A CRYSTALLOGRAPHIC STUDY ON LUMINESCENT GROUP 13 AND SELECTED LANTHANIDE TRIVALENT METAL COMPLEXES.

by

ORBETT T. ALEXANDER

A dissertation submitted to meet the requirements for the degree of

MAGISTER SCINTIAE

In the

DEPARTMENT OF CHEMISTRY

FACULTY OF NATURAL AND AGRICULTURAL SCIENCES

At the

UNIVERSITY OF THE FREE STATE

Supervisor: Prof. Hendrik G. Visser

Co-Supervisors: Prof. Hendrik C. Swart and Dr. Alice Brink.

February 215

ACKNOWLEDGEMENTS

Firstly I would like to thank my God for the countless blessings that you have bestowed on me, the strength, wisdom, understanding and perseverance you granted me with. Your love was, is and will always be enough for me, for that, I will always be grateful to you.

My sincere vote of thanks to Prof. Deon Visser for firstly believing in me. Thank you for your guidance, endurance, leadership, perseverance and support throughout the course of this work. Your enthusiasm for chemistry makes learning an adventure and I am honoured to be known as your student.

To Dr. Alice Brink, thank you for really making me believe in myself and also believing in me. I thank your support, advices, guidance, effort and your availability. You inspired me in so many ways and I will always cherish you for that. I am truly honoured.

To Prof. H.C. Swart. I thank you for the opportunity granted to work with you and also the support you gave me in many ways is highly appreciated. I am truly honoured to have worked with you.

To Dr. M.M. Duvenhage and the physics department personnel. My biggest thank you for the support, effort and time you gave me. You have contributed a major success in this journey and I appreciate it.

To Prof. A. Roodt. I would like to pass my vote of appreciation and gratitude for being such an inspiring leader. Your ecstasy for science rubs off to those around you and serves as an inspiration for one to archive. I am honoured to be called one of your students.

To Dr. Linette Twigge for all the help with the NMR studies. Thank you for your guidance and patience.

Thanks to my friends, fellow students and the personnel of the Chemistry Department at UFS who contributed in any way, for their support and enjoyable times we shared. Special thanks to the guys I have shared many laughs with, Penny Mokolokolo, Thabo Marake, Sipho Dlamini and Dumisani Kama. These guys have made this journey worth travelling.

Lastly, special thanks to my family. Without your unconditional love and support I wouldn't be where I am today. I will always love you.

I dedicate this work to my family: Motshedisi, Mannini, Ronnie, Ntsoaki, Itumeleng, Bokamoso, and Palesa Alexander. You all inspire me to do better than my best!

To My lovely Fiancé Thandiwe C. Mahlanyane and our little princess Olorato B. Alexander.

Special dedication to my late father……Lice William Alexander…..you taught me well papa. I appreciate all you have done for me, all the support, love, encouragements, advices and mostly the faith you had on me. You are the best father in the whole wide world and I thank God for you!

Abstract

Keywords: Aluminium, Gallium, 8-hydroxyquinoline, fluorescence, oleds, meridional, facial, Photoluminescence (PL).

The aim of this project is to try and understand the solid and solution state chemistry crystallography and NMR techniques to correlate the results thereof with the luminescence characteristics of the $M(N,O)_3$ complexes as described below and that was led by the prime solid state factors that hugely influences the luminescence characteristics differently than in the liquid state. Four complexes of the type $M(N,O)_3$ [M = Al, Ga, In. N,O = bidentate quinolinol type ligands: Ox = 8-hydroxyquinoline, 57dmOx = 5,7-dimethyl-8-hydroxyquinoline, 57dcOx = 5,7-dichloro-8-hydroxyquinoline] were synthesized. The obtained complexes were characterized by single crystal X-ray diffraction as well as other spectroscopic techniques (NMR, PL and UV-Vis) and includes the formation of the following *mer*-$[Al(Ox)_3]\cdot EtOH$, *mer*-$[(Ga(Ox)_3]\cdot 0.5\cdot EtOH$, *mer*-$[(Ga(57dmOx)_3]\cdot 0.5\cdot DCM$, *mer*-$[In(Ox)_3]\cdot 2H_2O$.Two more complexes of type $Ln(N,O)_3$ [Ln = Europium, N,O = 5,7-dichloro-8-hydroxyquinoline] which are $[Eu(57dcOx)_3]\cdot EtOH\cdot H_2O$ and κ^2-O,O'-$[Eu(57dcOx)_3\cdot EtOH]$.

The NMR solution studies gave some understanding with regard to the facial and meridional conformation of the complexes.

The crystal structures of *mer*-$[Al(Ox)_3]\cdot EtOH$, *mer*-$[(Ga(Ox)_3]\cdot 0.5\cdot EtOH$, and *mer*-$[In(Ox)_3]\cdot 2H_2O$, crystalizes in the same crystal system (monoclinic), space group ($P2_1/n$) and contain four number of molecules in the unit cell. That of *mer*-$[(Ga(57dmOx)_3]\cdot DCM$ crystallized in the triclinic crystal system ($P\bar{1}$) with two molecules in the unit cell. Complex : $[Eu(57dcOx)_3]\cdot EtOH\cdot H_2O$ and κ^2-O,O'-$[Eu(57dcOx)_3\cdot EtOH]$ crystallized in a trigonal and triclinic crystal system in space group $R\bar{3}$ and *P1* respectively.

Photoluminescence measurements were done on all the synthesized complexes. Change in intensity behaviour was observed as an influence of the metal and/or the ligand substitutions. The wavelength shifts were observed as a result of metal influence and also the influence from the geometrical conformation of the complexes (*mer*- or *fac*-).

Table of Contents

Abbriviations V

Abstract VI

1 Introduction and Aim 1

1.1 Introduction 1

1.2 Organic Light emitting Diodes (OLED's) 2

1.2.1 Why OLED's 2

1.3 Aim 3

2 Literature Studies 5

2.1 Introduction 5

2.2 Chemistry of Group 13 Metals Ions. 7

2.2.1 Aluminium (III) Metal. 7

2.2.2 A brief history of Gallium (III). 8

2.2.3 A brief history of Indium (III). 10

2.3 Lanthanide Metals Ion. 11

2.4 Luminescence 11

2.4.1 Photoluminescence 12

2.5 Chemistry Group 13 Metals Towards Photoluminescence 14

2.5.1 Introduction 14

2.6 Chemistry of Lanthanides Towards Photoluminescence 18

2.7 Factors affecting Fluorescence 20

2.7.1 Isomerism." 20

2.7.2 Structural Isomer 21

2.7.3 Molecular Packing 23

2.8 Organic light emitting diodes (OLEDs). 24

3 Synthesis of Metal Complexes 26

3.1 Introduction 26

3.2 Chemicals and Apparatus 28

3.3 General Synthesis Method For Mq3 Complexes. 28

3.3.1 Synthesis of *mer*-[*tris*-(8-hydroxyquinoline) aluminium (III)]·EtOH 29

3.3.2 Synthesis of [*tris*- (5,7-dimethyl-8-hydroxyquinoline) aluminium (III)] 29

3.3.3 Synthesis of [*tris*- (5,7-dichloro-8-hydroxyquinoline) aluminium (III)] 30
3.3.4 Synthesis of *fac*-[t*ris*-(8-hydroxyquinoline) gallium (III)]·0.5·EtOH 30
3.3.5 Synthesis of *mer*-[*tris*-(5,7-dimethyl-8-hydroxyquinoline) gallium (III)]·DCM 31
3.3.6 Synthesis of [*tris*-(5,7-dichloro-8-hydroxyquinoline) gallium (III)] 31
3.3.7 Synthesis of fac-[*tris*- (8-hydroxyquinoline) indium (III)]·$2H_2O$ 32
3.3.8 Synthesis of [*tris*- (5,7-dimethyl-8-hydroxyquinoline) indium (III] 32
3.3.9 Synthesis of [*tris*- (5,7-dichloro-8-hydroxyquinoline) indium (III)] 33
3.4 Synthesis of Lanthanide Complexes. 34
3.4.1 Synthesis Method For Respective Lanthanide Complexes. 35
3.5 Crystallized Complexes 36
3.6 Results and Discussions 37
3.6.1 8-Hydroxyquinoline complexes with Al, Ga and In metals 37
3.6.2 5,7-Dimethyl-8-Hydroxyquinoline 41
3.6.3 5,7-Dichloro-8-Hydroxyquinoline 44
3.7 Conclusions 46
4 X-RAY CRYSTALLOGRAPHIC STUDIES OF METAL-QUINOLATE COMPLXES 48
4.1 Introduction 48
4.2 Experimental 51
4.3 X-RAY Crystal Structures of $M(Ox)_3$ Complexes 52
4.3.1 4.3.1. *mer*-[*tris*-(8-Hydroxyquinoline) aluminium (III)] ·ethanol solvate (1) 52
4.3.2 mer-[tris-(8-Hydroxyquinoline) gallium (III)] 0.5·ethanol solvate (2) 60
4.3.3 *mer*-[*tris*-(5,7-Dimethyl-8-hydroxyquinoline)gallium (III)] dichloromethane solvate (3) 68
4.3.4 4.3.4. *mer*-[*tris*-(8-Hydroxyquinoline) indium (III)] ·$2H_2O$ (4) 73
4.4 Conclusion 81
5 X-RAY CRYSTALLOGRAPHIC STUDY OF LANTHANIDEQUINOLATE COMPLEXES. 84
5.1 Introduction 84
5.2 Experimental 86
5.3 X-RAY Crystal Structure of Lanthanides Complex 87
5.3.1 The crystal structure of: 87
[*tris*-(5,7-dichloro-8-hydroxyquinoline)·(diaqua)·europium(III)] water · ethanol solvate (5) 87
5.3.2 The crystal structure of: 95
κ^2-O,O'-*tris*-[(5,7-dichloro-8-hydroxyquinoline)(Methanol)Europium(III)] 95
5.4 Conclusions 106

6 Photoluminescence Studies of Group 13 Metal Ions.....108
6.1 Introduction.....108
6.2 Experimental.....110
6.3 Effects of substituents on the fluorescence of Mq_3 Complexes. 110
6.4 Effects of different group 13 metals on the fluorescence of $M(Ox)_3$ Complexes. 114
6.5 Eu complexes.....117
6.6 Conclusion 119
7 Theory of Characterization Techniques 120
7.1 Introduction.....120
7.2 Nuclear Magnetic Resonance Spectroscopy (NMR) 120
7.3 Magnetic Properties of Nuclei 120
7.3.1 Chemical Shifts.....122
7.3.2 Aromatics.....123
7.4 Ultraviolet/Visible Spectroscopy (UV/Vis) 125
7.5 X-ray Diffraction (XRD) 127
7.5.1 Bragg's Law. 128
7.5.2 Structure Factor. 129
7.5.3 The Phase Problem.....130
7.5.4 The Least-Squares Refinement. 131
7.6 Photoluminescence (PL) 132
7.6.1 The Electronic State 133
7.6.2 Radiative and Non-radiative Decay Pathways 134
7.6.3 Factors affecting Fluorescence Intensity.....135
7.7 Conclusions.....136
8 Evaluation of the Study 138
8.1 Introduction.....138
8.2 Scientific Relevance and Results Obtained.....138
8.2.1 Synthesis 138
8.2.2 X-ray Diffraction.....139
8.2.3 Luminescence studies 140

Appendix……

ABBREVIATIONS AND SYMBOLS

ABBREVIATION	MEANING
Ox	8-hydroxyquinoline
57dmOx	5,7-dimethyl-8-hydroxyquinoline
57dcOx	5,7-dichloro-8-hydroxyquinoline
β	Beta
γ	Gamma
α	Alpha
Å	Angstrom
π	Pi
°	Degree
°C	Degree celsius
g	grams
T	Temperature
Z	Number of molecules in a unit cell
PL	Photoluminescence
UV	Ultraviolet region in light spectrum
Vis	Visible region in light spectrum
NMR	Nuclear magnetic resonance spectroscopy
XRD	X-ray diffraction
λ	Wavelength
ppm	(Units of chemical shift) parts per million
DCM	Dichloromethane
UV	Ultraviolet in light Spectrum

Vis	Visible region in light spectrum
δ	Chemical Shift
EtOH	Ethanol
MeOH	Methanol
DCM	Dichloromethane
$CHCl_3$	Chloroform
H_2O	Water
Θ	Theta
Hz	Hertz
ε	Epsilon
%	Percent
ml	Mille litre
mmol	Mille moles

1 Introduction and Aim

1.1 Introduction

The energy demands on the world as we know it, is huge and still growing every year. The increased use of small mobile electronic devices has helped to influence the abrupt change of the energy landscape. There have been continuous efforts to harvest natural energy sources such as wind, water, and sunlight to satisfy both the environmental and clean energy issues and the limited energy resources crisis. Many research groups are involved in intense investigations on solar cells trying to carry out the mission of lowering energy consumption across the globe.[1,2,3]

South Africans use about 20 % of their available energy (electricity) for lighting systems, mostly through common incandescent light bulbs. Compared to traditional incandescent lights, energy-efficient light bulbs such as compact fluorescent lamps (CFLs), and light emitting diodes (LEDs) have the following advantages:

- Typically use about 25%-80% less energy than traditional incandescent, saving you money
- Can last 3 - 25 times longer.[4]

Considering the above, the research efforts to improve the science of LEDs by incorporating organic and inorganic based materials, is a must. Scientists strive to understand the factors that govern luminescence, and by so doing, improves it all the time.

[1] A. Mellit, A.M. Pavan, Solar Energy, 84(5), 807,2010.

[2] M.K. Nazeeruddin, E. Baranoff, M.Grätzel, Solar Energy, 85(6), 1172, 2011.

[3] T.M. Razykov, C.S. Ferekides, D. Morel, E. Stefanakos, H.S. Ullal, H.M. Upadhyaya, Solar Energy, 85, 8, 1580, 2011.

[4] http://energy.gov/energysaver/articles/how-energy-efficient-light-bulbs-compare-traditional-incandescents: Date Accessed: 01-February-2015.

1.2 Organic Light emitting Diodes (OLED's)

There are many technological display devices at this point in time. These various displays mainly consist of: inorganic light emitting diodes, liquid crystals, cathode ray tubes, plasmas etc. Although they have many advantages, one has to understand that these devices are not yet working at their respective optimum abilities. In terms of OLED research, factors like bulkiness, low viewing angle, colour tunability, high contrast and brightness, fast response time and many others, are still being improved upon on almost a daily basis.[5]

1.2.1 Why OLED's

One of the challenges of the digital era is the shortage of electricity turns out to be one of the major problems. Part of this problem can be ascribed to the present lighting system. For instance, tungsten filaments bulbs which tend to consume more power than other devices due their tendencies of converting a lot of their given energy as heat. To mention also mercury excited fluorescence bulbs that are non-ecofriendly, not disposable and has life of 1000h, are still being used by most households.[6]

Opposed to the above, OLEDs which are self-illuminating, eco-friendly and most importantly are power saving could solve this problem. Many OLEDs include inorganic complexes, like those formed between aluminium and its heavier group 13 icosagens with 8-hydroxyquinoline. The lanthanides can be excited with EM, however, the redistribution of their 4*f*-electron shell usually corresponds to forbidden *f-f* transitions resulting in low emission intensity. It was then seen fit to use antenna ligands to overcome this and use their spectral profiles together with the ligands fluorophore abilities to enhance the luminescence efficiency of the complexes.[7,8,9,10,11,12,] **Table 1.2.1.1** introduces a comparison between OLEDs and other lighting devices and highlights the reasons for this research.

[5] N.T. Kalyani, S.J. Dhoble, Renewable and Sustainable Energy Reviews, 16, 2696, 2012.

[6] M.H. Chang, D, Das, P.V. Varde, M. Pecht, Microelectronics Reliability, 52, 762, 2012.

[7] M.D. McGehee, T. Bergstedt, C . Zhang, A.P. Saab, M.B. O'Regan, G.C . Bazan, Adv. Mater,11, 1999.

[8] D. Zhao, Z. Hong, C. Liang, D. Zhao, X. Liu, W. Li, Thin Solid Films, 363, 208, 2000.

[9] C.J Liang, Z.R. Hong, X.Y. Liu, D.X. Zhao, D. Zhao, W.L. Li, Thin Solid Films, 14, 359, 2000.

[10]S.W. Pyo, S.P. Lee, H.S. Lee, O.K. Kwon, H.S. Hoe, S.H. Lee, Thin Solid Films, 232, 363, 2000.

[11] Zhu, Q. Jiang, Z. Lu , X. Wei, M. Xie, D. Zou, Synth. Met, 445, 111–2, 2000.

[12] D. Zhao, W. Li, Z. Hong, X. Liu, C. Liang, D. Zhao. J. Lumin., 82, 105, 1999, 2000.

Table 1.2.1.1: Technology landscape of LCDs, LED and OLED.[13]

Technology Feature	Active Matrix LCD	Passive Matrix LCD	LED	OLED
Brightness	Good	Good	Very good	Very good
Resolution	High	High	Low	High
Voltage	Low	Low	High	Low
Viewing angle	Medium	Poor	Excellent	Excellent
Contrast ratio	Excellent	Fair	Good	Excellent
Response time	Good	Poor	Fast	Very fast
Power Efficiency	Good	Good	Fair-good	Very good
Temperature range	Good	Poor	Very good	Very good
Form Factor	Thin	Thin	Wide	Very thin
Weight	Light	Light	Moderate	Light
Screen size	Small range	Small-medium	Small range	Small range
Cost	Average	Low	High	Below average
Applications	Laptops	Small displays	Signs, indicators	Multiple new/existing

1.3. Aim

The chemistry of $Al(Ox)_3$ for applications in the lighting industry was started in the 1980's by Tang and Van Slyke.[14] They found that when 8–hydroxyquinoline is chelated to the trivalent aluminium metal ion from Group 13 of the periodic table, to form a *tris*-coordinated homoleptic complex, light in the form of fluorescence is observed. The complex they made emitted a bright green light in the wavelength range of 500-520 nm. Since then, the chemistry of these $M(N^{\wedge}O)_3$ entities has never looked back.

This field of chemistry is not without challenges, isomerism being one of the largest. Research has shown that the *fac*-isomers of these types of complexes have higher intensities, but they are much more difficult to obtain. Furthermore, it seems that the *mer*-isomers are mostly preferred, resulting in very fast flip-over mechanisms from *fac-to-mer* with the reverse step very small.[15,16,17,18,19.]

[13] N.T. Kalyani, S.J. Dhoble, Renewable and Sustainable Energy Reviews, 44, 319, 2015.

[14] C. W. Tang, S. A. Van Slyke, Appl. Phys. 51, 913, 1987.

[15] M.J. Michalczyk, R. West, J. Michi, J. Am. Chem. Soc., 106, 821, 1983.

[16] N. Riddell, G. Arsenault. J. Klein, A. Lough, C.H. Marrin, A. Maclees, R. MacCrindle, G. Maclnuis, E. Sverk, S. Tittlemier, G.T. Tomy, Chemosphere, 74, 1538, 2009.

[17] Y. Kawano, H. Tobita, H. Ogina, Organometallics, 11, 499, 1991.

[18] R. Katakura, Y. Koide, Inorg. Chem., 45, 5730, 2006.

This first part of this study will investigate the coordinative and luminescent properties of M(N^O) complexes, with M = Al^{3+} to Ga^{3+} and In^{3+} and N^O = 8-hydroxyquinoline; *5,7* dichloro-8-hydroxyquioline and *5,7* dimethyl-8-hydroxyquinoline ligands.

Secondly, the coordination of a lanthanide metal ion, europium (Eu^{3+}), with 8-hydroxyquinoline will be investigated and the luminescence characteristics thereof will be studied. Europium complexes have been extensively used in this field of luminescence for its near IR sharp emission and characteristic spectral profile which influences the intensity and induces the delayed radiative emissions.[20,21,22]

The objectives of this study are therefore summarized as follows:

1. To synthesize the complexes of aluminium, gallium and indium with
   - ✓ 8–hydroxyquinoline
   - ✓ 5,7-dimethyl-8–hydroxyquinoline
   - ✓ 5,7-dichloro-8–hydroxyquinoline.
2. To synthesize complexes of Europium(III) with 5,7-dichloro-8–Hydroxyquinoline
3. To characterize the complexes with x-ray diffraction (XRD), nuclear magnetic resonance (NMR) and ultraviolet visible (UV/Vis) spectroscopies.
4. To study the luminescent properties of all the obtained complexes.
5. To further correlate the obtained information from the respective characterization techniques used to try and understand the subtle differences in coordination behavior of the these complexes and the luminescence properties thereof.

In the following chapter, a brief literature review of the development of these $M(N^{\wedge}O)_3$ type of complexes using Al^{3+}, Ga^{3+}, and In^{3+} metal ions and the chemistry of lanthanides particularly Eu^{3+} is presented, followed by the systematic presentation and discussion of experimental result.

[19] M. Colle, J. Gmeiner, W. Milius, H. Hillebrecht, W. Brutting, Adv. Func. Matter, 13, 108, 2003.

[20] J. Kido, Y. Okamoto, Chem. Rev., 102, 2357, 2002.

[21] M.F Reld, F.S. Richardson, Journ. of Phys. Chem., 88, 3579, 1984.

[22] N. Sabbatini, M. Guardigli, J.M. Lehn, Coord. Chem. Rev., 123,1-2, 201, 1993.

2 Literature Studies

2.1 Introduction

For the last two decades, the world has seen a great development in terms of research with the $Al(Ox)_3$ complex as the front runner in the field of organic light emitting devices (OLED's) which is commonly known as light emitting diodes.[1] Much of this interest is mainly because of the extra technical features it exhibits in flat panel displays that a typical conventional display device do not have.[2] Amongst many of the advantages of OLEDs are: high brightness and contrast, fast response time, wide viewing angle, high luminous efficiency, light weight and many others. Better yet, the field is still growing since the idea of developing white organic light emitters from OLED's for domestic, street lights and commercial use has brought the spot light and a necessary boost to the research activity in this field.[3]

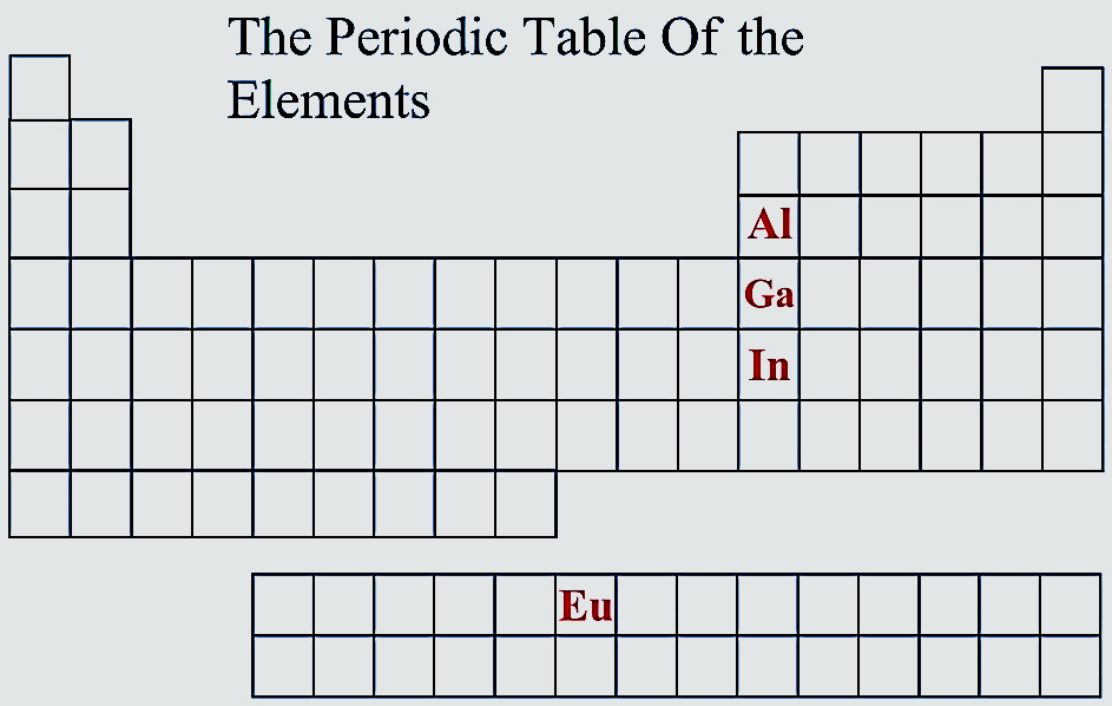

Figure 2.1.1: An outline of a periodic table displaying the metals of interest in this manuscript.

[1] C. W. Tang, S. A. Van Slyke, Appl. Phys. 51, 913, 1987.

[2] Z. Shen, P. E. Burrows, V. Bulovic, S. R. Forrest, M. E. Thompson, Science, 1997, 276, 2009.

[3] J. Signh, Organic light emitting devices, Croatia: Intech prepress, 2012.

The group 13 (aluminium, gallium, indium and thallium) cations have the potential to be Lewis acid catalysts and that is what brought much attention to the chemistry of these metals. There are chances that the transformations mostly conducted with neutral group 13 derivatives could possibly be accomplished with those that are cationic.[4] The major advantage besides the fact that they could easily be air stable, is that they can also enhances Lewis acidity. Despite the fact that the group 13 metals are deemed not essential to life, their trivalent metals are, nonetheless of great biological interest.[5]

Part of this thesis will also involve europium chemistry with the same ligand systems. The lanthanides have managed to reside under the spotlight due to their phenomenal and unmatched optical properties and their magnetic properties. They have shown their great potential hence it is used in applications such as optical glasses, telecommunications, lasers, lighting and displays and many others. They have earned respect from many coordination chemists after being thought of as minor actors in transition metal chemistry.[6]

The chemistry of this manuscript revolves around the group 13 metal ions namely: aluminium, gallium and indium. From the lanthanides column, the europium (Eu) metal ion was chosen for this project. Taking a peek at the icosagens, aluminium metal was the first to be used with the quinolinol systems and light was observed. Curiosity got the best of many scientist and the chemistry expanded down the boron group to gallium and indium. One of the factors that led to the aim of this project is to explore the chemistry of this $M(Ox)_3$ entities with gallium (Ga) and indium (In) metals and observe the change of chemistry thereof. Now the above mentioned metal ions are all trivalent metals.

[4] D. A. Atwood, Cationic group 13 complexes, Coordination Chemistry Reviews, 176, 407, 1998.

[5] A.J Downs, Chem. of aluminium, gallium, indium and thallium, USA: Chapman and Hall Inc.,1993.

[6] J.G. Bunzli, Lanthanide coordination chemistry, *Jour. of Coordination Chem*., 67, 23, 3706, 2014.

2.2 Chemistry of Group 13 Metals Ions.

2.2.1 Aluminium Metal.

Aluminium was first discovered back in 1825 by a Danish physicist named Hans Christian Oersted. The metal ore was originally proposed to be aluminum by Dany in 1807, which was roughly 18 years before the metal was officially discovered. However, right after the IUPAC adopted the name aluminum which soon after changed to be aluminium because of the "ium" suffix which most elements had, it became the house hold name to the world.[7] Aluminium stands to be the third most abundant element in the earth's crust (82g kg^{-1}, 8%) and furthermore, the most abundant metal. In many of quotidian applications, aluminium had become very useful in many ways and that is mainly because of the existing combination of the above indicated availability (8%) combined with its unique mechanical and electrical properties.[8] It is present in over 270 different minerals. The chief ore of aluminium is bauxite.[9]

Aluminium does not occur freely and is mostly found as oxides and silicates. This is largely due to the fact that it has strong affinity for oxygen. It has the ability to resist corrosion which is largely due to the phenomenon of passivation. It is a silvery white, soft, non-magnetic and ductile metal. It generally has the same chemical properties as gallium but differ in some aspects. Aluminium comprises of 8.1% of the earth's crust by mass and owing to its lightness 6.4 % on an atomic basis. Clay minerals such as kaolimite ($Al_2(OH)_4Si_2O_5$) and hydroxides are found from the weathering of igneous rocks that normally contain feldspars and micas. The main ore, bauxite, normally contains large amount of aluminium is then produced from leaching and weathering of silica. There are two forms in which Al_2O_3 is found; the gibbisite [$Al(OH)_3$], and/or the boehmite AlO(OH) form. Cryolite, $NaAlF_6$, it is now made

[7] Aluminium - Historical information. Available:
http://www.Webelements.com/Aluminium/history.html. Last accessed 24 January 2015.

[8] D.A. Atwood, B.C. Yearwood, The future of aluminium chemistry, Journ. of Organometallic Chem., 600, 186, 2000.

[9] Aluminium - Historical information. Available:
http://en.m.Wikipedia.org/ Aluminium/.html. Last accessed 24 January 2015.

synthetically because the source in which it was found, Greenland, has been depleted. It was used in the electrolytic production of metallic aluminium.[8,9,10]

Aluminium is one of those elements whose applications are seen or encountered on daily basis. In most cases it is alloyed and that somehow improves its mechanical properties. The beverage cans and aluminium foils are alloys of 92 % and 97 % aluminium. In addition, aluminium has been a key aspect in electrical transmission lines for power distribution. It is also used as sheet, tube and casting in transportation like aircrafts, automobiles, bicycles, etc. Furthermore, aluminium is used to form optical coatings where a thin layer of aluminium is deposited onto flat surfaces by physical and chemical vapor deposition.[9]

2.2.2 A brief history of Gallium (III).

Back in 1875 a French chemist by the name of Paul Emile Lecoq de Boisbaudran discovered and isolated an element called gallium. He managed to do so as he was also an investigator in the field of spectroscopy. He managed to discover the metal by its characteristic two violet spectral lines at 4172 Å and 4033 Å respectively. [11] However, 6 years before its discovery by the spectroscopy, Mendeleev had already predicted the metal. Gallium was the first element to be discovered spectroscopically and was also the first to be discovered as the three "eka" elements which were predicted by Mendeleev in 1870.[7,9]

Gallium does not occur free in its elemental state but as gallium (III) salt with trace amounts of zinc and bauxite ores. It can be obtained by smelting. It is silvery in colour and when solidified the metal expands by 3.1 %. Generally gallium has the same chemical properties as aluminum but differ in some respects. The metal gallium has a low melting temperature of 29.75 °C and a high boiling point of 1983-2070 °C.[12] The density of gallium is 5.904 g/ml (solid) at 29.6 °C and 6.095 g/ml (liquid) at 29.8 °C.[13]

Gallium can be found in all kinds of rocks. The proportion of gallium decreases as the basicity of the rock increases indicating preference towards acidic environments. Gallium is

[10] A.J Downs, Chem. of aluminium, gallium, indium and thallium, USA: Chapman and Hall Inc.,1993.

[11] M. E. Weeks, "Discovery of the Elements", J. Chem. Educ., Press, Easton, Pa., 1948.

[12] Liquid-Metals Handbook, Atomic Energy Commission, U.S. Government Printing Office, Washington, D.C., June 1, 31, 1950.

[13] Gallium - Historical information. Available:
http://www.Webelements.com/ Gallium /history.html. Last accessed 24 January 2015.

also found in bauxite as replacement for iron (Fe^{3+}) and with aluminium (Al^{3+}). The rare sulfide mineral called germanite, contains the highest gallium concentration (up to 1%). Nonetheless, the commercial production depends on recovery of less than 0.01 % found in bauxite, which is processed in large quantities for its aluminium.[13,1415]

The oldest application of gallium was that of a filler for high temperature thermometers. Gallium derivatives have many useful applications, for instance, GaAs is capable of converting electricity directly into coherent light.[16] Moreover, GaAs in some ways is the key component of light emitting diodes (LED's). Gallium is an excitant in phosphors for luminous paints and also in fluorescent lights. [17] It has two interesting isotopes (^{67}Ga and ^{72}Ga) which have been active for years in the radiopharmaceutical arena. ^{67}Ga have been used for inflammation and tumor imaging whereas ^{72}Ga have been useful in the treatment and diagnosis of bone cancer. [18]

2.2.3 A brief history of Indium (III).

Indium was discovered by F. Reich and H.T. Richter in 1863. These German chemists were testing zinc ores from the mines. Thallium was one of the key metals that was found in the nearby surroundings where these rocks were mined. The green spectral line emissions of thallium is the primary method of detection for it. However, blue line emissions were discovered indicating an unknown element in zinc ores. Later in 1864, the metal was isolated by Richter himself. This metal has the ability to stabilize non-ferrous metals and that was the first significant usage recorded in 1924.[19]

Indium is a very soft, silvery white and highly ductile. It consists of a mixture of 96% indium-115 and 4% indium-113, which are trivial. Indium's properties of being ductile and malleable get subjected to almost limitless deformation with a gravity of 7.3. It proves strength, hardness and corrosion resistance. The melting point of this metal is 156.6 ˚C (429.8

[14] Aluminium - Historical information. Available:
http://en.m.Wikipedia.org/ Aluminium/.html. Last accessed 24 January 2015.

[15] G. Phipps, C. Mikolajzak, T. Guckes, Renewable Energy Focus, 9(4), 56, 2008.

[16] R.R. Moskalyk, Mineral Engeneering, 16, 921, 2003.

[17] J. Dement, H.C. Dake, Rare Metals, Chemical Publishing Co., Brooklyn, N. Y., 28, 1946.

[18] H. C. Dudley, Naval Med. Research Inst., Rept. NM-011-013, 1949.

[19] J.F. Sidney, J. of Chem, 11 (5), 270, 1934.

K) and high boiling point of 2072 ˚C (2353 K).This indium metal ion burns at red heat to form a yellow oxide (In_2O_3). It has limited history available describing its environmental impact, hence, precautions should be taken regardless of the fact that is considers to have low toxicity. It is commonly found in association with zinc-bearing materials such as in solid solution in Sphalerite. Sphalerite is the most common mineral that contains zinc.[20]

Indium has a wide range of applications. Some of these applications in which indium are employed in are fabrication of germanium rectifiers, photo conductors and thermistors.[21] It is mostly used in thin film coatings such as prevalent LCD screens used in computer screens, gamma, CD and/or players, flat panel displays up to solar cells. Moreover, indium semiconductors are used in infrared detectors and high efficiency photovoltaic devices.[22]

2.3 Lanthanide Metals Ions.

Europium metal was discovered by a French chemist by the name of Eugene Anatole Damarcy in 1901. The metal ion was named after the continent Europe. This metal was one of the last of the rare earth's elements discovery. It is the most active of the lanthanides in that it can react with other elements more readily than any other lanthanides.[23]

This europium metal was one of the deposits in the element cerite and that discovery took hundred years. It is not abundant in the earth's surface.
The pure europium metal is silvery but if exposed to air it becomes dull. It has a melting point of 822 ˚C (1095 K) and a boiling point of 1529 ˚C (1802K). It is used in red phosphors in optical displayed and TV screens.[24,20]

[20] W. M. Haynes, ed., CRC Handbook of Chemistry and Physics, CRC Press/Taylor and Francis, 95th Ed., 2015.

[21] Economics of Indium, 1999.

[22] A.M. Alfantazi, R.R. Mosklyk, Minerals Eng, 16, 167, 2003.

[23] http://global.britannica.com/EBchecked/topic/196533/europium-Eu: Date accessed: 03-February-2015

[24] http://www.chemistryexplained.com/elements/C-K/Europium.html Date accessed: 03-February-2015

2.4 Luminescence[25,28]

Luminescence is light coming out from either chemical reactions, electrical energy, subatomic motions and/or stress on a crystal but not resulting from heat. The so called "cold light", is set to take place at normal and low temperatures only. The term luminescence was first introduced by a German physicist back in 1888 by the name of Eilhard Wiedemann.[26,27]

The concept of luminescent arises from the phenomenon of an energy source ejecting an atom out of its ground or lowest energy state into an excited or higher energy state. The electron then gives back the energy so it can fall back down to its ground state and in so doing, it gives off light.

There are several varieties of luminescence, each named according to what the source of energy is, or the key aspect that triggers luminescence. The types of emissions are:

- Chemiluminescence, an emission through a chemical reaction.
- Crystalloluminescence, an emission produced during crystallization.
- Electroluminescence, an emission resulting from an electric current passed through a substance.
- Mechanoluminescence, an emission resulting from a mechanical action on a solid.
- Photoluminescence, an emission resulting from absorption of photons.
- Radioluminescence, an emission as a result of bombardment by ionizing radiation.
- Thermoluminescence, the re-emission of absorbed energy when a substance is heated.

Luminescent compounds can be of very different kinds: **organic compounds**: aromatic hydrocarbons (naphthalene, anthracene, etc.), fluorescein, rhodamines, coumarins, oxazines, polyenes, diphenylpolyenes, aminoacids (tryptophan,tyrosine). **inorganic compounds**: uranyl ion (UO^{+2}), lanthanide ions (e.g. Eu^{3+}, Tb^{3+}), doped glasses e.g. with Nd, Mn, Ce, Sn.[28]

[25] http://www.wikipedia.org/wiki/Luminescence. Date accessed: 03-February-2015

[26] B. Valeur , M.N. Berberan-Santos, J. Chem. Education., 88 (6), 731, 2011.

[27] E. Wiedemann, On fluorescence and phosphorescence,*Annalen der Physik*,34: 446, 1888.

[28] B. Valeur, Molecular Fluorescence, New York: Wiley-VCH, 2001.

2.4.1 Photoluminescence

Photoluminescence is one of many forms of luminescence and it is mostly initiated by photo-excitation (excitation by photons).

Therefore its light emission is a result of absorption of photons. Photoluminescence processes can be classified by a direct relation between the energy of the exciting photon with respect to the emission. It can be found in two forms, namely, fluorescence and phosphorescence.

2.4.1.1 Fluorescence[29]

Fluorescence is the emission of light by a material that has absorbed light or other electromagnetic radiation. It is a form of luminescence mostly found as an optical phenomenon in cold bodies. In most cases, the emitted light has a longer wavelength, and therefore lower energy, than the absorbed radiation. The difference in energy between the absorbed and emitted photons ends up as vibration, heat or possibly molecular rotations. It is possible for a photon to be absorbed in an ultraviolet range and then emitted in the visible range. **Figure 2.4.1.1.1** shows the different applications of fluorescence.

Figure 2.4.1.1.1: Typical examples of different applications of fluorescent materials including fluorescent minerals.[29]

[29] http://en.wikipedia.org/wiki/Fluorescence. Date accessed: 03-February-2015.

2.4.1.2 Phosphorescence[30]

Phosphorescence is a form of photoluminescence that is directly related to fluorescence. The difference between the two is that phosphorescence has delayed emission and in contrast to that, fluorescence absorbed radiations are immediately re-emitted. This time factor that differentiates the two from each other is due to forbidden energy state transitions in quantum mechanics. These forbidden transitions occur less often in certain materials which might be due to the relaxations of transitions rules. The absorbed radiations can be re-emitted over a long period of time, however, compromising the light intensity of the material. It is for those reasons that phosphorescence is declared to be a process in which energy absorbed by a substance is released slowly in the form of light. **Figure 2.4.1.2.1** shows the different application of phosphorescence.

Figure 2.4.1.2.1: Typical examples of different applications of phosphorescent materials .[30]

These phosphorescence mechanisms are mostly used in the 'glow in the dark' materials. The idea behind it is to let the material absorb a certain amount of light and store it over a long period of time, especially when exposed to it (light), then re-emit when needed.

[30] http://en.wikipedia.org/wiki/Phosphorescence. Date accessed: 03-02-2015

2.5 Chemistry of Group 13 Metals towards Photoluminescence

2.5.1 Introduction

The coordination chemistry of 8-hydroxyquinoline with a variety of metal ions has been widely explored.[31,32,33] The ligand and its derivatives can stabilise various metal complexes due to its chelate-aromatic properties. 8-hydroxyquionolines are soluble in a majority of organic solvents. The derivatized entities such as the 8-hydroxyquinoline allow solvation of chelates in aqueous media and this widens the range of possible applications. These ligands are widely used in areas such as water treatment, food additives, radiopharmaceuticals, and (organic light emitting diodes) OLEDs.

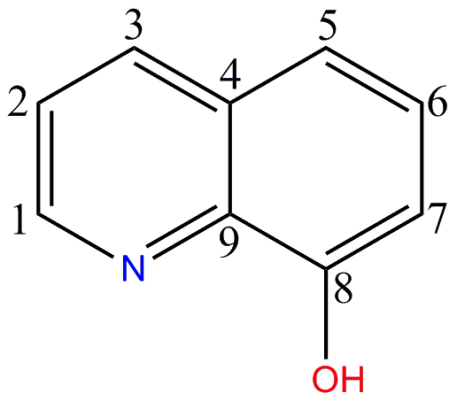

Figure 2.5.1.1: The schematic representation of 8-hydroxyquinoline.

Luminescent chemical sensors based on the increase in fluorescence brought about the introduction of a metal ion are attractive due to their ease of use and the high sensitivity even at low metal concentration. Free 8-hydroxyquinoline (**Figure 2.5.1.1**) is weakly luminescent if not nothing at all. Upon electron excitation, the OH group and the N atom of the pyridine group of these compounds become strongly acidic and basic respectively, resulting in excited state tautomerization as a result of coupled proton transfer and intra-molecular charge transfer. These tautomers turn out to be weakly luminescent. [34,35] The inclusion of a metal ion

[31] Y. Wang,W. Zhang, Y. Li, L. Ye and G. Yang, Chem. Mater.,11,530 (1999)

[32] L.S. Sapochak, F.E. Benincasa, R.S. Schofield, J.L. Baker, K.K.C. Riccio, D. Fogarty, H. Kohlmann, K.F. Ferris and P.E. Burrows, J. Am. Chem. Soc.,124 (21), 6119 (2002).

[33] P.J. Han, A.L. Rheingold and W.C. Trogler, Inorg.Chem., 52, 12033 (2013).

[34] R. E. Ballard, J. W. Edwards, J. Chem. Soc., 4668, 1964.

inhibits the degradation pathway and enhances the intensity. The fluorescence intensity enhancement is dependent on the nature of the metal ion. This effect provides opportunity to design more sensitive and selective 8-hydroxyquinolates. The optimisation of the OLEDs such as $Al(Ox)_3$, is subject to intense research particularly towards the development of blue light emitters through the modification of physiochemical properties such as control of the 1:3 geometry in $Al(Ox)_3$ with *fac* and *mer* ligand arrangement around the metal centre.

One of the major problems in the design and development of efficient OLEDS is the invariable truth that the 8-hydroxyquionoline ligands are open to coordination to a number of metal ions. There are numerous studies aimed towards the possible increase in selectivity of the ligands towards metal ions via the systematically functionalization of the ligands especially at positions 2, 5 and 7 of the ligand backbone (see **Figure 2.5.1.1**). Multi-dentate derivatives of quinolines provide high thermodynamic stability and selectivity due to the large stability constants. The potential fluorogenic properties of both O-TRENSOX (tris(2-aminoethyl)amine-sulfoxine) and (1-*n*-Butyl-8-hydroxyquinoline-7-carboxamide (n-BUSOX) was explored using aluminium(III) and gallium(III) in aqueous solutions.[36] The ligand

O-TRENSOX is composed of three 8-hydroxyquinoline subunits connected to a tris(2-aminoethyl)amine. The n-BUSOX is one arm of the TRENSOX.

[35] M. Goldman, E. L. Wehry, Anal. Chem., 42, 1178, 1970.

[36] F. Launay, V. Alain, E. Destandau, N. Ramos, E. Bardez, P. Baret**,** J-L Pierre**,** New J. Chem., 25, 1269, 2001.

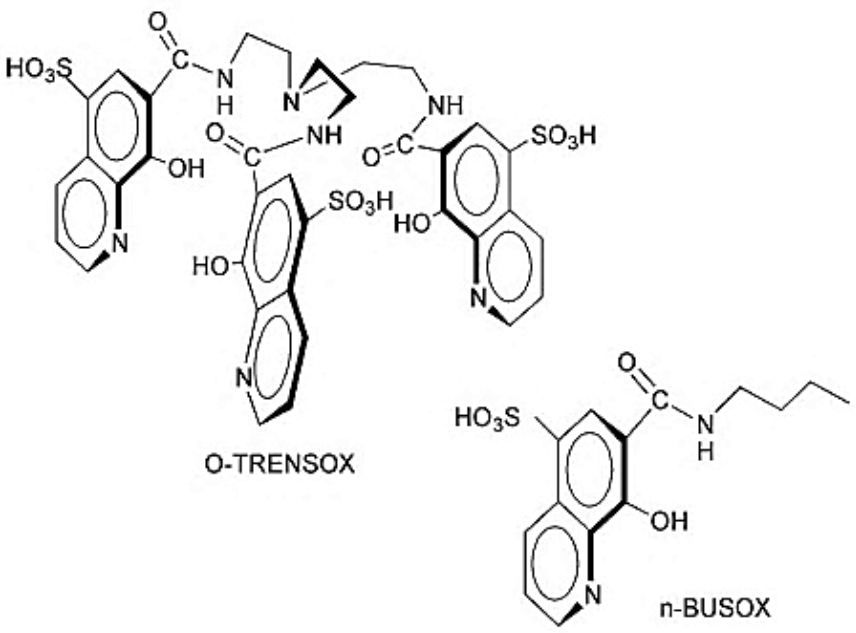

Figure 2.5.1.2: Structural representation of TRENSOX and n-BUSOX

The fluorescence spectra's of both aluminium(III) and gallium(III) were recorded in the same range in order to permit direct comparison. The ligands showed similar spectral profiles with no significant change in either the shape or the wavelength emission range of the chelates. The only notable difference was the slower level of emission the O-TRENSOX chelate. The results pointed out to an increase in fluorescence enhancement going from TRENSOX <8-HQn < n-BUSOX. This effect is opposite to what was expected and it was tentatively suggested that the difficulty in removing metallic impurities might be the reason to the minimal fluoro-genic enhancement by the TRENSOX. The fluorescence intensity was higher in aluminium than gallium. This effect might be due to the greater suppression of the photo-induced charge transfer within quinoline nucleus during excitation. Aluminium(III) has a higher charge density than gallium(III) making it a more suitable candidate for fluorescence.

The effect of a variety of functionalized ligands on the optical preference was evaluated. These studies highlighted the significance of tuning the electronic and steric properties of these ligands towards the overall performance of the complexes.[37,38,39]

[37] J. Cheng, H.D. Shieh, Analytical Science, 24, 235, 2008.

[38] A. Yuchi, H. Hiramatsu, M. Ohara, N. Ohata, Analytical Science, 19, 1177, 2003.

[39] J. Cheng, C.C. Chang, C.H. Chen, J. F. Chen, Analytical Science, 37, 20, 2004.

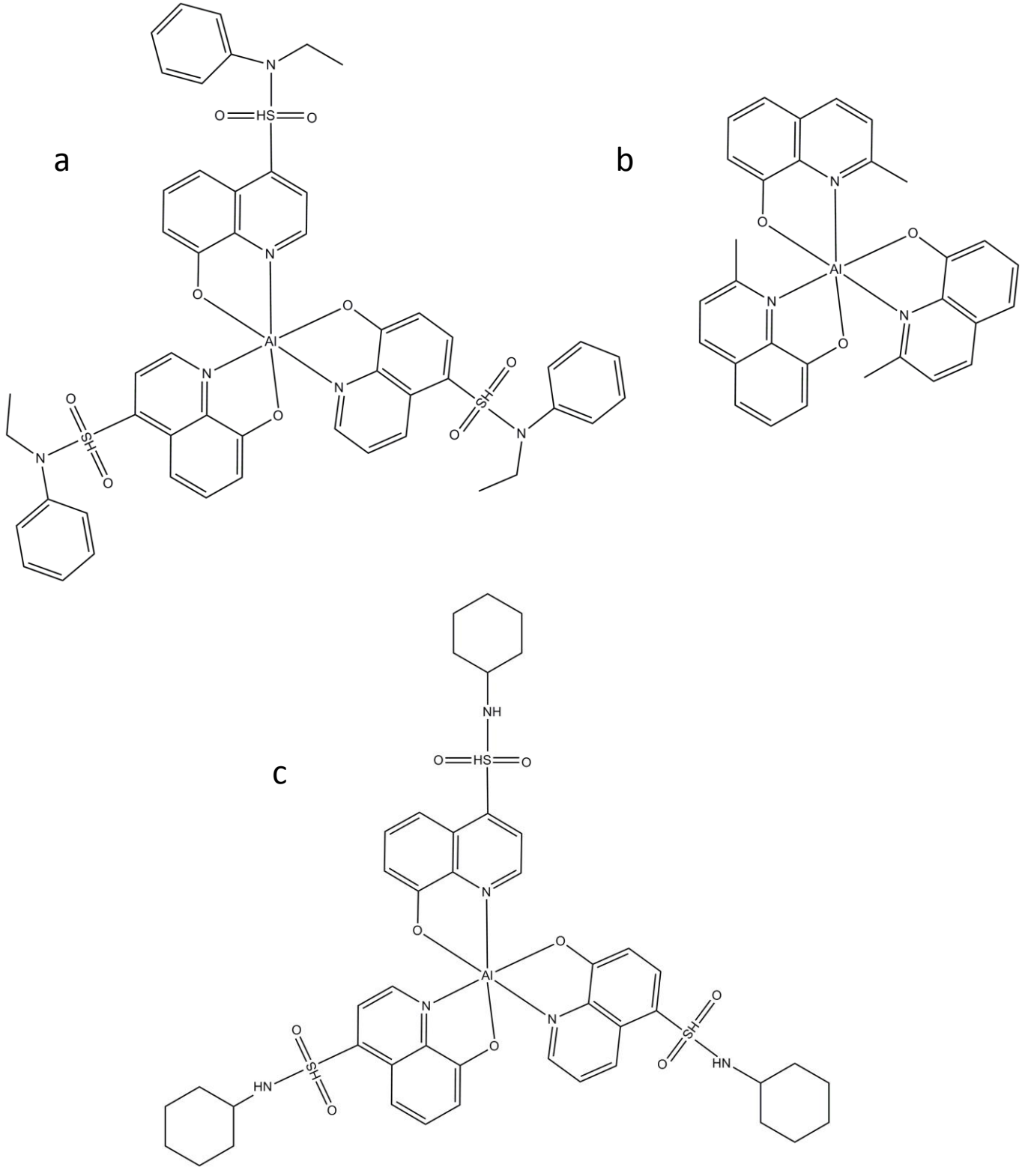

Figure 2.5.1.3: Structural representation of a) tris-(5-*N*-ethylamnilinesulfonamide-8-quinolinolato)aluminium(III), b) tris-(2-methyl-8-quinolinolato)aluminium(III) and c) tris-(5-piperidinylsulfonamide-8-quinolinolato)aluminium(III).

2.6 Chemistry of Lanthanides Towards Photoluminescence

The design and development of highly luminescent europium complexes, that can be used as active components for sensors and screens in electronic devices, has been subject to intense studies since the early 1990s. [40,41] The employment of lanthanide metal ions as emitting layers was motivated by the existence of well-defined emission bands due to their outer electron configuration. This property of lanthanide metal ions counteracts the broad, non-pure bands experienced when using material such organic metal complexes, organic dyes and organic polymers.

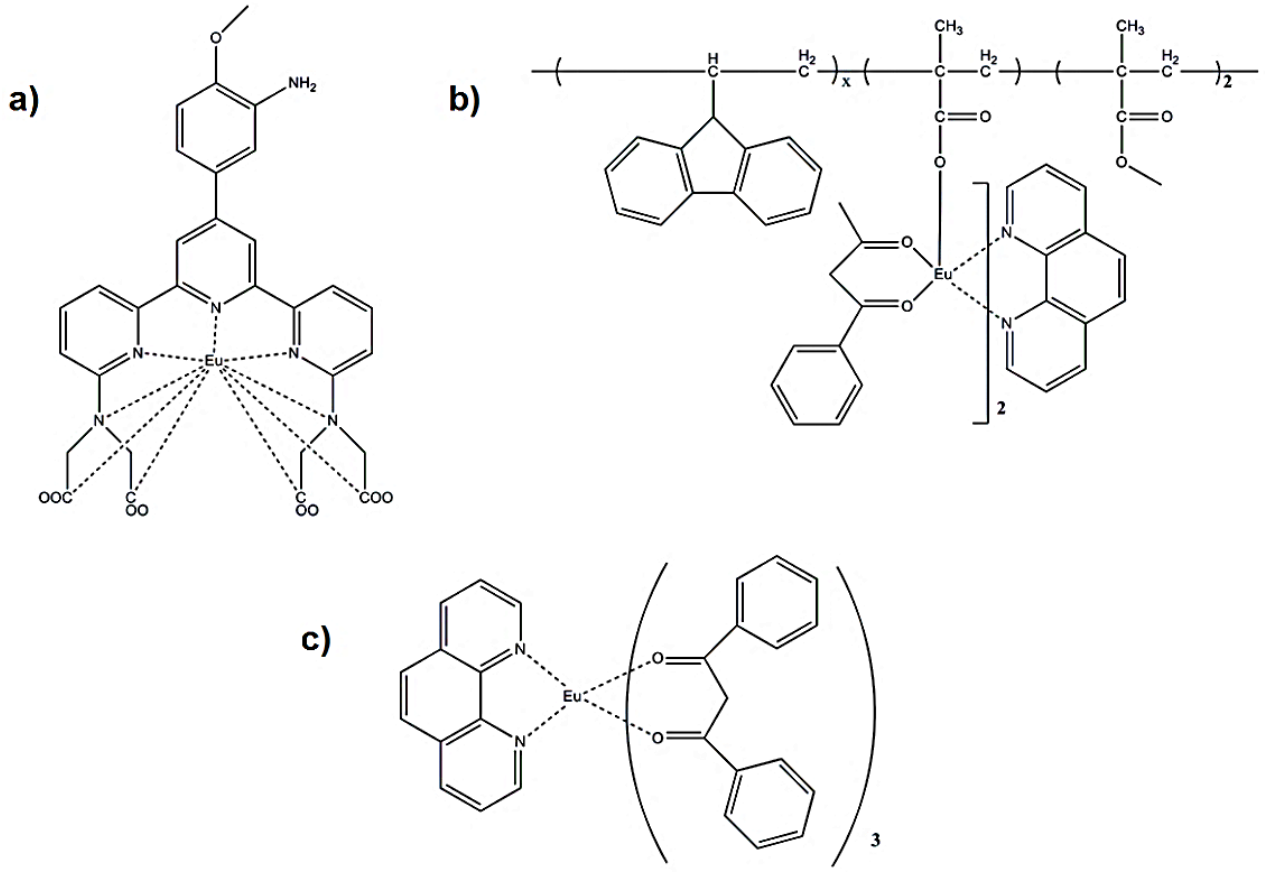

Figure 2.6.1: Typical lanthanide complex's used in the respective lanthanide bindings.

[40] V. Balzani,Tetrahedron, 48, 10443, 1992.

[41] F. Bodar-Houillon, A. Marsura, New J. Chem., 20, 1041, 1996.

Apart from the difference in spectral profiles of lanthanide complexes from the organic metal complexes, the excitation mechanism of the metal ion differs greatly to that of organic compounds. The excited triplet energy state of organic fluorescent compounds lowers though the deactivation processes without photon emission. A contrasting behaviour is observed for lanthanide complexes. For π-conjugated ligands such as β-diketone, metal ion excitation occurs through intra-molecular energy transfer from the triplet excited state of the ligands.[42,43] The excitation and energy transfer mechanisms for lanthanide chelates is shown in **Figure 2.6.2.**

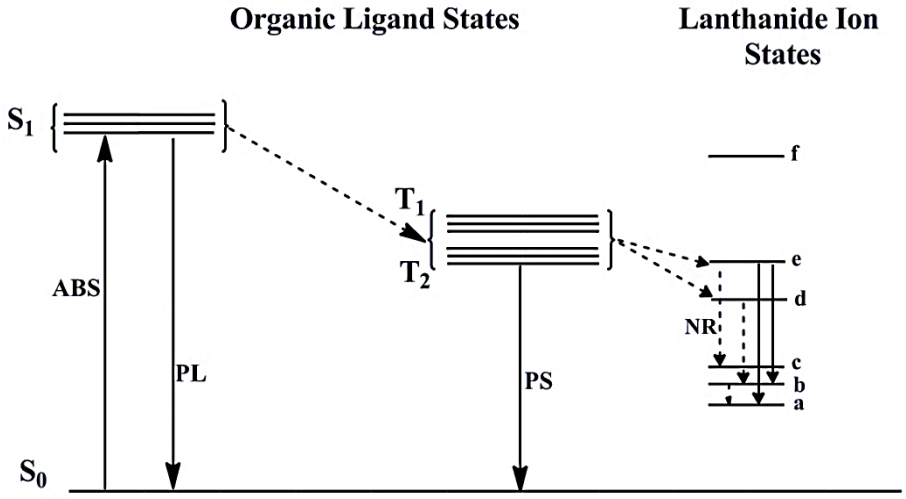

Figure 2.6.2: Energy transfer in lanthanide complexes: ABS= absorption, PS = phosphorescence, PL = photoluminescence, NR = non-radiative.[59]

The light emitted from lanthanides is commonly referred to as Time Resolved Fluorescence (TRF), since the light excitation and emission from lanthanides does not correspond to fluorescence. Eu^{3+} complexes do not fluorescence due to the efficient deactivation mechanism occurring in the aqua complex involving energy transfer from excited state Eu^{3+} to the OH groups which degrade rapidly in a non-emissive way.[44,45,46] In order to detect the lanthanide luminescence though TRF, the lanthanide chelate is attached to an organic linker, referred to as an "antenna". The linker absorbs the excited light and then transfers it to the triple state of the lanthanide ion Figure 2.6.2. Europium complexes are luminescent in

[42] R.E. Whanga, G.A. Crosby, J. Mol. Spectr., 8, 315, 1965.

[43] K.M.L. Bhaumi, M.A. El-Sayed, J. Chem. Lett., 657, 1965.

[44] Y. Haas, G. Stein, J. Chem. Phys.,76, 1093, 1972.

[45] R. S. Dickins, D. Parker, A. S. de Sousa, J. A. Williams, Chem. Soc., Chem. Commun., 697,1996.

[46] J. L Kropp,.; M. W. Windsor, J. Chem. Phys.,42, 1599, 1965.

aqueous solution, due to the presence of a photoactive chelator serving not only as a link between the lanthanide and the antenna, but also as a shield of the metal ion from coordination with water.

2.7 Factors affecting Fluorescence

2.7.1 Isomerism.[47,48,49]

2.7.1.1 Introduction

A German chemist by the name of F. Wohler, was the first to notice isomerism in the prepared silver cyanate complex. The word isomerism came from Greek word isomers (isos = equal, meros = a share).

Isomers are basically two or more compounds having the same molecular formula but different chemical and/or physical properties and the phenomenon is known as isomerism. Isomerism can be defined into two types namely:

- Structural isomerism (constitutional isomerism)
  - Optical isomerism
  - Geometrical isomerism
- Stereoisomerism (configurational isomerism)
  - Coordination isomerism
  - Ionization isomerism
  - Linkage isomerism

[47] N.N. Grenwood, A. Earnshaw, Chemistry of the elements, 2 Ed., Oxford: Butterworth Heinemann, 918, 1997.

[48] http://wwwchem.uwimona.edu.jm/courses/IC10Kiso.html. Date Accessed: 30-January-2015.

[49] http://en.wikipedia.org/wiki/Structural_isomer. Date Accessed: 30-January-2015.

2.7.2 Structural Isomer

Structural isomerism is one of the existing form of isomerism in which molecules with the same molecular formula have bonded together in different orders. For instance, these molecules each have a different structural formula, as opposed to stereoisomerism.

There are two main types of structural isomerism which are namely geometric isomerism, and optical isomerism. These stereoisomers are more involved in different arrangements of fragments of the molecule in space.

- **Geometrical isomerism**

This type of isomerism stands to be of most importance in square-planar and octahedral complexes.

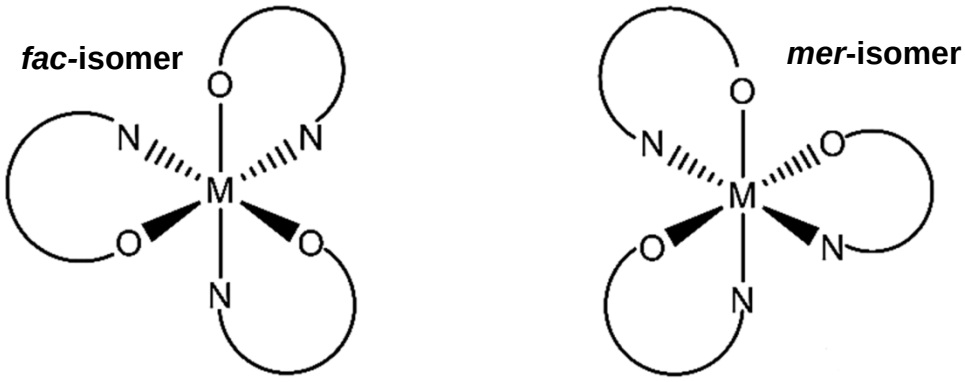

Figure 2.7.1.1: Geometrical isomerism in octahedral complexes

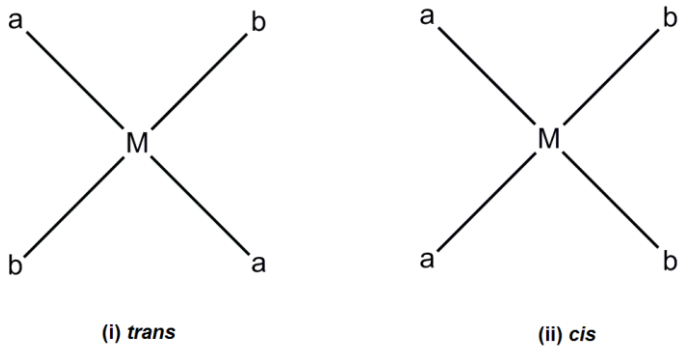

Figure 2.7.1.2: Geometrical isomerism in square planar complexes.

The phenomenon of isomers which possess the same molecular and structural formula but differ in the orientational occupancy of atoms or groups in space around the double bond is known as geometrical isomerism. Amongst many physical properties, UV/Vis spectra and the dipole moment are often of most importance in differentiating the geometrical isomers.

2.7.2.1 Effect of Temperature

Efforts has been made to tune the green emission typically of $Al(Ox)_3$ OLED's. The field became diversified so much that a lot of possibilities have be explored to archive that goal. Some have tried using multi-layer structures and some tried chemical doping. However, the intense effort directed towards the experimental and theoretical aspects is put on the $M(Ox)_3$ complexes, is continuously fuelled by the constant understating of the importance in resolving the isomerization problem in their chemistry.

The ^{1}H and ^{13}C investigation at room temperature reveal that only a mer-isomer can be obtained. It is further understood that some of the geometrical isomers are inter-convertable.[50,51,52] This inter-conversion can be temperature dependent. The *mer*-isomer is often more kinetically stable in solution at room temperature than *fac*-isomers. It is for such reason that the *fac*-isomer has a very short lifetime in solutions state. This short lifetime behaviour is in accordance with the *fac*-to-*mer* isomerization via ligand flip mechanism which indicates to be exceedingly fast compared to the reverse step. That leads to very difficult NMR-studies of these $M(Ox)_3$. Accordingly, polar protic solvents accelerate the *cis*-to-trans isomerisation process.[53,54,55]

[50] M.J. Michalczyk, R. West, J. Michi, J. Am. Chem. Soc., 106, 821, 1983.

[51] N. Riddell, G. Arsenault. J. Klein, A. Lough, C.H. Marrin, A. Maclees, R. MacCrindle, G. Maclnuis, E. Sverk, S. Tittlemier, G.T. Tomy, Chemosphere, 74, 1538, 2009.

[52] Y. Kawano, H. Tobita, H. Ogina, Organometallics, 11, 499, 1991.

[53] R. Katakura, Y. Koide, Inorg. Chem., 45, 5730, 2006.

[54] M. Muccini, M.A. Loi, K. Kenevey, R. Zamboni, N. Masciocchi, A. Sironi, Advanced Materials, 16, 861, 2004.

[55] M. Brinkmann, G. Gadret, M. Muccini, C. Taliani, N. Masciocchi, A. Sironi, J. Am. Chem. Soc., 122,5147, 2000.

2.7.3 Molecular Packing

Molecular packing in crystallography, is basically the arrangement of array of molecules in a unit cell. Since the unit cell is the smallest unit of volume, the observed properties in one unit cell becomes translational throughout the crystal.

There has been extensive research put out on the geometrical conformation of the $M(Ox)_3$ complex over the years and some achievements have been made.[55] The question of isomerism in this $M(Ox)_3$ entities have changed the landscape of the science of this molecular complexes. The discovery of the $Al(Ox)_3$ by Tang and Van Slyke was solely focused in obtaining high luminescence low-voltage driven devices.[55] However, it was not anticipated that the structural conformation of these complexes at this later stage, influenced by the orientation of ligands around the metal center, would highly influence the intensity and also the nature of emission thereof.

The recent focus has been on optimization of the OLED's devices optical characteristic, to improve the morphological stability, understanding of the charge transfer mechanism and the tuning of the OLED emission spectrum.[56,57,58] However, there are few systematic investigations of the correlation existing in between the molecular packing (see **Figure 2.8.1.2**) and the optical or electronic properties.

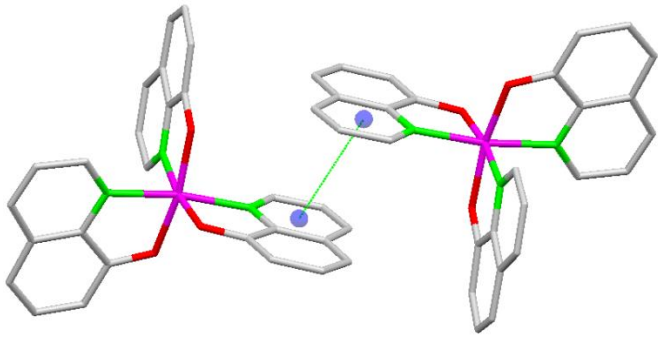

Figure 2.7.3.1: An outline of a π-π stacking between two neighbouring complexes.

[56] J. McElvain, H. Antoniadis, M.R. Hueeschen, J.N. Miller, D.M. Roitman, J.R. Sheats, R.L. Moon, J. Appl. Phys., 80, 6002, 1996.

[57] L.M. Do, E.M. Han, N. Yamomoto, M. Fujihira, Thin Solid Films, 273, 202, 1996.

[58] C.W. Tang, S.A. van Slyke, Chemi.

The molecules get arranged in such a way that the possible overlap of the π-orbitals between pairs of neighboring 8-hydroxyquinoline is minimized. Brinkmann *et al.*, demonstrated the influence of the orbital overlap on the optical properties and also the relative wavelength shifts observed in the photoluminescence spectra of different *fac*-$Al(Ox)_3$. It is further argued that there are rather strong reduced π-orbital overlap in *fac*-$Al(Ox)_3$ between neighboring complexes as compared in other phases. This indicates that the inter-molecular distance (particularly pi-staking) observed in the neighboring molecules is smaller for meridional isomers compared to facial isomers. Moreover, the density seem to impact the geometrical nature of these $M(Ox)_3$ in that the denser the packing, the more the red shift is observed.[55,59]

2.8 Organic light emitting diodes (OLEDs).

The field of organic opto-electronic devices has evolved over the years and have formed a tremendous field of research in both chemistry and physics. There has been an immense development towards this field of opto-electronic devices including organic resonant tunnels diodes[60,61], OLED's[62], organic photovoltaic[63], organic photo-transitions[64], organic photo-detector devices[65]. The idea of using organic material for lighting emitting diodes (OLED's) is fascinating owing to their attractive characteristics and relative ease of controlling their composition to tune their emission properties by chemical means.

[59] J. Kido, Y. Okamoto, Chem. Rev., 102(6), 2358, 2002.

[60] Y. Karzazi, J. Cornil, J. L. Bredas, J. Am. Chem. Soc., 123, 10076, 2001.

[61] Y. Karzazi, J. Cornil, J. L. Bredas, Nanotechnology, 14, 165, 2003.

[62] L. S. Hung, C. H. Chen, Mater. Sc. Eng., R 39, 143, 2002.

[63] G. Li, V. Shrotriya, J. S. Huang, Y. Yao, T. Moriarty, K. Emery, Y. Yang, Nature Mater., 4, 864, 2005.

[64] M. C. Hamilton, S. Martin, J. Kanicki, IEEE Trans. Electron Devices, 51, 877, 2004.

[65] P. Peumans, A. Yakimov, S. R. Forrest, J. Appl. Phys., 93, 3693, 2003.

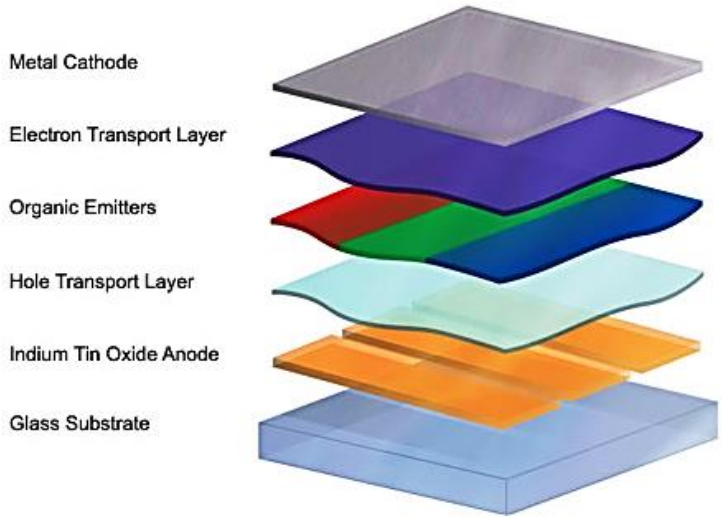

Figure 2.8.1: Organic Light Emitting Diode diagram.

The first organic electroluminescent (EL), discovered in 1963, was for instance based on anthracene single crystal in that an electric field was applied to it and it gave off blue electroluminescence; (Pope et al.,1963)[66] The known merits of OLEDs over other display technologies are: wider viewing angle, saturated emission color, high contrast, low cost, light weight, flexible, fast response time and the devices are normally flat and thin.[67]

An OLED is a solid-state semiconductor device with 100 to 500 nm thickness. This device consists of a conducting layer and an emissive layer, all together encrusted within two electrodes and deposited on a substrate. The conducting layer of the devise is made of organic plastic molecules that transport "holes" from the anode. The emissive layer is a film of organic compound that transport electrons from the cathode and emits light in response to an electric current. The conduction in organic layer is driven by delocalization of π electrons caused by conjugation over all or part of the organic molecule.[68]

[66] M. Pope, H.P. Kallmann, P. Maganate, J. Chem. Physics, 38, 2042, 1963.

[67] B. Geffroy, P. Le Roy, C. Prat, Polym. Int., 55, 572, 2006.

[68] Y. Karzazi, J. Mater. Environ. Sci. 5 (1), 1, 2014.

3 Synthesis of Metal Complexes

3.1 Introduction

This section describes the means by which the *tris*-coordinated N,O quinolinol coordination complexes were synthesized. The ligand 8-hydroxyquinoline was used as the parent ligand in addition to two derivatives. The *tris*-coordination of the ligand to the trivalent metal gives a neutral complex of the type $M(N^{\frown}O)_3$.

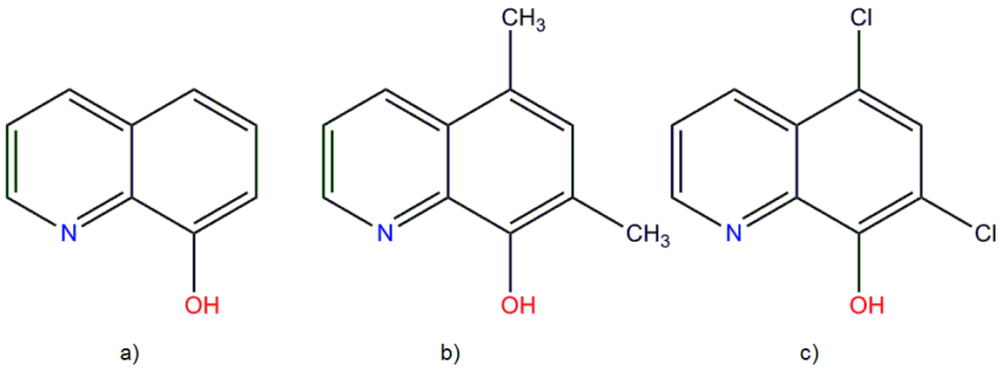

Figure 3.1.1: The schematic representation of the ligands used in this study.

The above ligands in **Figure 3.1.1**, are **a**) 8-hydroxyquinoline, **b**) 5,7-dimethyl-8-hydroxyquinoline and **c**) 5,7-dichloro-8-hydroxyquinoline. These ligands were coordinated to the metals: aluminium (Al), gallium (Ga) and indium (In) to form neutral homoleptic luminescent complexes.

Despite the fluorescent chemistry of these species; all the above shown ligands in **Figure 3.1.1** have the ability to give off luminescence in solution which is thought to assist if not influence the luminescent nature of the $M(Ox)_3$ complexes.

These $M(Ox)_3$ complexes are often found in two characteristic isomeric formations depending on the orientation of ligands around the metal center, namely, meridional (*mer*-) and facial (*fac*-) isomers as shown in **Figure 3.1.2.**

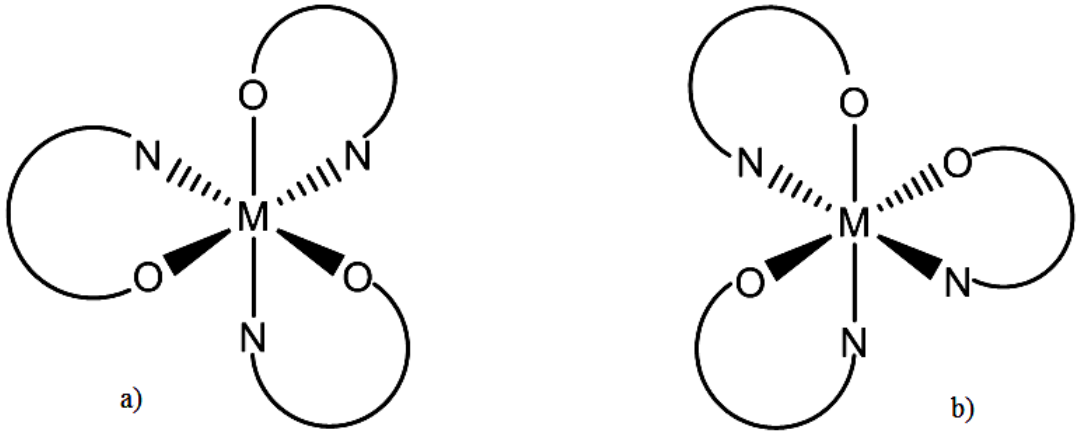

Figure 3.1.2: Schematic representation of a) facial isomer and b) meridional isomer.

The isomeric formation is often detected in octahedral complexes whereby six atoms are coordinated to the trivalent metal centers.[1] It is known that in solution state, *mer*-isomers is preferred above *fac*-isomers.[2] However, *fac*-isomeric derivatives are preferred in OLED's devises for its blue shifted fluorescence and reasonably high quantum yield.[3]

All of the aluminium, gallium and indium complexes synthesized were characterised using various techniques, including nuclear magnetic resonance (NMR), ultraviolet-visible (UV-Vis) spectroscopy and fluorescence spectroscopy. Single crystal X-ray diffraction (XRD) was used for characterisation of suitable crystalline material obtained. A detailed discussion of the complexes analysed by the X-ray diffraction is described in Chapter 4 and 5.

[1] J. E. Huheey, *Inorganic Chemistry*: Principles of structure and reactivity, Harper and Row, New York, 3rd edition, 489, 1983.

[2] R. Katakura, Y. Koide, Inorg. Chem., 45, 5730, 2006.

[3] M. Colle, J. Gmeiner, W. Milius, H. Hillebrecht, W. Brutting, Adv. Func. Matter, 13, 108, 2003.

3.2 Chemicals and Apparatus

All the reagents used for the synthesis and the characterization were of analytical grade. Unless otherwise stated, all commercially available reagents where used as received without further purification from Sigma-Aldrich, South Africa. All the ligands have been purchased unless otherwise stated.

All NMR data were obtained on a Bruker AXS 600 MHz (operating at 600.28 MHz for ^{1}H and 150.96 MHz for ^{13}C respectively) or Bruker AXS 300 MHz (operating at 300.13 MHz for ^{1}H and 75.48 MHz for ^{13}C nuclear magnetic resonance spectrometer using the mentioned deuterated solvent. Chemical shifts, δ, are reported in ppm with ^{1}H spectra calibrated relative to the residual $CHCl_3$ (7.24 ppm) and CH_2Cl_2 (5.32 ppm) peaks. ^{13}C spectra were calibrated relative to the residual CH_2Cl_2 (53.84 ppm) and $CHCl_3$ (77.16 ppm) peaks. Coupling constants, *J*, are reported in Hertz.

3.3 General synthetic method for $M(Ox)_3$ complexes.

The general synthetic method consists of the preparation of three solutions. Solution A was prepared by the addition of 8-hydroxyquinoline powder into absolute ethanol at 30-40 ˚C with full stirring until it dissolved completely. Solution B by dissolving metal salt [$M(NO_3)_3$ xH_2O] into distilled water. Solution C was prepared by dissolving NaOH in distilled water. Solution B was added to solution A with full stirring in a drop wise manner until all precipitates dissolved completely. As soon as the reactants are added, a sudden colour change from colourless to bright yellow appeared. The acidic mixture (pH 3) of the solution was adjusted by adding 2 M NaOH solution drop wise until pH 7-10. The precipitates were filtered using vacuum suction and washed several times with distilled water and ethanol (unless otherwise specified). The product was dried in a vacuum oven for over night and the yield recorded. Percentage yields were all calculated relative to the limiting reagents.

3.3.1 Synthesis of *mer*-[*tris*-(8-hydroxyquinoline) aluminium (III)]·EtOH

8-Hydroxyquinoline (0.3484 g, 2.4 mmol) was dissolved in 15 ml of absolute ethanol until the solute has dissolved completely. The ligand solution was then reacted with $Al(NO_3)_3 \cdot 9H_2O$ (0.30 g, 0.80 mmol) which was initially dissolved in 20 ml of distilled water. Upon addition of the metal solution, the reaction mixture precipitated. After addition, a solution of 2 M NaOH was used to adjust pH. The **Yield**: 0.2304 g, 57 %. The molar extinction coefficient from UV/Vis spectroscopy could not be obtained due to the solubility related problems.

UV-Vis (nm; L mol^{-1} cm^{-1}): λ_{max} = 342.6, $\varepsilon = 8 \times 10^4$.

^{1}H NMR (600 MHz, $CDCl_3$) δ 8.87 (dd, *J* = 4.7, 1.3 Hz, 1H), 8.83 (dd, *J* = 4.7, 1.1 Hz, 1H), 8.31 (dd, *J* = 8.3, 1.2 Hz, 1H), 8.25 – 8.20 (m, 2H), 7.52 (q, *J* = 8.0 Hz, 3H), 7.47 – 7.42 (m, 1H), 7.36 (dd, *J* = 11.4, 5.7 Hz, 1H), 7.24 (d, *J* = 3.7 Hz, 1H), 7.18 (dd, *J* = 8.3, 4.8 Hz, 1H), 7.15 – 7.06 (m, 6H).

^{13}C NMR (600 MHz, $CDCl_3$) δ 158.9, 158.8, 158.5, 144.8, 144.5 – 144.5, 142.3, 140.1, 139.6, 139.4, 139.4, 139.3, 139.3, 131.3, 130.9, 130.8, 129.7, 129.5, 129.3, 121.7, 121.6, 121.0, 113.5, 112.8, 112.4, 112.0, 111.8, 111.7.

3.3.2 Synthesis of *mer*-[*tris*- (5,7-dimethyl-8-hydroxyquinoline) aluminium (III)]

5,7-Dimethyl-8-hydroxyquinoline (0.2758g, 1.6 mmol) was dissolved in 15 ml of absolute ethanol until the solute has dissolved completely. The ligand solution was then reacted with $Al(NO_3)_3 \cdot 9H_2O$ (0.20g, 0.53 mmol) which was initially dissolved in 20 ml of distilled water. Upon addition of the metal solution, the reaction mixture precipitated. After addition, a solution of 2 M NaOH was used to adjust pH. The **Yield**: 0.1734 g, 60 %.

UV-Vis (nm; L mol^{-1} cm^{-1}): λ_{max} = 413.2, $\varepsilon = 2 \times 10^4$.

^{1}H NMR (600 MHz, $CDCl_3$) δ 8.78 (dd, *J* = 4.5, 1.2 Hz, 1H), 8.68 (dd, *J* = 4.7, 1.2 Hz, 1H), 8.33 (dd, *J* = 8.6, 1.3 Hz, 1H), 8.30 – 8.27 (m, 1H), 8.26 (dd, *J* = 3.8, 1.4 Hz, 1H), 7.37 (dd, *J* = 8.6, 4.7 Hz, 1H), 7.31 (dd, *J* = 8.6, 4.6 Hz, 1H), 7.24 (s, 1H), 7.22 (s, 2H), 7.14 – 7.10 (m, 2H), 2.52 – 2.46 (m, 9H), 2.39 – 2.33 (m, 9H).

^{13}C NMR (600 MHz, $CDCl_3$) δ 147.4, 144.5, 144.2, 142.0 – 141.9, 139.8 – 139.7, 139.0, 138.8, 136.4, 136.1 – 136.0, 136.0 – 135.8, 133.7, 133.5, 133.0, 130.8, 130.7, 126.9, 126.6, 26.6 – 126.4, 125.8, 123.7, 121.4, 121.3, 120.7, 120.5, 120.2, 120.1, 119.4.

3.3.3 Synthesis of [*tris*- (5,7-dichloro-8-hydroxyquinoline) aluminium (III)]

5,7-Dichloro-8-hydroxyquinoline (0.3202 g, 1.51 mmol) was dissolved in 15 ml of absolute ethanol until the solute has dissolved completely. The ligand solution was then reacted with $Al(NO_3)_3 \cdot 9H_2O$ (0.1913 g, 0.51 mmol) which was initially dissolved in 20 ml of distilled water. Upon addition of the metal solution, the reaction mixture precipitated. After addition, a solution of 2 M NaOH was used to adjust pH. The **Yield**: 0.1936 g, 57 %. The carbon NMR spectrum could not be obtained due to the concentration and solubility problem.

UV-Vis (nm; L mol^{-1} cm^{-1}): λ_{max} = 421.02.

^{1}H NMR (600 MHz, $CDCl_3$) δ 8.86 (dd, 3H), 8.51 (dd, *J* = 8.6 Hz, 3H), 7.61 (s, 3H), 7.58 (dd, 3H).

3.3.4 Synthesis of *fac*-[*tris*-(8-hydroxyquinoline) gallium (III)]·0.5·EtOH

8-Hydroxyquinoline (0.5182 g, 3.57 mmol) was dissolved in 15 ml of absolute ethanol until the solute has dissolved completely. The ligand solution was then reacted with $Ga(NO_3)_3 \cdot H_2O$ (0.3043 g, 1.19 mmol) which was initially dissolved in 20 ml of distilled water. Upon addition of the metal solution, the reaction mixture precipitated. After addition, a solution of 2 M NaOH was used to adjust pH. The **Yield**: 0.3626 g, 56 %.

UV-Vis (nm; L mol^{-1} cm^{-1}): λ_{max} = 378.6, ε = 1.11 ˣ 10^4.

^{1}H NMR (300 MHz, $CDCl_3$) δ: 8.88 (dd, 1H), 8.27 (dd, J = 23.0, 8.0 Hz, 2H), 7.50 (dd, J = 18.3, 10.2 Hz, 2H), 7.41 (t, J = 12.9 Hz, 1H), 7.15 (t, J = 7.1 Hz, 2H), 7.07 (dd, J = 8.2 Hz, 2H).

^{13}C NMR (600 MHz, CD_2Cl_2) δ: 139.7, 130.6, 121.5, 112.6, 112.2, 111.5, 53.8, 53.6, 53.4, 53.2, 53.0, 20.0.

3.3.5 Synthesis of *mer*-[*tris*-(5,7-dimethyl-8-hydroxyquinoline) gallium (III)]·DCM

5,7-Dimethyl-8-hydroxyquinoline (0.711 g, 4.11 mmol) was dissolved in 15 ml of absolute ethanol until the solute has dissolved completely. The ligand solution was then reacted with $Ga(NO_3)_3 \cdot H_2O$ (0.35 g, 1.37 mmol) which was initially dissolved in 20 ml of distilled water. Upon addition of the metal solution, the reaction mixture precipitated. After addition, a solution of 2 M NaOH was used to adjust pH. The **Yield:** 0.51 g, 55.5%

UV-Vis (nm; L mol^{-1} cm^{-1}): λ_{max} = 408.1, $\varepsilon = 8.8 \times 10^3$.

^{1}H NMR (600 MHz, $CDCl_3$) δ: 8.85 (d, *J* = 3.8 Hz, 1H), 8.74 (d, *J* = 3.9 Hz, 1H), 8.35 (d, *J* = 8.5 Hz, 1H), 8.33 (d, *J* = 8.2 Hz, 1H), 8.29 (d, *J* = 9.0 Hz, 1H), 7.38 (dd, *J* = 8.5, 4.7 Hz, 1H), 7.36 – 7.33 (m, 1H), 7.33 – 7.30 (m, 1H), 7.17 (dd, *J* = 8.1, 4.4 Hz, 1H), 2.52 (s, 3H), 2.49 (d, *J* = 2.7 Hz, 6H), 2.40 (s, 3H), 2.39 (d, *J* = 2.4 Hz, 6H).

^{13}C NMR (600 MHz, $CDCl_3$) δ: 156.8, 154.8, 154.1, 151.5, 147.7, 145.3, 144.0, 143.9, 142.9, 141.7, 141.6, 137.0, 136.6, 136.5, 136.4, 133.6, 133.6, 133.4, 133.1, 127.2, 127.1, 126.8, 121.8, 121.6, 121.1, 120.06, 119.9, 119.3, 117.4, 17.7, 17.6, 17.5, 17.0, 16.9, 16.8.

3.3.6 Synthesis of [*tris*-(5,7-dichloro-8-hydroxyquinoline) gallium (III)]

5,7-Dichloro-8-hydroxyquinoline (0.3763 g, 1.76 mmol) was dissolved in 15 ml of absolute ethanol until the solute has dissolved completely. The ligand solution was then reacted with $Ga(NO_3)_3 \cdot H_2O$ (0.15 g, 0.5867 mmol) which was initially dissolved in 20 ml of distilled water. Upon addition of the metal solution, the reaction mixture precipitated. After addition, a solution of 2 M NaOH was used to adjust pH. The **Yield**: 0.3287g, 79 %.

UV-Vis (nm; L mol^{-1} cm^{-1}): λ_{max} = 414.256.

^{1}H NMR (600 MHz, CDCl3) δ 8.86 (dd, J = 3.0 Hz, 1H), 8.52 (dd, J = 8.5 Hz, 1H), 7.61 (s, 1H), 7.58 (t, 1H), 2.17 (s, 9H).

^{13}C NMR (600 MHz, $CDCl_3$) δ: 149.3, 147.6, 138.7, 133.6, 128.3, 125.1, 122.5, 120.8, 115.4.

3.3.7 Synthesis of fac-[*tris*- (8-hydroxyquinoline) indium (III)]·$2H_2O$

8-Hydroxyquinoline (0.4632g, 3.19 mmol) was dissolved in 15 ml of absolute ethanol until the solute has dissolved completely. The ligand solution was then reacted with $In(NO_3)_3 \cdot 6H_2O$ (0.32 g, 1.06 mmol) which was initially dissolved in 20 ml of distilled water. Upon addition of the metal solution, the reaction mixture precipitated. After addition, a solution of 2 M NaOH was used to adjust pH. The **Yield**: 0.6325 g, 68 %.

UV-Vis (nm; L mol^{-1} cm^{-1}): λ_{max} = 381.5, $\varepsilon = 5.72 \times 10^3$.

^{1}H NMR (600 MHz, $CDCl_3$) δ: 8.57 (dd, *J* = 3.9 Hz, 1H), 8.30 (dd, *J* = 8.3, 1.3 Hz, 1H), 7.51 (dd, *J* = 8.0 Hz, 1H), 7.42 (dd, *J* = 8.3, 4.6 Hz, 1H), 7.28 (s, 1H), 7.19 (dd, 1H), 7.06 (dd, *J* = 7.8 Hz, 1H).

^{13}C NMR (600 MHz, $CDCl_3$) δ: 207.0, 159.2, 145.1, 140.4, 138.3, 130.9, 130.1, 121.1, 114.7, 112.0.

3.3.8 Synthesis of [*tris*- (5,7-dimethyl-8-hydroxyquinoline) indium (III]

5,7-Dimethyl-8-hydroxyquinoline (0.2517 g, 1.45 mmol) was dissolved in 15 ml of absolute ethanol until the solute has dissolved completely. The ligand solution was then reacted with $In(NO_3)_3 \cdot 6H_2O$ (0.1509 g, 0.50 mmol) which was initially dissolved in 20 ml of distilled water. Upon addition of the metal solution, the reaction mixture precipitated. After addition, a solution of 2 M NaOH was used to adjust pH. The **Yield**: 0.1942 g, 62 %. The molar extinction coefficient from UV/Vis spectroscopy, could not be obtained due to the solubility related problems

^{1}H NMR (600 MHz, $CDCl_3$) δ: 8.53 (dd, 1H), 8.36 (dd, *J* = 8.1 Hz, 1H), 7.35 (dd, 1H), 7.27 (s, 1H), 7.26 (s, 2H), 2.51 (s, 3H), 2.44 (s, 3H).

^{13}C NMR (600 MHz, $CDCl_3$) δ: 155.0, 144.4, 137.9, 136.7, 133.2, 127.2, 123.1, 119.3, 116.8.

3.3.9 Synthesis of [*tris*- (5,7-dichloro-8-hydroxyquinoline) indium (III)]

5,7-Dichloro-8-hydroxyquinoline (0.3312 g, 1.55 mmol) was dissolved in 15 ml of absolute ethanol until the solute has dissolved completely. The ligand solution was then reacted with $In(NO_3)_3 \cdot 6H_2O$ (0.1516 g, 0.50 mmol) which was initially dissolved in 20 ml of distilled water. Upon addition of the metal solution, the reaction mixture precipitated. After addition, solution of 2 M NaOH was used to adjust pH. The **Yield**: 0.2258 g, 60 %. The molar extinction coefficient from UV/Vis spectroscopy could not be obtained due to the solubility related problems.

^{1}H NMR (600 MHz, $CDCl_3$) δ: 8.85 (dd, 1H), 8.68 (dd, *J* = 8.6 Hz, 5H), 8.63 (dd, *J* = 4.1 Hz, 4H), 8.51 (dd, *J* = 8.9 Hz, 1H), 7.70 (s, 4H), 7.59 (dd, *J* = 8.4, 4.6 Hz, 6H).

^{13}C NMR (600 MHz, $CDCl_3$) δ: 154.1, 149.3, 146.7, 138.3, 138.2, 133.8, 130.9, 128.3, 126.5, 122.5, 121.9, 119.3, 114.1.

3.4 Synthesis of Lanthanide Complexes.

The synthesis of the lanthanide-quinolato complexes was aimed at having four homoleptic quinolate derivatives coordinated to the europium metal ion. The intent was well within reason due the the lanthanide contraction ability. The lanthanides have been active in the field of luminescence in many ways not to mention their involvement in medicinal chemistry.[4]

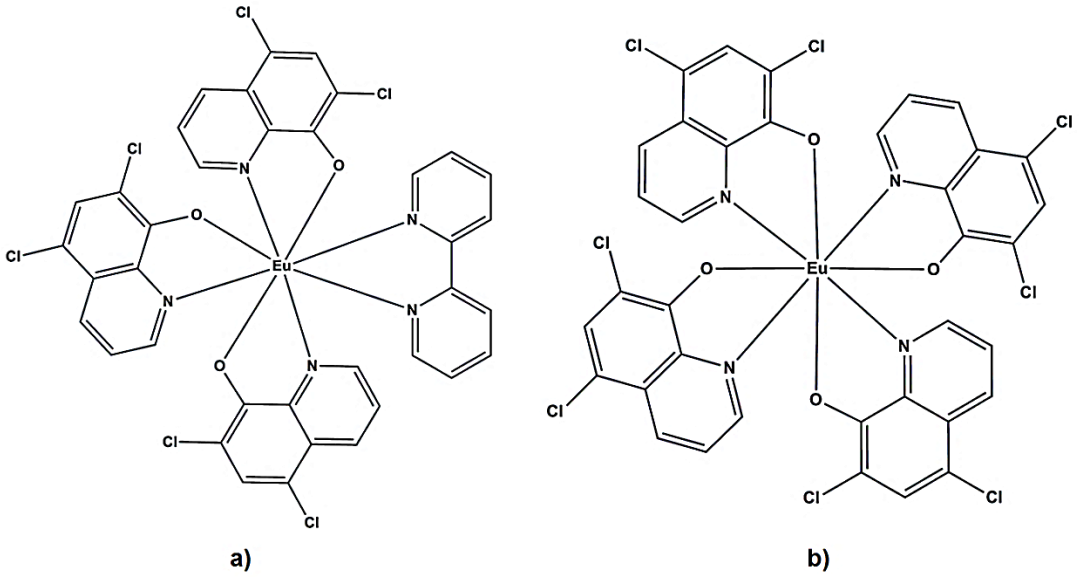

Figure 3.4.1: The schematic representation of the desired lanthanide complexes.

The complex obtained from the attempted synthesis of tetrakis-complex observed in **Figure 3.4.1. (a)**, was used as the starting material to obtain the complex **b)** observed in **Figure 3.4.1** but instead, the dimeric complex given in **Figure 3.4.2.2** was obtained. However, that did not stop science to take place in the space of the respective lanthanide complexes obtained hence reported in this manuscript as follows.

[4] J. Kido, Y. Okamoto, Chem. Rev., 102, 2357, 2002.

3.4.1 Synthesis method for lanthanide complexes.

3.4.1.1 Synthesis of [*tris*-(5,7-dichloro-8-hydroxyquinoline)$(H_2O)_2$Eu(III)] ·EtOH·H_2O

5,7-dichloro-8-hydroxyquinoline (0.7070 g, 3.33 mmol) in 15ml of absolute ethanol is reacted with $EuCl_3 \cdot 6H_2O$ (0.3078 g, 0.84 mmol) in 20ml of distilled water. NaOH (0.266 g, 6.5 mmol) in 10 ml of distilled water is later added. The suitable orange cubic crystals were obtained from ethanol solvent after one week. **Yield**: 0.4747 g, 68%. **UV-Vis** (nm; L mol^{-1} cm^{-1}): $\lambda_{max} = 408$, $\varepsilon = 5 \times 10^3$.

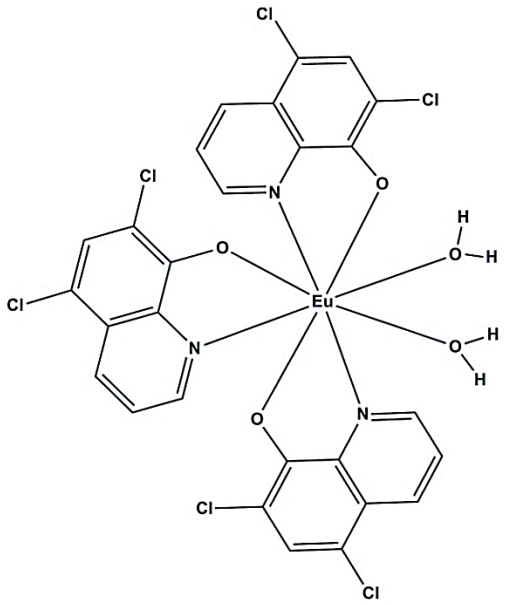

Figure 3.4.1.1: The schematic representation of the obtained lanthanide complex; namely: [*tris*-(5,7-dichloro-8-hydroxyquinoline)$(H_2O)_2$Eu(III)].

3.4.1.2 Synthesis of

κ^2-O,O'-*bis*-[*tris*-(5,7-dichloro-8hydroxyquinoline)(CH_3OH)Europium(III)]

[(5,7-dichloro-8-hydroxyquinoline)$(H_2O)_2$Eu(III)] (1 mg, 1.21 mmol) in 20ml of toluene was reacted with 2,2'-Bipyridine (1.9 mg, 1.2e-2 mmol) and the colour of the solution was yellow-orange during the reaction. The reaction was refluxed 120 ˚C using a Dean Stark setup to remove excess water.

The reaction was left to reflux for six hours with vigorous stirring. The reaction gradually turned to orange in colour. The reaction solution was filtered and layered with the methanol solution on top of the toluene solvent and then left for crystallization. Yellow-orange crystals suitable for x-ray diffraction were obtained within three days. **Yield**: 1.272 g, 64 %. The molar extinction coefficient could not be obtained due to the solubility related problems.

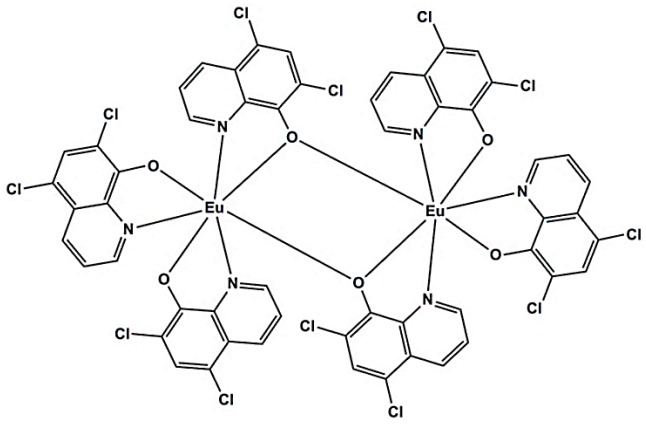

Figure 3.4.2.2: The schematic representation of the obtained lanthanide complex; namely: κ^2-O,O'-*bis*-[*tris*-(5,7-dichloro-8-hydroxyquinoline)(Methanol)Europium(III)]

3.5 Crystallized Complexes

Single crystals, suitable for x-ray diffraction were obtained for the following complexes:

3.5.1. *mer*-[*tris*-(8-hydroxyquinoline) Aluminium (III)] Ethanol Solvate
- $Al(Ox)_3$

3.5.2. *mer*-[*tris*-(8-hydroxyquinoline) Gallium (III)] Ethanol:
- $Ga(Ox)_3$

3.5.3. *mer*-[*tris*-(8-hydroxyquinoline) Indium (III)] Di-aqua:
- $In(Ox)_3$

3.5.4. *mer*-[*tris*-(5,7-dimethyl-8-hydroxyquinoline) Gallium(III)] Dichloromethane
- $Ga(57dmOx)_3$

3.5.5. [*tris*-(5,7-dichloro-8-hydroxyquinoline)(di-aqua) Europeum (III)] •Ethanol Water

3.5.6. κ^2-O,O'-*bis*-[*tris*-(5,7-dichloro-8-hydroxyquinoline)(Methanol)Europium(III)].

3.6 Results and Discussions

All the synthesized complexes were obtained as a yellowish or yellow-orange like powders. All obtained complexes were fluorescent as will be described in (chapter 6). The perplexing issue with these metal-quinolate complexes is mainly the geometrical conformation they normally resort to, which gets dictated by the orientation of the ligand around the metal center. These ligands are chelated to the trivalent metal center to form octahedral $M(N^{\frown}O)_3$ entities. As discussed in Paragraph **3.1**, two isomers are possible namely: (i) meridional (*mer*-) and (ii) facial (*fac*-). Since these complexes can be potential electroluminescent layers in the fabrication of the organic light emitting diodes, this observed isomerism is key to the subject in a way that it serves as an antenna towards the emission efficiency in the devices.[5,6] It is therefore a good opportunity to examine the coordination nature of these complexes and to what extend one can track down significant differences between their chemistry with group 13 (Al, Ga and In) metal ions. Part of this chapter gives us the opportunity to look into the NMR studies of these complexes.

3.6.1 8-Hydroxyquinoline complexes with Al, Ga and In metals

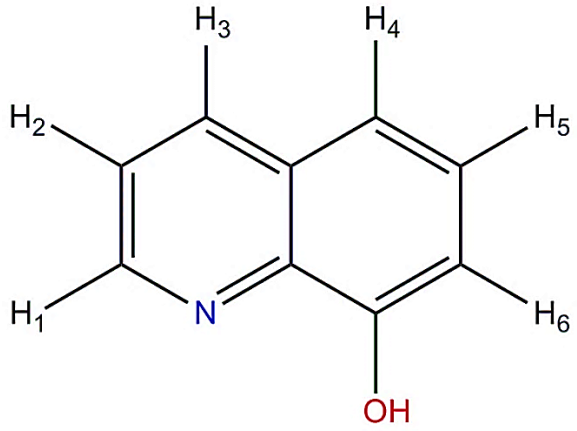

Figure 3.6.1.1: Schematic representation of 8-hydroxyquinoline with hydrogen labelings.

[5] M. Brinkmann, G. Gadret, M. Muccini, C. Taliani, N. Masciocchi, A. Sironi, J. Am. Chem. Soc., 122, 5147, 2000.

[6] M. Colle, R. E. Dinnebier, W. Brutting, Chem. Commun., 2908, 2002.

Each 8-hydroxyquinoline ligand has 6 H-atoms, all in chemically different environments. If one adds to that, the fact that three of these ligands are chelated to the metal ion, it is to be expected that NMR data could be complicated, especially considering the fact that two isomers are possible in solution. However, when one considers that the respective H-atoms in a *fac*-isomer all have similar chemical environments (i.e. H_1 in the first ligand has the same chemical environment as H_1 in the second ligand etc.) the spectra become less complicated, due to their only being one environment.

The respective H-atoms in *mer*-isomers do not experience similar environments, therefore leading to complicated spectra, difficult to attribute to specific signals, while the spectra for *fac*-isomers are less complicated. Another complication is the fact that the *fac*- and *mer*-isomer could be in conversional equilibrium in solution, also complicating the spectra.

The following paragraph discuss the spectra of $Al(Ox)_3$, $Ga(Ox)_3$ and $In(Ox)_3$. The respective ^1H and ^{13}C spectra are illustrated in **Figure 3.6.1.1** and **Figure 3.6.1.2**.

A. $Al(Ox)_3$

^1H NMR data indicates that a *mer*-isomer is mainly found in solution. This is supported by the ^{13}C NMR spectra where resonance peaks corresponding to more than 12 chemical environments are observed, This could possibly indicate that there is a thermal inter-conversion reaction between *mer*- and *fac*-isomers in solution which was not detected on ^1H NMR.

B. $Ga(Ox)_3$

^1H NMR data indicates that a *fac*-isomer is found in solution since 6 distinguishable chemical environments are found, however this is once again not supported by the ^{13}C NMR, possibly indicating the inter-conversion in the solution.

C. $In(Ox)_3$

Both 1H NMR and ^{13}C NMR spectra indicates the existence of only the *fac*-isomer in solution.

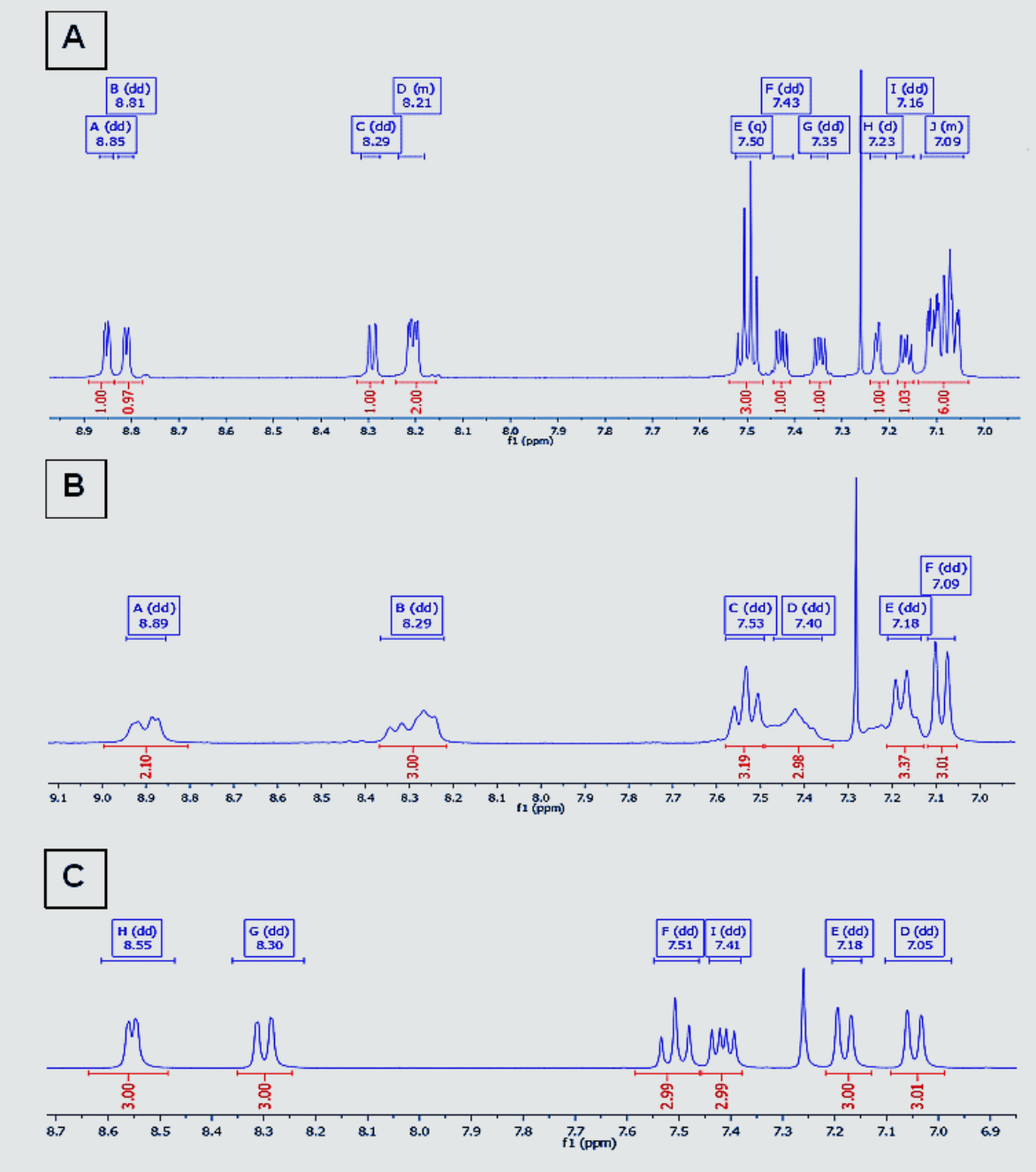

Figure 3.6.1.1: ^{1}H-NMR representations of different metal complexes (Al, Ga and In) with the same oxine ligand. Spectrum: A = *tris*-(8-hydroxyquinoline) aluminium (III), B = *tris*-(8-hydroxyquinoline) gallium (III) and C = *tris*-(8-hydroxyquinoline) indium (III). The spectrums were obtained in deuterated chloroform at 20˚C. The focus of all the spectrums is in the region of interest (aromatic region).

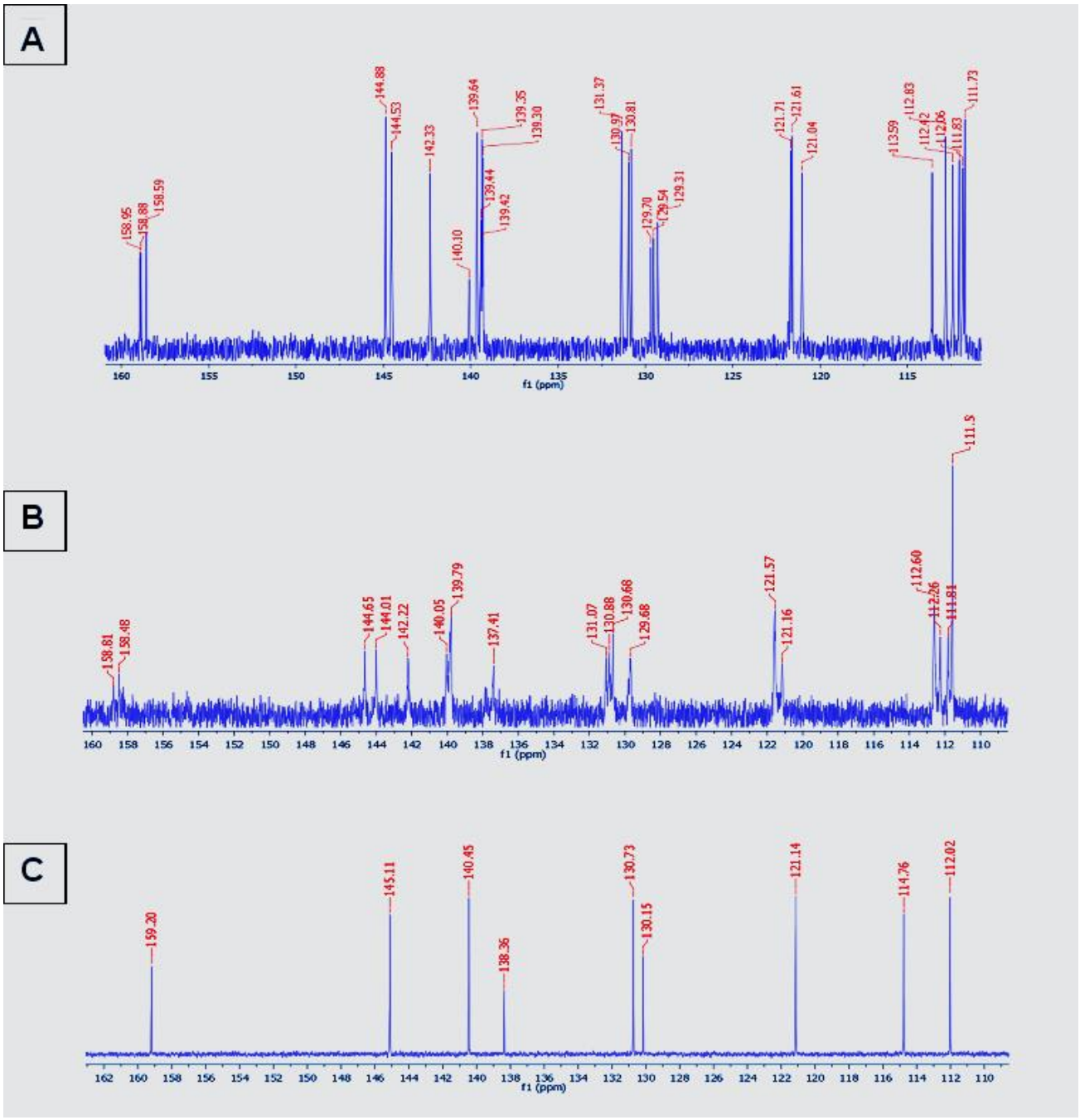

Figure 3.6.1.2: ^{13}C-NMR representations of different metal complexes (Al, Ga and In) with the same oxine ligand. Spectrum: A = *tris*-(8-hydroxyquinoline) aluminium (III), B = *tris*-(8-hydroxyquinoline) gallium (III) and C = *tris*-(8-hydroxyquinoline) indium (III). The spectrums were obtained in deuterated chloroform at 20˚C.

3.6.2 5,7-Dimethyl-8-Hydroxyquinoline

Each 5,7-dimethyl-8-hydroxyquinoline ligand has 4 H-atoms in the aromatic region, all in chemically different environments. The *fac*-isomer should give less complicated spectra than *mer*-spectra in that only four resonance environments must be seen in the aromatic region for four protons and more than four if *mer*-isomer. ^{13}C NMR spectra should give 9 resonance peaks accounting for all the ligands coordinated, however, if more than 9 peaks are observed, the *mer*-isomer is considered.

A. Al(57dmOx)$_3$

^{1}H NMR data indicates that a *mer*-isomer is found in solution. This is supported by the ^{13}C NMR spectra where resonance peaks corresponding to more than 9 chemical environments are observed, This could possibly indicate that there is an inter-conversion reaction between *mer*- and *fac*-isomers in solution which was not detected on ^{1}H NMR.

B. Ga(57dmOx)$_3$

^{1}H NMR data indicates that a *mer*-isomer is found in solution since 12 distinguishable chemical environments are found and also in correspondence with ^{13}C NMR. There are six chemical environments resonating upfield of the protons in the substituted methyl's correlating with the observed six carbon peaks.

C. In(57dmOx)$_3$

Both 1H NMR and ^{13}C NMR spectra indicates the existence of only the *fac*-isomer in solution.

The following paragraph discuss the spectra of Al(57dmOx)$_3$, Ga(57dmOx)$_3$ and In(57dmOx)$_3$. The respective ^{1}H and ^{13}C spectra are illustrated in **Figure 3.6.2.1** and **Figure 3.6.2.2**.

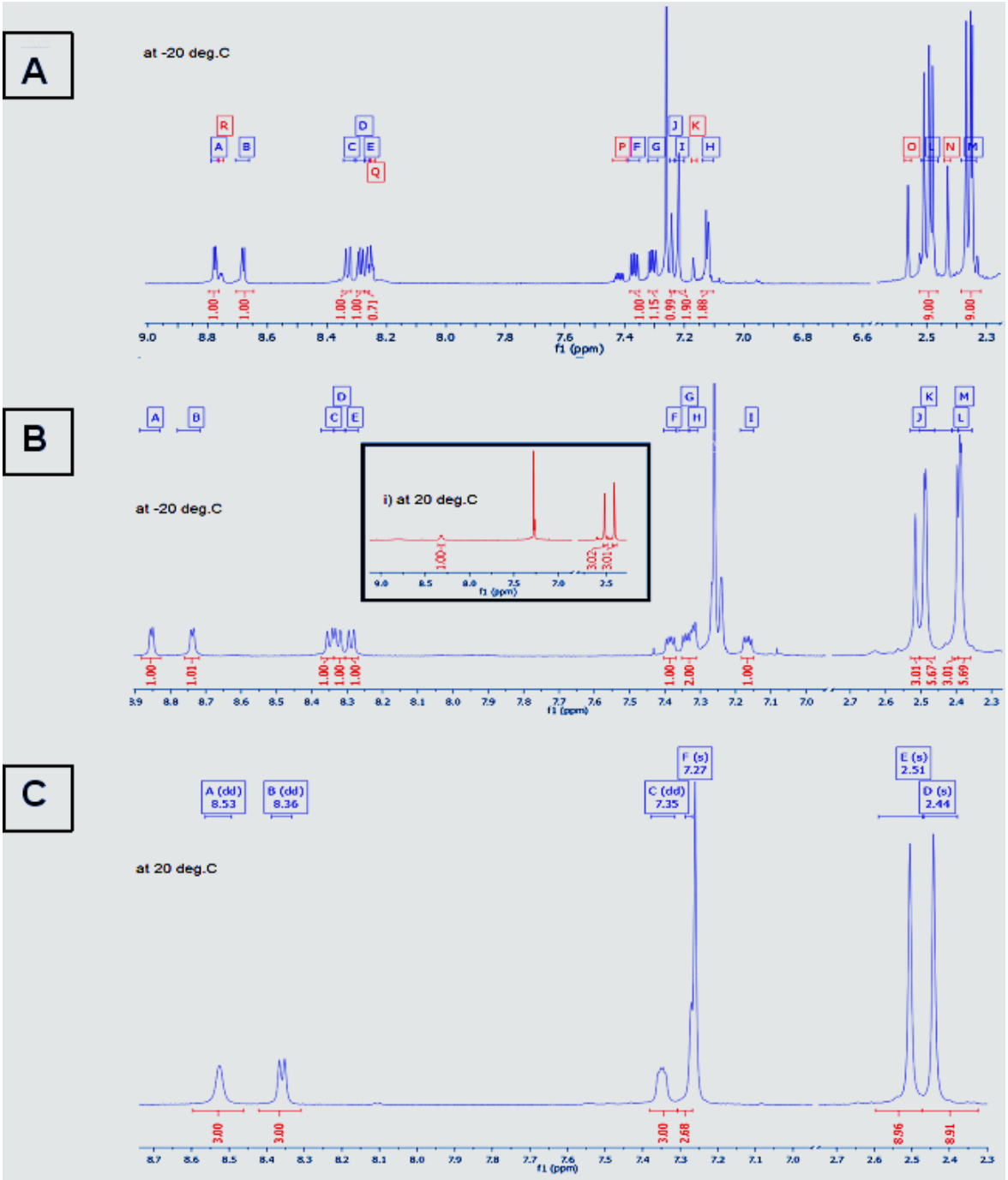

Figure 3.6.2.1: ^{1}H-NMR representations of different metal complexes (Al, Ga and In) with the same 5,7-dimethyl-8-hydroxyquinoline ligand. Spectrum: A = *tris*-(5,7-dimethyl-8-hydroxyquinoline) aluminium (III), B = *tris*-(5,7-dimethyl-8-hydroxyquinoline) gallium (III) and C = *tris*-(5,7-dimethyl-8-hydroxyquinoline) indium (III). The spectrums were obtained in deuterated chloroform. Spectrum: A and B were obtained at -20˚C and C at 20˚C. The focus of all the spectrums is in the region of interest (aromatic region).

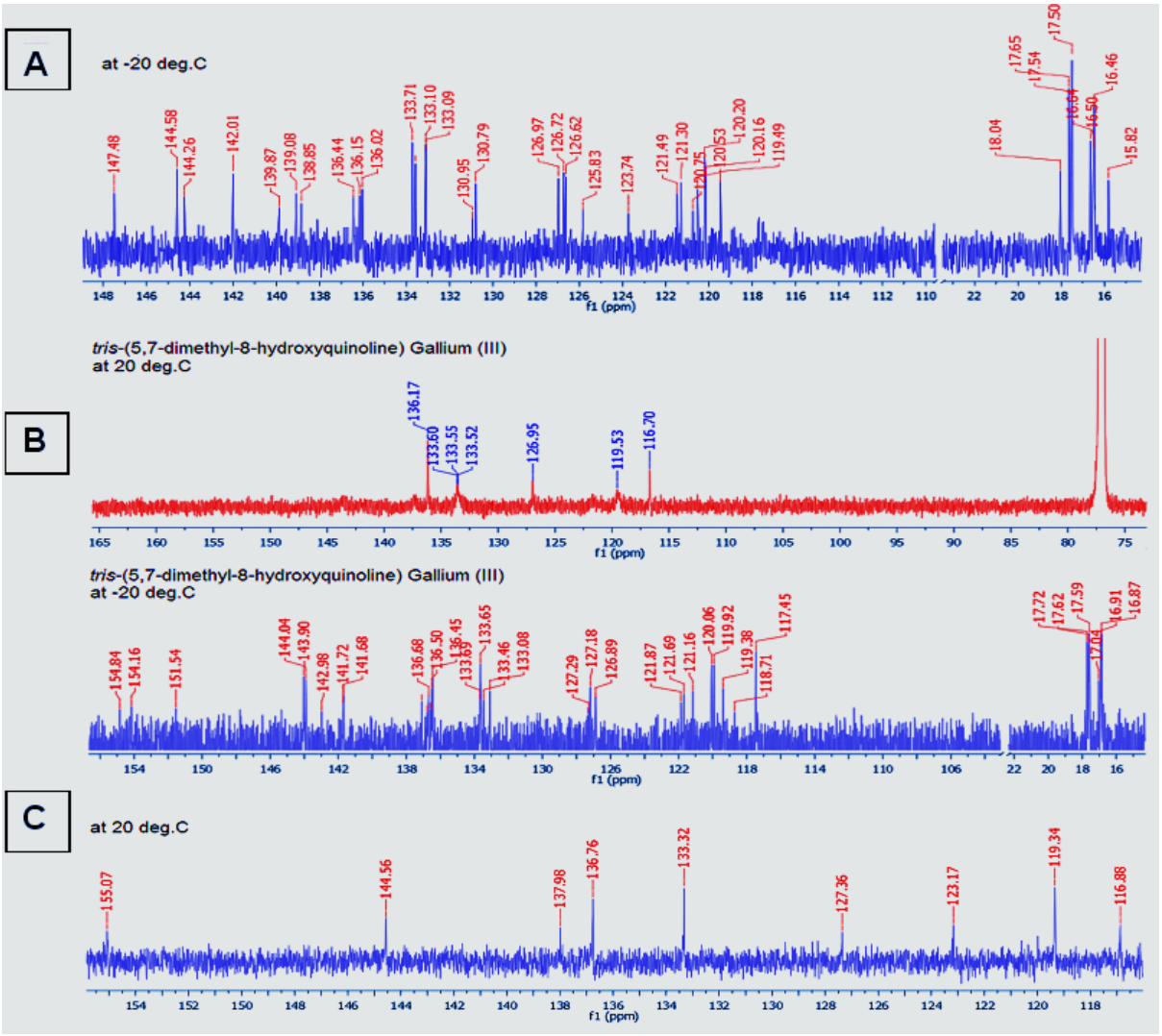

Figure 3.6.2.2: ^{13}C-NMR representations of different metal complexes (Al, Ga and In) with the same 5,7-dimethyl-oxine ligand. Spectrum: A = *tris*-(5,7-dimethyl-8-hydroxyquinoline) Aluminium (III), B = *tris*-(5,7-dimethyl-8-hydroxyquinoline) Gallium (III) and C = *tris*-(5,7-dimethyl-8-hydroxyquinoline) Indium (III). The spectrums were obtained in deuterated chloroform. Spectrum: A and B were obtained at -20˚C and C at 20˚C. The focus of all the spectrums is in the region of interest (aromatic region).

3.6.3 5,7-Dichloro-8-Hydroxyquinoline

Each 5,7-dichloro-8-hydroxyquinoline ligand has 4 H-atoms in the aromatic region, all in chemically different environment. The *fac*-isomer should give less complicated spectra than *mer*-spectra in that only four resonance environments must be seen in the aromatic region and more than four if *mer*-isomer. ^{13}C NMR spectra should give 9 resonance peaks accounting for all three ligands coordinated, however, if the peak are more than 9 then a *mer*-isomer is considered.

A. Al(57dcOx)$_3$

^{1}H NMR data indicates that a *mer*-isomer is found in solution. This is supported by the ^{13}C NMR spectra where resonance peaks corresponding to more than 9 chemical environments are observed, This could possibly indicate that there is an inter-conversion reaction between *mer*- and *fac*-isomers in solution which was not detected on ^{1}H NMR.

B. Ga(57dcOx)$_3$

^{1}H NMR data indicates that a *mer*-isomer is found in solution since 12 distinguishable chemical environments are found and also in correspondence with ^{13}C NMR. There are six chemical environments resonating upfield of the protons in the substituted methyl's correlating with the observed six carbon peaks.

C. In(57dcOx)$_3$

Both 1H NMR and ^{13}C NMR spectra indicates the existence of only the *fac*-isomer in solution.

The following paragraph discuss the spectra of $Al(57dcOx)_3$, $Ga(57dcOx)_3$ and $In(57dcOx)_3$. The respective ^{1}H and ^{13}C spectra are illustrated in **Figure 3.6.3.1** and **Figure 3.6.3.2**.

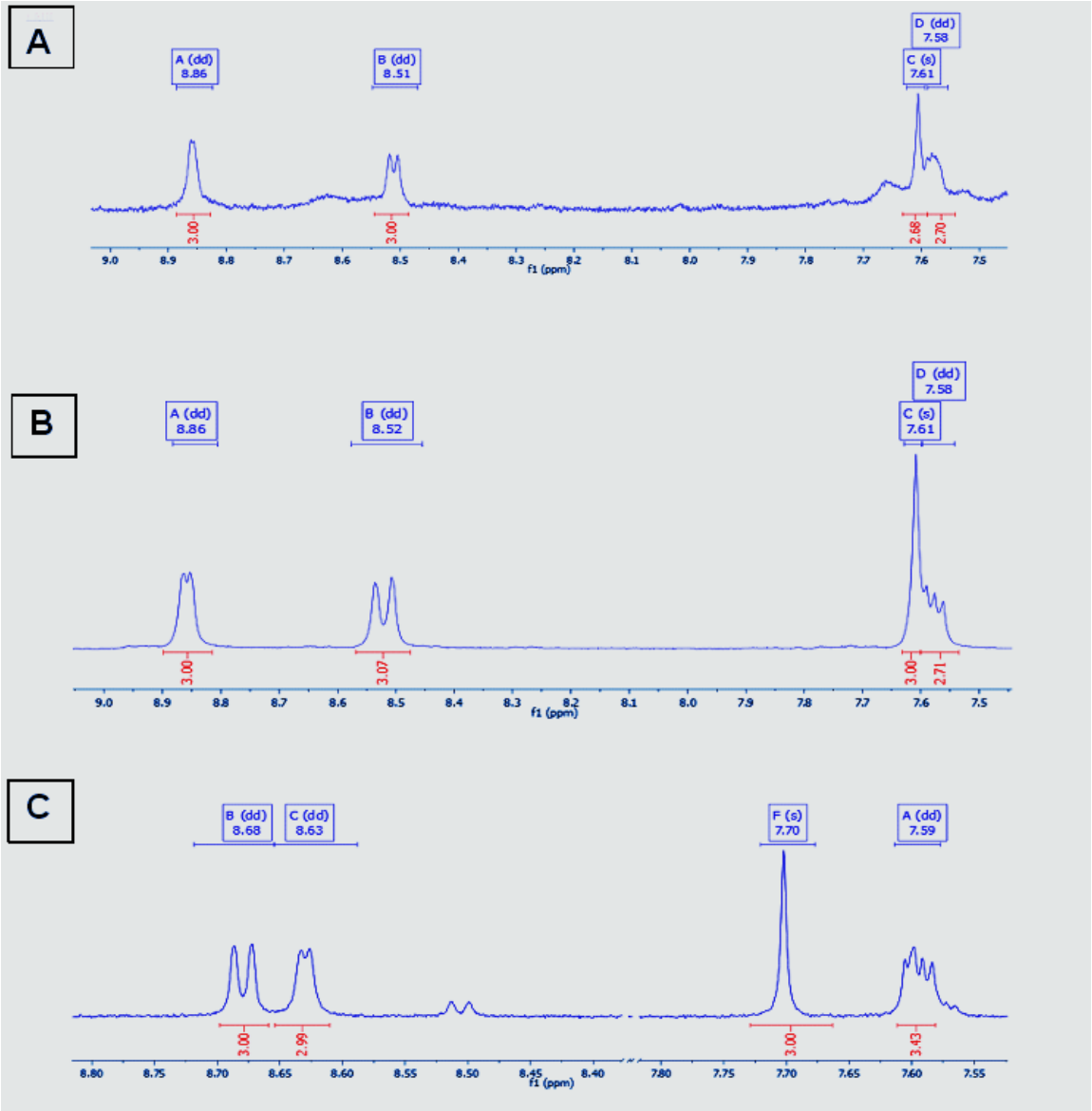

Figure 3.6.3.1: ^{1}H-NMR representations of different metal complexes (Al, Ga and In) with the same 5,7-dichloro-oxine ligand. Spectrum: A = *tris*-(5,7-dimethyl-8-hydroxyquinoline) Aluminium (III), B = *tris*-(5,7-dimethyl-8-hydroxyquinoline) Gallium (III) and C = *tris*-(5,7-dimethyl-8-hydroxyquinoline) Indium (III). The spectrums were obtained in deuterated chloroform at 20°C. The focus of all the spectrums is in the region of interest (aromatic region).

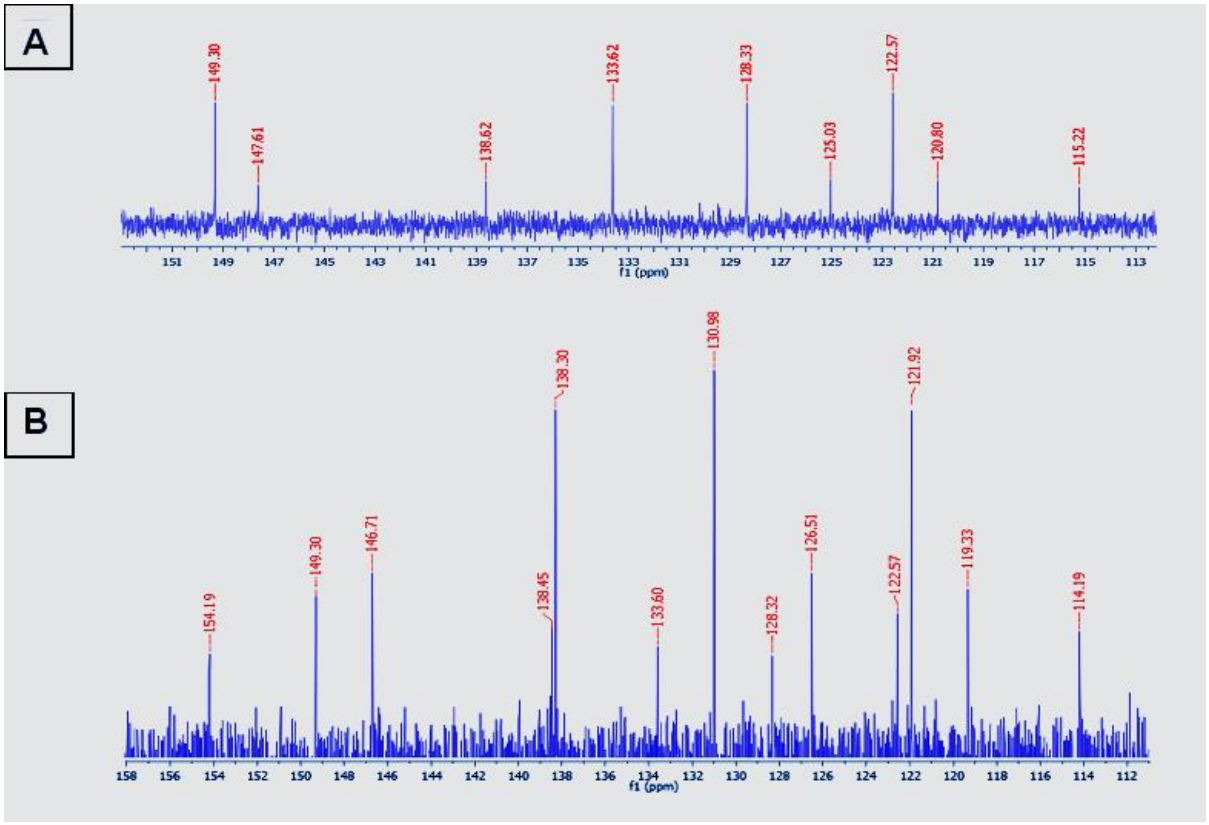

Figure 3.6.3.2: ^{13}C-NMR representations of different metal complexes (Al, Ga and In) with the same 5,7-dichloro-oxine ligand. Spectrum: A = *tris*-(5,7-dichloro-8-hydroxyquinoline) Gallium (III) and B = *tris*-(5,7-dichloro-8-hydroxyquinoline) Indium (III). The spectrums were obtained in deuterated chloroform at 20˚C. The focus of all the spectrums is in the region of interest (aromatic region).

3.7 Conclusions

All the ligand systems were successfully coordinated to the aluminium, gallium, indium and europium metal ions. The reactions were achieved without the need of inert environment. The synthesized complexes were obtained as a yellowish or yellow-orange like powder. The reactions were all performed on the bench. All obtained complexes were successfully fluorescent.

Table 3.7.1: Observed NMR results of group 13 metal complexes.

NMR Results of Group 13 metal complexes			
Metal	**Ox**	**57dmOx**	**57dcOx**
Al	*mer*	*mer*	*mer*
Ga	*fac*	*mer*	*mer*
In	*fac*	*fac*	*fac*

From **Table 3.7.1**, one can see that the Al and Ga complexes all form primarily *mer* complexes in solution, but strong evidence of inter-convertion reactions suggests that both *fac* and *mer* exists in solution. The indium complexes all form fac-isomers in solution. No evidence of inter-conversion reactions were found. [7,8,9]

The next chapter discusses the solid state properties of several of the complexes for which single crystal, suitable for X-ray diffraction studies were obtained.

Since the NMR studies of the europium complexes were not conducted due to its paramagnetic nature, the crystallography chapter is looked upon to exhibit the geometrical conformation of these lanthanide complexes in the solid state.

[7] R. Katakura, Y. Koide, *Inorg. Chem*., 45, 5730, 2006.

[8] M.H Wang, Y. Sawada, K. Saito, S. Horie, T. Uchida, M. Ohtsuka, S. Seki, S. Kobayashi, T. Arii, A. Kishi, T. Takahashi, Y. Nishimoto, T. Wakimoto, K. Monzen, I. Kashima, T. Nishikiori, L.X. Sun, R. Ozao, J. Therm. Anal. Calorim., 89, 2, 363, 2007.

[9] R. L. Martin, J.D. Kress, I.H. Campbell, D.L. Smith, *Phys. Rev. B*, 61, 15804, 2000.

4 X-RAY CRYSTALLOGRAPHIC STUDIES OF METAL-QUINOLATE COMPLEXES

4.1 Introduction

This chapter gives an insight to the coordination chemistry of three 8-hydroxyquinoline derivatives with the aluminium, gallium and indium trivalent metal centers.

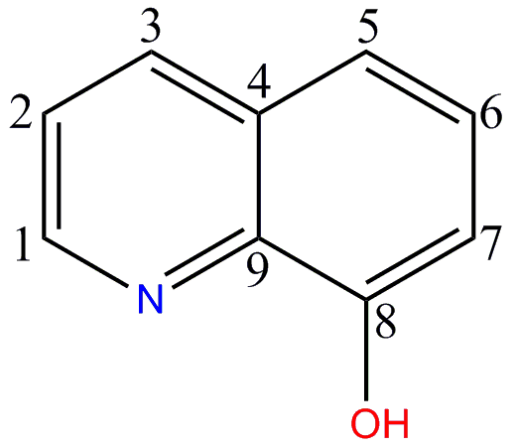

Figure 4.1.1: Schematic representation of 8-hydroxyquinoline.

The scheme given in **Figure 4.1.1**, is that of **8-hydroxyquinoline** (Oxine) which is the primary ligand used in this project. There are two other quinolinol derivatives used in this project namely; (i) 5,7-dimethyl-8-hydroxyquinoline and (ii) 5,7-dichloro-8-hydroxyquinoline. These functionalized quinolinol species, are substituted with the methyl and the chlorine atoms at the position five (5) and seven (7) as illustrated in **Figure 4.1.2**.

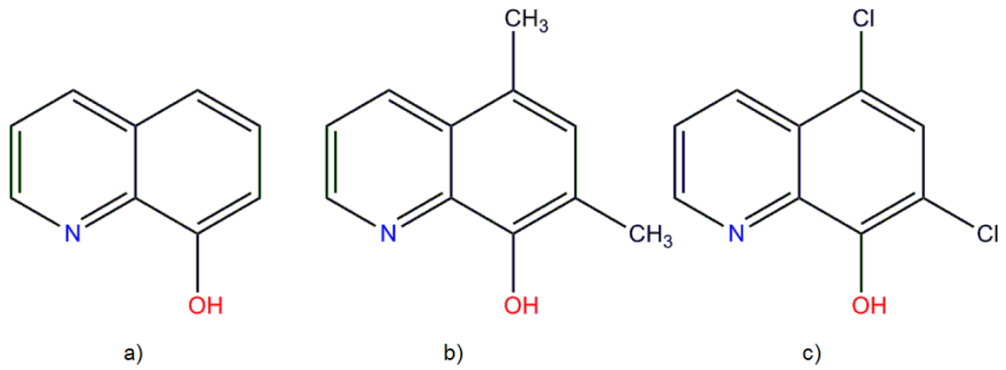

Figure 4.1.2: The schematic representation of functionalized and non-functionalized oxine derivatives. (a) 8-hydroxyquinoline, (b) 5,7-dimethyl-8-hydroxyquinoline and (c) 5,7-dichloro-8-hydroxyquinoline.

Quinolinol type ligands have wide applications in several fields of chemistry including the science of organic light emitting devices.[1] As mentioned earlier, the aim of this study is to investigate the coordination chemistry of these types of ligands to Al, Ga and In (group 13 metals) and to investigate the luminescence of the formed complexes.

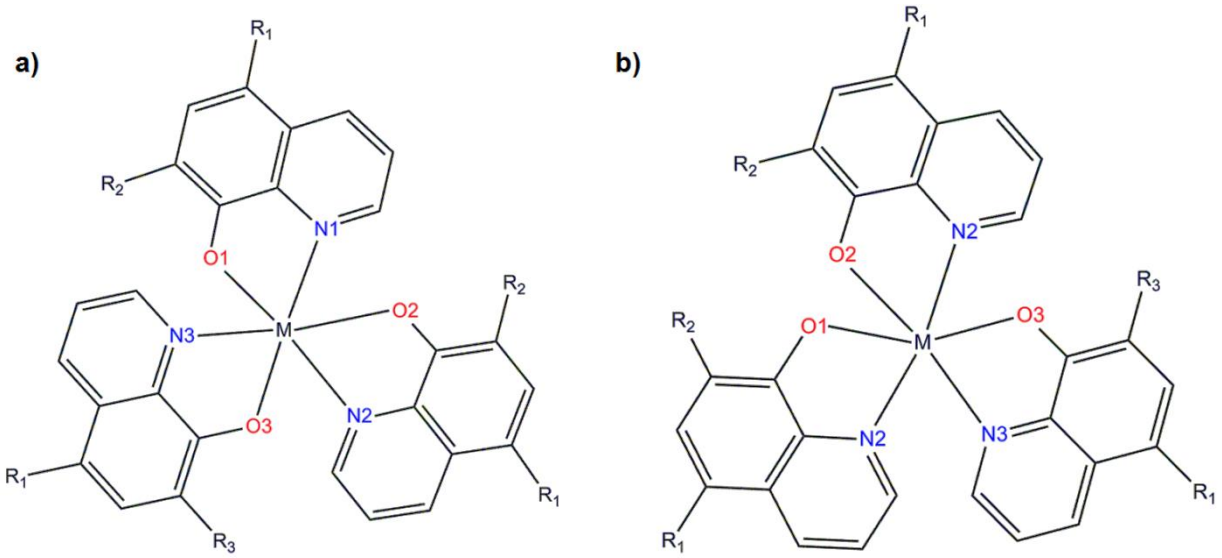

Figure 4.1.3: A typical schematic representation of a) facial and b) meridional $M(Ox)_3$ complexes.

[1] C.W. Tang, S.A. Van Slyke, Appl. Phys. Lett., 51, 913, 1987.

The two possible isomers, indicated in **Figure 4.1.3**, can form when quinolinol or its derivatives form tris complexes with a metal. It is further known that the *mer*-isomers are preferred over *fac*-isomers in solution.[2]

This chapter summarize the crystallographic data of complexes: *mer*-[$Al(Ox)_3$]·EtOH (**1**), *mer*-[$Ga(Ox)_3$]0.5·EtOH (**2**), *mer*-[$In(Ox_3)$]·$2H_2O$ (**4**), *mer*-[$Ga(57dmOx)_3$]·DCM (**3**).

The structural relationship will be compared to the solid state photoluminescence studies which will be discussed in chapter 6.

[2] M. Colle, J. Gmeiner, W. Milius, H. Hillebrecht, W. Brutting, Adv. Func. Matter, 13, 108, 2003.

4.2 Experimental

The intensity data were collected on a Bruker X8 Apex II 4K Kappa CCD diffractometer equipped with graphite monochromated Mo *K*α radiation, with a wavelength of 0.71073 Å; with both ω- and φ-scans at 100 K. All the cell refinements were performed with SAINT-Plus[3] and the data reduction was done with SAINT-Plus and XPREP. The software package SADABS[4] that utilizes the Sheldrick multi-scan technique were used to apply absorption correction. All the structures were solved with the use of the SIR-97[5] package, refinement was done with SHELXL- 97[6] and WinGX[7] and the molecular graphics were completed with DIAMOND[8] and MERCURY[9]. All the structures are shown with thermal ellipsoids drawn at a 50% probability level and all non-hydrogen atoms were anisotropically refined, unless otherwise stated. Methyl, methylene, methine and aromatic hydrogen atoms were placed in geometrically idealized positions, C-H = 0.95 to 1.00 Å, and they were constrained to ride on their parent atoms, $U_{iso}(H) = 1.5\ U_{eq}(C)$ and $1.2\ U_{eq}(C)$ respectively. The numbering on the quinoline rings, the first digit refers to the ring number while the second digit refers to the carbon atom in the ring.

All the atomic coordinates, anisotropic displacement parameters, bond distances, angles and hydrogen coordinates of all the crystals reported in this Chapter, are given in the supplementary data (Appendix A).

[3] Bruker, SAINT-Plus, Version 7.12 (including XPREP), Bruker AXS Inc., Madison, Wisconsin, USA, 2004.

[4] Bruker, SADABS, Version 2004/1, Bruker AXS Inc., Madison, Wisconsin, USA, 1998.

[5] A. Altomare, M.C. Burla, M. Camalli, G.L. Cascarano, C. Giacovazzo, A. Guagliardi, A.G.G. Moliterni, G. Polidori, R. Spagna, J. Appl. Cryst., 32, 837, 1999.

[6] G.M. Sheldrick, SHELXL97, Program for the refinement of crystal structures, University of Göttingen, Germany,1997.

[7] L.J. Farrugia, J. Appl. Cryst., 32, 837, 1999.

[8] K. Brandenburg, H. Putz, DIAMOND, Release 3.0c, Crystal Impact GbR, Bonn, Germany, 2008.

[9] I. Buno, J.A. Chisholm, P.R. Edgington, P. McCabe, E. Pidcock, L. Rodriguez-Monge, R. Taylor, J. van de Streek, P.A. Wood, J. Appl. Cryst, 41, 466, 2008.

4.3 X-ray Crystal Structures of $M(Ox)_3$ Complexes.

4.3.1 4.3.1. *mer*-[*tris*-(8-Hydroxyquinoline) aluminium (III)]·ethanol solvate (1)

The complex, *mer*-[$Al(Ox)_3$]·EtOH (**1**), was synthesized as described in **Paragraph 3.7.1** The asymmetric unit contains one full coordination compound plus an ethanol molecule. The complex crystallizes in a monoclinic crystal system in the $P2_1/c$ space group with four formula units per unit cell (Z = 4). The numbering scheme of the title complex is shown in **Figure 4.3.1.1**

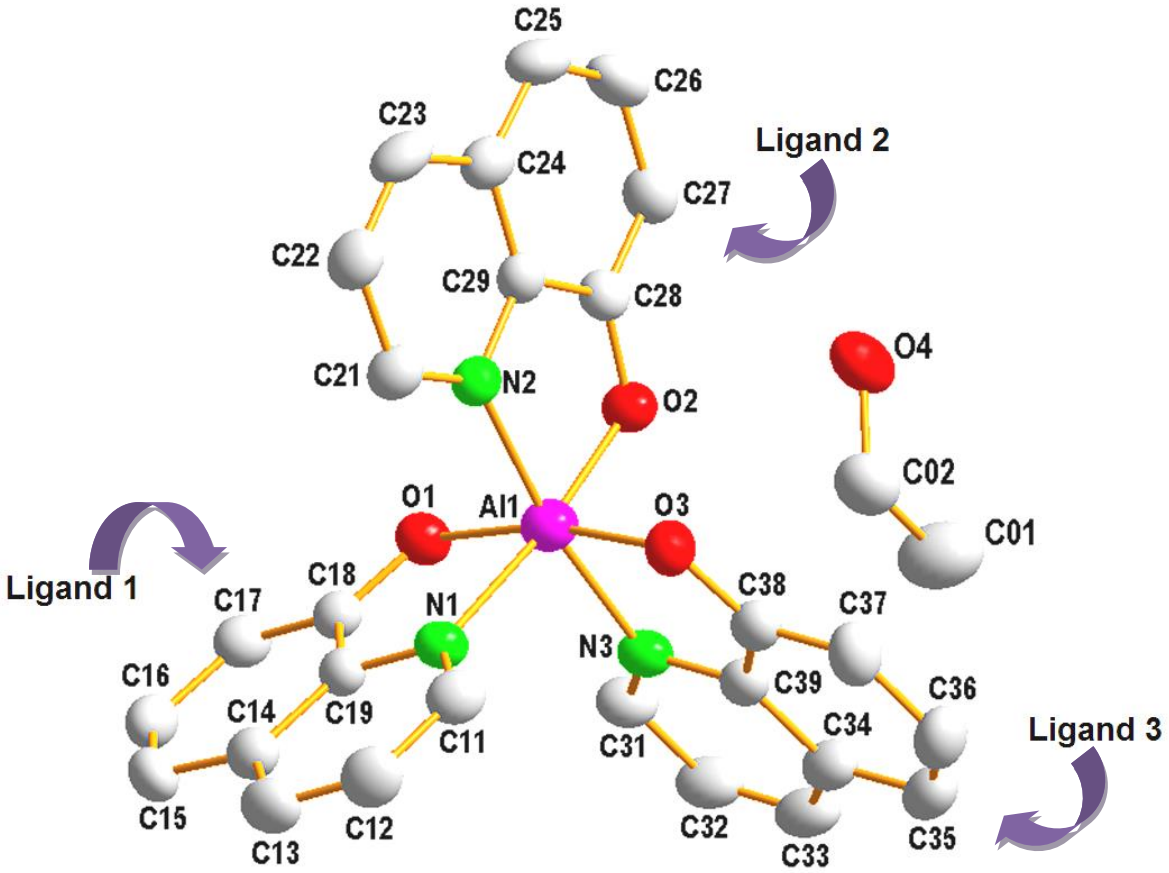

Figure 4.3.1.1: The representation of the molecular structure of *mer*-[$Al(Ox)_3$]·EtOH (1). Hydrogen atoms are omitted for clarity. Displacement ellipsoids are drawn at 50 % probability level.

Table 4.3.1.1: Crystal data and structure refinement for *mer*-[Al(Ox)$_3$]·EtOH (1).

Identification code	**Compound 1**	
Empirical formula	**$C_{29}H_{25}N_3O_4Al$**	
Formula weight	**506.50**	
Temperature	**100 K**	
Wavelength	**0.71073 Å**	
Crystal system	**Monoclinic**	
Space group	***P 2$_1$/c***	
Unit cell dimensions	**a = 11.136(5) Å**	**α= 90°**
	b = 13.188(5) Å	**β= 94.148(5)°**
	c = 16.637(5) Å	**γ = 90°**
Volume	**2436.9(16) Å^3**	
Z	**4**	
Density (calculated)	**1.381 g/cm^3**	
Absorption coefficient	**0.126 μ/mm^{-1}**	
F(000)	**1060**	
Crystal size	**0.661 × 0.492 × 0.275 mm^3**	
Theta range for data collection	**1.973 to 28.00°**	
Index ranges	**-14<=h<=14, -17<=k<=17, -21<=l<=21**	
Reflections collected	**70730**	
Independent reflections	**5875 [R_{int} = 0.0613, R_{sigma} = 0.0290]**	
Completeness	**99.7 %**	
Refinement method	**Full-matrix least-squares on F^2**	
Data / restraints / parameters	**5875/0/337**	
Goodness-of-fit on F^2	**1.579**	
Final R indices [I>2sigma(I)]	**R_1 = 0.1066, wR_2 = 0.3341**	
R indices (all data)	**R_1 = 0.1273, wR_2 = 0.3608**	
Largest diff. peak and hole	**3.86/-0.88 e.Å^{-3}**	

The geometrical conformation of **1** is distorted from octahedral geometry as illustrated in **Figure 4.3.1.2**.

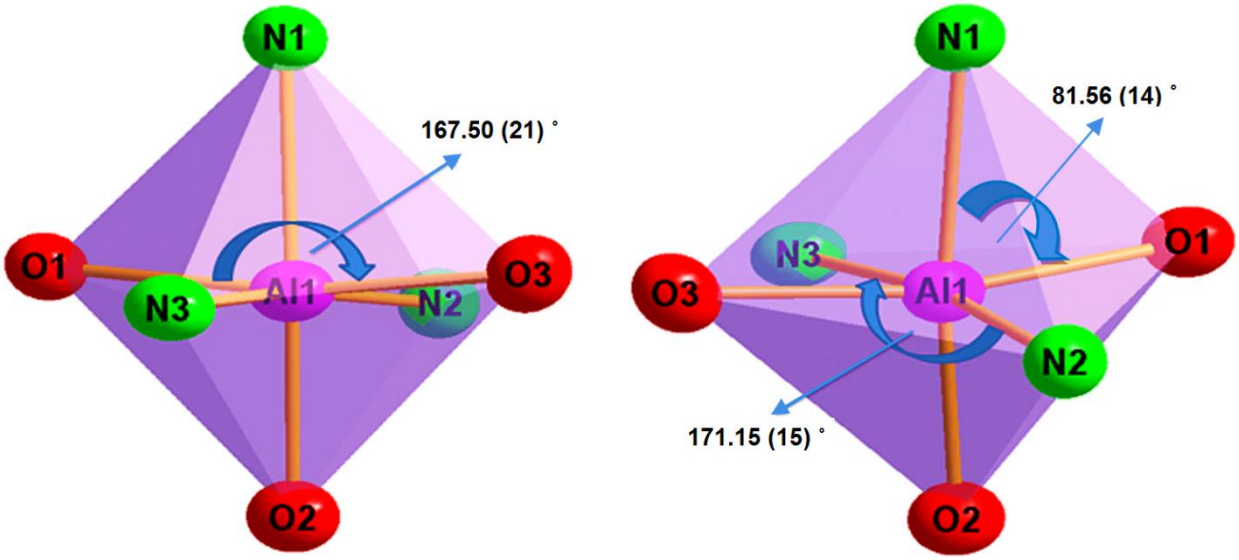

Figure 4.3.1.2: Illustration of an octahedral coordination polyhedron of 1.

The angles of O1-Al1-O3 and N2-Al1-N3 are 167.5 (21)˚ and 171.15 (15)˚ respectively as shown in **Figure 4.3.1.2**, illustrating the slight distortion mentioned. The respective Al-O and Al-N bond distance comparisons in each coordinated ligand are similar within experimental error and range from 1.860 (6) Å to 1.909 (8) Å for Al-O and 2.042 (6) Å to 2.083 (8) Å for Al-N bonds respectively, as illustrated in **Table 4.3.1.2**.

Table 4.3.1.2: Selected bond distances (Å) and selected angles (˚) of compound 1.

Selected bond distances		Selected bond angles	
Atom	**Distance (Å)**	**Atom**	**Angle (˚)**
Al1 - O1	1.889 (8)	O1 - Al1 - N1	81.56 (14)
Al1 - O2	1.860 (6)	O2 - Al1 - N2	83.49 (13)
Al1 - O3	1.909 (8)	O3 - Al1 - N3	82.51 (14)
Al1 - N1	2.083 (8)	O1 - Al - O3	167.45 (21)
Al1 - N2	2.066 (6)	N2 - Al - N3	171.14 (15)
Al1 - N3	2.042 (6)	N1 - Al - O2	173.18 (26)

The average bite angle of the ligand units of compound **1** for O-Al-N is 82.52 (14)˚ (**Table 4.3.1.2**) and all the bond distances are similar within experimental error.

All bond distances and angles are considered to be normal and fall within the range reported for similar complexes.[10,11]

The crystal structure is stabilized by C—H···O intra-molecular, O—H···O and C—H···O inter-molecular, π-π stacking and C—H···π interactions. These will be discussed in the following paragraph, see also **Table 4.3.1.3**.

The intra-molecular interaction is observed between a hydrogen atom of Ligand 1 and the neighbouring oxygen atom of Ligand 3 as illustrated in **Figure 4.3.1.3**.

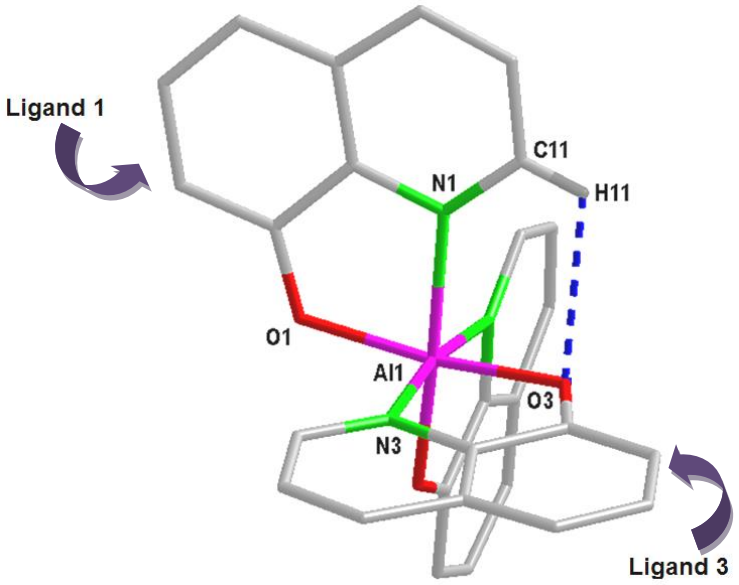

Figure 4.3.1.3: Intra-molecular hydrogen bond observed in 1. Hydrogen atoms, not taking part in the hydrogen bonding, are omitted for clarity. Hydrogen interactions are indicated by blue dotted lines.

[10] M. Ul-Haque, W. Horne, S.J. Lyle, J. of Crystallographic Research, 21 , 4, 1991.

[11] M. Brinkmann, G. Gadret, M. Muccini, C. Taliani, N. Masciocchi, A. Siron, J. Am. Chem. Soc., 122, 5147, 2000.

Table 4.3.1.3: Observed C—H···O and O—H···O hydrogen interactions in 1.

D—H···A		d (D—H) (Å)	d (H···A) (Å)	d (D···A) (Å)	D—H···A (°)
O4—H4···O3	**#0**	0.82	1.982 (3)	2.759 (5)	158
C11—H11···O3	**#0**	0.93	2.956 (3)	3.041 (5)	110
C15—H15···O1	**#1**	0.93	2.480 (3)	3.335 (5)	153
C23—H23···O1	**#2**	0.93	2.560 (3)	3.351 (5)	143

Symmetry transformations used to generate equivalent atoms:

[**#0** = x, y, z], [**#1** = 0.25-x, -0.5+y, 0.5-z], [**#2** = 2-x, -y, -z]

The C**—**H···O and O**—**H···O interactions are illustrated in **Figure 4.3.1.4** and also listed in **Table 4.3.1.3**.

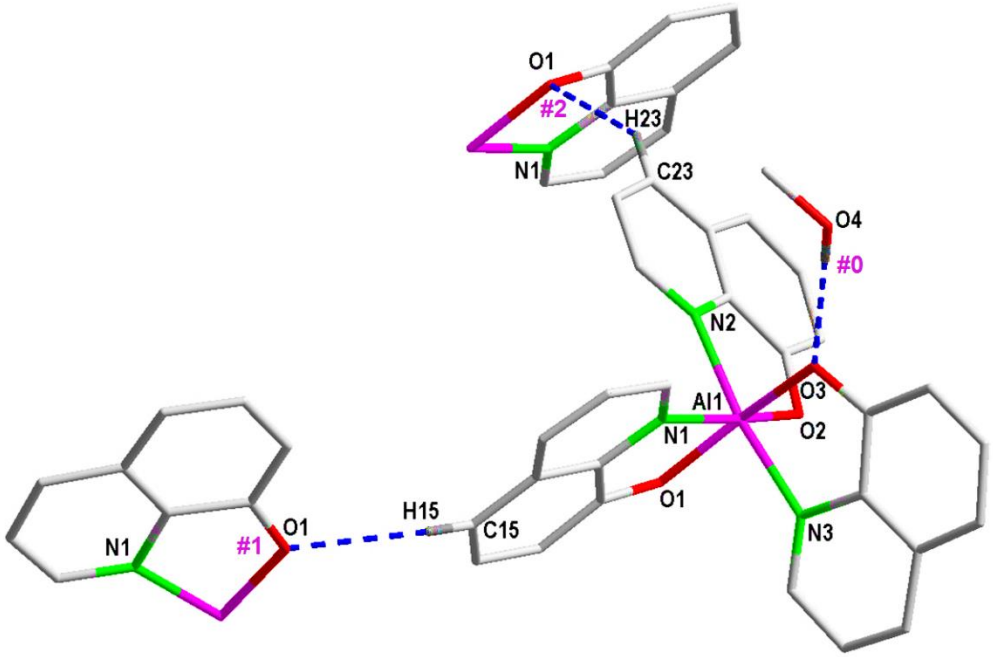

Figure 4.3.1.4: Inter-molecular hydrogen bonding observed in 1. Hydrogen atoms, not taking part in the hydrogen bonding, are omitted for clarity. Hydrogen interactions are indicated by blue dotted lines.

The intermolecular C—H···π and π-π stacking interactions further stabilize the crystal packing. These interactions are illustrated in **Figure 4.3.1.5** and **Figure 4.3.1.6.** The relevant data is given in **Tables 4.3.1.4** and **Table 4.3.1.5.**

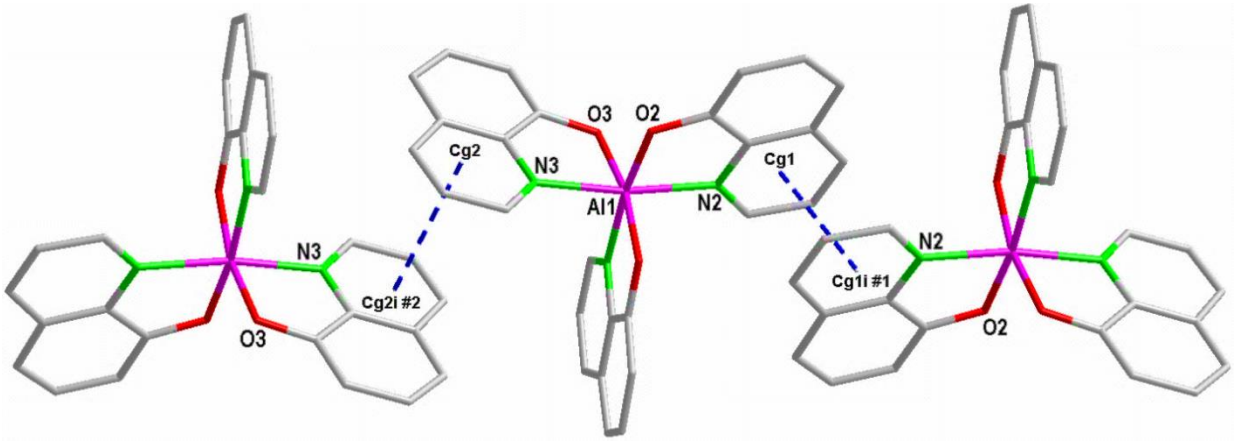

Figure 4.3.1.5: The schematic representation of the inter-molecular π-π stacking of 1. Hydrogen atoms have been omitted for clarity. Centroid atoms ending with 'i', resembles symmetry-generated molecules. The numbering of the nitrogen and oxygen denotes the number of the ligand coordinated.

The π-π stacking is observed between the neighbouring molecules with centroid-to-centroid distances of 3.536 (3) Å and 3.517 (4) Å respectively as indicated in **Table 4.3.1.4**. It is observed between pyridyl sides Ligand 2 and Ligand 3 of neighbouring molecules.

Table 4.3.1.4: Inter-molecular *π-π* Interactions of complex 1.

Centroid Atom	Centroid Atom	Distance between centroid atoms (Å)
Cg1	Cg1i **#1**	3.536(3)
Cg2	Cg2i **#2**	3.517(4)

Symmetry transformations used to generate equivalent atoms:
[**#1** = 1-x, -y, -z] and [**#2** = 2-x, -y,1-z]
Cg1 = Centroid atom of N2, C21, C22, C23, C24, C29.
Cg2 = Centroid atom of N3, C31, C32, C33, C34, C39.

The inter-molecular (C—H···π) interactions are illustrated in **Figure 4.3.1.6**. and listed in **Table 4.3.1.5**. These includes interactions between neighbouring $Al(Ox)_3$ molecules as well as influence from the solvent species.

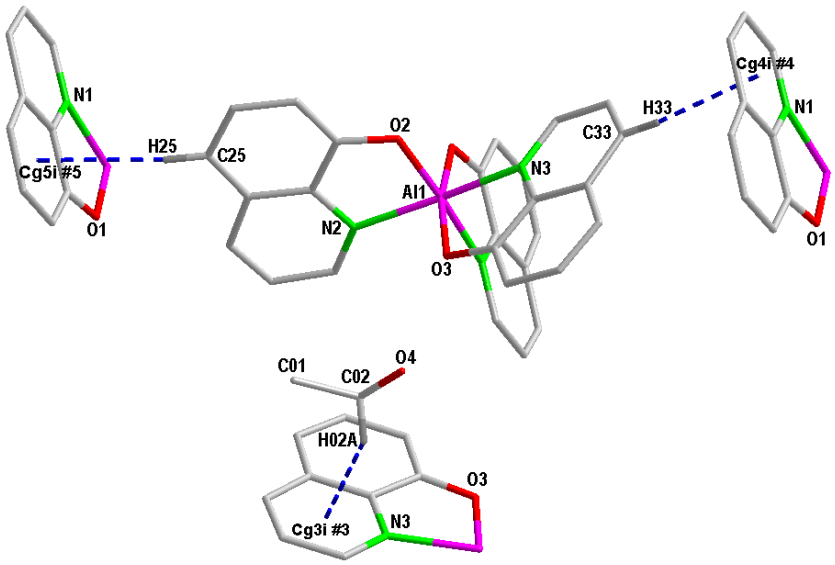

Figure 4.3.1.6: The geometrical representation of the C-H···π inter-molecular interactions in 1. Hydrogen atoms have been omitted for clarity. The numbering of the nitrogen and oxygen denotes the number of the ligand coordinated in the complex.

Table 4.3.1.5 C—H···π Interactions observed in 1.

C-H	Centroid Atom	d (H···Cg) (Å)	d (C···Cg) (Å)	C-H···Cg (°)
C02-H02	Cg3i **#3**	2.98	3.690 (8)	121
C25-H25	Cg5i **#5**	2.92	3.507 (6)	156
C33-H33	Cg4i **#4**	2.60	3.509 (6)	167

Symmetry transformations used to generate equivalent atoms:
[**#3** = 0.25-x, -0.5+y, 0.5-z], [**#4** = 2-x, -y,-z] and [**#5** = 2-x, -y, -z],
Cg3 = Centroid atom of N3, C31, C32, C33, C34, C39.
Cg4 = Centroid atom of N1, C11, C12, C13, C14, C19.
Cg5 = Centroid atom of C14, C15, C16, C17, C18, C19.

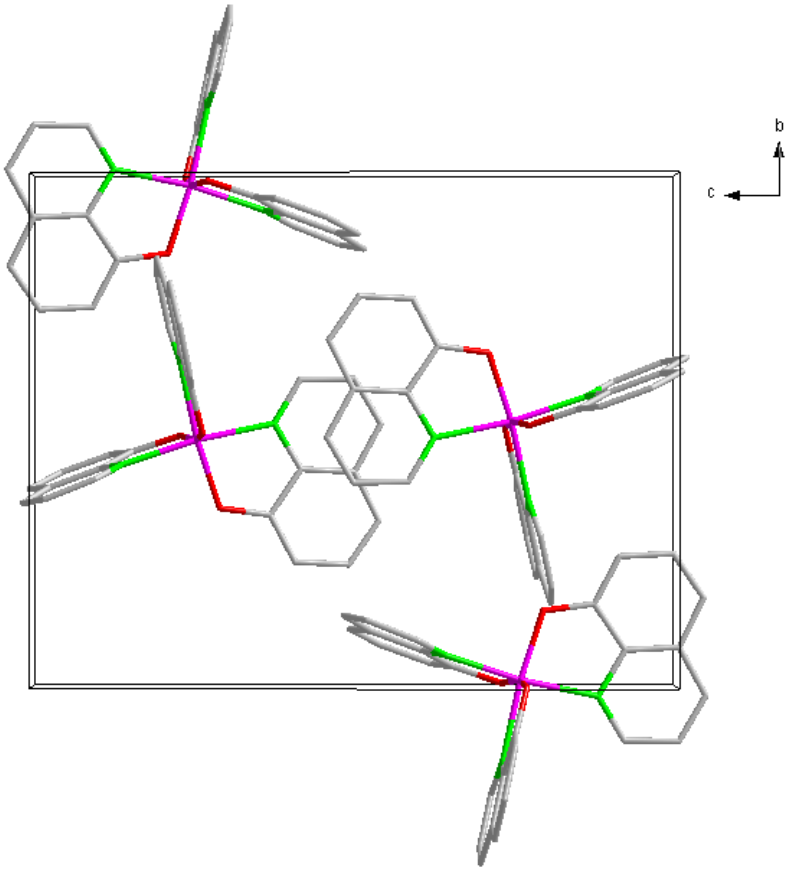

Figure 4.3.1.7: Molecular packing of 1.

Figure 4.3.1.7 displays the alternating zig-zag head to head packing of **1** when viewed along the *a*-axis.

4.3.2 mer-[tris-(8-Hydroxyquinolinato) gallium (III)] 0.5·ethanol solvate (2)

The complex *mer*-[Ga(Ox)$_3$]·0.5·EtOH (**2**), was synthesized as described in **Paragraph 3.7.4.** The asymmetric unit contains one full coordination compound and half occupancy ethanol molecule. The complex crystallizes in a monoclinic crystal system in the $P2_1/n$ space group with four formula units per unit cell (Z = 4). The numbering scheme of the title complex is shown in **Figure 4.3.1.1.**

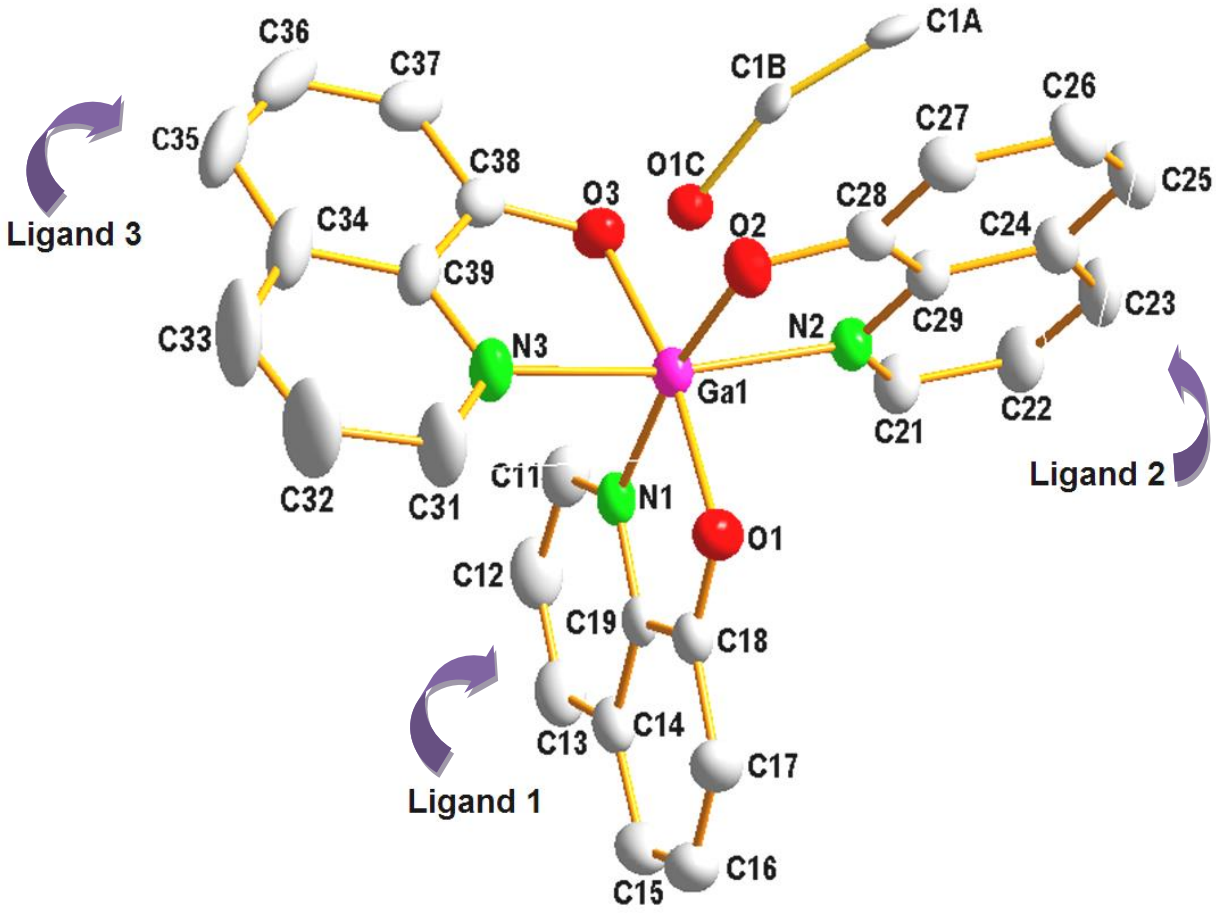

Figure 4.3.2.1: The representation of the molecular structure of *mer*-[Ga(Ox)$_3$]·0.5·EtOH (2). Hydrogen's atoms are omitted for clarity. Displacement ellipsoids are drawn at 50 % probability level.

Table 4.3.2.1: Crystal data and structure refinement for *mer*-[Ga(Ox)$_3$]·0.5·EtOH (2).

Identification code	Compound 2	
Empirical formula	C29 H20 Ga1 N3 O4	
Formula weight	544.20	
Temperature	100 K	
Wavelength	0.71073 Å	
Crystal system	Monoclinic	
Space group	*P 2$_1$/n*	
Unit cell dimensions	a = 10.944(5) Å	α= 90 °
	b = 13.123(5) Å	β= 97.523(5) °
	c = 16.864(5) Å	γ = 90 °
Volume	2401.1(16) Å^3	
Z	4	
Density (calculated)	1.505 Mg/m^3	
Absorption coefficient	1.189 mm^{-1}	
F(000)	1112	
Crystal size	0.326 x 0.394 x 0.652 mm^3	
Theta range for data collection	2.611 to 28.507°.	
Index ranges	-14<=h<=14, -17<=k<=17, -22<=l<=22	
Reflections collected	68758	
Independent reflections	6033 [R_{int} = 0.0661]	
Completeness	99.7 %	
Refinement method	Full-matrix least-squares on F^2	
Data / restraints / parameters	6033 / 24 / 352	
Goodness-of-fit on F^2	1.050	
Final R indices [I>2sigma(I)]	R1 = 0.0467, wR2 = 0.1237	
R indices (all data)	R1 = 0.0629, wR2 = 0.1335	
Largest diff. peak and hole	1.703 and -0.585 e.Å^{-3}	

The geometrical conformation of **2** is distorted from octahedral geometry as illustrated in **Figure 4.3.2.2**.

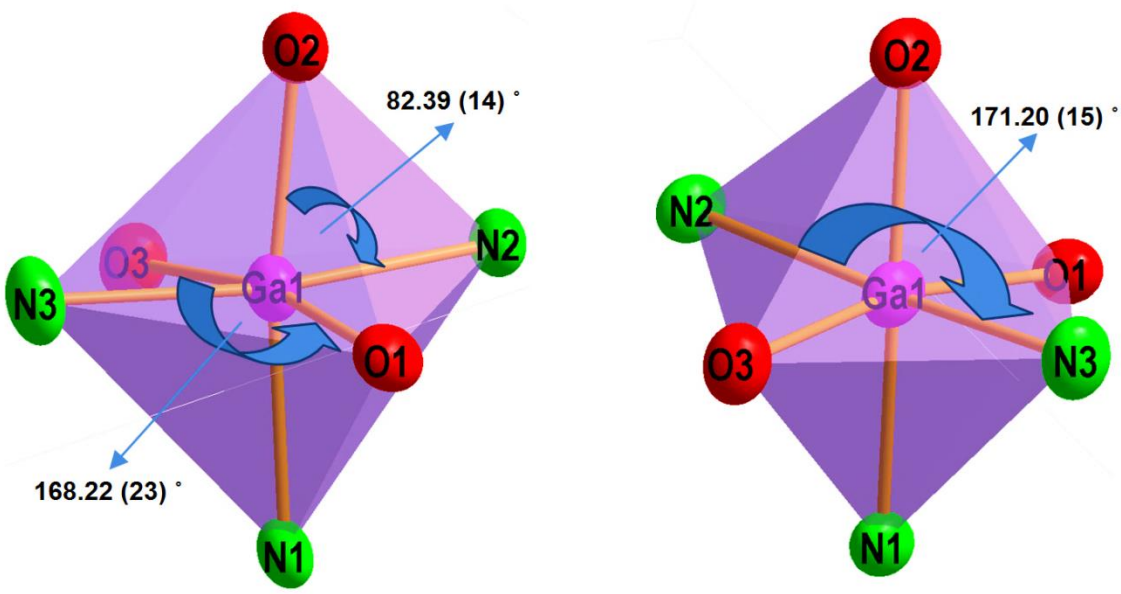

Figure 4.3.2.2: Illustration of an octahedral coordination polyhedron as found for the title compound viewed from the side.

The angles of O1-Ga1-O3 and N2-Ga1-N3 are 168.22 (23)˚ and 171.20 (15)˚ respectively as shown in **Figure 4.3.1.2**. The respective Ga-O and Ga-N bond distance comparisons in each ligand wing are similar within experimental error and ranges from 1.9335 (7) Å to 1.9468 (8) Å for Ga-O and 2.0720 (6) Å to 2.1125 (7) Å for Ga-N bonds respectively as illustrated in **Table 4.3.2.2**.

Table 4.3.2.2: Selected bond distances (Å) and selected angles (˚) of compound 2.

Selected bond distances		Selected bond angles	
Atom	**Distance (Å)**	**Atom**	**Angle (˚)**
Ga1 - O1	1.934 (7)	O1 - Ga1 - N1	80.968 (14)
Ga1 - O2	1.940 (9)	O2 - Ga1 - N2	82.391 (12)
Ga1 - O3	1.947 (8)	O3 - Ga1 - N3	82.010 (14)
Ga1 - N1	2.087 (6)	O1 - Ga - O3	115.574 (22)
Ga1 - N2	2.113 (7)	N2 - Ga - N3	114.057 (18)
Ga1 - N3	2.072 (6)	N1 - Ga - O2	114.225 (21)

The average bite angle of the ligand units of compound **2** for O-Ga-N is 81.79 (13)˚ as given in **Table 4.3.2.2** and the bond distances are similar within experimental error. All bond distances and angles are considered to be normal and fall within the range reported for similar complexes.[12,13]

The crystal structure is stabilized by C—H···O inter-molecular, π-π stacking and C—H···π interactions. These will be discussed in the following paragraph, see also **Table 4.3.2.3**.

The first two inter-molecular interactions are observed between respective hydrogen atoms of Ligand 1 and the respective oxygen atoms of Ligand 3 and Ligand 1 of the neighbouring $Ga(Ox)_3$ molecules. The other interaction is observed between the hydrogen atom of Ligand 2 and the oxygen atom of neighbouring Ligand 1.

The last inter-molecular interaction is from the hydrogen atom of the solvent moiety to the oxygen atom of the parent molecule. All these inter-molecular interactions are illustrated in **Figure 4.3.2.3**.

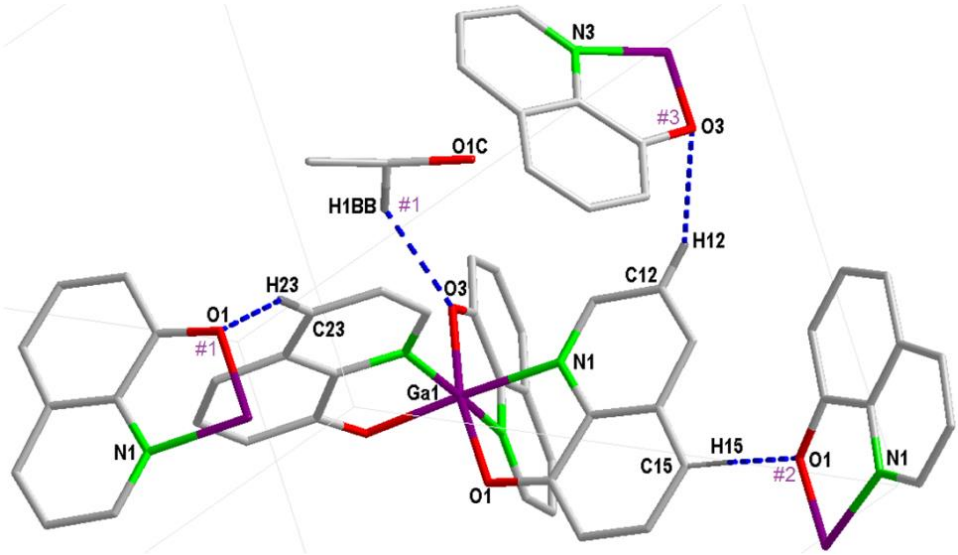

Figure 4.3.2.3: Inter-molecular hydrogen bonds observed in 2. Hydrogen atoms, not taking part in the hydrogen bonding, are omitted for clarity. Hydrogen interactions are indicated by blue dotted lines.

[12] Y. Wang, W. Zhang, Y. Li, L. Ye, G. Yang, Chem. Mater., 11, 530, 1999.

[13] M. Rajeswaran, V.V. Jarikov, Acta Cryst., E60, m217-m218, 2004.

Table 4.3.2.3: Observed C—H···O hydrogen interactions in 2.

D—H···A	d (D—H) (Å)	d (H···A) (Å)	d (D···A) (Å)	D—H···A (˚)
C1B—H1BB····O3 **#1**	0.97	2.50	3.344 (8)	146
C15—H15·····O1 **#2**	0.93	2.47	3.312 (6)	151
C12—H12·····O3 **#3**	0.93	2.57	3.293 (6)	134
C23—H23·····O1 **#1**	0.93	2.59	3.421 (6)	149

Symmetry transformations used to generate equivalent atoms: [**#1** = 1.5-x, 0.5+y, 0.5-z], [**#2** = 2-x, -y, -z] and [**#3** = 2.5-x, 0.5+y, 0.5-z]

The intermolecular C—H···π and π-π stacking interactions further stabilize the crystal packing. These interactions are illustrated in **Figure 4.3.2.4** and **Figure 4.3.2.5.** The relevant data is given in **Tables 4.3.2.4** and **Table 4.3.2.5.**

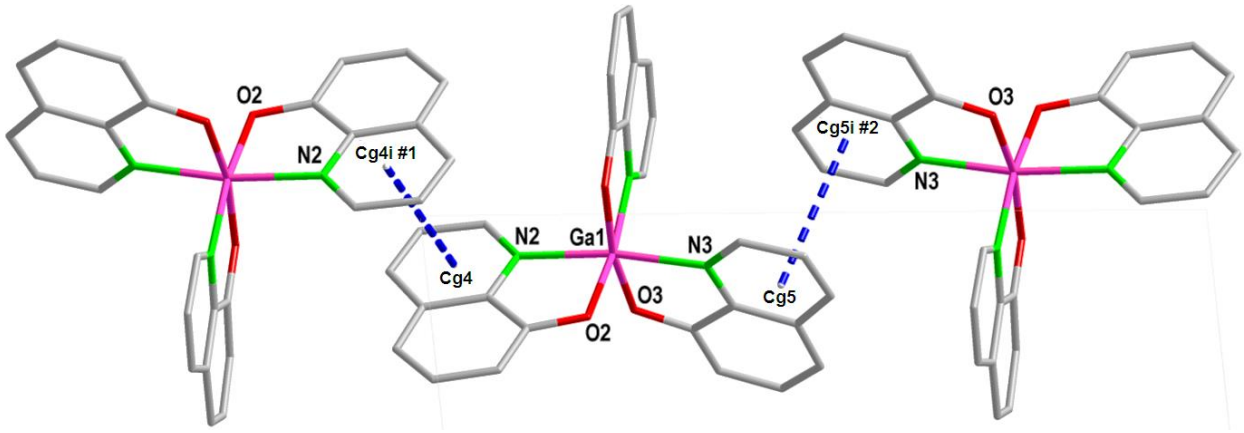

Figure 4.3.2.4: The schematic representation of the inter-molecular π-π stacking of 2. Hydrogen atoms have been omitted for clarity. Centroid atoms ending with 'i', resembles symmetry-generated molecules. The numbering of the nitrogen and oxygen denotes the number of the ligand coordinated.

π-Stacking is observed between the neighbouring molecules with centroid-to-centroid distances of 3.587(3) Å and 3.739(4) Å respectively as indicated in **Table 4.3.2.4**. The π-stacking is observed between pyridyl sides Ligand 2 and Ligand 3 of neighbouring $Ga(Ox)_3$ molecules.

Table 4.3.2.4: π-π Interactions observed between the pyridyl rings of the main and symmetry-generated molecules.

Centroid Atom	Centroid Atom	Distance between centroid atoms (Å)
Cg4	Cg4i **#1**	3.587(3)
Cg5	Cg5i **#2**	3.739(4)

Symmetry transformations used to generate equivalent atoms:
[**#1** = 2-x, -y, -z] and [**#2** = 2-x, -y,1 -z]
Cg1 = Centroid atom of N2, C26, C25, C29, C28, C27.
Cg2 = Centroid atom of C11, C12, C13, C14, C15, C16

The inter-molecular C—H···π interactions are illustrated in **Figure 4.3.2.5** and listed in **Table 4.3.2.5**. These includes interactions between neighbouring $Ga(Ox)_3$ molecules as well as influence from the solvent species.

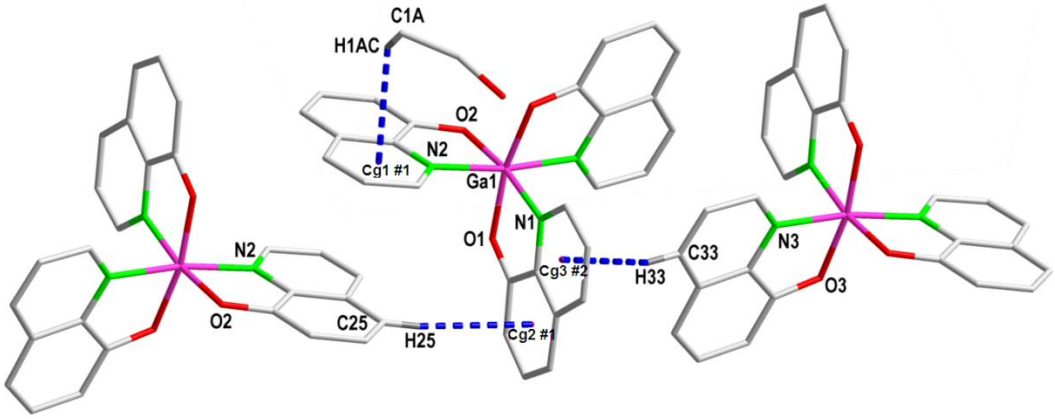

Figure 4.3.2.5: The geometrical representation of the C−H···π inter-molecular interactions of 2. Hydrogen atoms have been omitted for clarity. The numbering of the nitrogen and oxygen denotes the number of the ligand coordinated.

Table 4.3.2.5 C—H···π Interactions observed in 2.

C-H	Centroid Atom	d (H···Cg) (Å)	d (C···Cg) (Å)	C-H···Cg (°)
C1A-H1AC	Cg1 **#1**	3.00	3.690(8)	130
C25-H25	Cg4 **#1**	2.88	3.800(6)	173
C33-H33	Cg3 **#2**	2.61	3.507(6)	162

Symmetry transformations used to generate equivalent atoms:
[**#1** = 2-x, -y, -z] and [**#2** = 2-x, -y, 1-z]
Cg3 = Centroid atom of N1, C16, C15, C19, C18, C17.
Cg4 = Centroid atom of N3, C36, C35, C39, C38, C39.

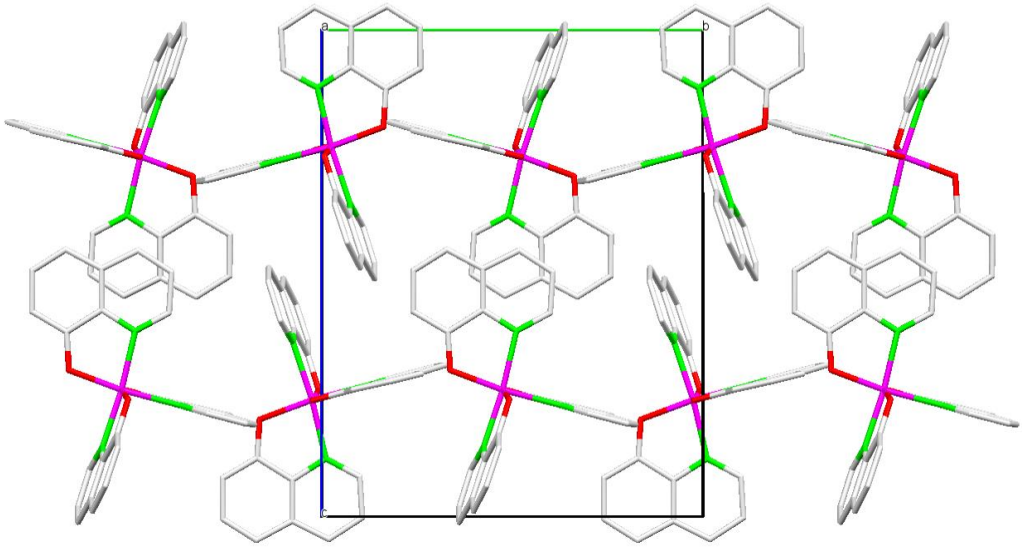

Figure 4.3.2.6: Molecular packing of 2.

The packing pattern represented in **Figure 4.3.2.6** is an alternating zig-zag head to head column packing as viewed along the c-axis.

4.3.3 *mer*-[*tris*-(5,7-Dimethyl-8-hydroxyquinolinato)gallium (III)] dichloromethane solvate (3)

The complex *mer*-[Ga(57dmOx)$_3$]·DCM (**3**), was synthesized as described in **Paragraph 3.7.5.** The asymmetric unit contains one full coordination compound and a dichloromethane molecule. The complex crystallizes in a triclinic crystal system in the $P\bar{1}$ space group with two formula units per unit cell (Z = 2). The numbering scheme of the title complex is shown in **Figure 4.3.1.1.**

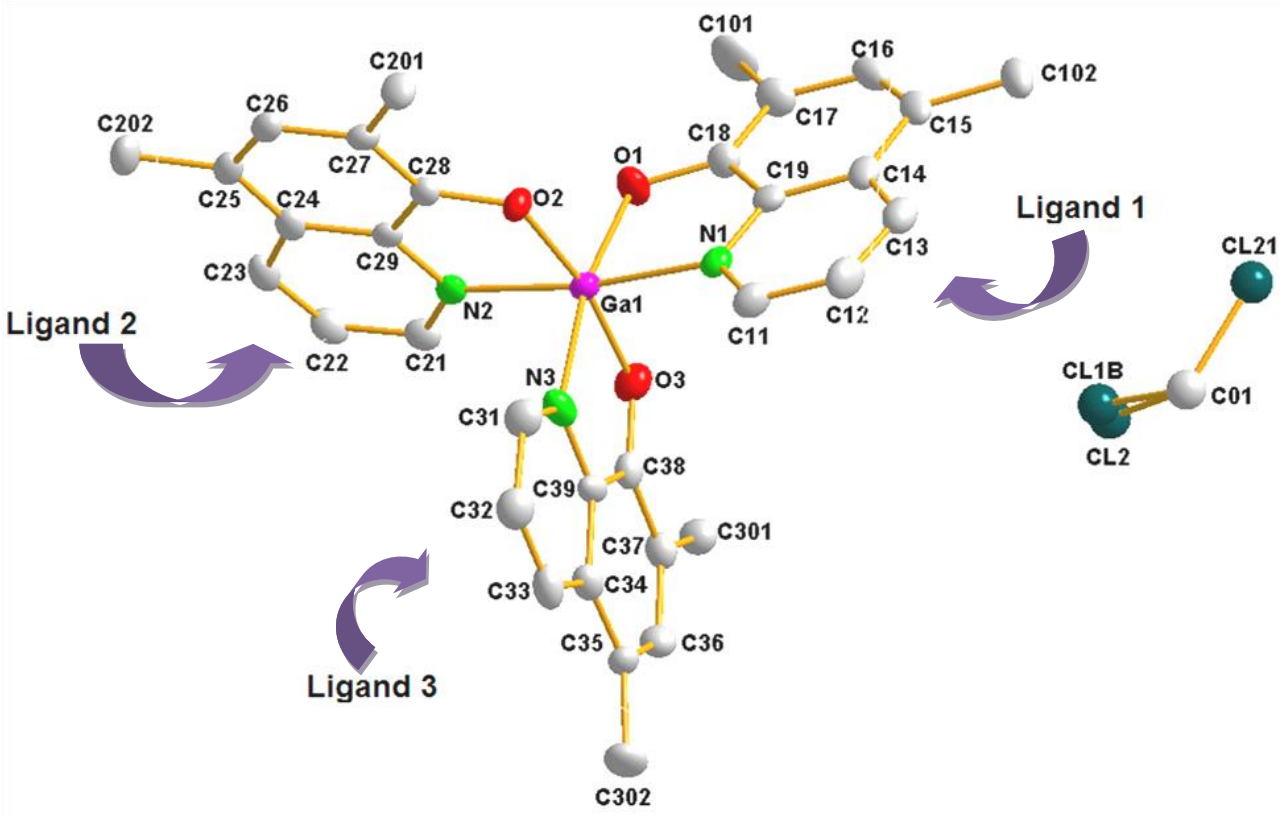

Figure 4.3.3.1: The representation of the molecular structure of *mer*-[Ga(57dmOx)$_3$]·DCM. Hydrogen's atoms are omitted for clarity. The solvent atoms are isotropically refined for clarity on the naming of the chlorine atoms that are distorted. The anisotropic displacement parameters of these solvent atoms show overlapping with large ellipsoids. Displacement ellipsoids are drawn at 50 % probability level.

Table 4.3.3.1. Crystal data and structure refinement for *mer*-[Ga(57dmOx)$_3$]·DCM (3).

Identification code	Compound 4	
Empirical formula	C34 H32 Cl2 Ga N3 O3	
Formula weight	671.24	
Temperature	100 K	
Wavelength	0.71073 Å	
Crystal system	Triclinic	
Space group	$P\bar{1}$	
Unit cell dimensions	a = 11.217(5) Å	α= 101.315(5) °.
	b = 11.283(5) Å	β= 97.324(5) °.
	c = 13.660(5) Å	γ = 113.366(5) °.
Volume	1515.2(11) Å^3	
Z	2	
Density (calculated)	1.471 Mg/m^3	
Absorption coefficient	1.125 mm^{-1}	
F(000)	692	
Crystal size	0.380 x 0.409 x 0.598 mm^3	
Theta range for data collection	2.031 to 28.309°.	
Index ranges	-14<=h<=14, -15<=k<=15, -18<=l<=18	
Reflections collected	21151	
Independent reflections	7408 [R(int) = 0.0422]	
Completeness	99.4 %	
Refinement method	Full-matrix least-squares on F^2	
Data / restraints / parameters	7408 / 5 / 411	
Goodness-of-fit on F^2	1.075	
Final R indices [I>2sigma(I)]	R1 = 0.0557, wR2 = 0.1282	
R indices (all data)	R1 = 0.0890, wR2 = 0.1436	
Largest diff. peak and hole	0.941 and -0.765 e.Å^{-3}	

The geometrical conformation of **3** is disordered from octahedral geometry as illustrated in **Figure 4.3.3.2**.

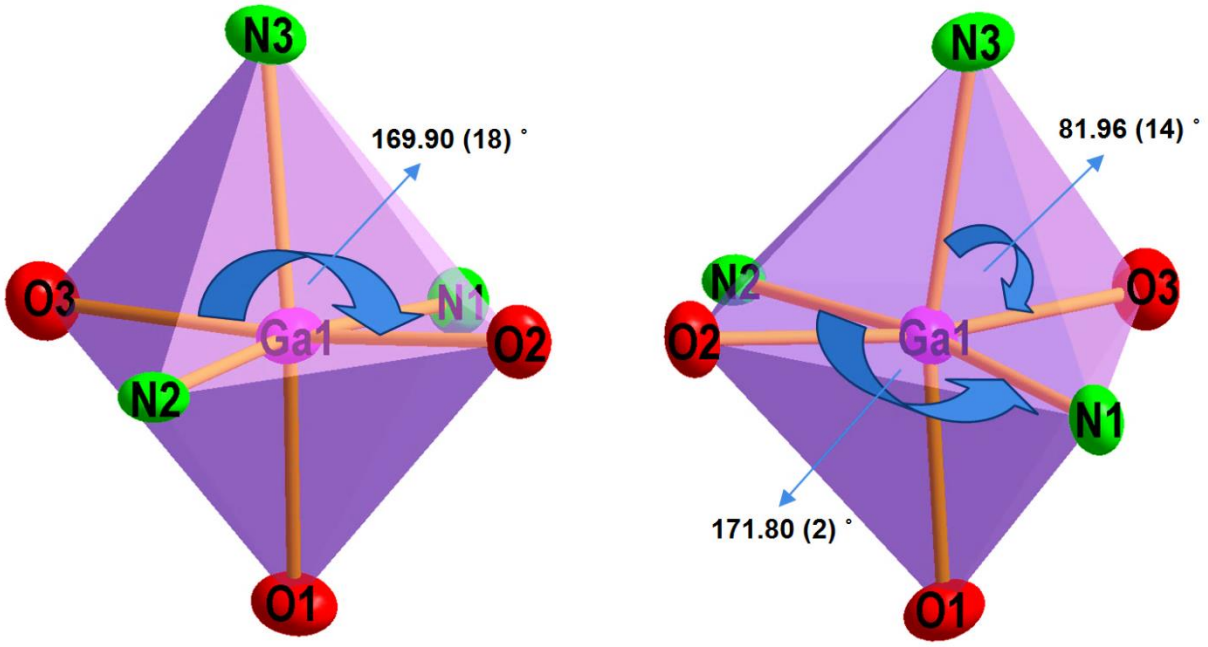

Figure 4.3.3.2. Illustration of the distorted octahedral coordination polyhedron as found for the title compound viewed from the side.

The angles of O2-Ga1-O3 and N2-Ga1-N1 are 169.9 (18)˚ and 171.8 (2)˚ respectively as shown in **Figure 4.3.3.2**, illustrating the slight distortion mentioned. The respective Ga-O and Ga-N bond distance comparisons in each ligand wing are similar within experimental error and ranges from 1.9434 (6) Å to 1.9502 (5) (8) Å for Ga-O and 2.0722 (7) Å to 2.1009 (7) Å for Ga-N bonds respectively as illustrated in **Table 4.3.3.2**.

Table 4.3.3.2: Selected bond distances (Å) and angles (˚) of 3.

Selected bond distances		Selected bond angles	
Atom	**Distance (Å)**	**Atom**	**Angle (˚)**
Ga1 - O1	1.949 (8)	O1 - Ga1 - N1	81.960 (14)
Ga1 - O2	1.943 (6)	O2 - Ga1 - N2	81.927 (12)
Ga1 - O3	1.950 (5)	O3 - Ga1 - N3	81.961 (14)
Ga1 - N1	2.093 (6)	O1 – Ga1 – O3	168.27 (21)
Ga1 - N2	2.101 (7)	N2 – Ga1 – N3	171.22 (15)
Ga1 - N3	2.072 (7)	N1 – Ga1 – O2	171.78 (15)

The average bite angle of the ligand units O-Ga-N is 81.94 (13)˚ and the bond distances are similar within experimental error.

All bond distances and angles are considered to be normal and fall within the range reported for similar complexes.[12,13.]

The structure is stabilized by C—H···O and C—H···Cl inter-molecular interactions as indicated in **Figure 4.3.3.3**. These will be discussed in the following paragraph, see also **Table 4.3.3.3**.

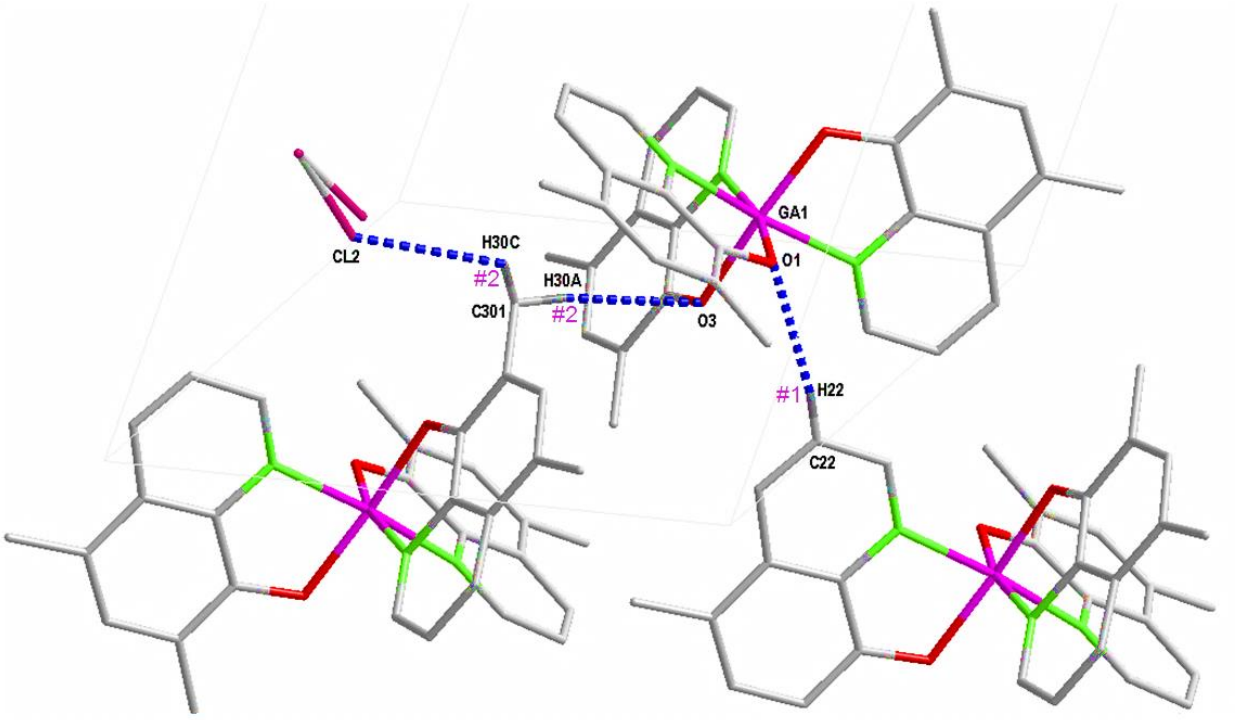

Figure 4.3.3.3: Hydrogen bonding observed for *mer*-[Ga(57dmOx)$_3$]·DCM (3). Hydrogen atoms, not taking part in the hydrogen bonding, are omitted for clarity. Hydrogen interactions are indicated by blue dotted lines.

The first observed C—H···O interaction is between the hydrogen atom in Ligand 2 of the neighbouring molecule and the oxygen atom in Ligand 1 of the parent molecule. Another interaction observed is between the hydrogen atom in Ligand 3 of the neighbouring molecule and the oxygen atom in Ligand 3 of the parent molecule.

The C—H···Cl hydrogen interaction is observed between the distorted dichloromethane solvent molecule and the hydrogen atom in Ligand 3 of the neighbouring molecule.

Table 4.3.3.3: Observed hydrogen bonding interactions in 3.

D—H···A	d (D—H) (Å)	d (H···A) (Å)	d (D···A) (Å)	D—H···A (°)
C28—H28····O1 **#1**	0.93	2.40	3.306 (5)	163
C301—H30A···O3 **#2**	0.96	2.59	3.534 (6)	167
C301—H30C···Cl2 **#2**	0.96	2.44	3.432 (10)	127

Symmetry transformations used to generate equivalent atoms:

[**#1** = 1-x, -y, -z] and [**#2** = 1-x, 1-y, -z]

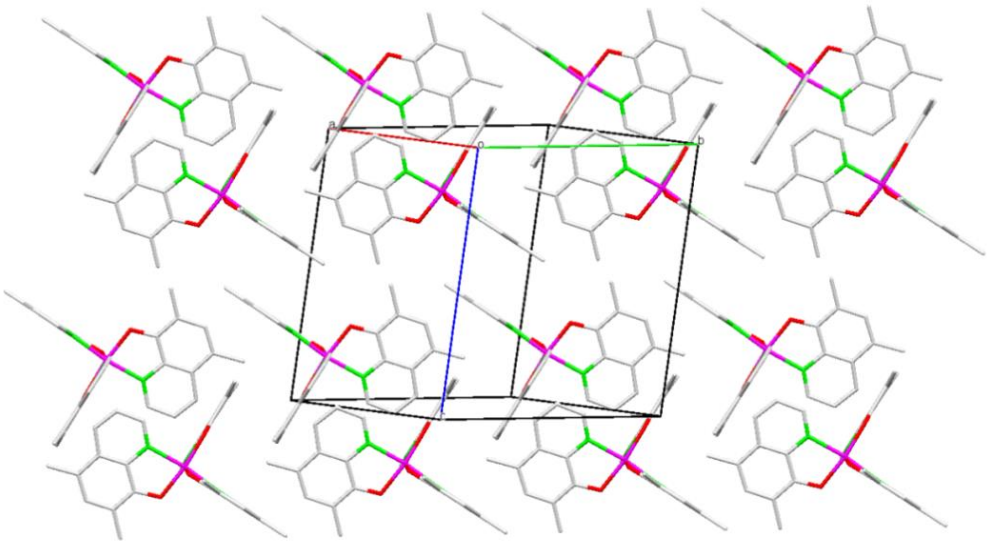

Figure 4.3.3.5: Molecular packing of 3.

The packing illustrated above is showing head-to-tail row packing as viewed along the [110] plane in the unit cell.

4.3.4 4.3.4. *mer*-[*tris*-(8-Hydroxyquinolinato) indium (III)] ·diaqua (4)

The complex *mer*-[In(Ox_3)]·$2H_2O$ (**4**), was synthesized as described in **Paragraph 3.7.7.** The asymmetric unit contains one full coordination compound and two water molecules. The complex crystallizes in a monoclinic crystal system in the $P2_1/n$ space group with four formula units per unit cell (Z = 4). The numbering scheme of the title complex is shown in **Figure 4.3.4.1.**

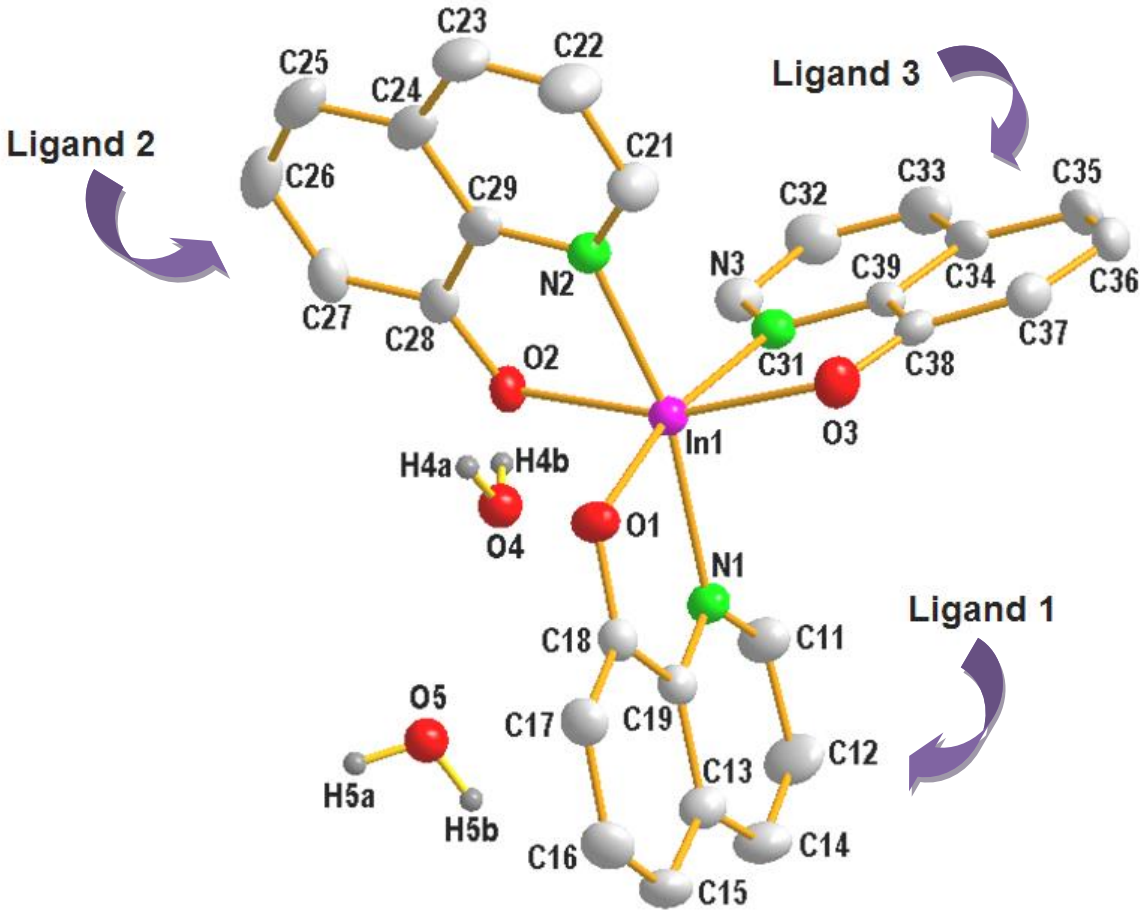

Figure 4.3.4.1: The representation of the molecular structure of *fac*-[In(Ox_3)]·$2H_2O$ (4). Hydrogen atoms are omitted for clarity. Displacement ellipsoids are drawn at 50 % probability level.

Table 4.3.4.1: Crystal data and structure refinement of *mer*-[In(Ox$_3$)]·2H$_2$O (4).

Identification code	Compound 4	
Empirical formula	$C_{27}H_{22}N_3O_5In$	
Formula weight	583.04	
Temperature	100 K	
Wavelength	0.71073 Å	
Crystal system	Monoclinic	
Space group	*P* $2_1/n$	
Unit cell dimensions	a = 11.391 (5) Å	α= 90 °
	b = 12.771 (5) Å	β= 94.441(5) °
	c = 16.910 (5) Å	γ = 90°
Volume	2452.7(16) Å^3	
Z	4	
Density (calculated)	1.579 g/cm^3	
Absorption coefficient	1.007 μ/mm^{-1}	
F(000)	1175	
Crystal size	0.142 x 0.205 x 0.356 mm^3	
Theta range for data collection	4 to 56°.	
Index ranges	$-15 \leq h \leq 15, -16 \leq k \leq 16, -22 \leq l \leq 22$	
Reflections collected	68421	
Independent reflections	5898 [R_{int} = 0.1216, R_{sigma} = 0.0556]	
Completeness	99.7 %	
Refinement method	Full-matrix least-squares on F^2	
Data / restraints / parameters	5898/0/327	
Goodness-of-fit on F^2	1.045	
Final R indices [I>2sigma(I)]	R_1 = 0.0427, wR_2 = 0.0967	
R indices (all data)	R_1 = 0.0645, wR_2 = 0.1095	
Largest diff. peak and hole	1.43 and -1.24 e.Å^{-3}	

The geometrical conformation of **4** is severely distorted from octahedral geometry as illustrated in **Figure 4.3.4.2**.

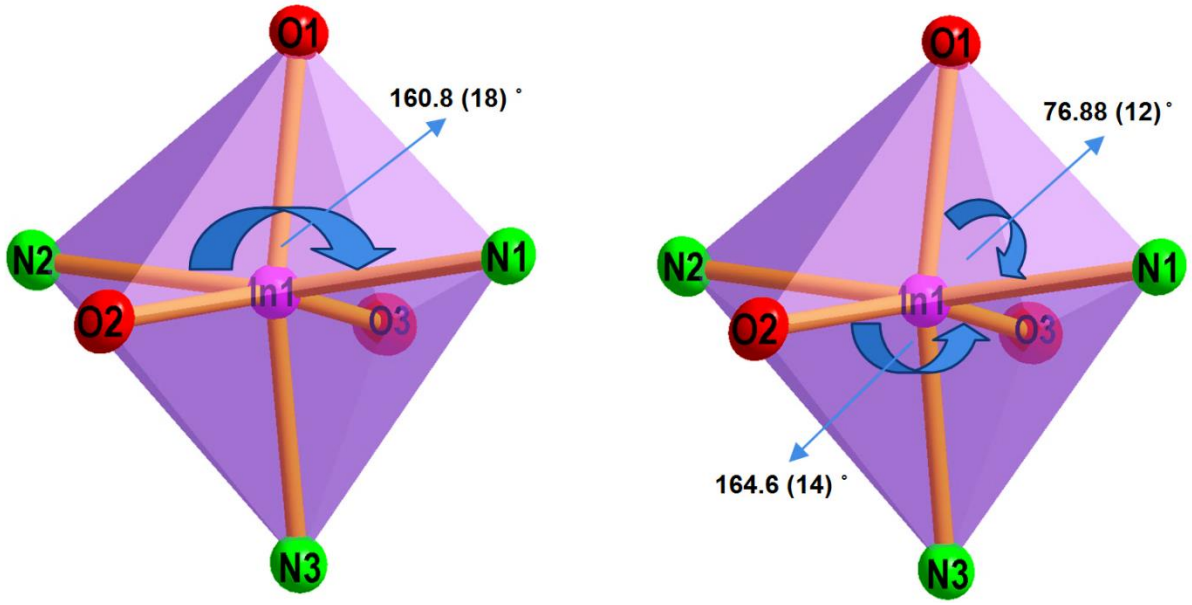

Figure 4.3.4.2: Illustration of an octahedral coordination polyhedron as found for the title compound.

The angles of O2-Ga1-O3 and N1-Ga1-N2 are 164.6 (14)˚ and 160.8 (18)˚ respectively as shown in **Figure 4.3.4.2**. There is a similar distortion observed as also seen in all above discussed crystal structures.

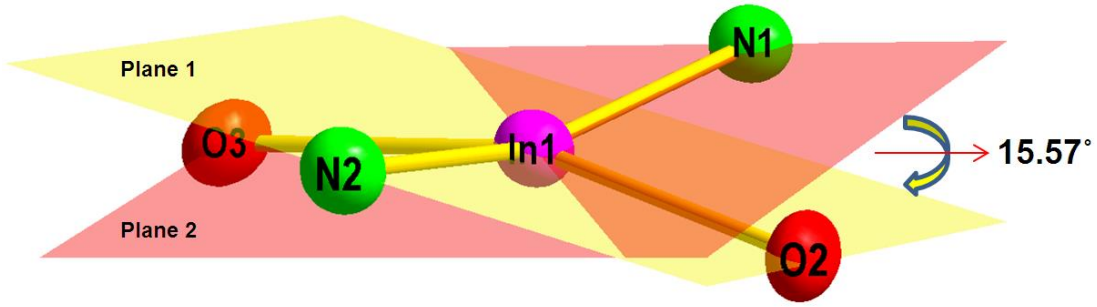

Figure 4.3.4.3: Partial structure view of 4 showing the twisted square planar conformation illustrated by two planes.

The planes constructed in **Figure 4.3.4.3** are to illustrate the distortion with an angle of deviation of 15.57˚.

The respective In-O and In-N bond distance comparisons in each ligand wing are similar within experimental error and ranges from 2.120 (9) Å to 2.143 (8) Å for In-O and 2.231 (6) Å to 2.253 (8) Å for In-N bonds respectively as illustrated in **Table 4.3.4.2**.

The average bite angle of the ligand units (O-Ga-N) of the title compound is 76.76 (13)˚ as illustrated in **Table 4.3.4.2** .

Table 4.3.4.2: Selected bond distances (Å) and selected angles (˚) of 4.

Selected bond distances		Selected bond angles	
Atom	**Distance (Å)**	**Atom**	**Angle (˚)**
In1 - O1	2.135 (7)	O1 - In1 - N1	76.882 (12)
In1 - O2	2.143 (8)	O2 - In1 - N2	76.856 (13)
In1 - O3	2.120 (9)	O3 - In1 - N3	76.548 (13)
In1 - N1	2.241 (6)	O2 - In1 – O3	169.94 (18)
In1 - N2	2.231 (6)	N1 - In2 – N3	171.78 (20)
In1 - N3	2.253 (8)	N1- In1 – O1	168.24 (24)

All bond distances and angles are considered to be normal and fall within the range reported for similar complexes.[14.]

The structure is stabilized by C—H···O and O—H···O inter-molecular interactions as indicated in **Figure 4.3.4.3.** These will be discussed in the following paragraph, see also **Table 4.3.4.3.**

[14] M. Rajeswaran, V.V. Jarikov, Acta Cryst., E59, m306, 2003.

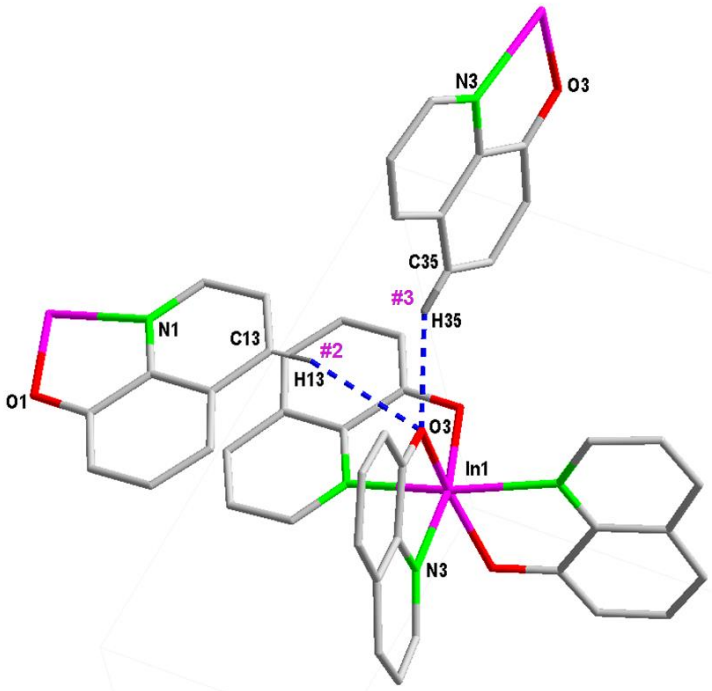

Figure 4.3.4.4: Schematic representation showing the inter-molecular C—H···O interactions in 4. Hydrogen atoms, not taking part in hydrogen bonding are omitted for clarity

There is a C—H···O interaction observed between the two respective hydrogen atoms from Ligand 1 and Ligand 3 of symmetry generated neighbouring molecules and the oxygen atom in Ligand 3 of the parent molecule.

The observed O—H···O inter-molecular interaction is between the hydrogen atom of the symmetry generated neighbouring water molecule and the oxygen atom in Ligand 1 of the parent structure. Similarly the same type of interaction is observed between the hydrogen atom of the neighbouring water molecule and the oxygen atom of in Ligand 2 of the parent structure.

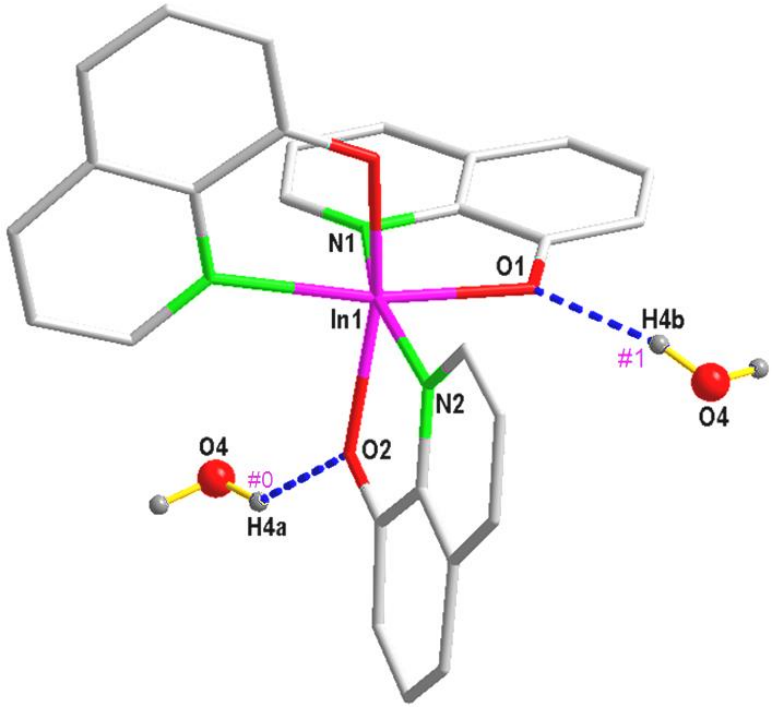

Figure 4.3.4.4: Schematic representation showing the O—H···O hydrogen bonding in 4. Hydrogen atoms, not taking part in hydrogen bonding are omitted for clarity.

Table 4.3.4.3: Observed hydrogen bonding in 4.

D—H···A		d (D—H) (Å)	d (H···A) (Å)	d (D···A) (Å)	D—H···A (°)
O4—H4a····O2	**#0**	0.85	2.12 (2)	2.820 (4)	140
O4—H4b····O1	**#1**	0.85	2.10 (4)	2.908 (4)	158
C13—H13···O3	**#2**	0.93	2.55 (3)	3.380 (5)	149
C35—H35····O3	**#3**	0.93	2.33 (3)	3.171 (5)	150

Symmetry transformations used to generate equivalent atoms:

[**#0** = x, y, z]; [**#1** = 1.5-x, -0.5-y, 0.5-z]; [**#2** = 2-x, 1-y, -z] and [**#3** = 2-x, -0.5+y, 0.5-z]

The intermolecular π-π stacking interactions further stabilize the crystal packing. These interactions are illustrated in **Figure 4.3.4.7.** The relevant data is given in **Tables 4.3.4.4.**

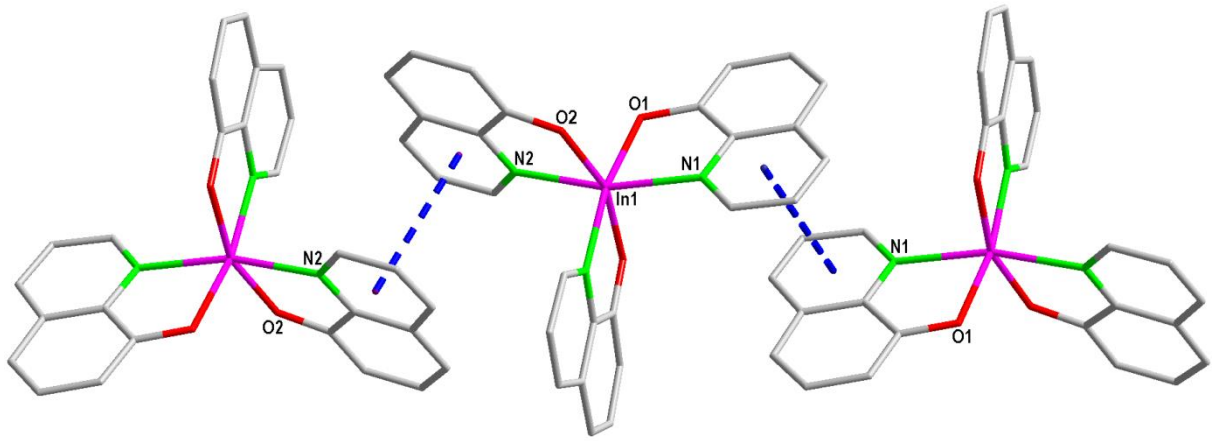

Figure 4.3.4.7: The schematic representation of the inter-molecular π-π stacking in 4. Hydrogen atoms have been omitted for clarity. Centroid atoms ending with 'i', resemble symmetry-generated molecules. The numbering of the nitrogen and oxygen denotes the number of the ligand coordinated.

The π-π stacking is observed between the neighbouring molecules with centroid-to-centroid distances of 3.678(10) Å and 3.719(14) (4) Å respectively as indicated in **Table 4.3.4.4**. The π-stacking is observed between pyridyl rings of Ligand 1 and Ligand 2 of symmetry generated neighbouring molecules.

Table 4.3.4.4: *π-π* stacking observed between the pyridyl rings of the main and symmetry-generated molecules of 4.

Centroid Atom	Centroid Atom	Distance between centroid atoms (Å)
Cg1	Cg1i **#1**	3.678(10)
Cg2	Cg2i **#2**	3.719(14)

Symmetry transformations used to generate equivalent atoms:
[**#1** = 2-x, 1-y, 1-z] and [**#2** = 2-x, 1-y, -z]
Cg1 = Centroid atom of N1, C11, C12, C13, C14, C19.
Cg2 = Centroid atom of N2, C21, C22, C23 C24, C29.

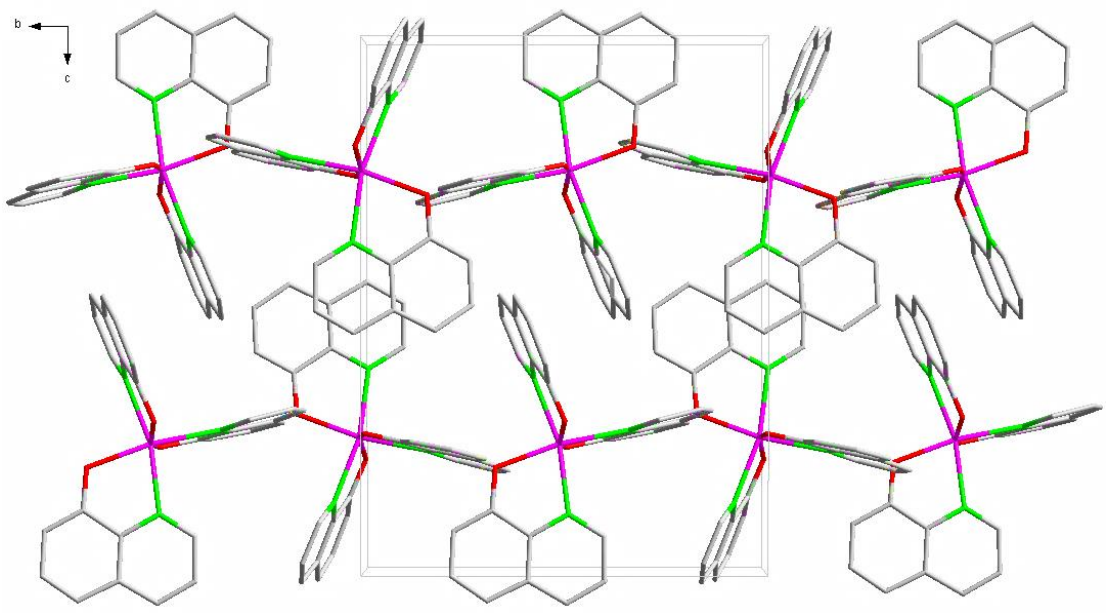

Figure 4.3.4.8: Molecular packing (4).

The zig-zag head-to-tail packing of the unit cell represented in **Figure 4.3.4.8** as viewed along the *c-axis*.

4.4 Conclusion

Crystal structures of the following complexes for group 13 metal complexes namely:

- *mer*-[*tris*-(8-Hydroxyquinoline) aluminium (III)] ·ethanol solvate [**1**]
- *mer*-[*tris*-(8-Hydroxyquinoline) gallium (III)] ·0.5 ethanol solavate [**2**]
- *mer*-[*tris*-(5,7-Dimethyl-8-hydroxyquinoline) gallium (III)] dichloromethane solvate [**3**]
- *mer*-[*tris*-(8-Hydroxyquinoline) indium (III)] ·diaqua solvate [**4**]

were analyzed and discussed in this chapter. A crystallographic investigation of the complexes in this study was considered important to fully understand the geometrical conformation and coordination chemistry of these complexes and ultimately correlate with the results obtained from other characterization techniques.

All complexes with non-functionalized ligand species namely complex **1**, **2** and **4**, crystallizes in a monoclinic crystal system. However, complex **3**, which is a dimethyl-substituted ligand, crystallized in triclinic crystal system. Complex **1** was refined in $P2_1/c$ whereas **2** and **4** were both refined in a non-standard $P2_1/n$ space group. They could not be solved in the standard equivalent setting which is $P2_1/c$, which resulted in unstable refinements. Complex **1**, **2** and **4** has four formula units in the unit cell (Z = 4) and complex **3** have two formula units in the unit cell (Z = 2). The crystal structures of all four complexes were stabilized by variety hydrogen bonding, namely by C—H···O, O—H···O, C—H···π and π-π stacking interactions.

The respective data collection of the latter mentioned crystals was a success despite the difficulties of obtaining high quality data for some of these crystals like in the case of compound **1.**

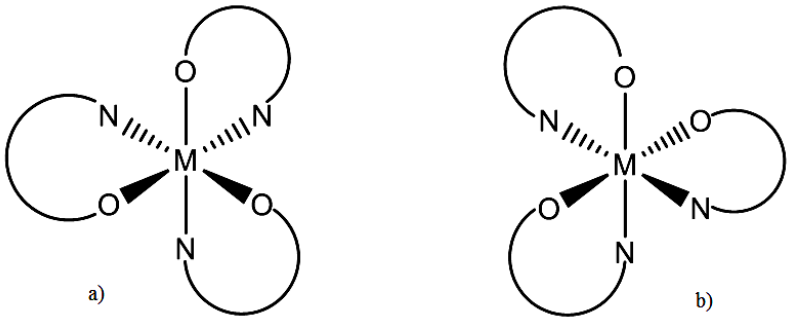

Figure 4.4.1: Schematic representation of a) facial isomer and b) meridional isomer.

The solution NMR studies have suggested a facial isomer for both the gallium and indium complex. This prediction comes from both the ^{1}H and ^{13}C NMR experiments. However, the solid state data obtained here indicates that only *mer*-isomer is formed. The perturbations of the complexes were suggested to be induced by the existing inter-conversion which morely favours the meridional isomer.

Significant differences are observed in the bite angles of the respective complexes recorded in **Table 4.4.2**. The bite angles of an octahedron molecular geometry are ideally expected to be 90˚ with equal bond distances. The average bite angles of the complexes as we go down the group 13 metals from aluminium to indium are:

- aluminium complex is 82.524 (14) ˚
- gallium complexes is 81.789 (13) and 81. 949 (13) ˚
- indium complex is 76.762 (13)˚

In general, the metal to ligand bond distances increases as expected when moving from aluminium (Al) down to indium (In).

5 X-RAY CRYSTALLOGRAPHIC STUDY OF LANTHANIDE QUINOLATE COMPLEXES.

5.1 Introduction

This chapter gives an insight to the coordination chemistry of the quinolinol derivatives with the lanthanide metal ion europium (Eu).

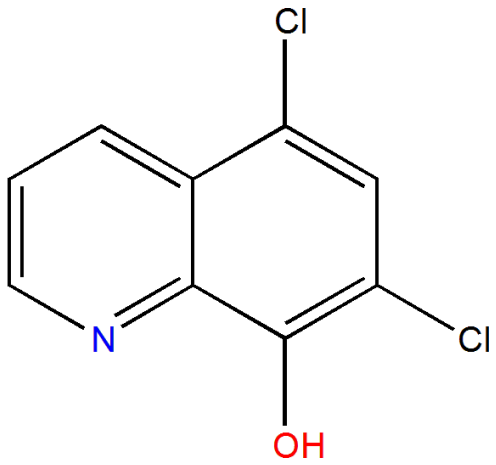

Figure 5.1.1: Schematic representation of a dichloro-functionalized quinolinol ligand.

The scheme given in **Figure 5.1.1**, is that of 5,7-dichloro-8-hydroxyquinoline as one of the primary ligands used in this project. There have been great achievements from the 1980's with the organic light emitting diodes using such ligand systems.[12] The on-going investigations have been conducted to improve the chemistry thereof in order to manipulate their luminescent abilities. However, it has been a great difficulty in fine tuning the emission colour without affecting the electroluminescence material's physical properties.

[1] C.W. Tang, S.A. Van Slyke, Appl. Phys., 51, 913(1987).

[2] C.W. Tang, S.A. Van Slyke, C.H. Chen, J. Appl. Phys., 65, 3610 (1989).

8-hydroxyquinoline is one of the ligand species that is deemed proper due to its good chelatoaromatic properties which in turn influence the stability of the chelate metal complex in a positive way.[3] The observed ligand in **Figure 5.1.1**; is to be coordinated to the lanthanide metal in great concern of the luminescence properties thereof.

The synthesis of the lanthanide-quinolinol complex was aimed at having four homoleptic quinolate derivatives coordinated to the europium metal ion. The intent was well within reason due to the history of the lanthanide contraction ability. The lanthanides have been active in the field of luminescence in many ways including their involvement in the medicinal chemistry in the development of potential magnetic resonance imaging agents.[4] Lanthanide ions have the ability to exhibit extremely sharp emission bands near infrared region and can be accounted for in terms of inter-configurational *4f-4f* radiative transitions.[5] Moreover, looking at the spectral profile of the complex, the excitation mechanism of the central metal ion differs from others in that Eu(III) excited states are only slightly lower in energy than the excited states of typical organic ligands. Their excitations are via intra-molecular energy transfers from the triplet excited states of the ligand and that possess no limitations in the internal quantum efficiency of the device using lanthanides complexes as emitters.[2,6]

This chapter entails two crystal structures of the europium (Eu) metal ion and the above shown ligand. The crystal structures of *tris*-[(5,7-dichloro-8-hydroxyquinoline)$(H_2O)_2$Eu(III)] $\cdot EtOH \cdot H_2O$ and the dimerized complex of κ^2-O,O'-*tris*-[(5,7-dichloro-8-hydroxyquinoline)(methanol)Eu(III)] are discussed in detail.

[3] K.K. Zborowski, M. Sola, J. Poater, L.M. Proniewicz, Cent. Eur. J. Chem, 11, 655, 2013.

[4] J. Kido, Y. Okamoto, Chem. Rev., 102, 2357, 2002.

[5] M.F Reld, F.S. Richardson, J. of Phys. Chem., 88, 3579, 1984.

[6] N. Sabbatini, M. Guardigli, J.M. Lehn, Coord. Chem. Rev., 123,1-2, 201, 1993.

5.2 Experimental

The intensity data were collected on a Bruker X8 Apex II 4K Kappa CCD diffractometer equipped with graphite monochromated Mo *K*α radiation, with a wavelength of 0.71073 Å; with both ω- and φ-scans at 100 K. All the cell refinements were performed with SAINT-Plus[7] and the data reduction was done with SAINT-Plus and XPREP. The software package SADABS[8] that utilizes the Sheldrick multi-scan technique were used to apply absorption correction. All the structures were solved with the use of the SIR-97[9] package, refinement was done with SHELXL-97[10] and WinGX[11] and the molecular graphics were completed with DIAMOND[12] and MERCURY[13]. All the structures are shown with thermal ellipsoids drawn at a 50% probability level and all non-hydrogen atoms were anisotropically refined, unless otherwise stated. Methyl, methylene, methine and aromatic hydrogen atoms were placed in geometrically idealized positions, C-H = 0.95 to 1.00 Å, and they were constrained to ride on their parent atoms, $U_{iso}(H) = 1.5\ U_{eq}(C)$ and $1.2\ U_{eq}(C)$ respectively. For the numbering of the quinoline rings, the first digit refers to the ring number while the second digit refers to the carbon atom in the ring.

All the atomic coordinates, anisotropic displacement parameters, bond distances, angles and hydrogen coordinates, of all the crystals reported in this Chapter, are given in the supplementary data (Appendix A).

[7] Bruker, *SAINT-Plus*, Version 7.12 (including XPREP), Bruker AXS Inc., Madison, Wisconsin, USA, 2004.

[8] Bruker, SADABS, Version 2004/1, Bruker AXS Inc., Madison, Wisconsin, USA, 1998.

[9] A. Altomare, M.C. Burla, M. Camalli, G.L. Cascarano, C. Giacovazzo, A. Guagliardi, A.G.G. Moliterni, G. Polidori, R. Spagna, *J. Appl. Cryst*., 32, 837, 1999.

[10] G.M. Sheldrick, *SHELXL97*, Program for the refinement of crystal structures, University of Göttingen, Germany,1997.

[11] L.J. Farrugia, *J. Appl. Cryst*., 32, 837, 1999.

[12] K. Brandenburg, H. Putz, *DIAMOND*, Release 3.0c, Crystal Impact GbR, Bonn, Germany, 2008.

[13] I. Buno, J.A. Chisholm, P.R. Edgington, P. McCabe, E. Pidcock, L. Rodriguez-Monge, R. Taylor, J. van de Streek, P.A. Wood, *J. Appl*. Cryst, 41, 466, 2008.

5.3 X-ray Crystal Structure of Lanthanides Complex

5.3.1 The crystal structure of:

[*tris*-(5,7-dichloro-8-hydroxyquinoline)·(diaqua)·europium(III)] water · ethanol solvate (5)

The complex, $[Eu(57dcOx)_3]\cdot EtOH\cdot H_2O$ (**5**), was synthesized as described in **Paragraph 3.8.1.1.** The asymmetric unit contains one full coordination compound, an ethanol molecule and a water molecule. The complex crystallizes in a trigonal crystal system in the $R\bar{3}$ space group with four formula units per unit cell (Z = 18). The numbering scheme of the title complex is shown in **Figure 5.3.1.1**

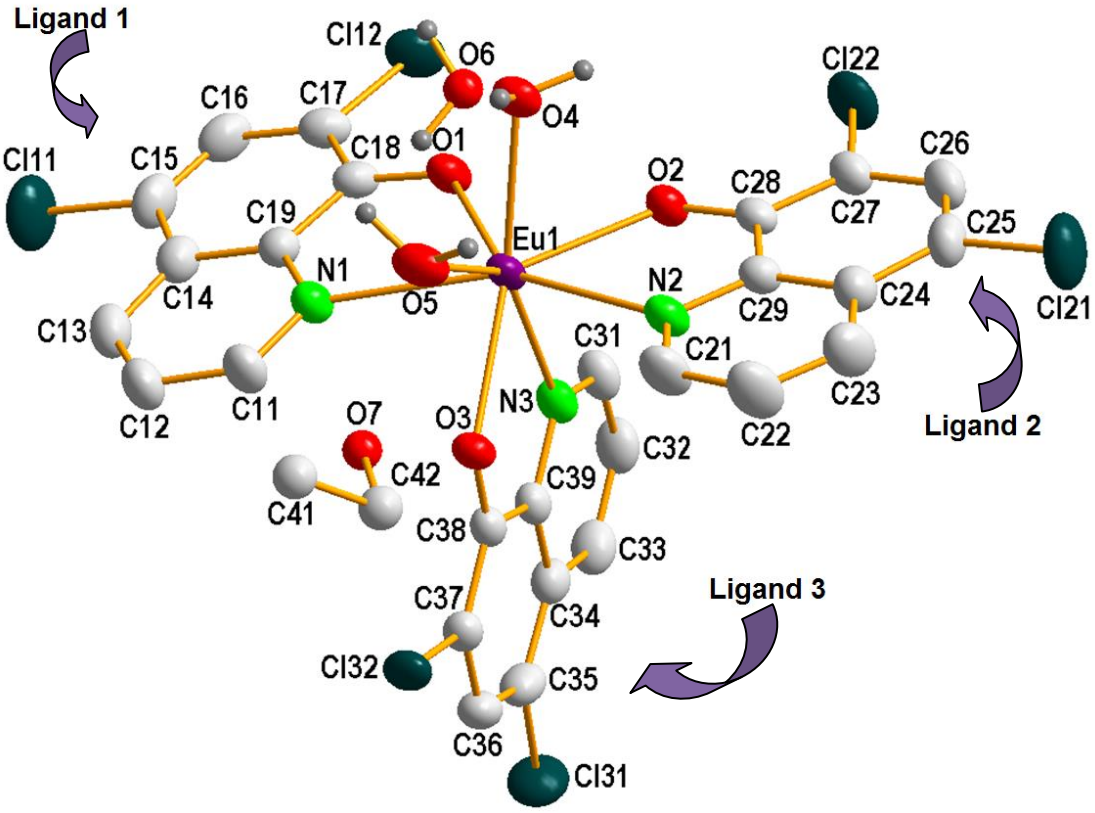

Figure 5.3.1.1: The representation of the molecular structure of (5). Hydrogen atoms are omitted for clarity. Displacement ellipsoids are drawn at 50 % probability.

Table 5.3.1.1: Crystal data and structure refinement of 5.

Identification code	**Compound 5**	
Empirical formula	**$C_{29}Cl_6EuN_3O_6H_{22}$**	
Formula weight	**879.16**	
Temperature	**100.0 K**	
Wavelength	**0.71073 Å**	
Crystal system	**Trigonal**	
Space group	**$R\bar{3}$**	
Unit cell dimensions	**a = 21.678 (2) Å**	**α= 90 °**
	b = 21.678 (2) Å	**β= 90 °**
	c = 37.361 (4) Å	**γ = 120°**
Volume	**15205(4) $Å^3$**	
Z	**18**	
Density (calculated)	**1.728 Mg/m^3**	
Absorption coefficient	**2.377 mm^{-1}**	
F(000)	**7800.0**	
Crystal size	**0.375 × 0.368 × 0.298 mm^3**	
Theta range for data collection	**6.142 to 56.726**	
Index ranges	**$-28 \le h \le 28$, $-28 \le k \le 28$, $-49 \le l \le 49$**	
Reflections collected	**187325**	
Independent reflections	**8436 [R_{int} = 0.0699, R_{sigma} = 0.0238]**	
Completeness	**99.6 %**	
Refinement method	**Full-matrix least-squares on F^2**	
Data / restraints / parameters	**8436 / 0 / 422**	
Goodness-of-fit on F^2	**1.085**	
Final R indices [I>2sigma(I)]	**R_1 = 0.0314, wR_2 = 0.0870**	
R indices (all data)	**R_1 = 0.0440, wR_2 = 0.0966**	
Largest diff. peak and hole	**1.50 / -0.67 $Å^{-3}$**	

The geometrical conformation of **5** shows a distortion from square antiprismatic molecular geometry as illustrated in **Figure 5.3.1.2**.

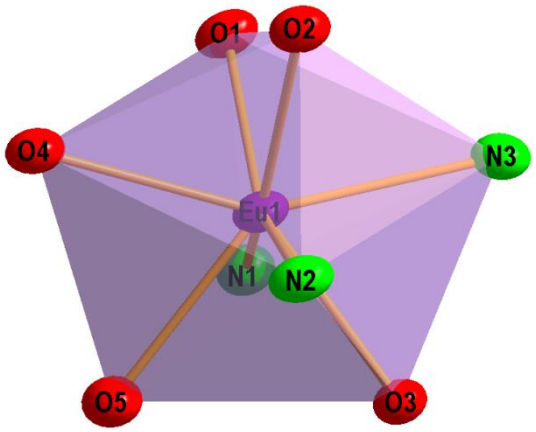

Figure 5.3.1.2: Illustration of a square anti-prismatic coordination polyhedron as found for the title compound.

Table 5.3.1.2: Selected bond distances (Å) and angles (°) of compound 5.

Bond Distances (Å)			
Eu1 - O1	2.343 (2)	**Eu1 - O5**	2.432 (2)
Eu1 - O2	2.365 (2)	**Eu1 - N1**	2.606 (2)
Eu1 - O3	2.387 (2)	**Eu1 - N2**	2.568 (3)
Eu1 - O4	2.455 (2)	**Eu1 - N3**	2.519 (2)
Bond Angles (°)			
N1 - Eu1 - O1	64.742 (4)	**O1 - Eu1 - O2**	79.13 (14)
N2 - Eu1 - O2	65.225 (4)	**N1 - Eu1 - N2**	151.13 (5)
N3 - Eu1 - O3	66.213 (4)	**O3 - Eu1 - O5**	140.69 (5)
O4 - Eu1 - O5	67.480 (4)	**O4 - Eu1 - N3**	151.35 (5)

The respective Eu-O and Eu-N bond distance comparisons in each ligand wing are slightly out of range from 2.343 (2) Å to 2.387 (2) Å for Eu-O and 2.519 (2) Å to 2.606 (2) Å for Eu-N bonds distance as illustrated in **Table 5.3.1.2**.

The average bite angle of the ligand units (O-Eu-N) of the title compound is 65.39 (4) ° as they are all listed in **Table 5.3.1.2**.

All bond distances and angles are considered to be normal and fall within the range reported for similar complexes.[14,15.]

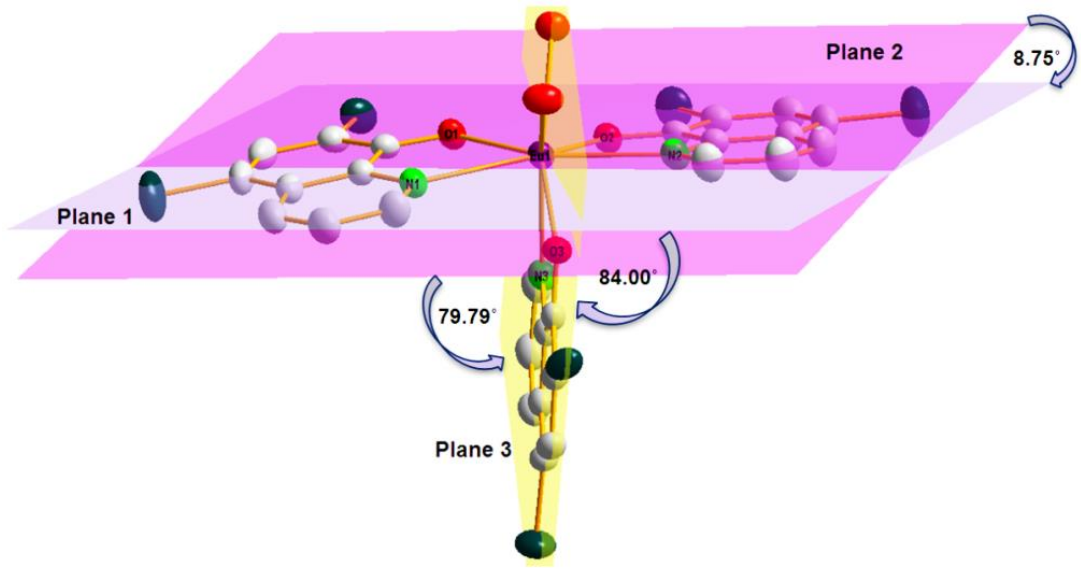

Figure 5.3.1.3: Illustration of the relations between the equatorial and perpendicular constructed planes of 5.

Table 5.3.1.3: Dihedral angles between the constructed planes in compound 5.

Plane Angles (°)	
Plane 1 & 2	8.750
Plane 2 & 3	79.79
Plane 3 & 1	84.00

Plane 1: Eu1, O1, N1, C11, C12, C13, C14, C15, C16, C17, C18, C19, Cl11, Cl12.

Plane 2: Eu1, O2, N2, C21, C22, C23, C24, C25, C26, C27, C28, C29, Cl21, Cl22.

Plane 3: Eu1, O3, N3, C31, C32, C33, C34, C35, C36, C37, C38, C39, Cl31, Cl32.

[14] Z. Chen, Y. Gu, X. Song, Y. Liu, Y. Peng, H. Liang, Euro. J. of Med. Chem., 59, 194, 2013.

[15] Z. Chen, Y. Gu, X. Song, Y. Liu, Y. Peng, Q. Pin, H. Liang, Euro. J. of Med. Chem., 59, 168, 2013.

The constructed planes as illustrated in **Figure 5.3.1.3**, assists in understanding of the respective positions of each ligand relative to each other around the metal center. The deviation angle between plane 1 and plane 2 is 8.750˚. The relevant data is recorded in **Table 5.3.1.3**.

The crystal structure is stabilized by O—H···O and C—H···Cl intra-molecular, O—H···O, C—H···Cl and C—H···O inter-molecular interactions. These will be discussed in the following paragraph, see also **Table 5.3.1.4**.

The O—H···O intra-molecular interaction is observed between a hydrogen atom of the coordinated water molecule and the oxygen atom of another neighbouring coordinated water molecule as illustrated in **Figure 5.3.1.4**.

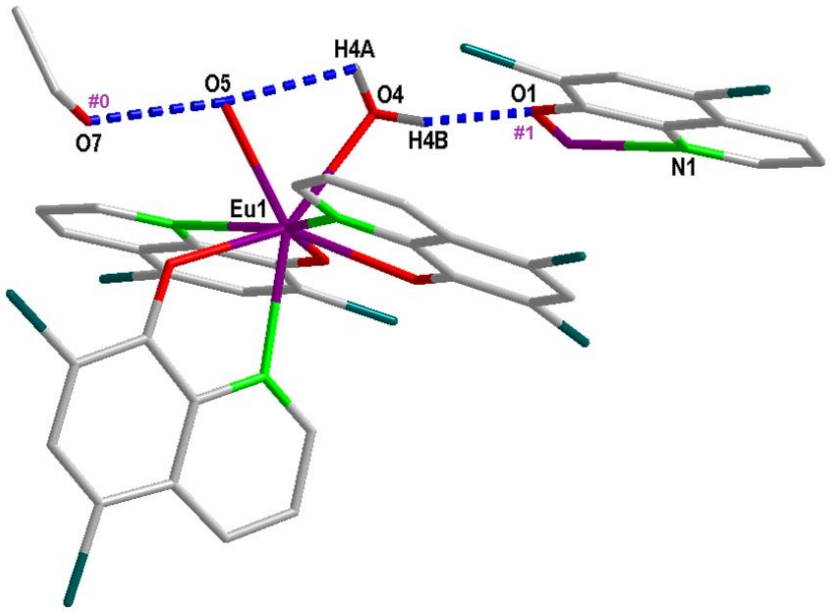

Figure 5.3.1.4: O—H•••O type of hydrogen bonding observed in 5. Hydrogen atoms not taking part in the hydrogen bonding are omitted for clarity. Hydrogen interactions are indicated by blue dotted lines.

The observed C—H···O inter-molecular interaction is between the hydrogen atom of one of the coordinated water molecules and the oxygen atom of the neighbouring ethanol solvent.

The last C—H···O inter-molecular interaction observed is between the hydrogen atom of the other coordinated water molecule and the oxygen atom in Ligand 1 of the symmetry generated neighbouring molecule.

Table 5.3.1.4: Observed O—H•••O hydrogen bonding in 5.

D—H···A	d (D—H) (Å)	d (H···A) (Å)	d (D···A) (Å)	D—H···A (°)
O7—H7•••O5 **#0**	0.84	1.860 (3)	2.597 (4)	146
O4—H4A•••O5 **#0**	0.91	2.350 (3)	2.715 (4)	104
O4—H4B•••O1 **#1**	0.91	1.850 (2)	2.680 (3)	151

Symmetry transformations used to generate equivalent atoms:

[**#0** = x, y, z] and [**#1** = 1-x, 1-y, 1-z]

The inter- and intra-molecular C—H···Cl interactions, further stabilize the crystal packing. These interactions are illustrated in **Figure 5.3.1.5**. The relevant data is given in **Tables 5.3.1.5**.

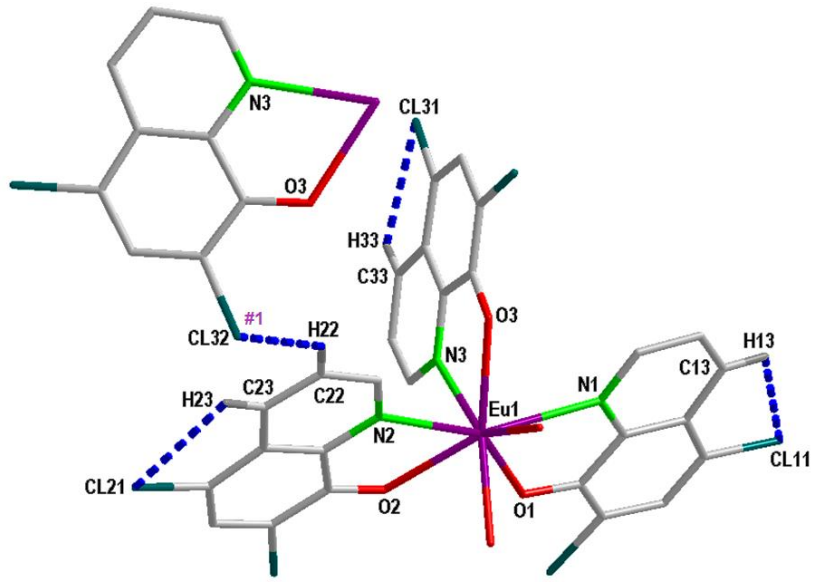

Figure 5.3.1.5: C—H•••Cl type of hydrogen bonding observed in 5. Hydrogen atoms, not taking part in the hydrogen bonding, are omitted for clarity. Hydrogen interactions are indicated by blue dotted lines.

The intra-molecular and inter-molecular C—H•••Cl interactions are illustrated in **Figure 5.3.1.5**. The hydrogen bonding is summarized in **Table 5.3.1.5**.

There are both inter and intra-molecular interactions.

There are three C—H•••Cl intra-molecular interactions observed and another C—H•••Cl inter-molecular interaction observed in **Figure 5.3.1.5,** further stabilizing the crystal packing.

Table 5.3.1.5: Observed C—H•••Cl hydrogen bonding in 5.

D—H•••A	d (D—H) (Å)	d (H•••A) (Å)	d (D•••A) (Å)	D—H•••A (°)
C13—H13•••Cl11 **#0**	0.95	2.716 (1)	3.093 (5)	146
C23—H23•••Cl21 **#0**	0.95	2.739 (2)	3.107 (5)	104
C33—H33•••Cl31 **#0**	0.95	2.736 (2)	3.105 (5)	104
C22—H22•••Cl32 **#1**	0.95	2.820 (1)	3.573 (5)	133

Symmetry transformations used to generate equivalent atoms: [**#0** = x, y, z] and [**#1** = 1-x, 1-y, 1-z]

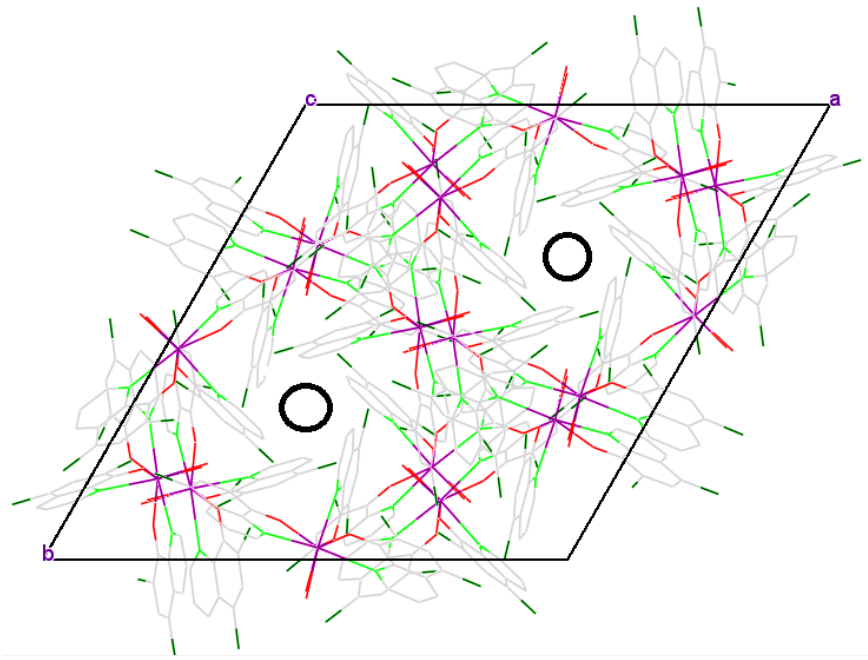

Figure 5.3.1.6: Molecular packing 5.

The observed molecular packing in **Figure 5.3.1.6** shows a tight packing of eighteen molecules in one unit cell along the *c*-axis. It appears to form two pseudo rings systems constructed by the packing of **5** (indicated by rings in Figure 5.3.1.6).

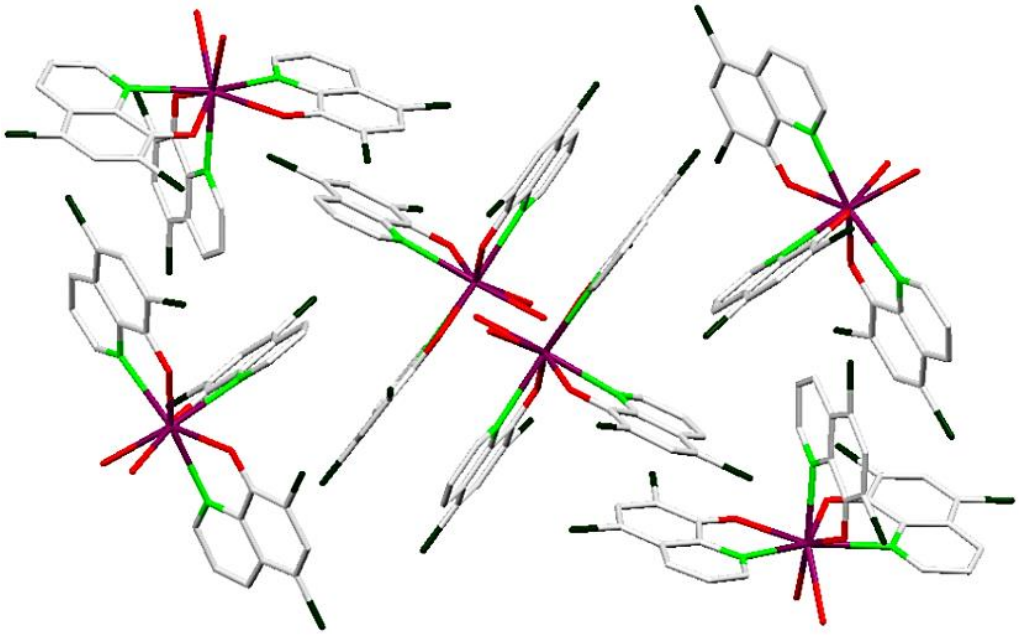

Figure 5.3.1.7: The packing of one-third of compound 5 in the unit cell.

There appears to be three distinct groupings in one unit cell amounting to eighteen molecules per unit cell along the *a*,*b*-axis. Focusing on one group to look at any systematic packing, it appears that the center molecules pack head to head.

5.3.2 The crystal structure of:

κ^2-O,O'-*tris*-[(5,7-dichloro-8-hydroxyquinoline)(Methanol)Europium(III)]

The complex, κ^2-O,O'-[Eu(57dcOx)$_3$·EtOH] (**5**), was synthesized as described in **Paragraph 3.8.1.2.** The asymmetric unit contains one full coordination compound. The complex crystallizes in a triclinic crystal system in the *P1 space* group with one formula units per unit cell (Z = 1). The numbering scheme of the title complex is shown in **Figure 5.3.2.1**

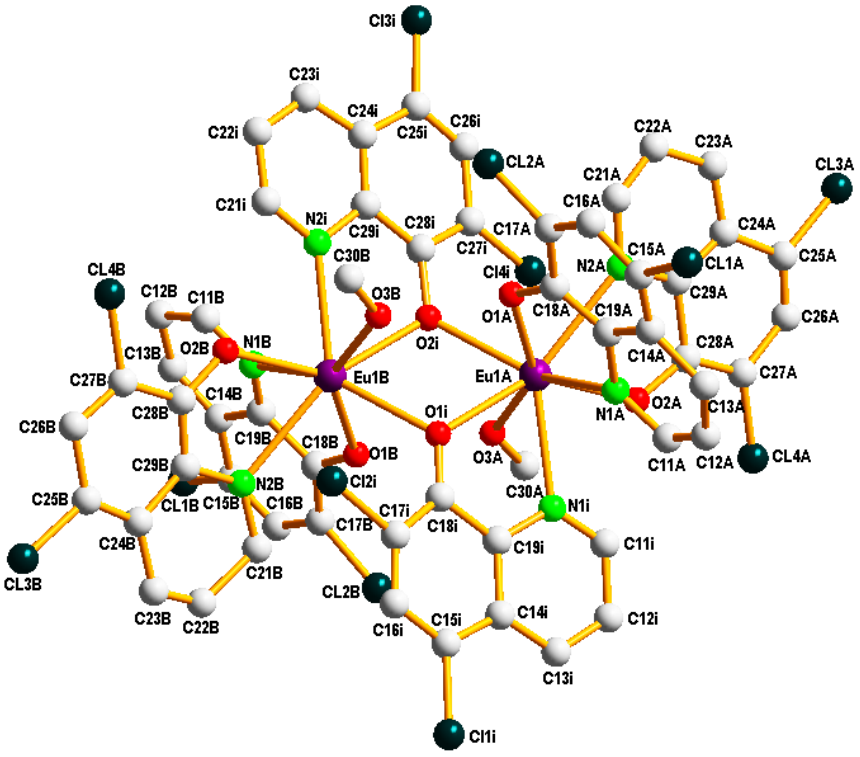

Figure 5.3.2.1: The representation of the molecular structure of (6). The structural model shows isotropic displacement parameter for better visibility of the atoms and naming. Hydrogen atoms are omitted for clarity. The solvent molecule of this crystal structure is toluene and it cannot be displayed since it is highly disordered. The naming in which atoms are marked 'i', are those from the ligand that bridges the two metal ions to form the dimer.

Due to the complexity of the europium complex as well as the disorder found in several atoms which cannot at present be defined due to instability of the least square refinement, the crystal structure of compound **6** is here refined isotropically. Attempts to obtain crystal with improved crystallinity are currently being conducted.

Table 5.3.2.1: Crystal data and structure refinement of 6.

Identification code	**Compound 6**	
Empirical formula	$C_{56}H_{30}N_6O_8Cl_{12}Eu_2$	
Formula weight	**1854.16**	
Temperature	**100.0 K**	
Wavelength	**0.71073 Å**	
Crystal system	**Triclinic**	
Space group	***P1***	
Unit cell dimensions	**a = 10.720 (5) Å**	**α= 65.288(5) °**
	b = 12.232 (5) Å	**β= 71.325(5) °**
	c = 14.267(5)Å	**γ = 88.067(5)°**
Volume	**1599.1(11)Å^3**	
Z	**1**	
Density (calculated)	**1.925 Mg/m^3**	
Absorption coefficient	**2.513 mm^{-1}**	
F(000)	**892.0**	
Crystal size	**0.122 × 0.189 × 0.221 mm^3**	
Theta range for data collection	**5.78 to 56.73**	
Index ranges	**$-14 \le h \le 14$, $-16 \le k \le 16$, $-16 \le l \le 18$**	
Reflections collected	**34962**	
Independent reflections	**14631 [R_{int} = 0.0607, R_{sigma} = 0.1083]**	
Completeness to theta = 26.000°	**99.6 %**	
Refinement method	**Full-matrix least-squares on F^2**	
Data / restraints / parameters	**14631/3/759**	
Goodness-of-fit on F^2	**1.018**	
Final R indices [I>2sigma(I)]	**R_1 = 0.0652, wR_2 = 0.1797**	
R indices (all data)	**R_1 = 0.1058, wR_2 = 0.2211**	
Largest diff. peak and hole	**3.80/-1.23Å^{-3}**	

In κ^2-O,O'-*tris*-[(5,7-dichloro-8-hydroxyquinoline)(methanol)Eu(III)] (**6**), there is one molecule in an asymmetric unit cell in a dimeric formation.

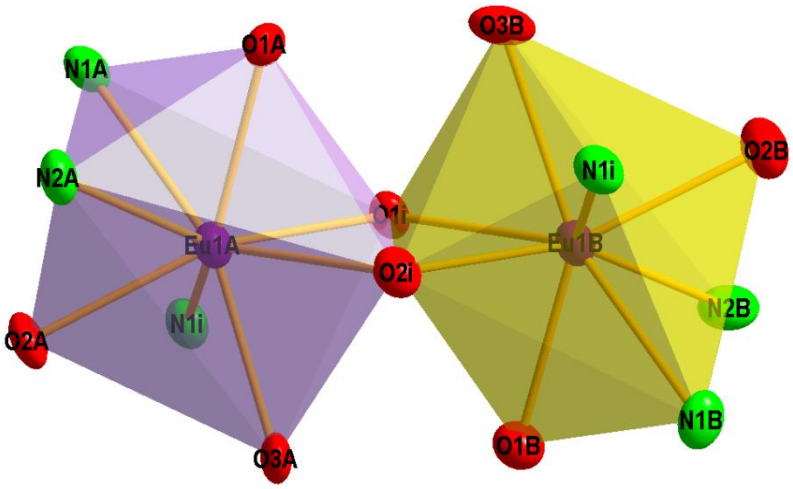

Figure 5.3.2.2: Illustration of a square anti-prismatic coordination polyhedron as found for the title compound.

Table 5.3.2.2: Selected bond distances (Å) and angles (°) of compound 6.

Bond Distances (Å)			
Eu1A-N1A	2.660 (7)	**Eu1A-O1A**	2.349 (9)
Eu1A-N2A	2.651 (7)	**Eu1A-O2A**	2.266 (7)
Eu1A-N1i	2.575 (9)	**Eu1A-O1i**	2.427 (7)
Eu1B-N1B	2.589 (6)	**Eu1B-O1B**	2.381 (9)
Eu1B-N2B	2.670 (7)	**Eu1B-O2B**	2.303 (7)
Eu1B-N2i	2.576 (10)	**Eu1B-O2i**	2.395 (7)
Bond Angles (°)			
N1A - Eu1A - O1A	65.89 (14)	**N1B - Eu1b - O1B**	64.30 (17)
N2A - Eu1A - O2A	65.96 (16)	**N2B - Eu1B - O2B**	64.42 (16)
N1i - Eu1A - O1i	66.41 (16)	**N2i -Eu1B - O2i**	64.59 (16)
O2i - Eu1A - O3A	71.95 (17)	**O1i - Eu1B - O3B**	70.23 (17)
Eu1A- O2i - Eu1B	109. 62 (18)	**Eu1B - O1i - Eu1A**	108. 76 (18)

The respective Eu-O and Eu-N bond distance comparisons in each ligand wing are slightly out of range from 2.266 (7) Å to 2.427 (7) Å for Eu-O and 2.575 (9) Å to 2.670 (7) Å for Eu-N bonds as illustrated in **Table 5.3.2.2**.

The bite angles are close to what was observed in **5**; whereby the average bite angles of the ligand units (O-Eu-N) of the title compound is 66.086 (15)˚ from the **A** side and 64.436 (16)˚ from the **B** side of **6**.

All bond distances and angles are considered to be normal and fall within the range reported for similar complexes[16].

In **Figure 5.3.2.3**, there is a flat plane made up by Eu1B, O1i, Eu1A, O2i atoms. The four atoms that makes plane 1 gives a rectangular shape in the heart of the dimer. The plane angles are tabled below.

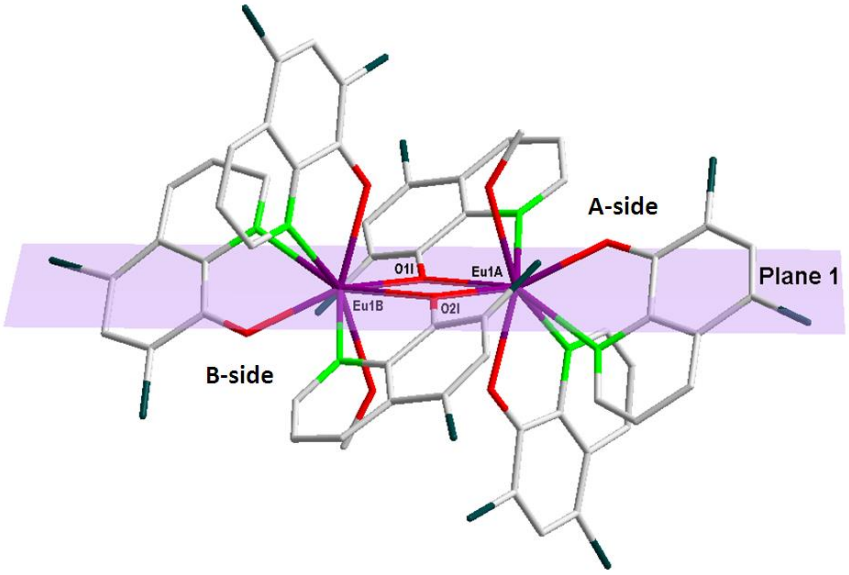

Figure 5.3.2.3: Illustration showing the flat equatorial plane of 6. The ending alphabets in the naming of the atoms denote the molecular side of the atom as dictated by the metal atoms.

[16] C.S. Erasmus, J.C.A. Boeyens, Acta Cryst., B26, 1843, 1970.

In **Figure 5.3.2.4** and **Figure 5.3.2.5**, planes are constructed to calculate the relations of the preferred ligand orientations around the metal center. The dihedral angles are indicated in **Table 5.3.1.3**.

Table 5.3.1.3: Dihedral angles between the constructed planes in compound 6.

	Dihedral Angle (˚)
Plane 1& 2	88.57
Plane 1& 3	88.45
	Dihedral Angle (˚)
Plane 4 & 5	81.97
Plane 6 & 7	82.68

Plane 1:Eu1B-O1i-Eu1A-O2i.
Plane 2: Eu1A, C11A, C12A, C13A, C14A, C15A, C16A, C17A, C18A, C19A, N1A, O1A, Cl1A, Cl2A
Plane 3: Eu1B, C11B, C12B, C13B, C14B, C15B, C16B, C17B, C18B, C19B, N1B, O1B, Cl1B, CL2B
Plane 4: Eu1A, C21A, C22A C23A, C24A, C25A, C26A, C27A, C28A, C29A, N2A, O2A, CL3A, CL4A.
Plane 5: Eu1A, C11A, C12A C13A, C14A, C15A, C16A, C17A, C18A, C19A, N1A, O1A, CL1A, CL2A
Plane 6: Eu1B, CA1B, C12B, C13B, C14B, C15B, C16B, C17B, C18B, C19B, N1B, O1B, CL1B, CL2B.
Plane 7: Eu1B, C21B, C22B, C23B, C24B, C25B, C26B, C27B, C28B, C29B, N2B, O2B, CL3B, CL4B.

The constructed planes below illustrate the relation of ligands and their relative orientation around the metal center.

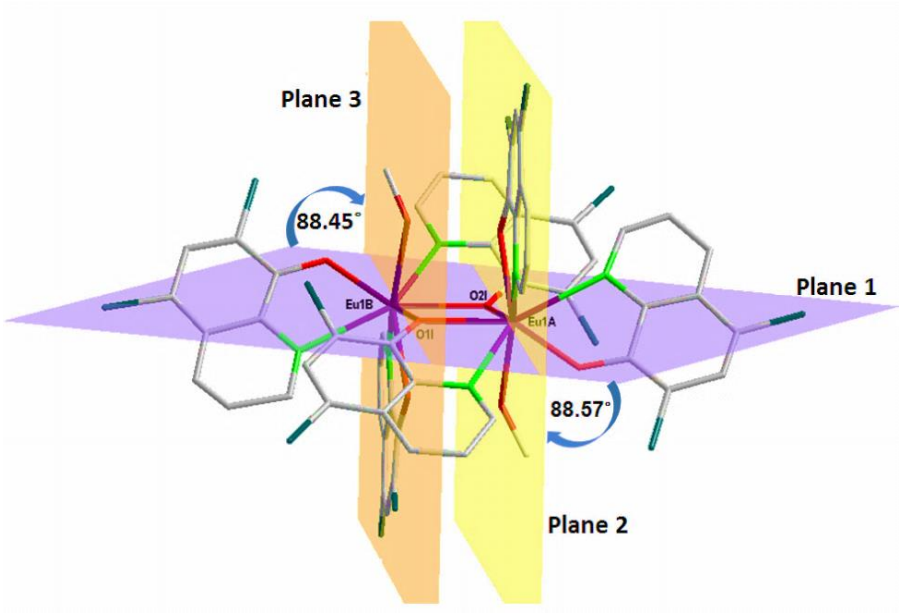

Figure 5.3.2.4: Illustration of the relations between the equatorial and perpendicular planes of 6.

Two planes are nearly perpendicular to plane 1, 2 and 3 constructed from both the **A** side and the **B** side of the molecule respectively, with dihedral angles of 88.57˚ and 88.45˚ respectively.

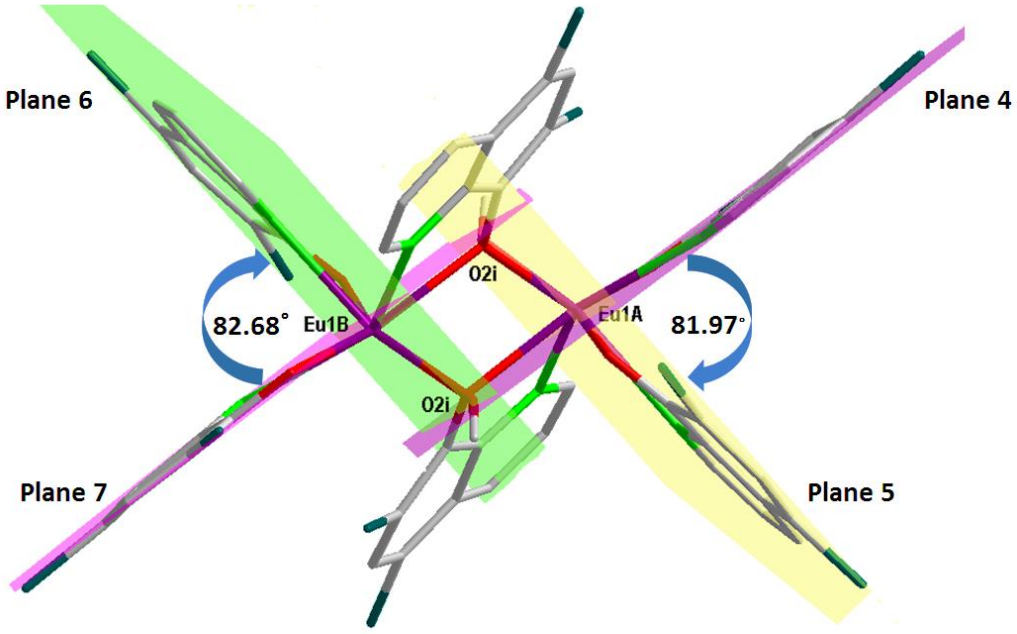

Figure 5.3.2.5: Illustration of the relations between the equatorial and perpendicular planes of 6.

In **Figure 5.3.2.5**, planes constructed are to view how the ligand wings accommodated each other in **6**.

There are two intra-molecular interactions observed between the hydrogen atoms from the two bridging ligands to the oxygen atoms of Ligand 2 in the **A** side and Ligand 2 in the **B** side respectively.

Furthermore, another intra-molecular interaction is observed between the hydrogen atom of Ligand 2 and the oxygen atom if Ligand 1. All this interactions are illustrated below in **Figure 5.3.2.6**.

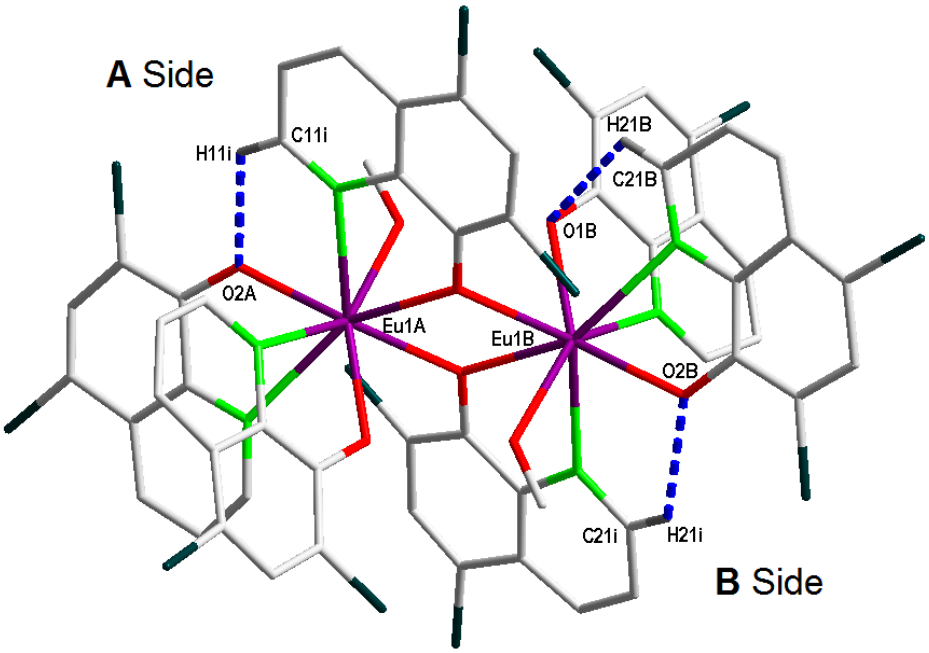

Figure 5.3.2.6: Schematic representation showing the C—H•••O hydrogen bonding in 6. Hydrogen atoms, not taking part in hydrogen bonding are omitted for clarity.

Table 5.3.2.4: Observed C—H•••O hydrogen bonding in 6.

D—H•••A	d (D—H) (Å)	d (H•••A) (Å)	d (d•••A) (Å)	D—H•••A (°)
C11i—H 11i •••O2A	0.93	2.336 (9)	2.93 (4)	122
C21B—H21B ••• O1B	0.93	2.593 (10)	3.07 (3)	115
C21i—H21i ••• O2B	0.93	2.442 (9)	3.06 (4)	125

The intermolecular π-π stacking and C—Cl•••π interactions, further stabilize the crystal packing. These interactions are illustrated in **Figure 5.3.2.7, Figure 5.3.2.8 and Figure 5.3.2.9.** The relevant data is given in **Tables 5.3.2.5** and **Tables 5.3.2.7.**

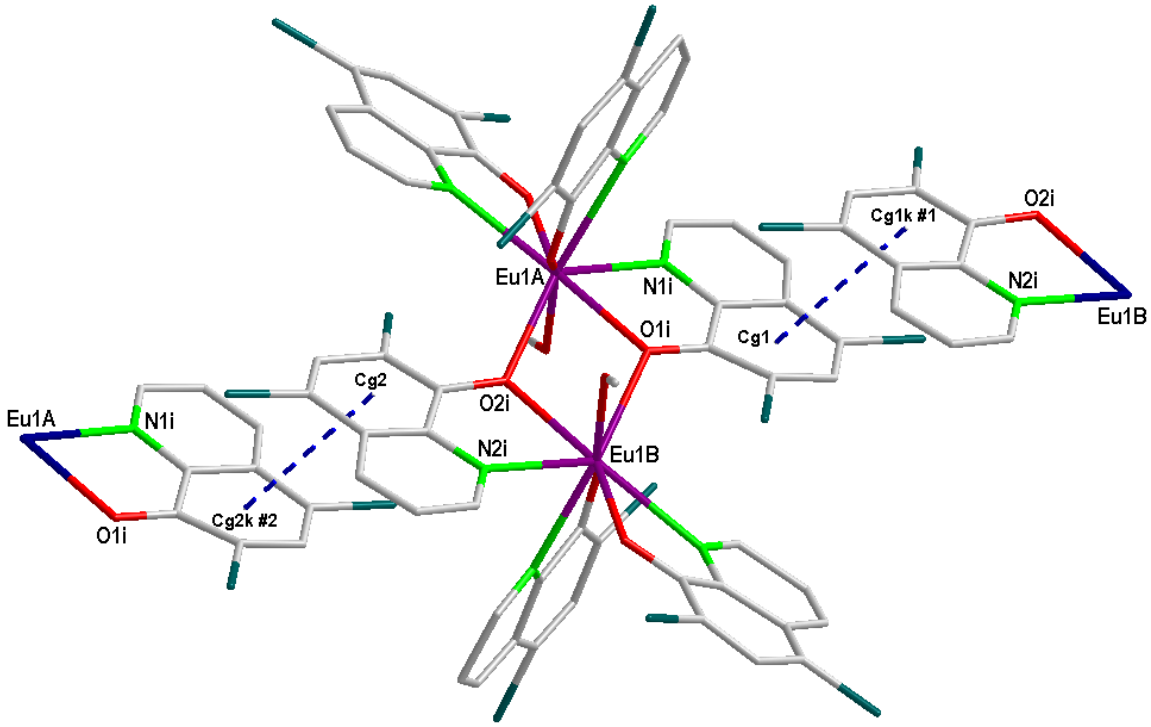

Figure 5.3.2.7: The schematic representation of the inter-molecular π-π-stacking of 6. Hydrogen atoms have been omitted for clarity. Centroid atoms ending with 'k', resembles symmetry-generated molecules. The numbering on the nitrogen and oxygen atoms denotes the number of the ligand coordinated around the metal centre.

The π-π stacking is observed between the neighbouring molecules with centroid-to-centroid distances of 3.70 (2) Å and 3.70 (2) Å respectively as indicated in **Table 5.3.2.5.** The π-stacking is observed between phenoxide rings of the bridging ligands and the neighbouring bridging ligand of symmetry generated neighbouring molecules.

Table 5.3.2.5: *π-π* Interactions observed between the bridging phenoxide rings of 6.

Centroid Atom	Centroid Atom	Distance between centroid atoms (Å)
Cg1	Cg2k **#1**	3.70 (2)
Cg2	Cg2k **#2**	3.70 (2)

Symmetry transformations used to generate equivalent atoms:
[**#1** = 1+x, +y, +z] and [**#2** = -1+x, +y,+z]
Cg1 = Centroid atom of C14i, C15i, C16i, C17i, C18i, C19i.
Cg2 = Centroid atom of C24i, C25i, C26i, C27i, C28i, C29i.

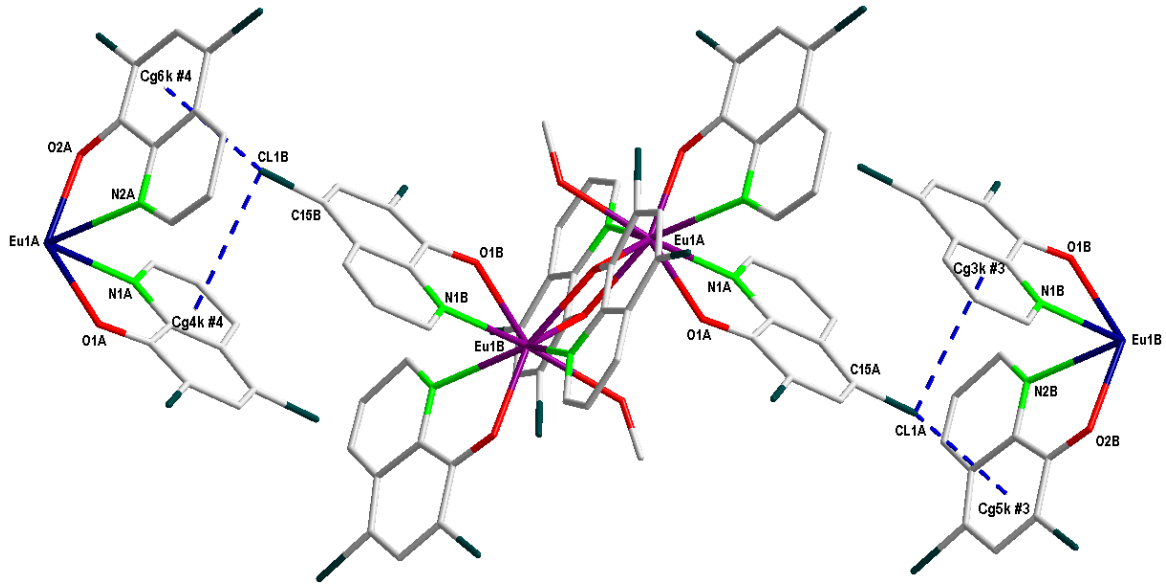

Figure 5.3.2.8: The geometrical representation of the C—Cl•••π inter-molecular interactions of 6. Hydrogen atoms have been omitted for clarity. Centroid atoms ending with 'k', resembles symmetry-generated molecules. The numbering of the nitrogen and oxygen denotes the number of the ligand coordinated.

The observed intra-molecular interaction is from the bifurcated chlorine atom in Ligand 1 in the **B** side of the molecule to the respective centroids in the phenoxide ring of Ligand 2 and the pyridyl ring of Ligand 1 of the **A** side of the neighbouring molecule.

The same interaction is observed on the **A** side of the parent structure. All the data for the interactions is tabled just below.

Table 5.3.2.6: C—Cl•••π Interactions observed in 6.

C—Cl	Centroid Atom	d (H•••Cg) (Å)	d (C•••Cg) (Å)	C—H•••Cg (˚)
C15A – Cl1A	Cg3k **#3**	3.570 (17)	3.95 (4)	90
C15A – Cl1A	Cg5k **#3**	3.463 (19)	5.11 (4)	160
C15B – Cl1B	Cg4k **#4**	3.584 (18)	3.92 (4)	87
C15B – Cl1B	Cg6k **#4**	3.430 (2)	5.17 (4)	167
C15i – Cl1i	Cg3k **#5**	3.323 (15)	4.42 (3)	116
C25i – Cl3i	Cg4K **#6**	3.354 (16)	4.37 (3)	117
C17i – Cl2i	Cg7 **#0**	3.497 (16)	3.98 (3)	92

Symmetry transformations used to generate equivalent atoms:
[**#0** = x, y, z], [**#3** = x, -1+y, 1+z], [**#4** = x, 1+y, -1+z], [**#5** = 1+x, y, z], [**#6** = -1+x, y, z].
Cg3 = Centroid atom of N1B, C11B, C12B, C13B, C14B, C19B.
Cg4 = Centroid atom of N1A, C11A, C12A, C13A, C14A, C19A.
Cg5 = Centroid atom of C24B, C25B, C26B, C27B, C28B, C29B.
Cg6 = Centroid atom of C24A, C25A, C26A, C27A, C28A, C29A.
Cg7 = Centroid atom of N2B, C11B, C22B, C23B, C24B, C29B. . .

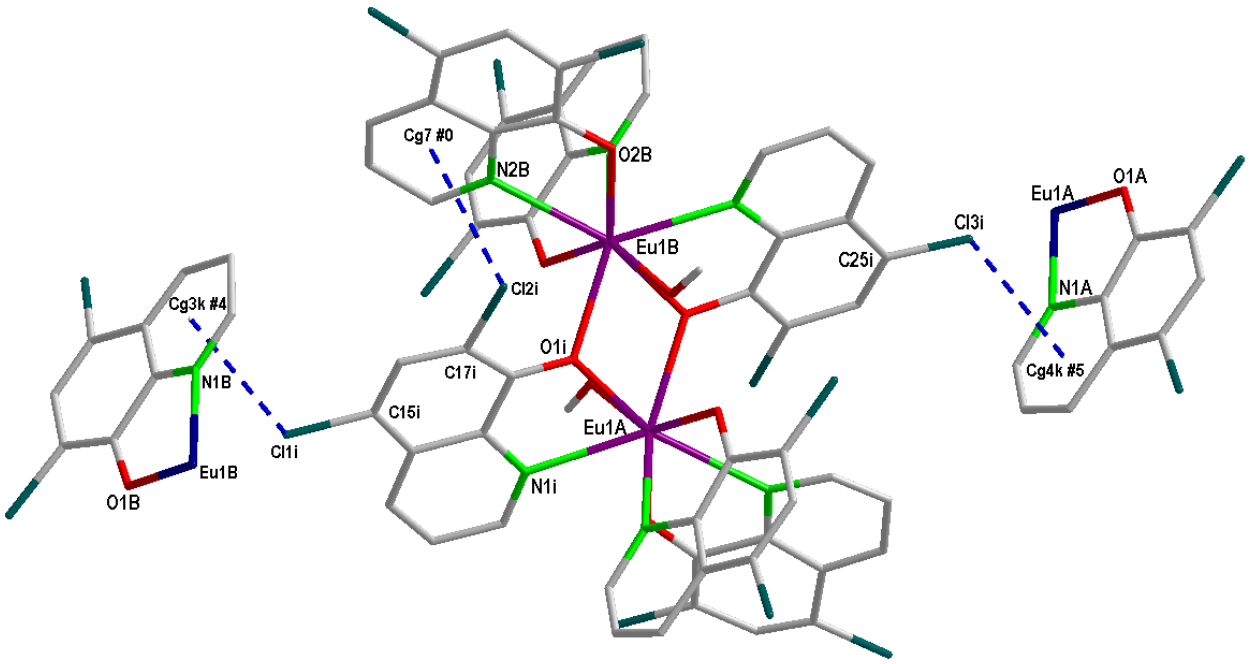

Figure 5.3.2.9: The geometrical representation of the C—Cl•••π inter-and intra-molecular interactions in 6. Hydrogen atoms have been omitted for clarity. Centroid atoms ending with 'k', resembles symmetry-generated molecules. The numbering of the nitrogen and oxygen denotes the number of the ligand coordinated.

There is an inter-molecular interaction of the same type occurring on both sides of the parent structure between the hydrogen atoms of the respective bridging ligands and the centroid of the pyridyl ring of the neighbouring molecules of Ligand 1 of the **A** side and Ligand 3 of the **B** side.

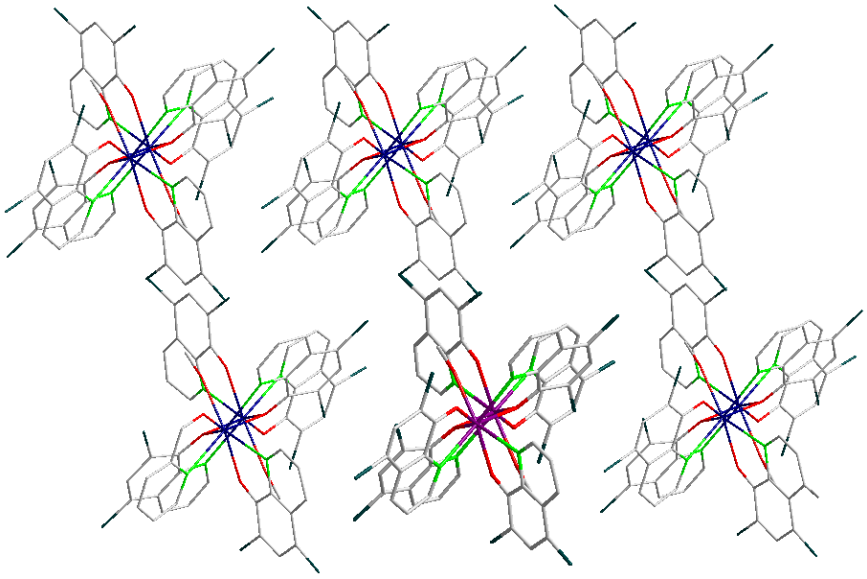

Figure 5.3.2.10: Packing of six unit cells of 6. The molecules with thinner bonds designs are symmetry generated molecules.

The lattice packing of 6 is observed in **Figure 5.3.2.10** along the *ab*-axis.

5.4 Conclusions

The crystal structures of two lanthanide metal complexes namely:

- *fac*-[(5,7-dichloro-8-hydroxyquinoline)$(H_2O)_2$Eu(III)] •EtOH•H_2O [**5**]
- κ^2-O,O'-*tris*-[(5,7-dichloro-8-hydroxyquinoline)Methanol Europium(III)] **[6]**

were analyzed and discussed in this chapter. A crystallographic investigation of the complexes in this study was considered important to fully understand the coordination chemistry of these complexes.

Compound **5** crystallizes in a trigonal crystal system, whereas compound **6**, crystallized in triclinic crystal system. Compound **5** was refined in a $R\bar{3}$ space group whereas compound **6** was refined in the $P\bar{1}$ space group. Complex **5** has eighteen formula units in the unit cell (Z = 18) and complex **6** has only one formula unit in the unit cell (Z = 1). The crystal structures of both complexes were stabilized by variety of hydrogen bond interactions namely: C—Cl•••π, C—H•••Cl, C—H•••π, π- π stacking interactions.

The selected bond angles and selected bond distances of interest are given in **Table 5.3.1**.
Complexes **5** and **6** have similar bond distances and angles. The Eu – O bond distances for compound **5** ranges from 2.343 (2) Å to 2.455 (2) Å and for compound **6** ranges from 2.266 (7) Å to 2.427 (7) Å for the **A** side and 2.303 (7) Å to 2.395 Å for the **B** side. The Eu – N bond distances of compound **6** ranges from 2.575 (9) Å to 2.660 (7) Å in the **A** side of the molecule and range from 2.576 (2) Å to 2.670 (2) Å in the **B** side of the molecule whereas in compound **5** the range is from 2.519 to 2.606(2). The respective average bite angles of the ligand pieces of **5** and **6** are 66.08 (15)˚ and 65.39 (4)˚ respectively as they are listed in **Table 5.3.1** .[17]

These above crystal structures compares well with those in literature.[17]

[17] P.J. Han, A.L. Rheighgold, W.C Togler, Inorg. Chem., 2003.

Table 5.3.1: Selected bond distances and bond angles of interest of both compound 5 and 6.

Bond Distances (Å)							
6				**5**			
Eu1A-N1A	2.660 (7)	**Eu1A-O1A**	2.349 (9)	**Eu1 - O1**	2.343 (2)	**Eu1-O5**	2.432 (2)
Eu1A-N2A	2.651 (7)	**Eu1A-O2A**	2.266 (7)	**Eu1 - O2**	2.365 (2)	**Eu1-N1**	2.606 (2)
Eu1A-N1i	2.575 (9)	**Eu1A-O1i**	2.427 (7)	**Eu1 - O3**	2.387 (2)	**Eu1-N2**	2.568 (3)
Eu1B-N1B	2.589 (6)	**Eu1B-O1B**	2.381 (9)	**Eu1 - O4**	2.455 (2)	**Eu1-N3**	2.519 (2)
Eu1B-N2B	2.670 (7)	**Eu1B-O2B**	2.303 (7)				
Eu1B-N2i	2.576 (10)	**Eu1B-O2i**	2.395 (7)				
Bond Angles (˚)							
N1A - Eu1A - O1A	65.89 (14)	**N1B - Eu1b - O1B**	64.30 (17)	**N1 - Eu1 - O1**	64.742 (4)	**Eu1 - O1 - C18**	125.014(7)
N2A - Eu1A - O2A	65.96 (16)	**N2B - Eu1B - O2B**	64.42 (16)	**N2 - Eu1 - O2**	65.225 (4)	**Eu1 - O2 - C29**	123.286(7)
N1i - Eu1A - O1i	66.41 (16)	**N2i -Eu1B - O2i**	64.59 (16)	**N3 - Eu1 - O3**	66.213 (4)	**Eu1 - O3 - C38**	121.046(7)
O2i - Eu1A - O3A	71.95 (17)	**O1i - Eu1B - O3B**	70.23 (17)	**O4 - Eu1 - O5**	67.480 (4)		
Eu1A- O2i - Eu1B	109. 62(18)	**Eu1B - O1i - Eu1A**	108. 76(18)				

6 Photoluminescence Studies of Group 13 Metal Ions and Lanthanide Ion.

6.1 Introduction

Tang and Van Slyke used *tris*-(8-hydroxyquinoline) aluminium $Al(Ox)_3$ as both the emissive and electron transporting layer in the development of the first multi-layered organic light emitting diode (OLED) in 1987.[1] Since then substantial progress has been made in the field, leading to more and more commercial OLED products (screens for mp3 players, cellphones and cameras). $Al(Ox)_3$ is still used in these devices due to its thermal stability, relatively good electron mobility and high fluorescence efficiency.[2] The emission of $Al(Ox)_3$ originates from the ligand's electronic $\pi - \pi^*$ transitions. These transitions are from the highest molecular orbital (HOMO) (situated on the phenoxide ring) to the lowest unoccupied molecular orbital (LUMO) (situated on the pyridyl ring).[2] The highest electron density of the HOMO of Alq_3 is located on the C-5, C-7 and C-8 positions of the phenoxide ring and for the LUMO on the C-2 and C-4 positions of the pyridyl ring[2] as positions are illustrated in **Figure 6.1.1**. It is predicted that the substituents on these respective positions can lead to either a blue or red shift and in the process tunning the emission color of $Al(Ox)_3$ chemically.[3,4]

The effect of substituents on the fluorescence maximum is investigated in this chapter. There are nine complexes synthesized in this manuscript with each three of group 13 metals ions (Al, Ga and In). The three ligands used in the synthesis of these respective complexes are:

[1] C.W. Tang, S.A. Van Slyke, Appl. Phys., 51, 913, 1987.

[2] M.M. Shi, J.J. Lin, Y.W. Shi, M. Ouyang, M. Wang and H.Z. Chen, Mater. Chem. Phys., 115, 841, 2009.

[3] A. Irfan, R. Cui, J. Zhang and L. Hao, Chem. Phys., 364, 39, 2009.

[4] Y. Qin, I. Kiburu, S. Shah and F. Jakle, Org. Lett., 8, 5227, 2006.

- 8-hydroxyquinoline
- 5,7-Dimethyl-8-hydroxyquinoline
- 5,7-Dichloro-8-hydroxyquinoline.

The respective ligand substitutions are on the position 5 and 7 of the phenoxide ring. The relative carbon positions are indicated in **Figure 6.1.1**. These nine complexes comprises of three metal complexes for each metal ion with each of the above given ligand derivatives. Moreover, the structural conformations of all these complexes is closely monitored to investigate the impact it has on the luminescent characteristic of these respective complexes.

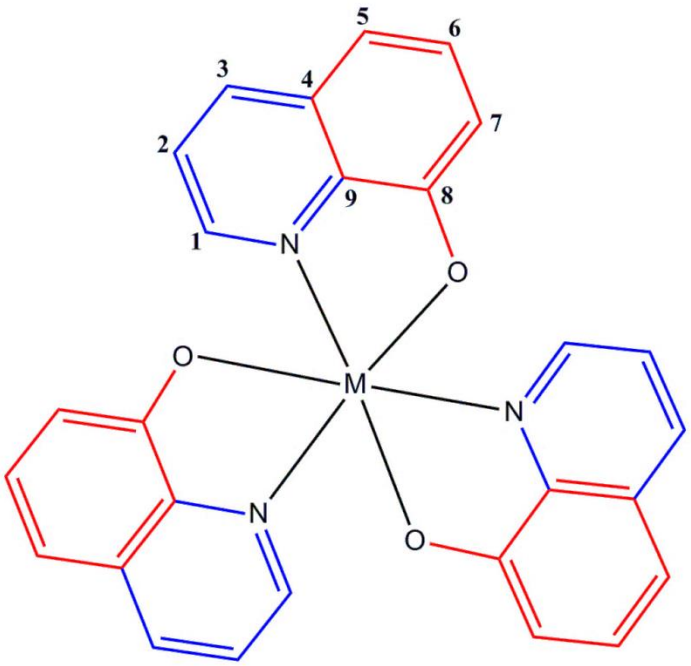

Figure 6.1.1: Schematic diagram of a typical $M(Ox)_3$ complex. The red ring indicates the phenoxide side and the blue ring indicates the pyridyl side in the quinolinol ligand structure. The numbering of the one ligand wing indicates the relative carbon positions in the respective ligand wings.

6.2 Experimental

The photoluminescence (PL) spectra of the different samples were taken using a Cary Eclipse spectrophotometer equipped with a 15 W Xenon flash lamp that flashes at a rate of 80 flashes per second with an average pulse width of 2-3 μs. A slide width of 2.5 nm was used (unless otherwise stated).

6.3 Effects of substituents on the fluorescence of $M(Ox)_3$ Complexes.

Figure 6.4.1. shows the solid state excitation and emission spectra of the three $[Al(Ox)_3]\cdot EtOH$ derivatives. All the samples were excited at 343 nm. This wavelength correlates with a higher energy electronic transition (S_4 and above).[5,6.] The $[Al(Ox)_3]\cdot EtOH$ sample has an emission peak at 517 nm. This can be interpreted as the Franck-Condon (or Stokes) shift, which results from large conformational energy changes upon optical excitation. The broadness of the peak can also be attributed to these conformational changes, due to strong exciton-phonon couplings.[7] In literature $Al(Ox)_3$ is known as a singlet emitter.[8] The emission is due to the relaxation of an excited electron from the S_1-S_0 level.

The highest electron density of $[Al(Ox)_3]\cdot EtOH$ HOMO is located at the C-5, C-7 and C-8 positions of the phenoxide oxygen. It is predicted that an electron-withdrawing group at these positions will lead to a blue shift in the emission spectrum. In the case of $[5dcAl(Ox)_3]$, a red shift of ~ 13 nm to 530 nm was observed. Shi et al. [5] found that in the case of $5FAl(Ox)_3$ the lone electron pair on the F atom and the high electron density at the C-5 position will cause the F group to take part in forming the HOMO of $Al(Ox)_3$ through a conjugation effect, giving rise to the higher HOMO-LUMO gap and a red shift in the emission peaks. The Cl substituents in

[5] V.V.N. Ravi Kishore, A. Aziz, K.L. Narasimhan, N. Periasamy, P.S. Meenakshi and S. Wategaonkar. Synth. Met. 126, 199, 2002.

[6] W. Stampor, J.Kalinowski, G. Marconi, P. Di Marco, V Fattori and G. Giro, Chem. Phys. Lett., 283, 373, 1998.

[7] P.E. Burrows, Z. Shen, V. Bulovic, D.M. McCarty and S.R. Forrest, J. Appl. Phys., 79, 7991,1996.

[8] A.D. Walser, R. Priestley and R. Dorsinville. Synth. Met. 102, 1552, 1999.

[57dcAl$(Ox)_3$] also contain lone electron pairs, which might cause the HOMO level to be higher leading to the observed red shift.

57dmAl$(Ox)_3$ shows a red shift of 41 nm to 558 nm in its emission spectrum. A similar shift was found by Singh et al.[9] in 57dmZn$(Ox)_3$ to 560 nm. The shift is due to a decrease in the band gap of the material. Qin et al.[4] reported that electron-donating groups and groups capable of extended π conjugation at the 5 position of the phenoxide ring should lead to higher HOMO levels and smaller HOMO-LUMO gaps, thus resulting in a red shift.

There was a significant decrease in the PL intensity [57dcAl$(Ox)_3$] and [57dmAl$(Ox)_3$] compared to that of Al$(Ox)_3$. Sapochak et al. suggested that the stronger coupling of the metal-ligand stretching coordinating to the electronic transition in Al$(Ox)_3$ may provide additional paths for non-radiative decay.[10] The decrease in the PL intensity is therefore reasonable, because the conjugated effect makes the coupling of the metal-ligand stronger which will lead to an increase in the energy loss in the excited state vibration.

The [57dmGa$(Ox)_3$]·DCM, [57dcGa$(Ox)_3$], [57dmIn$(Ox)_3$] and [57dcIn$(Ox)_3$] samples are showing the same behavior as the [Al$(Ox)_3$]·EtOH samples (**Figure 6.4.1 (a)** and **(b)**). Zhang et al.[12] reports that the luminescence of the ligand is strongly affected by the electron cloud overlapping between the ligand and metal ion. Regardless of the direction of energy transfer (metal to ligand (fluorescence) or ligand to metal (phosphorescence)), the electron cloud between the metal and ligand strongly determines the efficiency of intra-molecular transfer. By attaching substituents to the quinoline ligand the electron cloud of the ligand is altered and should lead to a change in emission wavelength.

All the samples are showing one broad emission peak. The [57dmGa$(Ox)_3$]·DCM sample is red shifted by ~ 48 nm from 520 nm – 568 nm and the [57dcGa$(Ox)_3$] sample by ~ 25 nm to 545 nm. The [57dmIn$(Ox)_3$] sample is red shifted by ~ 46 nm from 515 nm to 561 nm and the [57dcIn$(Ox)_3$] sample by ~ 29 nm to 544 nm.

[9] K. Singh, A. Kumar, R. Srivastava, P.S. Kadyan, M.N. Kamalasanan and I. Singh, Opt. Mater., 34, 221, 2011.

[10] L.S. Sapochak, A. Padmaperuma, N. Washton, F. Endrino, G.T. Schmett, J. Marshall, D. Fogerty, P.E. Burrows and S.R. Forrest, J. Am. Chem. Soc., 123, 6300, 2001.

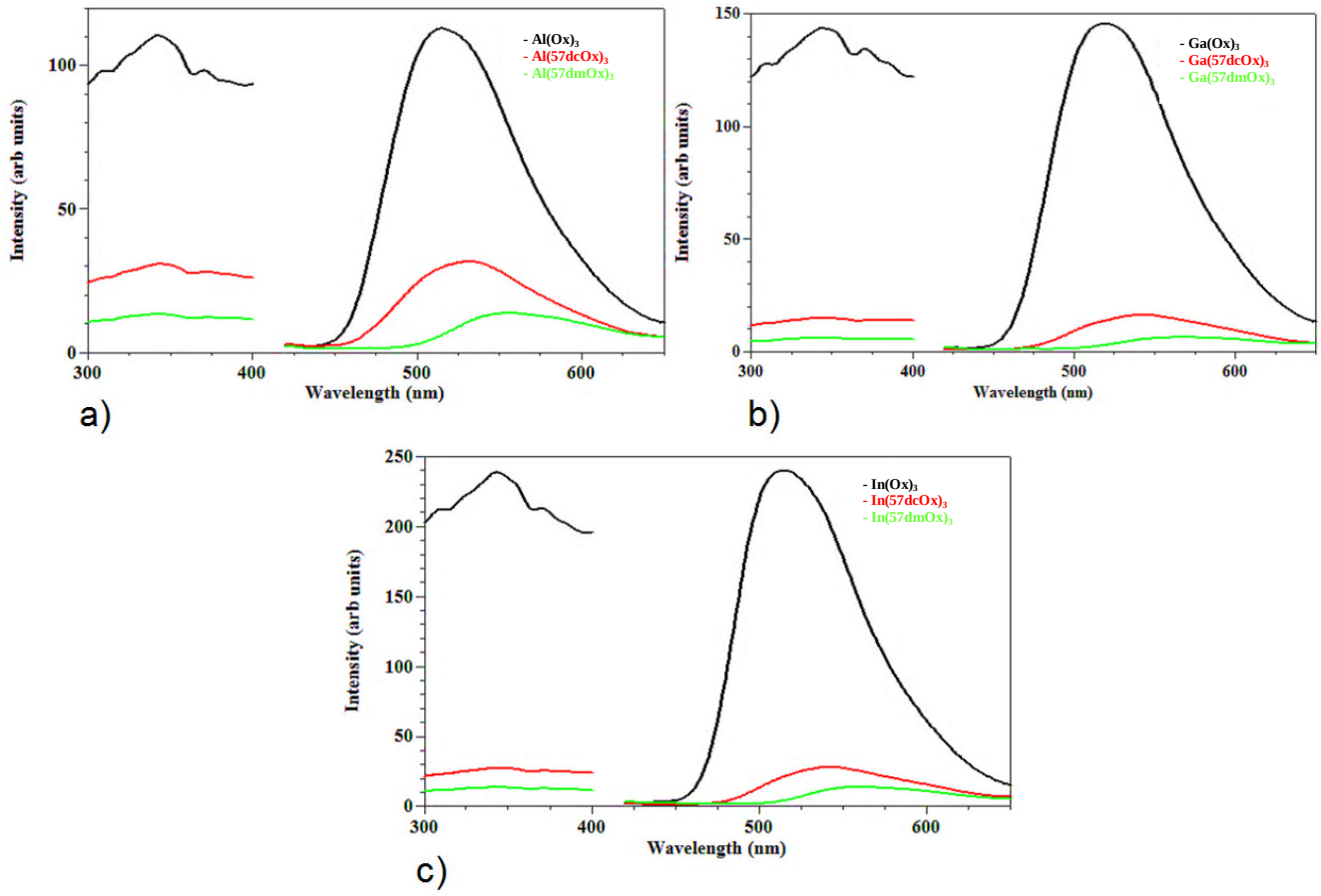

Figure 6.4.1: Fluorescence spectrums of all group 13 metal complexes with respective ligand derivatives. The solvent molecules are not included in the naming of the complexes for clarity purposes.

Figure 6.4.2 shows the emission spectra for the (a) 5,7-dichloro and (b) 5,7-dimethyl substituted quinolinol with various group 13 metal ions. It can be seen that the respective metal ions are not effecting the emission maximum as it was anticipated. Both the Ga and In complexes are slightly red shifted from the Al complexes.

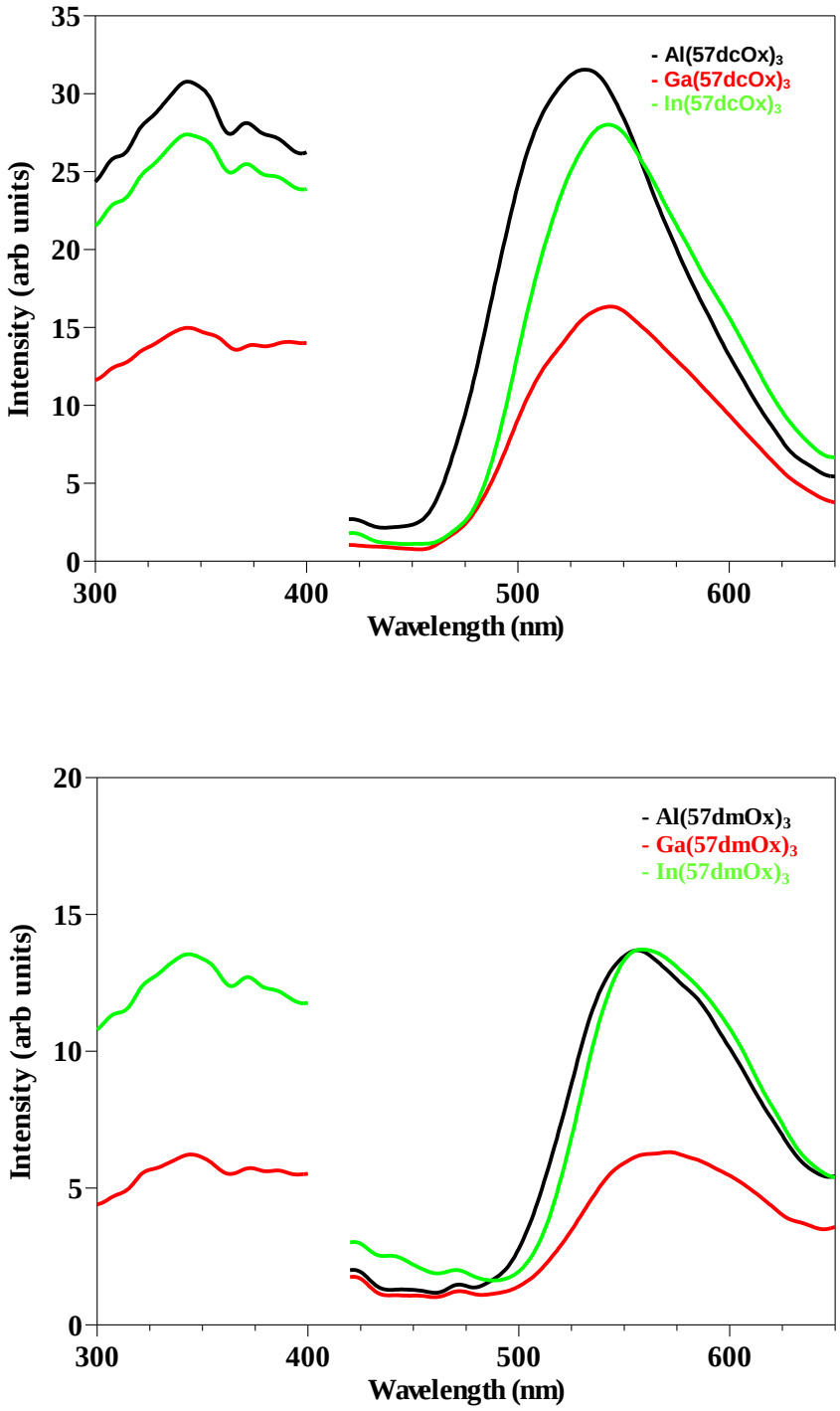

Figure 6.4.2: Fluorescence spectrums of all group 13 metal complexes with respective modified ligand derivatives. The solvent molecules are not included in the naming of the complexes for clarity purposes.

6.4 Effects of different group 13 metals on the fluorescence of $M(Ox)_3$ Complexes.

It is known that the emission of $M(Ox)_3$ compounds originates from the ligand's electronic π- π* transitions. This is from the highest occupied molecular orbital (HOMO) that is mainly situated on the phenoxide ring to the lowest unoccupied molecular orbital (LUMO) situated on the pyridyl ring[2]. The nature of the metal ion has, however, been shown to influence the emission color, stability, efficiency and evaporation of the metal complex.[11] Not all metals can be coordinated with the 8-hydroxyquinoline ligand and still be used as fluorescent materials. A few general rules which govern the fluorescence of metal chelates of 8-hydroxyquinolinehave been formulated:

- Chelates with metal ions that are paramagnetic are essentially non-fluorescent due to a high rate of intersystem crossing from the singlet to triplet state (e.g. Cr, Ni).

- Fluorescence is reduced with increasing atomic number of the metal ion, also caused by an increase in the rate of intersystem crossing, known as the heavy atom effect. For example, *mer*-$[Al(Ox)_3]\cdot EtOH$ will be more fluorescent than *fac*-$[Ga(Ox)_3]\cdot 0.5\cdot EtOH$ which, in turn, is more fluorescent than $In(Ox)_3$.

- As the covalent nature of the metal-ligand bonding (primarily metal-nitrogen) is increased, the emission shifts to longer wavelengths. For example, the chelates formed by In will emit at longer wavelengths than those formed by Al. On the other hand, more ionic-metal-ligand bonding results in a blue shift. For example, $Mg(Ox)_2$ will emit at a shorter wavelength compared to $Zn(Ox)_2$.

[11] C.H. Chen and J. Shi, Coord. Chem. Rev., 171,161, 1998.

The effect that Al^{3+}, Ga^{3+} and In^{3+} have on the luminescent properties of $M(Ox)_3$ was investigated. **Figure 6.5.1** shows the absorption and emission spectra of the three $M(Ox)_3$ samples. The *mer*-$[Al(Ox)_3]\cdot EtOH$ sample has an emission maximum at 517 nm, while the *fac*-$[Ga(Ox)_3]\cdot 0.5\cdot EtOH$ and *fac*-$[In(Ox)_3]\cdot 2H_2O$ samples have maximums at 520 nm and 515 nm respectively. The emission of *mer*-$[Al(Ox)_3]\cdot EtOH$ corresponds to that in literature[8], but the emission of *mer*-$[Ga(Ox)_3]\cdot 0.5\cdot EtOH$ and *fac*-$[In(Ox)_3]\cdot 2H_2O$ are blue shifted from that reported for *mer*-$Ga(Ox)_3$ and *mer*-$In(Ox)_3$ in literature.[12] It is reported that *fac*-$Al(Ox)_3$ shows a blue shift of 0.2 eV.[13,14] Brinkmann et al. also reports a blue shift in *fac*-$Ga(Ox)_3$.[15]

From NMR studies(see chapter 3), it can be seen that *mer*-$[Al(Ox)_3]\cdot EtOH$ isomer was synthesized, but that *fac*-$[Ga(Ox)_3]\cdot 0.5\cdot EtOH$ and *fac*-$[In(Ox)_3]\cdot 2H_2O$ were of facial isomer. The *fac*-$[Ga(Ox)_3]\cdot 0.5\cdot EtOH$ sample is blue shifted by ~ 0.11 eV and the Inq_3 sample is blue shifted by 0.9 eV from the values reported in literature for meridional isomer. It is believed that the different packing of the crystal together with the changed symmetry of the molecule are responsible for the blue shift.[13]

The $In(Ox)_3$ sample shows the highest intensity. This is contradictory to the heavy atom effect, where *mer*-$[Al(Ox)_3]\cdot EtOH$ is supposed to have the highest intensity. The *mer*-$[Al(Ox)_3]\cdot EtOH$ was however subjected to long time exposure to atmospheric conditions, before the fluorescence measurements were done. It is known that Alq_3 will decompose to non-radiative product when stored under atmospheric conditions.[16] The phenoxide ring will rupture and form C=O and C-OH bonds when in contact with O_2 and H_2O in the atmosphere.

[12] V.K. Shukla and S. Kumar, Photonics, India, Proceedings, 439, 2004.

[13] M. Cölle, R.E. Dinnebier and W. Brutting, Chem. Commun., 2908, 2002.

[14] A. Curioni, M. Boero and W. Andreoni, Chem. Phys, Lett. 294, 263, 1998.

[15] M. Brinkmann, B. Fite, S. Pratontep and C. Chaumont, Chem. Mater., 16, 4627, 2004.

[16] F.P. Rosseli, W.G. Quirino, C. Legnani, V.L. Calil, K.C. Teixeira, A.A. Leitao, R.B. Capaz, M. Cremona and C.A. Achete, Org. Electron., 10**,** 1417, 2009.

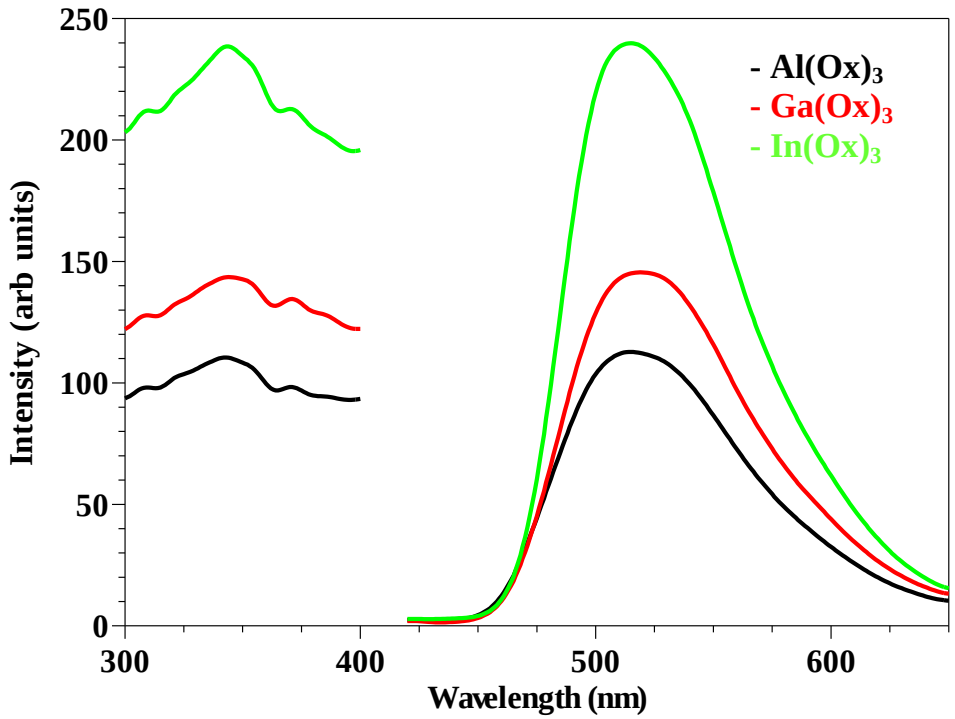

Figure 6.5.1: Fluorescence spectrums of all group 13 metal complexes. The solvent molecules are not included in the naming of the complexes for clarity purposes.

The central metal ion plays two kinds of roles:

- It decreases intra-molecular vibration and increases the energy of the radiative transition.
- It modulates the excited state of the ligand through charge transfer.

Uncoordinated 8-hydroxyquinoline does not show any emission because of its intra-molecular freedom (**Figure 6.5.2**). The introduction of metal ions effectively reduces the loss of intra-molecular energy and facilitates strong emission.

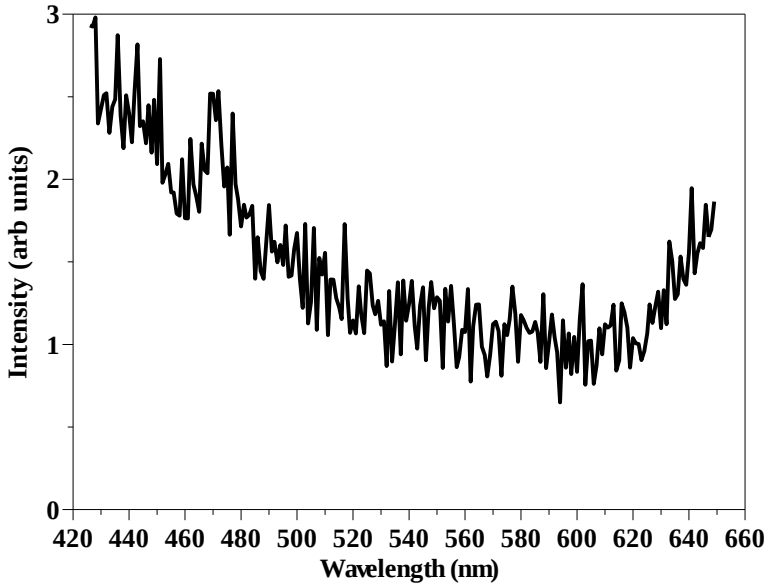

Figure 6.5.2: Fluorescence spectrum of 8-hydroxyquinoline excited at 343 nm.

6.5 Europium complexes

Figure 6.6.1 shows the fluorescence spectrum of the two **Eu complexes**. Both samples were excited at 334 nm and a slit width of 5 nm was used. Three distinct peaks can be seen for both the complexes. The first peak is assigned to singlet emission of the quinoline nucleus.[17] The other two peaks are assigned to the 5d-4f transition of Eu^{2+}.[11] The reason that two peaks are observed might be ascribed to different forms of the complex or the splitting of the 5d and 4f levels. Eu^{3+} emission is observed at 590 nm – 700 nm.[18] Further measurements needs to be done in this region to confirm if any Eu^{3+} emission is present. Laser PL measurements with a 325 nm HeCd laser as excitation source might also be helpful to determine the Eu^{3+} emission, as no second order excitation source is observed with this setup.

[17] F. Rizzo, F. Meinardi, R. Tubino, R. Pagliarin, G. Dellepiane and A. Papagni, Synthetic Met., 159, 356, 2009.

[18] J.C. Zhang, Y.Z. Long, H.D. Zhang, B. Sun, W.P. Hanab and X.Y. Sunc, J. Mater. Chem. C., 2, 312, 2014.

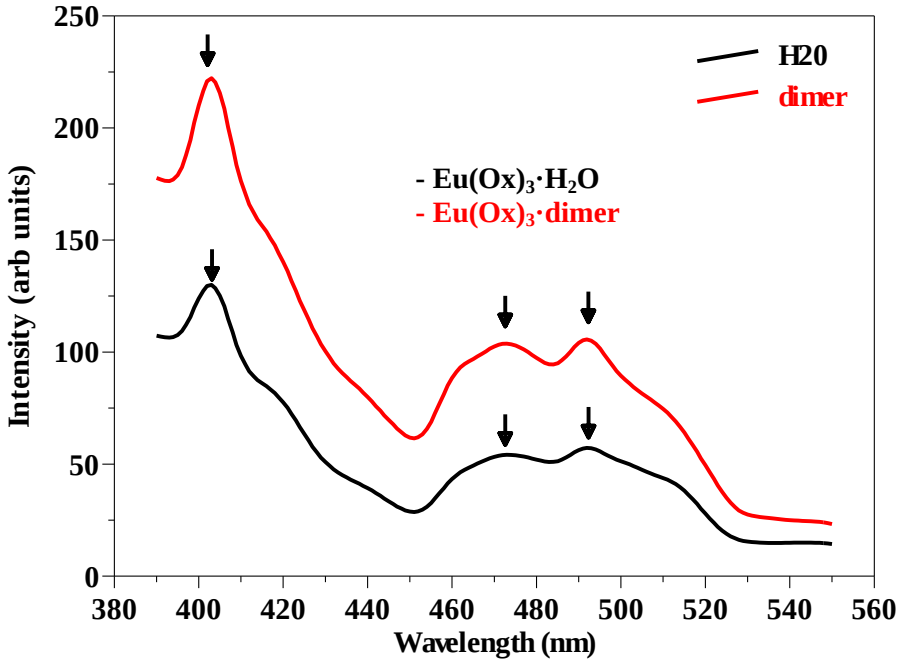

Figure 6.5.1: Emission of Europium complexes excited at 334 nm. The solvent molecules are not included in the naming of the complexes for clarity purposes.

6.6 Conclusion

All the $M(Ox)_3$ samples were excited at 343 nm and this wavelength correlates with a higher energy electronic transition (S_4 and above). All the samples showed singlet emission (S_1-S_0) that is characteristic of quinoline samples. The substituted samples showed a red shift in their emission spectrum that can be ascribed to the modification of the HOMO LUMO energy gap by die substituents. Due to the heavy atom effect it is expected that samples with a heavier metal center should be red shifted as well as experience a decrease in their intensity. In our case there was not a big shift between the different metal samples. This is due to the fact that the *fac*-$[Ga(Ox)_3]\cdot 0.5\cdot EtOH$ and *fac*-$[In(Ox)_3]\cdot 2H_2O$ samples are facial and not meridional. It has been reported that the facial isomer is blue shifted from the *mer*-isomer. It is believed that the different packing of the crystal together with the changed symmetry of the molecule are responsible for the blue shift.

Three peaks are observed for the Eu complexes. The first peak is assigned to singlet emission of the quinoline nucleus while the other two peaks are assigned to the 5d-4f transition of Eu^{2+}. More measurements should be performed between 590 nm and 700 nm to see if there are any emission from Eu^{3+}.

7 Theory of Characterization Techniques

7.1 Introduction

All the complexes synthesized were characterized using various research techniques, including nuclear magnetic resonance (NMR), ultraviolet-visible (UV-Vis) spectroscopy and photoluminescence (PL). A brief description of the theory behind the above mentioned research techniques will be discussed in this chapter.

7.2 Nuclear Magnetic Resonance Spectroscopy (NMR)

Nuclear magnetic resonance spectroscopy is in the elucidation of molecular structures through measurements of their interaction in an oscillating electromagnetic field with a collection of nuclei submerged in a strong external magnetic field. This phenomenon is supported by the discovery made in 1902 by a Nobel Prize winner physicist P. Zeeman that the nuclei of certain atoms behaved mysteriously when subjected to a strong external magnetic field.[1]

7.3 Magnetic Properties of Nuclei

A hydrogen (H) atom composed of a single proton and a single electron is regarded as the simplest atom found in almost all organic compounds. The atom is often denoted by ^{1}H, whereby the super-script indicates the sum of the atom's protons and neutrons. The angular momentum properties of the hydrogen nucleus remain to be the fundamental aspect of it as far as NMR is concerned. This angular momentum properties of hydrogen nucleus, resembles those of a classical spinning particle. That is largely because the general magnetic field that possesses a magnetic moment (μ) is generated by the spinning hydrogen nucleus that is positively charged. The magnetic moment (μ) has both the magnitude and direction and that automatically makes a vector.

[1] Macomber R.A, A complete introduction to modern NMR spectroscopy, John Wiley & Sons, Inc., 1998,

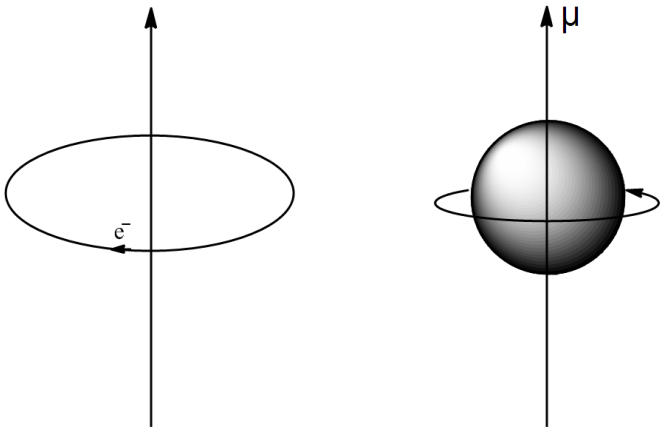

Figure 7.2.1.1: Angular momentum between a charge moving in a circle and a spinning nucleus.[3]

NMR experiments turn to exploit the magnetic properties of nuclei to give detailed information about the molecular structure. The overall spin of the nucleus is defined by the combined spin properties of protons and neutrons in the nuclei of normally heavier elements.

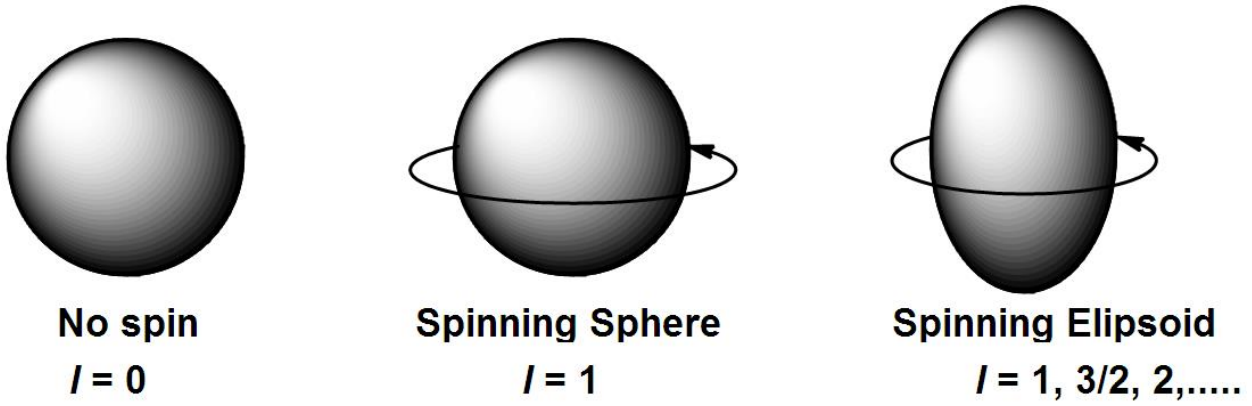

Figure 7.2.1.2: Three classes of nuclei[3]

It is when both the atomic number and the atomic mass are even that the nucleus has no magnetic properties and that is signified by a zero value of its spin quantum number (*I*).The nuclei with zero spin quantum number are considered to be the spinning carbon (^{13}C) and oxygen (^{16}O) are the typical examples of this non-spinning nuclei. But, commonly known nuclei with spin of ½ include ^{1}H, ^{13}C, ^{15}N, ^{19}F, ^{29}Si and ^{31}P. Moreover, all the nuclei that fall within the l = ½ class are the most easily examined by the NMR experiment.[3]

7.3.1 Chemical Shifts

An effective magnetic field, is the sum of the many contributions of which amongst them is the interaction with unpaired electrons. These unpaired electrons tend to decrease the external magnetic field as they experience an induced magnetic field which opposes the external magnetic field.

Nuclei in suitable chemical compounds are normally used as standards triggered by the fact that nuclei in a diamagnetic molecule experienced a smaller magnetic field than the free nuclei. Tetramethylsilane (TMS) is commonly used in proton NMR. Such an effective magnetic field experienced by such protons is:

$$B = B_o (1 - \sigma_{TMS}) \quad 7.1$$

Whereby σ is the shielding constant and $B_0\sigma$ is the induced magnetic field which opposes to B_0. This electronic modulation of the B_0 field is termed shielding.

The nature of the surrounding electrons dictated the actual field of a given nucleus. The variation of the resonance frequency with shielding has been termed the chemical shift. The expression for the resonance frequency in terms of shielding is:

$$\upsilon_o = \frac{\Upsilon B_0 (1-\sigma)}{2\pi} \quad 7.2$$

At constant $B_{0,}$ decreased shielding (deshielding) is induced by higher resonance frequency (υ_o) due to the negative sign in equation 2.

7.3.2 Aromatics

The deshielding of the sp^2-carbon atoms augmented by the diamagnetic anisotropic of benzene ring tends to yield a very high frequency (low field) position for benzene, δ 7.27. Both the inductive and resonance effects of substituents are similar to those in alkenes. The chemical shifts appear to be different between toluene and nitrobenzene due to this substitution effects.

Nitrobenzene

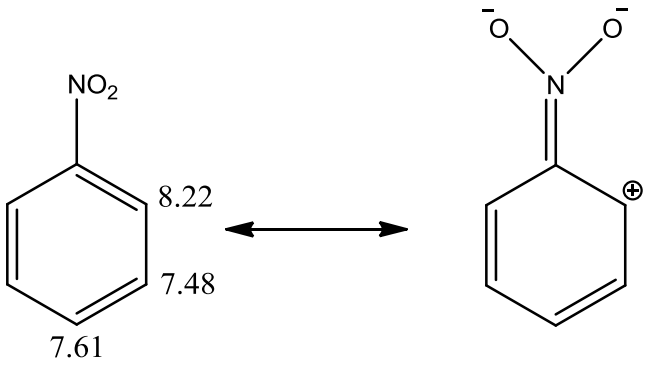

Anisole

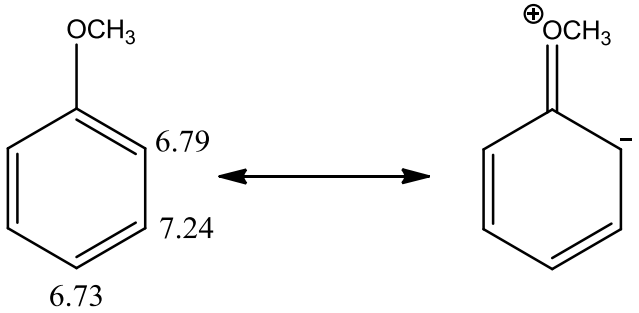

The inductive effect of the heteroatom highly influences the high frequency chemical shift of the α-proton in heterocyclics as in pyridine and pyrole.

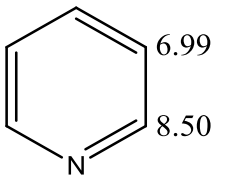

Pyridine

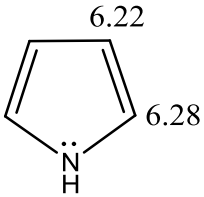

Pyrole

The addition of the substituents parameter to the shift of the benzene results in the overall shift of a particular proton as shown in the relationship:

$$\delta = 7.27 + \sum S_i \qquad 7.3$$

For instance, looking at the values in Table 1 below, there are two examples to show how the equation works. The spectrum of 4-chlorobenzaldehyde contains two doublets centered at δ 7.75 and 7.50. The calculated resonance positions for H_a are 7.79 (7.27 + 0.58 - 0.06) and for H_b is 7.50 (7.27 + 0.02 + 0.21). As for the observed resonances for 4-methoxybenzoic acid, centered at δ 8.08 and 6.98, resulted to calculated positions of δ 7.98 for H_a and 6.98 for H_b according to Equation 3.

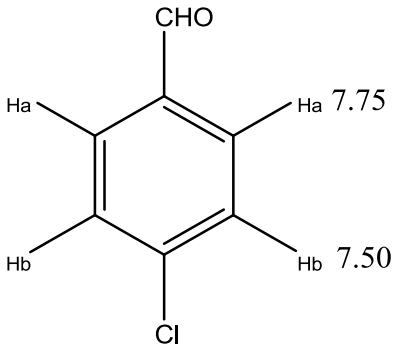

4-Chlorobenzaldehyde

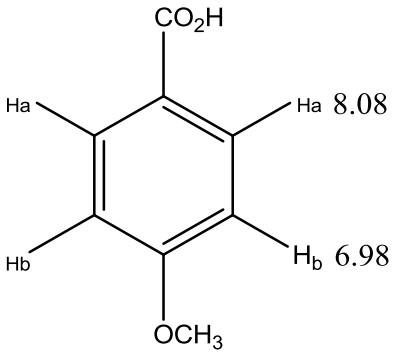

4-Methoxybenzoic acid

The identity of the substituents may be known for multiply substituted aromatic rings; however, their relative positions may be compromised.[2,3]

[2] I. Bertini, C. Luchinat, G. Parigi; Solution NMR of Paramagnetic Molecules, Amsterdam, Elsevier, 2001.

[3] J.B. Lambert, E.P. Mazzola, Nuclear Magnetic Resonance Spectroscopy, New Jersey: Pearson Edu. Inc., 2013.

Table 7.2.2.1: Substituted parameters for aromatic protons shift.[3]

Substituent	S_{ortho}	S_{meta}	S_{para}
CH_3	-0.17	-0.09	-0.18
CH_2CH_3	-0.15	-0.06	-0.18
NO_2	0.95	0.17	0.33
Cl	0.02	-0.06	-0.04
Br	0.22	-0.13	-0.33
I	0.4	-0.26	-0.03
CHO	0.58	0.21	-0.03
OH	-0.5	-0.14	0.27
NH_2	-0.75	-0.24	-0.4
CN	0.27	0.11	-0.63
CO_2H	0.8	0.14	0.3
CO_2CH_3	0.74	0.07	0.2
$COCH_3$	0.64	0.09	0.3
OCH_3	-0.43	-0.09	-0.37
$OCOCH_3$	-0.21	-0.02	-0.13
$N(CH_3)_2$	-0.6	-0.1	-0.62
SCH_3	0.37	0.2	0.1

7.4 Ultraviolet/Visible Spectroscopy (UV/Vis)

The ultraviolet/visible spectroscopy is a useful analytical tool that can be extensively used to identify functional groups and to further exploit the content of a particular substance. This technique comprises of only a small part of the electromagnetic spectrum. This electromagnetic spectrum consists of other forms of radiation namely, radio, infrared (IR), cosmic and x-ray.
The equation given below defines the energy association with the electromagnetic radiation:

$$E = h\upsilon \qquad 7.4$$

Where E is the energy, h is Planck's constant and υ is frequency.

The combination of alternating electric and magnetic field that travels through space with a wave motion is considered to be electromagnetic radiation. Due to the fact that radiation behaves more like a wave; it can either be classified as a wavelength or the frequency which are related by the following equation:

$$\upsilon = \frac{c}{\lambda} \qquad 7.5$$

Where υ is the frequency, c is the speed of light and lastly λ is the wavelength.

UV/vis is based on electrons absorbing energy. The electrons normally get prompted from the ground state (from the highest occupied molecular orbit- HOMO) to an excited state (lowest unoccupied molecular orbital- LUMO) if the valence electrons get to absorb light, either visible or ultraviolet. The wavelength in which the molecules absorb energy is dictated by how tightly the valence electrons are bound to the atom. The electrons in the double and triple bonds are easily excited because they are not strongly held.
There are three types of electron orbitals that valence electrons can occupy:

- Single (σ) bonding
- Double or Triplet (π) bonding and lastly
- Non-bonding (lone pair electrons) orbitals.

The energy thereof, increases from the single orbitals throughout to the non-bonding orbitals.[4]

[4] T. Owen, of Fundamental modern UV/Vis spectroscopy, Germany, Agilent technologies, 2000.

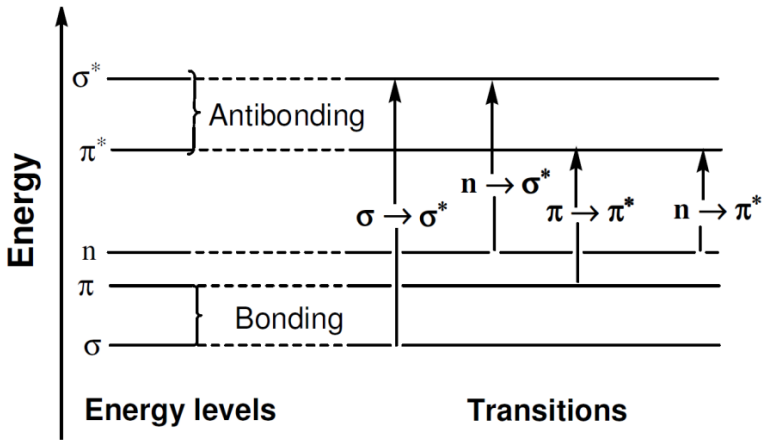

Figure 7.3.2: Electron transitions in ultraviolet/visible spectroscopy.[5]

7.5 X-ray Diffraction (XRD)

X-ray diffraction is a useful tool used for the determination of structures of crystalline material based of how they diffract x-ray radiation. The first prediction that crystals would exhibit diffraction qualities when bombarded with x-ray beam was suggested by a German physicist Max Von Laue. Crystals are made up of regular arrangement of molecules in one or many orientations. This repetitive arrangement of molecules is known as the unit cell. The unit cell is defined as the smallest repeating unit of atoms used to describe a crystal.

The phenomenon has flourished since then and today is well known as x-ray diffraction. It occurs when the x-ray, wavelength (λ) and the interatomic distance (d) The crystal has the same order of magnitude (ca. 10^{-10} m or 1 Å). W.L. Bragg presented a simple explanation for the angles observed in diffracted x-ray beam and that was a year later after Von Laue had created the diffraction patterns. W.L. Bragg was able to analyzed the first crystalline structures of potassium chloride (KCl) and that of sodium chloride (NaCl) successfully by x-ray crystallography. This new technique opened a wide range of opportunities in the field of x-ray crystallography for physicist and chemist to date.[6]

[6] W.L Bragg, Proceedings of the Royal Society, A89, 248, 1914.

7.5.1 Bragg's Law.

Bragg's assumption states that when a monochromatic x-ray beam is incident into the surface of a crystal, it is reflected. However, some of the x-ray beam penetrates deeper into the crystal and undergo a similar process within the crystal. All the reflected x-rays from a given plane remain in phase after reflection whereas the two x-rays reflected from the neighboring planes are in general out of phase after reflection. This is due to the longer path length travelled by the x-rays. Bragg's law is given by equation 7.11.

$$n\lambda = 2d_{hkl}Sin\ \theta \qquad 7.11$$

where *n* represents an integer, λ wavelength, d_{hkl} the distance between the successive parallel crystal planes and lastly θ the angle of incidence and reflection.

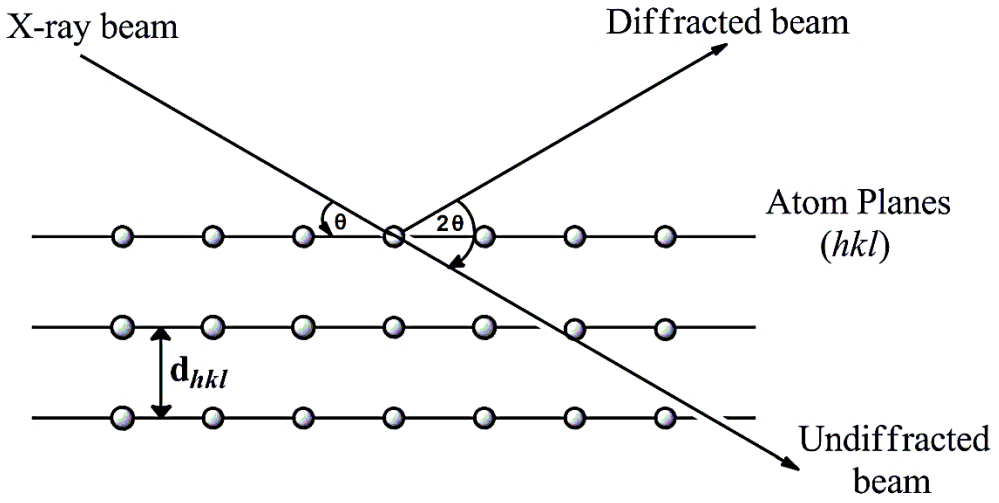

Figure 7.4.1: Bragg's description of X-ray Diffraction.[6]

7.5.2 The Phase Problem.

The image of the atoms from the diffracted rays is obtained from the help of the structure factor functions and Bragg's equation. The reflections that are obtained from the x-ray diffractometer provide an array of intensities which are directly proportional to the square of the amplitude of the diffracted waves. That often results to a loss of information and this inability to determine the phase is called the phase problem and it can be overcome by using a number of means. The most common methods include the Patterson function and Direct methods.

7.5.2.1 Direct Methods.

Direct methods are commonly used to solve molecular structures of light atoms. These methods are able to calculate the phase difference directly from the amplitudes of normalized structural factors. An estimation of the strongly scattered beams from their measured intensities direct methods in particular, turn to be useful in determining good phase information.

7.5.2.2 Patterson Methods.

In 1934 Patterson linked the Fourier transform of the intensities with the electron density map. This came as a solution to a problem faced with about the measured intensities in an XRD experiment not yielding any information on the phase of the refractions.

$$p(u,v,w) = V^{-1}\sum_h\sum_k\sum_l(|(f_{hkl})|)^2\exp[-2\pi i\ (hx_j + ky_j + lz_j)] \quad 7.12$$

$$p(u,v,w) = \int p(r)p(r=u)d^3r \quad 7.13$$

The Patterson function look to be an electron density map with peak of positive electron density in various positions. However, these various positions are not of atoms in the structure. The Patterson peaks shows only where the atoms lie relative to each other but not relative to the unit cell. They are proportional in size to the product of the atomic number of the two atoms involved.[7]

[7] W. Clegg, Crystal Structure determination, New York: Oxford University Press, Inc., 1998.

7.5.3 Structure Factor.

There are two parameters that can be associated with each reflection in crystal diffraction pattern; they are namely:

- Amplitude ($|F(hkl)|$) and
- The phase (Φ) of the diffracted wave.

The quality that express these parameters for any diffracted x-ray is called the structure factor [F(hkl)]. There is a direct relation between the structure factor and the intensity of the reflected beam $\sqrt{I_{hkl}}$ which express the combined scattering of all atoms in the unit cell, compared to that of a single electron. The total scattering of all atoms in the unit cell is given as:

$$\mathrm{F}\,(hkl) = \sum_{j=1}^{N} f_j \exp[i2\pi\,(hx_j + ky_j + lz_j)] \qquad 7.14$$

Where f_j is the scattering factor of each of the N atoms and $(x_j + y_j + z_j)$ are the coordinates of each atom in the unit cell.

The formula given in Equation 7.12 indicates that the structure factor magnitude depends only on the relative disposition of the N atoms in the unit cell and the on the atomic scattering factors. The equation represents a wavelet with amplitude of f_j and phase (Φ) $[2\pi(hx_j + ky_j + lz_j)]$ which expresses the path length for each scattering wavelet. The scattering wavelet by the N atoms in the unit cell results in the structure factor, F (hkl).[8]

The equation can also be re-written as:

$$\mathrm{F}\,(hkl) = \sum_{j=1}^{N} f_j \exp[cos2\pi\,(hx_j + ky_j + lz_j)] + i\sin 2\pi\,(hx_j + ky_j + lz_j) \qquad 7.15$$

The square of the amplitude of the wave turns to be proportional to the energy in the cosine wave.

[8] L.V. Azároff, Elements of x-ray crystallography, New York: McGraw-Hill, Inc.,1968.

7.5.4 The Least-Squares Refinement.

The least square refinement process is a very useful tool for the single crystal x-ray diffraction (XRD) experiment. It assists in comparing the experimental structure factors to the calculated one. The main aim is to get the correct desired atomic structure of the obtained crystal and hence the comparison. The values converge as the experimental data agrees with the calculated one and that is measured by the residual or R-factor and the weighted R (wR).[9]

7.5.4.1 The Residual Factors.

There are various factors or rather 'R-factors' that assists in the better judgement of the quality of the model. During refinement, these factors should converge to at minimum to indicate signal how good the model prediction is. The three most used residual factors are:

- The weighted R-factor (wR^2) :
  This residual is most closely related to the refinement against squared structure factors.

$$wR = \left[\frac{\sum w\,(f_0^2 - f_c^2)}{\sum w f_0^2}\right]^{1/2} \qquad 7.16$$

  The weighting factor looks closely in every single reflection to restore confidence in the accuracy of the fitting. Better yet, it is derived from the standard uncertainties of the measured reflections.

- The second one is that of the un-weighted residual factor (R1)
  This residual is based mostly of F-values:

$$R = \frac{\sum||f_0| - |f_c||}{\sum|f_0|} \qquad 7.17$$

- The last residual factor is the goodness of fit (GOOF):

[9] G. Rhodes, Crystallography made crystal clear: A guide for users of macromolecular models, 2nd Ed.,Academic Press, San Diego, 2000.

$$S = \left[\frac{\sum w\,(f_0^2 - f_c^2)}{(N_R - N_p)}\right]^{1/2} \qquad 7.18$$

Where: N_R is the number of the independent reflections and N_P of the refined parameters. Theoretically, the Goof value should be close to **1** to signal a proper adjusted weighted sheme. Other values suggest that there are some problems with the data and/or the refinement itself. There are two aspects that frequently lead to these problems[10]:

- Failure to perform a proper absorption corrections
- Refinement in the wrong space group.

7.6 Photoluminescence (PL)

Photoluminescence (PL) spectroscopy is a efficient, contactless, nondestructive, widely used technique for the analysis of the optoelectronic properties of semiconductors, which requires very little sample manipulation. Photoluminescence is defined as the spontaneous emission of light from a material under optical excitation and can be therefore used to provide detailed information on discrete electronic states involving both intrinsic optical processes and about the wide variety of defect which are endemic in practical semiconductor materials and extrinsic optical processes.

7.6.1 The Electronic State

Fluorescence and phosphorescence are photon emission processes that happen to occur during molecular relaxation from electronic states. The chemical compound that has the ability to give off light or rather polyatomic fluorescent molecules are commonly called fluorophores. This process takes place during the transition between the electronic and vibrational states of fluorophores. In 1933, a Polish physicist named Alexander Jablonski, first proposed a diagram

[10] P. Muller, R. Herbst-Irmer, A.L. Spek, T.R. Schneider, M.R Sawaga, Crystal structure refinement: a crystallographer's guide to SHELXL, 8th Ed., Oxford University press, New York, 2006.

that illustrates the electronic states of a molecule and the transitions thereof. The diagram was created to describe the absorption and emission of light, see **Figure 7.5.1.**

The observed electronic states are spilt into multiple sublevels representing the vibrational mode of the molecule. The energies of the vibrational levels are separated by about 100 cm^{-1}. The electronic excited states also have specific polarization properties. Fluorophores are preferentially excited when the polarization of light is aligned along a specific molecular axis. In general, the excitation and emission dipoles do not coincide.

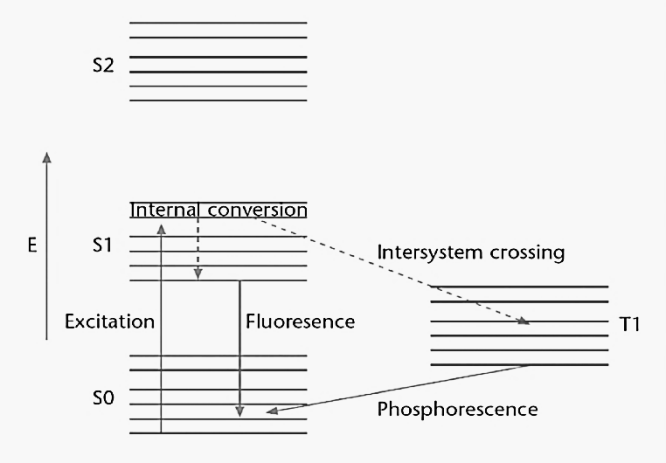

Figure 7.5.1: The Jablonski diagram of fluorophore excitation, radiative decay and nonradiative decay pathways. E denotes the energy scale; S_0 is the ground singlet electronic state; S1 and S2 are the successively higher energy excited singlet electronic states. T1 is the lowest energy triplet state.[11]

7.6.2 Radiative and Non-radiative Decay Pathways

The molecular de-excitation accompanied by photon emission are two processes that are described by the radiative decay. However, molecules in the electronic excited state can relax by non-radiative process. This process take place when excitation energy is not converted into photons; dissipated by thermal processes such as vibrational relaxation and collisional quenching. The temporal evolution of the excited state can be described by:

$$\frac{dN}{dt} = -(\Gamma + k)\, N \qquad 7.19$$

$$N = N_0 e^{-(\Gamma+k)t} = N_0 e^{-t/\Gamma} \quad 7.20$$

Where Γ and k are radiative and non-radiative decay rates respectively, N is the fraction of flourophore in the excited states. The combine rate of the radiative and non-radiative pathways is measured by the fluorescence lifetime, τ:

$$\tau = \frac{1}{\Gamma+k} \quad 7.21$$

But now in the absence of the non-radiative decay processes, the intrinsic lifetime of the fluorophores becomes;

$$\tau = \frac{1}{\Gamma} \quad 7.22$$

The efficiency of the flourophore can be quantified by the fluorescence quantum yield, Q:

$$Q = \frac{\Gamma}{\Gamma+k} = \frac{\tau}{\tau_0} \quad 7.23$$

7.6.3 Factors affecting Fluorescence Intensity

There are several factors that contribute to the non-radiative decay pathway of the fluorophore and reduce the fluorescence intensities. The non-radiative decay processes can be classified as:

$$k = k_{ic} + k_{ec} + k_{is} \quad 7.24$$

Where: k_{ic} is the rate of internal conversion is, k_{ec} is the rate of external conversion and lastly k_{is} is the rate of the intersystem crossing.

The conversion of the electric energy to the vibrational energy of the fluorophore is termed internal conversion. This internal conversion is set to decrease the fluorescence intensity with

rising temperature and that is due to the fact that vibrational processes are driven by thermal process. The process where the fluorophore loses electronic energy to its environment through collision with other solutes is described by the external conversion called collisional quenching. Oxygen is considered to be among solute molecules that are fluorescence quenchers. The collisional quenching rate can be expressed as:

$$k_{ec} = k_0[Q] \tag{7.25}$$

Where k_0 is related to the diffusivity and the hydro-dynamics radii of the reactants and [Q] is the concentration of the quencher.

In a situation where collisional quenching is dominant, Equation 7.19, predicts that fluorescence lifetime decreases with quenching concentration:

$$\frac{\tau_0}{\tau} = (1 + k_0\tau_0[Q] \tag{7.26}$$

The steady state intensity, F, looks to be declining relative to the fluorescence intensities in the absence of a quencher, F_0. This effect is described by the Stern volmer equation:

$$\frac{F_0}{F} = (1 + k_0\tau_0[Q]) \tag{7.27}$$

Fluorescence signal reduction can also result from ground state process, steady state quenching. In some instance, a fluorophore get chemically bound to a quencher to form a dark complex. Fluorescence intensities decrease with steady state quenching:

$$\frac{F_0}{F} = 1 + k_s[Q] \tag{7.28}$$

Where k_s is the association constant of the quencher and the fluorophore. The excited states are not involved hence the fluorescence lifetime is not affected by the steady state quenching.[11,12,13,14.]

[11] P.T.C. So, C.Y Dong, Fluorescence Spectroscopy, Encyclopedia of Life Science, USA: Macmillan Publishers Ltd., 2002.

[12] R.S. Becker, Theory and interpretation of fluorescence and phosphorescence, New York: Wiley. 1969.

[13] J.B. Birks, Photo physics of aromatic molecules, New York: Wiley, 1970.

7.7 Conclusions

In conclusion, the advantages of the methods for characterization to be used during this project have been presented in this chapter.

The UV/Vis spectroscopy worked as an important tool in helping to correlate the respective absorption wavelengths of the respective coordination complexes in question. The obtained absorption wavelengths were then used as a starting point in finding the optimum excitation wavelengths in the photoluminescence spectroscopy.

The nuclear magnetic resonance spectroscopy was applied to test for the extent of coordination chemistry of the metal-quinolato complexes. Since the geometrical conformation of these complexes is a great issue, NMR technique assisted in the understanding of the solution chemistry.

Photoluminescence spectroscopy helped in shedding more light in respect to the geometrical conformations suggested by the solution NMR studies. One other aspect is the influence of the isomerization observed in NMR studies on the fluorescence of these complexes.

Finally, X-ray crystallography is a valuable tool for determination of complex structure. It correlated the solid state configurations of these complexes with the solution state results and lastly the nature of the coordination chemistry of these $M(N\hat{}O)_3$ entities.

[14] J.R. Lakowicz, Principles of fluorescence spectroscopy, New York: Plenum Press,1999.

8 Evaluation of the Study

8.1 Introduction

One of the original motivations of this study was to gain further knowledge into the coordinative and the luminescent properties of the M(N^O) (M =Al^{3+}, Ga^{3+} and In^{3+}) entities as potential electroluminescent agents in the manufacturing of OLED's devices. The great concern with these group 13 metal-quinolate complexes is the geometrical isomerization they normally resort to and that was one of the key aspects to explore. The coordination nature was tested with a range of ligands of quinolinol specie, from the 8-hydroxquinoline to 5,7-dimethyl-8-hydroxyquinoline and lastly 5,7-dichloro-8-hydroxyquinoline.

On the same breath, the same mandate was planned for the europium metal ion. Apart from the fact that lanthanides chemistry is totally different from the aluminium triad metals, it also has the ability to influence the luminescent properties of the whole complexes by being the center of luminescence.

Finally, the coordination of the quinolinol derivatives with group 13 metal ions was explored and the NMR studies revealed the nature of the complexes. The coordination chemistry of the lanthanide complexes with a 5,7-dichloro substituted quinolinol ligand species also prevailed and the luminescent properties of the respective metal complexes was successfully studied.

The findings of this investigation are briefly discussed below.

8.2 Scientific Relevance and Results Obtained.

8.2.1 Synthesis

In this study, three bidentate N,O ligands were used for all the coordination chemistry exercised in this manuscript. These quinolinol ligand derivatives were selected for their differences in electronic properties induced by their peripheral substitution on the back bone of the ligand itself (see **Figure 3.1.1.**)

The following complexes were successfully synthesized and characterized:

All these *tris*-coordinated complexes were highly stable, both in solid and solution state. NMR studies showed different behavior as one moves from Al^{3+} down to In^{3+}. Most of the isolated complexes of aluminium and gallium were isolated in the solid state in the *mer*–isomeric forms, but in solution, both isomeric forms were observed in some cases.

The synthesis of the lanthanide-quinolinol complexes was difficult compared to the group 13 metal complexes. Several different synthesic methods were also tested but the results were not as anticipated. In the end, two complexes were synthesized successfully, namely

8.2.1. *mer*-[*tris*-(8-hydroxyquinoline) Aluminium (III)] Ethanol Solvate

- *mer*-[Al(Ox)$_3$]·EtOH

8.2.2. *mer*-[*tris*-(8-hydroxyquinoline) Gallium (III)] Ethanol:

- *mer*-[Ga(Ox)$_3$]·0.5·EtOH

8.2.3. *mer*-[*tris*-(8-hydroxyquinoline) Indium (III)] Di-aqua:

- *mer*-[In(Ox)$_3$]·2H$_2$O

8.2.4. *mer*-[*tris*-(5,7-dimethyl-8-hydroxyquinoline) Gallium(III)] Dichloromethane

- *mer*-[Ga(57dmOx)$_3$]·DCM

8.2.5. [*tris*-(5,7-dichloro-8-hydroxyquinoline)(di-aqua) Europeum (III)] •Ethanol Water

-[Eu(57dcOx)$_3$]·EtOH·H$_2$O

8.2.6. κ^2-O,O'-*bis*-[*tris*-(5,7-dichloro-8-hydroxyquinoline)(Methanol)Europium(III)].

-κ^2-O,O'-[Eu(57dcOx)$_3$·EtOH]

8.2.2 X-ray Diffraction

Six suitable crystals for X-ray diffraction were obtained and characterized in detail with single crystal X-ray diffraction techniques as well as other spectroscopic techniques. Three complexes of the 8-hydroxyquinoline ligand, coordinated to Al, Ga and In respectively, crystallized in the same crystal system (monoclinic), space group ($P2_1/n$) and contain the same number of molecules in the unit cell. The crystallographic results correlate well with both NMR and Fluorescence results. It was discovered in literature that the longer the distance (weak π-stacking) between the π-π stacking of the above discussed complexes with none-functionalized quinolinol ligands are, the better the luminescence is (see **Par. 2.6.2.**).

The other complex with 5,7-dimethyl-8-hydroxyquinoline coordinated to the gallium (Ga) metal, crystallized in a triclinic crystal system, space group of $P\bar{1}$ and contained two molecules per unit cell. There were minor solvent disorders in this crystal structure.

The two europium crystal structures obtained were suitable for x-ray diffraction and were both collected. The first complex, $[Eu(57dcOx)_3(H_2O)_2]\cdot EtOH\cdot H_2O$, is made up of *tris*-coordination of 5,7-dichloro-8-hydroxyquinoline to the europium metal and two aqua molecules to complete a square anti-prismatic coordination polyhedron. The structure crystallized in a trigonal crystal system with $R\bar{3}$ space group.

Good quality crystals of the dimer, κ^2-O,O'-$[Eu(57dcOx)_3\cdot EtOH]$ was also obtained and its crystal data was collected with the X-ray diffraction technique. Although the data was good, the crystal had a disordered toluene solvent that could not be solved. This europium-dimer complex crystallized in the triclinic crystal system and space group of *P1*.

8.2.3 Luminescence studies

The luminescence studies of the group 13 metals were successfully completed and it correlated well with what was obtained in NMR studies as far as *mer*- and *fac*-isomers are concerned. Two important aspects of photoluminescence differentiate *mer*- and *fac*-isomers from each other. These are intensity and wavelength shifts. The relative intensities of the complexes that were deemed facial isomers were higher than those of *mer*-isomers as per literature. All the $M(Ox)_3$ samples were excited at 343 nm and in general a red shift corresponding to the size of the metal used, was obtained. The *fac*-isomers of indium and gallium did not adhere to this rule as expected.

The luminescence studies of the europium complexes reported low intensities for both complexes, with the dimer the highest. The lower intensities of the di-aqua complex is probably due to quenching (see **Par. 2.5.** for references).

Appendix

A. *mer*-[*tris*-(8-Hydroxyquinoline) aluminium (III)] ·ethanol solvate (1)

Table A.1: Fractional Atomic Coordinates ($\times 10^4$) and Equivalent Isotropic Displacement Parameters ($Å^2 \times 10^3$) for *mer*-[$Al(Ox)_3$]·EtOH.

Atom	*x*	*y*	*z*	U(eq)
C11	2544(6)	427(5)	3455(3)	46.4(16)
C12	1450(6)	471(6)	3777(4)	63(2)
C13	1359(8)	811(6)	4569(5)	77(2)
C14	2338(8)	1120(6)	5043(4)	73(2)
C15	3490(7)	1105(5)	4734(4)	58.8(19)
C16	4578(8)	1418(6)	5132(4)	73(2)
C17	5616(7)	1338(6)	4793(4)	68(2)
C18	5608(6)	965(5)	4005(4)	60.8(19)
C19	3569(6)	753(4)	3942(4)	47.6(17)
C21	3717(6)	-981(5)	845(4)	53.0(17)
C22	3420(6)	-986(6)	8(4)	61(2)
C23	3298(6)	-119(6)	-403(4)	62(2)
C24	3480(6)	817(5)	-2(4)	51.9(18)
C25	3397(6)	1750(6)	-378(4)	66(2)
C26	3640(6)	2620(6)	88(4)	65(2)
C27	3942(5)	2558(5)	915(4)	55.1(18)
C28	4008(5)	1651(5)	1305(3)	45.7(17)
C29	3772(5)	767(5)	827(3)	43.6(16)
C31	3721(6)	-2026(5)	2894(4)	55.5(18)
C32	4037(6)	-3022(5)	3053(4)	58.9(19)
C33	5185(7)	-3322(5)	3047(4)	63(2)
C34	6098(5)	-2606(4)	2871(3)	48.2(17)
C35	7333(6)	-2817(6)	2842(4)	62(2)
C36	8092(6)	-2051(6)	2693(4)	62(2)
C37	7705(5)	-1055(5)	2533(4)	53.5(18)
C38	6494(5)	-830(5)	2519(3)	45.0(16)
C39	5707(5)	-1627(5)	2703(3)	41.4(16)
C41	290(11)	9053(9)	749(7)	138(4)
C42	660(8)	8562(7)	1483(5)	90(3)
N11	4629(4)	679(4)	3595(3)	47.5(14)
N21	3875(4)	-127(4)	1246(3)	44.5(14)
N31	4527(4)	-1339(4)	2710(3)	45.5(14)
O11	2739(4)	110(3)	2714(3)	50.8(13)
O21	4285(4)	1522(3)	2083(2)	52.2(13)

O31	6015(4)	66(3)	2349(3)	49.6(12)
O44	625(6)	9185(4)	2151(4)	88.6(18)
Al1	4355.7(10)	192.5(9)	2438.8(7)	11.5(7)

Table A.2: Hydrogen Atom Coordinates (Å×104) and Isotropic Displacement Parameters (Å2×103) for *mer*-[Al(Ox)$_3$]·EtOH.

Atom	*x*	*y*	*z*	U(eq)
H12	766	275	3470	75
H13	612	826	4776	93
H14	2251	1338	5565	88
H16	4573	1688	5645	88
H17	6328	1526	5073	81
H18	6329	919	3765	73
H21	3802	-1590	1118	64
H22	3309	-1595	-261	73
H23	3093	-132	-952	74
H25	3185	1799	-926	79
H26	3599	3248	-159	78
H27	4102	3147	1206	66
H31	2928	-1832	2917	67
H32	3451	-3486	3165	71
H33	5387	-3990	3156	75
H35	7620	-3469	2924	74
H36	8905	-2191	2697	74
H37	8255	-553	2438	64
H41A	326	8587	312	207
H41B	810	9613	668	207
H41C	-514	9292	771	207
H41D	89	9741	856	207
H41E	-396	8715	499	207
H41F	929	9036	396	207
H42A	147	7985	1551	107
H42B	1469	8315	1451	107
H44	873	8876	2554	133

Table A.3: Anisotropic Displacement Parameters ($Å^2×10^3$) for *mer*-$[Al(Ox)_3]·EtOH$.

Atom	U_{11}	U_{22}	U_{33}	U_{23}	U_{13}	U_{12}
C11	53(4)	48(4)	39(4)	-2(3)	9(3)	6(3)
C12	57(4)	65(5)	69(5)	-8(4)	17(4)	9(4)
C13	76(6)	86(6)	74(5)	2(5)	28(5)	16(4)
C14	96(6)	76(5)	50(4)	-6(4)	18(4)	18(5)
C15	80(5)	55(4)	41(4)	-1(3)	4(4)	4(4)
C16	103(7)	65(5)	50(4)	-2(4)	-8(5)	-3(5)
C17	70(5)	73(5)	58(5)	-7(4)	-4(4)	-7(4)
C18	64(5)	64(5)	54(4)	1(4)	-2(4)	-9(4)
C19	61(4)	40(4)	43(4)	1(3)	11(3)	2(3)
C21	58(4)	53(4)	48(4)	-7(3)	4(3)	-1(3)
C22	61(4)	67(5)	55(4)	-14(4)	9(3)	-2(4)
C23	58(4)	85(6)	42(4)	0(4)	3(3)	-11(4)
C24	46(4)	66(5)	44(4)	1(3)	7(3)	1(3)
C25	65(5)	84(6)	48(4)	22(4)	-6(3)	1(4)
C26	60(4)	64(5)	70(5)	19(4)	1(4)	6(4)
C27	54(4)	52(4)	59(4)	1(3)	3(3)	4(3)
C28	45(4)	47(4)	44(4)	6(3)	-2(3)	4(3)
C29	37(3)	49(4)	45(4)	1(3)	1(3)	0(3)
C31	53(4)	57(5)	55(4)	7(3)	-2(3)	-14(3)
C32	63(5)	41(4)	74(5)	-4(3)	12(4)	-11(3)
C33	79(5)	42(4)	67(4)	5(3)	3(4)	9(4)
C34	58(4)	39(4)	48(3)	-4(3)	2(3)	6(3)
C35	58(5)	64(5)	63(4)	3(4)	2(3)	19(4)
C36	47(4)	81(6)	58(4)	4(4)	6(3)	10(4)
C37	39(4)	62(4)	58(4)	1(3)	0(3)	6(3)
C38	43(4)	47(4)	45(3)	1(3)	3(3)	3(3)
C39	38(4)	49(4)	37(3)	-1(3)	2(3)	-1(3)
N11	46(3)	49(3)	46(3)	-4(2)	-3(3)	-4(2)
N21	43(3)	44(3)	45(3)	-2(2)	1(2)	0(2)
N31	46(3)	45(3)	45(3)	4(2)	1(2)	-1(3)
O11	43(3)	58(3)	52(3)	-4(2)	4(2)	6(2)
O21	60(3)	50(3)	46(3)	-1(2)	2(2)	-1(2)
O31	40(3)	46(3)	62(3)	4(2)	3(2)	0(2)
Al1	12.5(10)	12.2(9)	9.9(9)	-0.2(5)	1.1(6)	1.0(5)

Table A.4: Bond Lengths for *mer*-[Al(Ox)$_3$]·EtOH.

Atom	Atom	Length/Å	Atom	Atom	Length/Å
C11	C12	1.377(9)	C28	O21	1.325(7)
C11	C19	1.428(9)	C29	N21	1.378(8)
C11	O11	1.339(7)	C31	C32	1.390(9)
C12	C13	1.408(10)	C31	N31	1.335(8)
C13	C14	1.370(12)	C32	C33	1.349(10)
C14	C15	1.426(10)	C33	C34	1.444(9)
C15	C16	1.410(11)	C34	C35	1.418(9)
C15	C19	1.413(9)	C34	C39	1.393(8)
C16	C17	1.334(12)	C35	C36	1.361(10)
C17	C18	1.407(10)	C36	C37	1.413(10)
C18	N11	1.309(8)	C37	C38	1.389(9)
C19	N11	1.363(8)	C38	C39	1.426(8)
C21	C22	1.413(10)	C38	O31	1.328(7)
C21	N21	1.323(8)	C39	N31	1.379(7)
C22	C23	1.341(10)	C41	C42	1.424(14)
C23	C24	1.419(10)	C42	O44	1.393(10)
C24	C25	1.388(10)	N11	Al1	2.038(5)
C24	C29	1.402(9)	N21	Al1	2.070(5)
C25	C26	1.409(10)	N31	Al1	2.090(5)
C26	C27	1.401(9)	O11	Al1	1.906(4)
C27	C28	1.370(9)	O21	Al1	1.862(4)
C28	C29	1.434(9)	O31	Al1	1.886(4)

Table A.5: Bond Angles for *mer*-[Al(Ox)$_3$]·EtOH.

Atom	Atom	Atom	Angle/°	Atom	Atom	Atom	Angle/°
C12	C11	C19	117.9(6)	C35	C36	C37	123.2(6)
O11	C11	C12	125.8(6)	C38	C37	C36	119.4(6)
O11	C11	C19	116.3(5)	C37	C38	C39	117.2(6)
C11	C12	C13	120.5(7)	O31	C38	C37	125.1(6)
C14	C13	C12	122.0(7)	O31	C38	C39	117.7(5)
C13	C14	C15	119.8(6)	C34	C39	C38	123.0(5)
C16	C15	C14	127.0(7)	N31	C39	C34	123.1(6)
C16	C15	C19	115.4(7)	N31	C39	C38	113.9(5)
C19	C15	C14	117.6(7)	O44	C42	C41	113.3(9)
C17	C16	C15	122.0(7)	C18	N11	C19	118.8(5)
C16	C17	C18	118.5(7)	C18	N11	Al1	130.6(5)
N11	C18	C17	122.7(7)	C19	N11	Al1	110.4(4)
C15	C19	C11	122.2(6)	C21	N21	C29	118.5(5)
N11	C19	C11	115.3(5)	C21	N21	Al1	132.8(4)
N11	C19	C15	122.5(6)	C29	N21	Al1	108.6(4)

N21	**C21**	**C22**	121.2(6)	**C31**	**N31**	**C39**	118.6(5)
C23	**C22**	**C21**	120.6(7)	**C31**	**N31**	**Al1**	131.4(4)
C22	**C23**	**C24**	120.3(6)	**C39**	**N31**	**Al1**	110.0(4)
C25	**C24**	**C23**	124.4(6)	**C11**	**O11**	**Al1**	115.2(4)
C25	**C24**	**C29**	119.5(6)	**C28**	**O21**	**Al1**	115.9(4)
C29	**C24**	**C23**	116.0(6)	**C38**	**O31**	**Al1**	116.7(4)
C24	**C25**	**C26**	118.5(6)	**N11**	**Al1**	**N21**	171.0(2)
C27	**C26**	**C25**	121.4(6)	**N11**	**Al1**	**N31**	95.6(2)
C28	**C27**	**C26**	121.4(6)	**N21**	**Al1**	**N31**	91.3(2)
C27	**C28**	**C29**	117.0(5)	**O11**	**Al1**	**N11**	82.55(19)
O21	**C28**	**C27**	125.5(6)	**O11**	**Al1**	**N21**	91.94(19)
O21	**C28**	**C29**	117.5(5)	**O11**	**Al1**	**N31**	88.05(19)
C24	**C29**	**C28**	122.1(6)	**O21**	**Al1**	**N11**	90.1(2)
N21	**C29**	**C24**	123.3(6)	**O21**	**Al1**	**N21**	83.39(19)
N21	**C29**	**C28**	114.6(5)	**O21**	**Al1**	**N31**	173.13(19)
N31	**C31**	**C32**	121.7(6)	**O21**	**Al1**	**O11**	96.44(19)
C33	**C32**	**C31**	120.7(6)	**O21**	**Al1**	**O31**	94.50(18)
C32	**C33**	**C34**	119.9(6)	**O31**	**Al1**	**N11**	91.2(2)
C35	**C34**	**C33**	125.9(6)	**O31**	**Al1**	**N21**	95.5(2)
C39	**C34**	**C33**	115.9(6)	**O31**	**Al1**	**N31**	81.65(19)
C39	**C34**	**C35**	118.2(6)	**O31**	**Al1**	**O11**	167.42(19)
C36	**C35**	**C34**	118.9(6)				

Table A.6: Torsion Angles for *mer*-[Al(Ox)$_3$]·EtOH.

A	**B**	**C**	**D**	**Angle/°**	**A**	**B**	**C**	**D**	**Angle/°**
C11	C12	C13	C14	0.8(12)	C28	O21	Al1	N11	-174.7(4)
C11	C19	N11	C18	180.0(6)	C28	O21	Al1	N21	-1.0(4)
C11	C19	N11	Al1	3.5(6)	C28	O21	Al1	O11	-92.2(4)
C12	C11	C19	C15	0.5(10)	C28	O21	Al1	O31	94.0(4)
C12	C11	C19	N11	179.1(5)	C29	C24	C25	C26	1.6(10)
C12	C11	O11	Al1	177.7(5)	C29	C28	O21	Al1	1.1(7)
C12	C13	C14	C15	0.3(12)	C31	C32	C33	C34	-0.2(10)
C13	C14	C15	C16	178.4(7)	C32	C31	N31	C39	-2.1(9)
C13	C14	C15	C19	-0.9(11)	C32	C31	N31	Al1	179.8(5)
C14	C15	C16	C17	177.6(7)	C32	C33	C34	C35	-179.8(6)
C14	C15	C19	C11	0.5(10)	C32	C33	C34	C39	-1.0(9)
C14	C15	C19	N11	-178.0(6)	C33	C34	C35	C36	-177.9(6)
C15	C16	C17	C18	2.4(11)	C33	C34	C39	C38	179.9(5)
C15	C19	N11	C18	-1.4(9)	C33	C34	C39	N31	0.7(9)
C15	C19	N11	Al1	-177.9(5)	C34	C35	C36	C37	-2.6(10)
C16	C15	C19	C11	-178.8(6)	C34	C39	N31	C31	0.8(9)
C16	C15	C19	N11	2.6(9)	C34	C39	N31	Al1	179.3(5)
C16	C17	C18	N11	-1.0(11)	C35	C34	C39	C38	-1.1(9)
C17	C18	N11	C19	0.5(10)	C35	C34	C39	N31	179.6(5)
C17	C18	N11	Al1	176.1(5)	C35	C36	C37	C38	-0.4(10)

C19	**C11**	**C12**	**C13**	-1.2(10)	**C36**	**C37**	**C38**	**C39**	2.6(9)
C19	**C11**	**O11**	**Al1**	-1.7(7)	**C36**	**C37**	**C38**	**O31**	-177.5(6)
C19	**C15**	**C16**	**C17**	-3.2(11)	**C37**	**C38**	**C39**	**C34**	-1.8(9)
C21	**C22**	**C23**	**C24**	0.8(11)	**C37**	**C38**	**C39**	**N31**	177.5(5)
C22	**C21**	**N21**	**C29**	-1.5(9)	**C37**	**C38**	**O31**	**Al1**	-176.0(5)
C22	**C21**	**N21**	**Al1**	-177.8(5)	**C38**	**C39**	**N31**	**C31**	-178.5(5)
C22	**C23**	**C24**	**C25**	178.7(7)	**C38**	**C39**	**N31**	**Al1**	0.0(6)
C22	**C23**	**C24**	**C29**	-0.8(10)	**C38**	**O31**	**Al1**	**N11**	92.6(4)
C23	**C24**	**C25**	**C26**	-177.9(6)	**C38**	**O31**	**Al1**	**N21**	-93.4(4)
C23	**C24**	**C29**	**C28**	178.5(6)	**C38**	**O31**	**Al1**	**N31**	-2.9(4)
C23	**C24**	**C29**	**N21**	-0.4(9)	**C38**	**O31**	**Al1**	**O11**	32.5(11)
C24	**C25**	**C26**	**C27**	-1.0(10)	**C38**	**O31**	**Al1**	**O21**	-177.2(4)
C24	**C29**	**N21**	**C21**	1.5(9)	**C39**	**C34**	**C35**	**C36**	3.3(9)
C24	**C29**	**N21**	**Al1**	178.7(5)	**C39**	**C38**	**O31**	**Al1**	3.9(7)
C25	**C24**	**C29**	**C28**	-1.0(10)	**N21**	**C21**	**C22**	**C23**	0.4(10)
C25	**C24**	**C29**	**N21**	-179.9(6)	**N31**	**C31**	**C32**	**C33**	1.8(10)
C25	**C26**	**C27**	**C28**	-0.4(10)	**O11**	**C11**	**C12**	**C13**	179.4(7)
C26	**C27**	**C28**	**C29**	1.0(9)	**O11**	**C11**	**C19**	**C15**	180.0(6)
C26	**C27**	**C28**	**O21**	-180.0(6)	**O11**	**C11**	**C19**	**N11**	-1.4(8)
C27	**C28**	**C29**	**C24**	-0.3(9)	**O21**	**C28**	**C29**	**C24**	-179.4(5)
C27	**C28**	**C29**	**N21**	178.6(5)	**O21**	**C28**	**C29**	**N21**	-0.5(8)
C27	**C28**	**O21**	**Al1**	-177.9(5)	**O31**	**C38**	**C39**	**C34**	178.3(5)
C28	**C29**	**N21**	**C21**	-177.5(5)	**O31**	**C38**	**C39**	**N31**	-2.4(8)
C28	**C29**	**N21**	**Al1**	-0.3(6)					

B. *mer*-[*tris*-(8-Hydroxyquinoline) gallium (III)] 0.5•ethanol solvate (2)

Table B.1: Fractional Atomic Coordinates ($\times 10^4$) and Equivalent Isotropic Displacement Parameters ($Å^2 \times 10^3$) for *mer*-[$Ga(Ox)_3$]·0.5·EtOH (2).

Atom	*x*	*y*	*z*	U(eq)
Ga01	9227.1(3)	247.2(2)	2398.2(2)	27.04(11)
O2	9068.7(19)	1625.4(15)	1993.7(11)	33.9(4)
O3	7526.4(19)	73.0(16)	2594.2(12)	35.0(4)
O1	10997.4(18)	226.1(15)	2385.2(12)	31.6(4)
N2	8785(2)	-111.8(18)	1189.4(13)	29.6(5)
N1	9572(2)	-1292.3(18)	2716.1(12)	27.8(5)
N3	9433(2)	750(2)	3572.3(14)	37.2(6)
C8	9246(3)	-3009(2)	3092.1(19)	42.9(7)
C26	10387(5)	1403(4)	4815(2)	75.2(14)
C10	8838(2)	1685(2)	1206.8(16)	30.4(6)
C9	10463(3)	-3229(2)	3110.1(18)	43.2(7)
C3	13290(3)	-1801(3)	2776.2(19)	45.2(8)
C20	6181(3)	345(3)	3587(2)	45.9(8)
C27	9301(5)	1383(4)	5114(2)	71.3(13)
C23	8202(4)	1049(3)	4647.6(19)	51.3(9)
C7	8818(3)	-2020(2)	2886.2(17)	36.9(6)
C22	7026(4)	1010(3)	4891(2)	61.8(11)
C12	8489(3)	2590(3)	-57(2)	43.7(7)
C25	10425(4)	1083(3)	4030.7(19)	56.4(10)
C4	12582(3)	-2612(3)	2934.9(18)	43.0(7)
C21	6054(4)	670(3)	4370(3)	59.2(11)
C24	8334(3)	727(2)	3861.6(17)	35.2(6)
C1	11543(2)	-651(2)	2570.7(15)	29.3(5)
C2	12801(3)	-826(3)	2603.9(18)	38.7(7)
C19	7313(3)	359(2)	3314.3(17)	32.8(6)
C18	8306(3)	-194(3)	-467.1(17)	41.0(7)
C14	8420(3)	769(2)	-89.4(16)	34.4(6)
C16	8655(3)	-999(2)	815.8(17)	35.7(6)
C11	8739(3)	2593(2)	786.5(18)	37.7(6)
C13	8332(3)	1713(3)	-489.0(18)	42.8(7)
C15	8671(2)	766(2)	755.5(15)	28.9(5)
C5	11305(3)	-2474(2)	2929.4(16)	34.4(6)
C17	8414(3)	-1065(2)	-21.4(18)	41.4(7)
C6	10795(2)	-1502(2)	2741.5(14)	27.3(5)
O4A	10019(8)	-3911(7)	5136(6)	76.8(12)
C2B	10549(10)	-4202(11)	6028(6)	43(2)

C1A	10965(6)	-3223(5)	6693(4)	116(2)
C2A	10376(14)	-4076(12)	6214(7)	55(3)
O4B	10159(5)	-4743(4)	5331(3)	76.8(12)

Table B.1: Hydrogen Atom Coordinates (Å×10^4) and Isotropic Displacement Parameters (Å^2×10^3) for *mer*-[Ga(Ox)$_3$]·0.5·EtOH (2).

Atom	*x*	*y*	*z*	U(eq)
H8	8698	-3509	3215	51
H26	11099	1628	5128	90
H9	10744	-3884	3243	52
H3	14133	-1898	2783	54
H20	5492	118	3251	55
H27	9273	1593	5638	86
H7	7983	-1877	2870	44
H22	6910	1215	5404	74
H12	8431	3210	-327	52
H25	11171	1104	3823	68
H4	12938	-3248	3045	52
H21	5277	652	4537	71
H2	13323	-293	2511	46
H18	8157	-234	-1022	49
H16	8725	-1596	1116	43
H11	8837	3208	1061	45
H13	8167	1737	-1044	51
H17	8329	-1698	-270	50

Table B.3: Anisotropic Displacement Parameters (Å^2×10^3) for *mer*-[Ga(Ox)$_3$]·0.5·EtOH (2).

Atom	U_{11}	U_{22}	U_{33}	U_{23}	U_{13}	U_{12}
Ga01	30.07(17)	31.87(18)	19.16(16)	-2.01(11)	3.1(1)	1.16(12)
O2	44.4(11)	32(1)	24.5(10)	-4.3(8)	1.9(8)	1.5(9)
O3	30.4(10)	42.3(11)	32.0(11)	-4.1(8)	3.3(8)	1.9(8)
O1	29.7(10)	33.2(10)	32.3(10)	4.2(8)	5.7(8)	-0.2(8)
N2	36.5(12)	31.8(12)	20.7(11)	-2.3(8)	4.5(9)	2.5(10)
N1	32.7(11)	32.3(12)	18.7(10)	-0.6(8)	4.1(8)	-3.5(9)
N3	40.8(13)	49.9(15)	20.9(11)	-4.9(10)	4.4(9)	-6.3(12)
C8	58(2)	34.2(15)	36.3(16)	-2.5(12)	7.0(14)	-14.1(14)
C26	83(3)	108(4)	34(2)	-25(2)	1.3(19)	-34(3)
C10	30.4(13)	32.7(14)	27.9(14)	0(1)	3.6(10)	0.4(11)

C9	67(2)	30.8(15)	32.2(16)	-2.5(12)	6.9(14)	2.3(14)
C3	35.2(16)	64(2)	35.8(17)	1.9(15)	3.0(12)	13.2(15)
C20	40.6(17)	44.3(18)	56(2)	15.4(15)	16.7(15)	8.9(14)
C27	104(4)	83(3)	28.7(19)	-20.2(19)	14(2)	-20(3)
C23	81(3)	47.0(19)	30.2(16)	-3.9(14)	24.0(16)	-3.1(18)
C7	39.9(15)	41.4(16)	29.8(15)	-4.6(12)	6.3(11)	-9.1(13)
C22	93(3)	56(2)	45(2)	2.2(17)	42(2)	10(2)
C12	48.7(18)	41.6(17)	40.1(17)	14.1(13)	3.3(13)	-2.1(14)
C25	55(2)	86(3)	26.9(16)	-12.4(17)	1.7(14)	-24(2)
C4	51.0(18)	44.8(17)	32.5(16)	0.9(13)	3.5(13)	18.9(15)
C21	67(3)	53(2)	68(3)	19.9(19)	48(2)	19.6(19)
C24	47.2(17)	34.2(15)	26.6(14)	0.3(11)	13.6(12)	0.9(13)
C1	33.0(13)	36.3(14)	18.3(12)	0.6(10)	2.3(10)	0.3(11)
C2	29.1(14)	54.9(19)	32.5(15)	4.9(13)	5.0(11)	0.7(13)
C19	36.5(14)	29.8(14)	33.5(15)	4.6(11)	10.2(11)	5.5(11)
C18	53.3(19)	49.1(18)	20.7(14)	-5.4(12)	4.6(12)	-5.3(15)
C14	37.4(15)	41.1(16)	24.9(13)	1.5(11)	4.6(11)	-0.5(13)
C16	47.9(17)	33.1(14)	26.8(14)	-2.4(11)	6.7(12)	1.2(12)
C11	41.4(16)	32.5(15)	38.8(16)	0.8(12)	3.8(12)	1.7(12)
C13	52.7(19)	49.7(18)	25.3(15)	6.7(12)	2.3(13)	-2.1(15)
C15	31.8(13)	31.5(14)	23.5(13)	-0.5(10)	4.6(10)	0.5(11)
C5	48.8(17)	33.4(14)	20.8(13)	-2.1(10)	3.4(11)	5.0(12)
C17	56.6(19)	39.2(16)	28.3(15)	-10.6(12)	5.3(13)	-1.8(14)
C6	33.3(13)	34.2(14)	14.5(11)	-1.8(9)	3.2(9)	1.7(11)
O4A	69(3)	66(3)	98(3)	-9(2)	20(2)	-13(2)
C2B	43(4)	67(5)	24(5)	-11(4)	27(4)	-3(3)
C1A	109(5)	100(5)	134(6)	-25(4)	-1(4)	38(4)
C2A	78(6)	74(6)	24(4)	-8(4)	43(4)	-13(5)
O4B	69(3)	66(3)	98(3)	-9(2)	20(2)	-13(2)

Table B.4: Bond Lengths for *mer*-[Ga(Ox)$_3$]·0.5·EtOH (2).

Atom	Atom	Length/Å	Atom	Atom	Length/Å
Ga01	**O2**	1.933(2)	**C20**	**C19**	1.377(4)
Ga01	**O3**	1.946(2)	**C27**	**C23**	1.417(6)
Ga01	**O1**	1.941(2)	**C23**	**C22**	1.403(6)
Ga01	**N2**	2.087(2)	**C23**	**C24**	1.416(4)
Ga01	**N1**	2.112(2)	**C22**	**C21**	1.363(6)
Ga01	**N3**	2.071(2)	**C12**	**C11**	1.414(4)
O2	**C10**	1.320(3)	**C12**	**C13**	1.361(5)
O3	**C19**	1.321(4)	**C4**	**C5**	1.408(4)
O1	**C1**	1.315(3)	**C24**	**C19**	1.436(4)

N2	**C16**	1.323(4)	**C1**	**C2**	1.390(4)
N2	**C15**	1.361(4)	**C1**	**C6**	1.436(4)
N1	**C7**	1.319(4)	**C18**	**C14**	1.413(4)
N1	**C6**	1.361(3)	**C18**	**C17**	1.365(5)
N3	**C25**	1.322(4)	**C14**	**C13**	1.407(4)
N3	**C24**	1.356(4)	**C14**	**C15**	1.415(4)
C8	**C9**	1.360(5)	**C16**	**C17**	1.405(4)
C8	**C7**	1.407(5)	**C5**	**C6**	1.412(4)
C26	**C27**	1.351(7)	**O4A**	**C2B**	1.586(13)
C26	**C25**	1.393(5)	**O4A**	**C2A**	1.822(16)
C10	**C11**	1.382(4)	**O4A**	**O4B**	1.145(10)
C10	**C15**	1.426(4)	**C2B**	**C1A**	1.726(14)
C9	**C5**	1.413(4)	**C2B**	**O4B**	1.392(12)
C3	**C4**	1.364(5)	**C1A**	**C2A**	1.477(16)
C3	**C2**	1.402(5)	**C2A**	**O4B**	1.718(12)
C20	**C21**	1.412(5)	**O4B**	**O4B**[1]	1.311(10)

[1]2-X,-1-Y,1-Z

Table B.5: Bond Angles for *mer*-[Ga(Ox)$_3$]·0.5·EtOH (2).

Atom	Atom	Atom	Angle/°	Atom	Atom	Atom	Angle/°
O2	**Ga01**	**O3**	97.26(9)	**C22**	**C21**	**C20**	122.6(3)
O2	**Ga01**	**O1**	93.03(8)	**N3**	**C24**	**C23**	122.3(3)
O2	**Ga01**	**N2**	82.41(9)	**N3**	**C24**	**C19**	115.3(2)
O2	**Ga01**	**N1**	171.78(8)	**C23**	**C24**	**C19**	122.4(3)
O2	**Ga01**	**N3**	91.89(10)	**O1**	**C1**	**C2**	124.8(3)
O3	**Ga01**	**N2**	92.00(9)	**O1**	**C1**	**C6**	118.4(2)
O3	**Ga01**	**N1**	89.30(9)	**C2**	**C1**	**C6**	116.8(3)
O3	**Ga01**	**N3**	82.06(9)	**C1**	**C2**	**C3**	120.6(3)
O1	**Ga01**	**O3**	168.17(9)	**O3**	**C19**	**C20**	125.3(3)
O1	**Ga01**	**N2**	95.15(9)	**O3**	**C19**	**C24**	118.1(3)
O1	**Ga01**	**N1**	81.00(8)	**C20**	**C19**	**C24**	116.6(3)
O1	**Ga01**	**N3**	91.81(9)	**C17**	**C18**	**C14**	120.3(3)
N2	**Ga01**	**N1**	92.46(9)	**C18**	**C14**	**C15**	116.4(3)
N3	**Ga01**	**N2**	171.21(10)	**C13**	**C14**	**C18**	125.1(3)
N3	**Ga01**	**N1**	93.92(10)	**C13**	**C14**	**C15**	118.5(3)
C10	**O2**	**Ga01**	114.02(17)	**N2**	**C16**	**C17**	121.8(3)
C19	**O3**	**Ga01**	114.24(19)	**C10**	**C11**	**C12**	120.4(3)
C1	**O1**	**Ga01**	115.63(17)	**C12**	**C13**	**C14**	119.5(3)
C16	**N2**	**Ga01**	131.4(2)	**N2**	**C15**	**C10**	115.6(2)
C16	**N2**	**C15**	119.5(2)	**N2**	**C15**	**C14**	122.4(3)

C15	**N2**	**Ga01**	109.12(17)	**C14**	**C15**	**C10**	121.9(3)
C7	**N1**	**Ga01**	130.7(2)	**C4**	**C5**	**C9**	125.7(3)
C7	**N1**	**C6**	119.2(3)	**C4**	**C5**	**C6**	118.7(3)
C6	**N1**	**Ga01**	110.11(17)	**C6**	**C5**	**C9**	115.6(3)
C25	**N3**	**Ga01**	130.0(2)	**C18**	**C17**	**C16**	119.6(3)
C25	**N3**	**C24**	119.7(3)	**N1**	**C6**	**C1**	114.9(2)
C24	**N3**	**Ga01**	110.27(19)	**N1**	**C6**	**C5**	123.2(3)
C9	**C8**	**C7**	119.7(3)	**C5**	**C6**	**C1**	121.9(2)
C27	**C26**	**C25**	119.0(4)	**C2B**	**O4A**	**C2A**	11.8(7)
O2	**C10**	**C11**	124.0(3)	**O4B**	**O4A**	**C2B**	58.7(7)
O2	**C10**	**C15**	118.7(2)	**O4B**	**O4A**	**C2A**	66.3(7)
C11	**C10**	**C15**	117.3(3)	**O4A**	**C2B**	**C1A**	118.0(9)
C8	**C9**	**C5**	120.7(3)	**O4B**	**C2B**	**O4A**	44.7(5)
C4	**C3**	**C2**	122.8(3)	**O4B**	**C2B**	**C1A**	162.5(10)
C19	**C20**	**C21**	120.7(4)	**C2A**	**C1A**	**C2B**	12.2(6)
C26	**C27**	**C23**	121.5(3)	**C1A**	**C2A**	**O4A**	118.4(10)
C22	**C23**	**C27**	126.4(3)	**C1A**	**C2A**	**O4B**	149.4(9)
C22	**C23**	**C24**	118.2(4)	**O4B**	**C2A**	**O4A**	37.6(4)
C24	**C23**	**C27**	115.4(3)	**O4A**	**O4B**	**C2B**	76.7(7)
N1	**C7**	**C8**	121.6(3)	**O4A**	**O4B**	**C2A**	76.1(8)
C21	**C22**	**C23**	119.4(3)	**O4A**	**O4B**	**O4B**[1]	103.6(8)
C13	**C12**	**C11**	122.3(3)	**C2B**	**O4B**	**C2A**	9.9(8)
N3	**C25**	**C26**	122.1(4)	**O4B**[1]	**O4B**	**C2B**	177.6(8)
C3	**C4**	**C5**	119.2(3)	**O4B**[1]	**O4B**	**C2A**	172.5(8)

[1]2-X,-1-Y,1-Z

Table B.6: Torsion Angles for *mer*-[Ga(Ox)$_3$]·0.5·EtOH (2).

A	B	C	D	Angle/°	A	B	C	D	Angle/°
Ga01	**O2**	**C10**	**C11**	-177.3(2)	**C4**	**C5**	**C6**	**N1**	179.6(2)
Ga01	**O2**	**C10**	**C15**	3.2(3)	**C4**	**C5**	**C6**	**C1**	-1.1(4)
Ga01	**O3**	**C19**	**C20**	177.6(2)	**C21**	**C20**	**C19**	**O3**	-179.9(3)
Ga01	**O3**	**C19**	**C24**	-1.7(3)	**C21**	**C20**	**C19**	**C24**	-0.5(4)
Ga01	**O1**	**C1**	**C2**	-179.4(2)	**C24**	**N3**	**C25**	**C26**	0.9(6)
Ga01	**O1**	**C1**	**C6**	1.6(3)	**C24**	**C23**	**C22**	**C21**	-0.2(6)
Ga01	**N2**	**C16**	**C17**	-176.5(2)	**C2**	**C3**	**C4**	**C5**	-0.2(5)
Ga01	**N2**	**C15**	**C10**	-1.6(3)	**C2**	**C1**	**C6**	**N1**	178.9(2)
Ga01	**N2**	**C15**	**C14**	177.5(2)	**C2**	**C1**	**C6**	**C5**	-0.4(4)
Ga01	**N1**	**C7**	**C8**	-179.5(2)	**C19**	**C20**	**C21**	**C22**	-0.1(5)
Ga01	**N1**	**C6**	**C1**	1.4(3)	**C18**	**C14**	**C13**	**C12**	-178.4(3)
Ga01	**N1**	**C6**	**C5**	-179.3(2)	**C18**	**C14**	**C15**	**N2**	-0.7(4)
Ga01	**N3**	**C25**	**C26**	179.3(4)	**C18**	**C14**	**C15**	**C10**	178.4(3)
Ga01	**N3**	**C24**	**C23**	-178.8(3)	**C14**	**C18**	**C17**	**C16**	-0.8(5)
Ga01	**N3**	**C24**	**C19**	0.9(3)	**C16**	**N2**	**C15**	**C10**	-179.3(3)

O2	**C10**	**C11**	**C12**	-180.0(3)	**C16**	**N2**	**C15**	**C14**	-0.3(4)
O2	**C10**	**C15**	**N2**	-0.9(4)	**C11**	**C10**	**C15**	**N2**	179.5(3)
O2	**C10**	**C15**	**C14**	180.0(2)	**C11**	**C10**	**C15**	**C14**	0.4(4)
O1	**C1**	**C2**	**C3**	-177.4(3)	**C11**	**C12**	**C13**	**C14**	-0.1(5)
O1	**C1**	**C6**	**N1**	-2.0(3)	**C13**	**C12**	**C11**	**C10**	0.3(5)
O1	**C1**	**C6**	**C5**	178.7(2)	**C13**	**C14**	**C15**	**N2**	-179.2(3)
N2	**C16**	**C17**	**C18**	-0.2(5)	**C13**	**C14**	**C15**	**C10**	-0.2(4)
N3	**C24**	**C19**	**O3**	0.5(4)	**C15**	**N2**	**C16**	**C17**	0.7(4)
N3	**C24**	**C19**	**C20**	-178.9(3)	**C15**	**C10**	**C11**	**C12**	-0.4(4)
C8	**C9**	**C5**	**C4**	179.5(3)	**C15**	**C14**	**C13**	**C12**	0.1(5)
C8	**C9**	**C5**	**C6**	0.5(4)	**C17**	**C18**	**C14**	**C13**	179.7(3)
C26	**C27**	**C23**	**C22**	-179.0(5)	**C17**	**C18**	**C14**	**C15**	1.2(5)
C26	**C27**	**C23**	**C24**	1.0(7)	**C6**	**N1**	**C7**	**C8**	-0.1(4)
C9	**C8**	**C7**	**N1**	-0.7(5)	**C6**	**C1**	**C2**	**C3**	1.6(4)
C9	**C5**	**C6**	**N1**	-1.3(4)	**O4A**	**C2B**	**C1A**	**C2A**	104(5)
C9	**C5**	**C6**	**C1**	177.9(2)	**O4A**	**C2B**	**O4B**	**C2A**	-86(6)
C3	**C4**	**C5**	**C9**	-177.6(3)	**O4A**	**C2A**	**O4B**	**C2B**	92(6)
C3	**C4**	**C5**	**C6**	1.4(4)	**C2B**	**O4A**	**C2A**	**C1A**	107(5)
C27	**C26**	**C25**	**N3**	-0.7(8)	**C2B**	**O4A**	**C2A**	**O4B**	-48(4)
C27	**C23**	**C22**	**C21**	179.9(4)	**C2B**	**O4A**	**O4B**	**C2A**	10.2(8)
C27	**C23**	**C24**	**N3**	-0.8(5)	**C2B**	**O4A**	**O4B**	**O4B**[1]	-177.5(8)
C27	**C23**	**C24**	**C19**	179.5(3)	**C2B**	**C1A**	**C2A**	**O4A**	-58(4)
C23	**C22**	**C21**	**C20**	0.4(6)	**C2B**	**C1A**	**C2A**	**O4B**	-27(3)
C23	**C24**	**C19**	**O3**	-179.8(3)	**C1A**	**C2B**	**O4B**	**O4A**	-7(3)
C23	**C24**	**C19**	**C20**	0.8(4)	**C1A**	**C2B**	**O4B**	**C2A**	-92(7)
C7	**N1**	**C6**	**C1**	-178.2(2)	**C1A**	**C2A**	**O4B**	**O4A**	-48(2)
C7	**N1**	**C6**	**C5**	1.1(4)	**C1A**	**C2A**	**O4B**	**C2B**	44(5)
C7	**C8**	**C9**	**C5**	0.4(5)	**C2A**	**O4A**	**C2B**	**C1A**	-55(4)
C22	**C23**	**C24**	**N3**	179.2(3)	**C2A**	**O4A**	**C2B**	**O4B**	128(5)
C22	**C23**	**C24**	**C19**	-0.5(5)	**C2A**	**O4A**	**O4B**	**C2B**	-10.2(8)
C25	**N3**	**C24**	**C23**	-0.2(5)	**C2A**	**O4A**	**O4B**	**O4B**[1]	172.3(8)
C25	**N3**	**C24**	**C19**	179.6(3)	**O4B**	**O4A**	**C2B**	**C1A**	177.7(9)
C25	**C26**	**C27**	**C23**	-0.3(8)	**O4B**	**O4A**	**C2A**	**C1A**	154.3(11)
C4	**C3**	**C2**	**C1**	-1.4(5)	**O4B**	**C2B**	**C1A**	**C2A**	109(6)

C. *mer*-[*tris*-(5,7-Dimethyl-8-hydroxyquinoline) gallium (III)] dichloromethane solvate (3)

Table C.1: Fractional Atomic Coordinates ($\times 10^4$) and Equivalent Isotropic Displacement Parameters ($Å^2 \times 10^3$) for *mer*-[Ga(57dmOx)$_3$]·DCM (3).

Atom	*x*	*y*	*z*	U(eq)
Ga1	3267.2(5)	1671.2(5)	2872.7(4)	21.34(17)
O2	3991(4)	1467(4)	4166(3)	31.1(8)
O3	2303(3)	1915(3)	1693(2)	23.5(7)
O1	5074(3)	2704(3)	2747(3)	29.9(8)
N1	3522(4)	119(4)	1945(3)	22.7(8)
N3	3075(4)	3343(4)	3627(3)	20.7(8)
N2	1482(4)	300(4)	3105(3)	27.1(9)
C15	1100(5)	-1320(5)	5257(4)	26.6(10)
C3	7411(6)	1595(6)	1644(4)	34.2(12)
C24	1291(5)	3294(5)	1196(4)	23.4(9)
C30	3300(5)	5162(5)	4986(4)	29.8(10)
C4	6634(6)	268(6)	1182(4)	31.5(11)
C8	3058(6)	-2082(5)	956(4)	37.0(12)
C11	7906(6)	3934(6)	2706(6)	47.0(15)
C34	5185(7)	4845(7)	1563(5)	50.0(16)
C22	4848(6)	1046(6)	6095(4)	35.4(12)
C9	4352(6)	-1634(6)	834(4)	34.3(12)
C33	798(6)	2458(5)	94(4)	31.8(11)
C23	1996(5)	2948(5)	1915(4)	22.2(9)
C27	2156(5)	4889(5)	3266(4)	24.6(9)
C13	3451(5)	342(5)	5479(4)	28.4(10)
C10	7190(7)	-624(7)	598(5)	43.8(15)
C12	3113(5)	633(5)	4549(4)	27.9(10)
C26	1443(5)	5234(5)	2522(4)	25.9(10)
C28	2411(5)	3751(4)	2945(4)	21.8(9)
C6	4801(5)	578(5)	1814(4)	24.6(9)
C1	5622(5)	1965(5)	2273(4)	27.2(10)
C25	1048(5)	4437(5)	1522(4)	26.2(10)
C5	5277(5)	-287(5)	1261(4)	28.2(10)
C31	2640(5)	5591(5)	4324(4)	28.9(10)
C14	2440(6)	-629(5)	5791(4)	33.0(11)
C19	-845(6)	-1234(5)	2843(4)	36.1(12)
C7	2678(5)	-1154(5)	1534(4)	29.8(11)

C21	115(7)	-2352(6)	5658(5)	45.9(15)
C32	1138(6)	6427(5)	2818(5)	35.7(12)
C20	-545(6)	-1562(5)	3727(5)	34.9(12)
C17	1776(5)	-37(5)	4015(4)	27.7(10)
C2	6945(5)	2480(6)	2187(4)	33.9(11)
C29	3477(5)	4004(5)	4608(4)	25.4(10)
C16	745(5)	-1004(5)	4353(4)	28.9(10)
C18	249(5)	-267(5)	2557(4)	33.5(11)
Cl1	5635(4)	6258(3)	2683(4)	44.6(11)
Cl2	6514(4)	5125(9)	856(3)	44.4(12)
Cl3	5282(10)	6183(6)	2318(9)	52(3)
Cl4	6424(7)	5407(15)	912(5)	37(3)

Table C.2. Hydrogen coordinates (x 10^4) and isotropic displacement parameters ($Å^2$x 10^3) for *mer*-[Ga(57dmOx)$_3$]·DCM (3).

Atoms	x	y	z	U(eq)_
H(3)	8292	1949	1601	40
H(30)	3619	5623	5669	35
H(8)	2462	-2961	675	44
H(11A)	7429	4471	2708	70
H(11B)	8589	4211	2332	70
H(11C)	8295	4006	3393	70
H(22A)	5183	387	6139	52
H(22B)	4861	1498	6768	52
H(22C)	5377	1668	5768	52
H(9)	4609	-2238	466	40
H(33A)	107	1604	49	47
H(33B)	1530	2354	-146	47
H(33C)	468	2915	-312	47
H(10A)	7061	-1357	883	62
H(10B)	8124	-93	662	62
H(10C)	6734	-938	-109	62
H(25)	599	4666	1036	31
H(31)	2507	6338	4571	34
H(14)	2681	-819	6389	40
H(19)	-1703	-1610	2457	42
H(7)	1817	-1454	1623	33
H(21A)	-233	-3205	5163	66

H(21B)	-582	-2101	5772	66
H(21C)	569	-2387	6289	66
H(32A)	1961	7232	3032	50
H(32B)	686	6344	3362	50
H(32C)	589	6455	2232	50
H(20)	-1225	-2186	3919	41
H(29)	3887	3699	5063	29
H(18)	78	-37	1962	40
H(34A)	5200(40)	4160(40)	1850(30)	29(11)
H(34B)	4420(60)	4590(60)	1110(40)	60(17)

Table C.3: Anisotropic Displacement Parameters ($Å^2×10^3$) for *mer*-[Ga(57dmOx)$_3$]·DCM (3).

Atom	**U_{11}**	**U_{22}**	**U_{33}**	**U_{23}**	**U_{13}**	**U_{12}**
Ga1	20.7(3)	20.1(3)	24.9(3)	9.77(19)	6.47(19)	8.4(2)
O2	31.3(19)	30.8(18)	31.4(19)	10.7(15)	1.7(15)	14.3(16)
O3	30.4(18)	20.3(15)	22.6(16)	6.6(13)	4.5(13)	13.7(14)
O1	20.6(17)	28.0(18)	39(2)	5.4(15)	11.1(15)	9.2(14)
N1	24(2)	23.0(19)	22.0(19)	9.7(15)	3.2(15)	10.4(16)
N3	15.4(18)	20.2(18)	26.6(19)	8.6(15)	6.7(15)	6.1(15)
N2	19.2(19)	22.8(19)	34(2)	2.5(17)	8.5(17)	5.4(16)
C15	31(3)	23(2)	33(3)	14(2)	15(2)	14(2)
C3	32(3)	54(3)	28(3)	19(2)	12(2)	26(3)
C24	23(2)	26(2)	26(2)	13.1(19)	9.6(18)	11.1(19)
C30	24(2)	30(3)	30(3)	5(2)	7(2)	8(2)
C4	37(3)	53(3)	23(2)	19(2)	11(2)	33(3)
C8	51(3)	27(3)	33(3)	4(2)	9(2)	20(3)
C11	21(3)	45(3)	63(4)	7(3)	15(3)	5(2)
C34	50(4)	45(3)	50(4)	23(3)	20(3)	9(3)
C22	32(3)	41(3)	39(3)	17(2)	11(2)	18(2)
C9	50(3)	37(3)	27(3)	12(2)	12(2)	27(3)
C33	38(3)	38(3)	24(2)	9(2)	4(2)	22(2)
C23	20(2)	24(2)	27(2)	10.8(18)	9.3(18)	10.3(18)
C27	19(2)	22(2)	34(3)	9.3(19)	11.5(19)	7.4(18)
C13	28(3)	32(3)	29(2)	7(2)	8(2)	17(2)
C10	57(4)	67(4)	37(3)	23(3)	23(3)	49(4)
C12	32(3)	28(2)	30(2)	7(2)	10(2)	18(2)
C26	22(2)	20(2)	39(3)	12(2)	11(2)	9.6(19)
C28	19(2)	20(2)	28(2)	10.7(18)	10.5(18)	6.3(17)
C6	28(2)	31(2)	22(2)	15.3(19)	7.7(18)	17(2)

C1	24(2)	33(3)	29(2)	9(2)	5.5(19)	15(2)
C25	21(2)	27(2)	37(3)	16(2)	13(2)	12.4(19)
C5	38(3)	36(3)	22(2)	13(2)	9(2)	24(2)
C31	22(2)	22(2)	39(3)	5(2)	13(2)	6.1(19)
C14	37(3)	35(3)	35(3)	14(2)	15(2)	20(2)
C19	40(3)	31(3)	39(3)	9(2)	10(2)	17(2)
C7	36(3)	21(2)	28(2)	6.3(19)	3(2)	10(2)
C21	48(4)	39(3)	60(4)	27(3)	33(3)	15(3)
C32	38(3)	23(2)	54(3)	11(2)	16(3)	18(2)
C20	31(3)	32(3)	43(3)	2(2)	7(2)	18(2)
C17	37(3)	19(2)	36(3)	12.2(19)	22(2)	14(2)
C2	25(3)	40(3)	36(3)	11(2)	8(2)	13(2)
C29	18(2)	28(2)	25(2)	5.7(19)	5.0(18)	5.5(19)
C16	29(3)	24(2)	38(3)	10(2)	14(2)	13(2)
C18	28(3)	32(3)	38(3)	8(2)	6(2)	12(2)

Table C.4: Bond Lengths for *mer*-[Ga(57dmOx)$_3$]·DCM (3).

Atom	Atom	Length/Å	Atom	Atom	Length/Å
Ga1	**O2**	1.943(4)	**C8**	**C9**	1.379(9)
Ga1	**O3**	1.951(3)	**C8**	**C7**	1.420(7)
Ga1	**O1**	1.947(4)	**C11**	**C2**	1.518(8)
Ga1	**N1**	2.091(4)	**C34**	**Cl1**	1.829(8)
Ga1	**N3**	2.070(4)	**C34**	**Cl2**	1.834(9)
Ga1	**N2**	2.098(4)	**C34**	**Cl3**	1.608(10)
O2	**C12**	1.311(6)	**C34**	**Cl4**	1.720(10)
O3	**C23**	1.333(5)	**C22**	**C13**	1.486(7)
O1	**C1**	1.337(6)	**C9**	**C5**	1.406(8)
N1	**C6**	1.367(6)	**C23**	**C28**	1.420(6)
N1	**C7**	1.321(6)	**C27**	**C26**	1.421(7)
N3	**C28**	1.378(6)	**C27**	**C28**	1.422(6)
N3	**C29**	1.321(6)	**C27**	**C31**	1.422(7)
N2	**C17**	1.407(7)	**C13**	**C12**	1.417(7)
N2	**C18**	1.315(7)	**C13**	**C14**	1.410(8)
C15	**C14**	1.402(8)	**C12**	**C17**	1.399(7)
C15	**C21**	1.503(7)	**C26**	**C25**	1.385(7)
C15	**C16**	1.404(7)	**C26**	**C32**	1.509(6)
C3	**C4**	1.361(8)	**C6**	**C1**	1.419(7)
C3	**C2**	1.430(8)	**C6**	**C5**	1.426(7)
C24	**C33**	1.509(7)	**C1**	**C2**	1.393(7)
C24	**C23**	1.393(6)	**C19**	**C20**	1.371(8)

C24	**C25**	1.421(6)	**C19**	**C18**	1.441(8)
C30	**C31**	1.372(7)	**C20**	**C16**	1.404(7)
C30	**C29**	1.407(7)	**C17**	**C16**	1.440(7)
C4	**C10**	1.533(7)	**Cl1**	**Cl3**	0.564(9)
C4	**C5**	1.426(8)			

Table C.5: Bond Angles for *mer*-[Ga(57dmOx)$_3$]·DCM (3).

Atom	Atom	Atom	Angle/°	Atom	Atom	Atom	Angle/°
O2	**Ga1**	**O3**	169.97(15)	**O3**	**C23**	**C24**	124.0(4)
O2	**Ga1**	**O1**	89.50(16)	**O3**	**C23**	**C28**	118.4(4)
O2	**Ga1**	**N1**	95.59(15)	**C24**	**C23**	**C28**	117.6(4)
O2	**Ga1**	**N3**	91.17(15)	**C26**	**C27**	**C28**	118.5(4)
O2	**Ga1**	**N2**	81.88(17)	**C26**	**C27**	**C31**	125.1(4)
O3	**Ga1**	**N1**	91.86(14)	**C31**	**C27**	**C28**	116.4(4)
O3	**Ga1**	**N3**	82.01(14)	**C12**	**C13**	**C22**	119.9(5)
O3	**Ga1**	**N2**	91.28(16)	**C14**	**C13**	**C22**	121.7(5)
O1	**Ga1**	**O3**	98.26(15)	**C14**	**C13**	**C12**	118.4(5)
O1	**Ga1**	**N1**	81.56(15)	**O2**	**C12**	**C13**	123.2(5)
O1	**Ga1**	**N3**	93.95(15)	**O2**	**C12**	**C17**	119.5(5)
O1	**Ga1**	**N2**	168.17(16)	**C17**	**C12**	**C13**	117.3(5)
N1	**Ga1**	**N2**	91.18(16)	**C27**	**C26**	**C32**	120.9(5)
N3	**Ga1**	**N1**	171.84(15)	**C25**	**C26**	**C27**	117.3(4)
N3	**Ga1**	**N2**	94.31(15)	**C25**	**C26**	**C32**	121.8(5)
C12	**O2**	**Ga1**	114.9(3)	**N3**	**C28**	**C23**	115.1(4)
C23	**O3**	**Ga1**	114.2(3)	**N3**	**C28**	**C27**	121.7(4)
C1	**O1**	**Ga1**	114.3(3)	**C23**	**C28**	**C27**	123.2(4)
C6	**N1**	**Ga1**	109.9(3)	**N1**	**C6**	**C1**	115.6(4)
C7	**N1**	**Ga1**	130.1(4)	**N1**	**C6**	**C5**	122.0(5)
C7	**N1**	**C6**	120.0(4)	**C1**	**C6**	**C5**	122.4(5)
C28	**N3**	**Ga1**	110.3(3)	**O1**	**C1**	**C6**	118.0(4)
C29	**N3**	**Ga1**	129.8(3)	**O1**	**C1**	**C2**	123.9(5)
C29	**N3**	**C28**	119.9(4)	**C2**	**C1**	**C6**	118.0(5)
C17	**N2**	**Ga1**	108.3(3)	**C26**	**C25**	**C24**	124.5(4)
C18	**N2**	**Ga1**	131.9(4)	**C4**	**C5**	**C6**	118.4(5)
C18	**N2**	**C17**	119.7(5)	**C9**	**C5**	**C4**	125.2(5)
C14	**C15**	**C21**	120.0(5)	**C9**	**C5**	**C6**	116.5(5)
C14	**C15**	**C16**	117.1(5)	**C30**	**C31**	**C27**	120.6(4)
C16	**C15**	**C21**	122.9(5)	**C15**	**C14**	**C13**	124.9(5)
C4	**C3**	**C2**	124.0(5)	**C20**	**C19**	**C18**	116.6(5)
C23	**C24**	**C33**	119.9(4)	**N1**	**C7**	**C8**	121.9(5)

C23	**C24**	**C25**	118.8(4)	**C19**	**C20**	**C16**	123.7(6)
C25	**C24**	**C33**	121.3(4)	**N2**	**C17**	**C16**	120.9(5)
C31	**C30**	**C29**	119.2(5)	**C12**	**C17**	**N2**	115.3(4)
C3	**C4**	**C10**	121.5(5)	**C12**	**C17**	**C16**	123.8(5)
C3	**C4**	**C5**	118.3(5)	**C3**	**C2**	**C11**	119.9(5)
C5	**C4**	**C10**	120.2(5)	**C1**	**C2**	**C3**	118.8(5)
C9	**C8**	**C7**	118.6(5)	**C1**	**C2**	**C11**	121.2(5)
Cl1	**C34**	**Cl2**	111.8(4)	**N3**	**C29**	**C30**	122.0(4)
Cl3	**C34**	**Cl1**	17.4(4)	**C15**	**C16**	**C17**	118.5(5)
Cl3	**C34**	**Cl2**	114.5(5)	**C20**	**C16**	**C15**	125.6(5)
Cl3	**C34**	**Cl4**	104.7(7)	**C20**	**C16**	**C17**	115.9(5)
Cl4	**C34**	**Cl1**	104.3(6)	**N2**	**C18**	**C19**	123.1(5)
Cl4	**C34**	**Cl2**	11.3(4)	**Cl3**	**Cl1**	**C34**	58.5(8)
C8	**C9**	**C5**	121.0(5)	**Cl1**	**Cl3**	**C34**	104.1(9)

Table C.6: Torsion Angles for *mer*-[Ga(57dmOx)$_3$]·DCM (3).

A	**B**	**C**	**D**	**Angle/°**	**A**	**B**	**C**	**D**	**Angle/°**
Ga1	**O2**	**C12**	**C13**	179.4(4)	**C12**	**C17**	**C16**	**C20**	179.2(4)
Ga1	**O2**	**C12**	**C17**	0.8(5)	**C26**	**C27**	**C28**	**N3**	-178.8(4)
Ga1	**O3**	**C23**	**C24**	-178.9(4)	**C26**	**C27**	**C28**	**C23**	0.4(7)
Ga1	**O3**	**C23**	**C28**	1.3(5)	**C26**	**C27**	**C31**	**C30**	178.9(5)
Ga1	**O1**	**C1**	**C6**	7.6(6)	**C28**	**N3**	**C29**	**C30**	-2.6(7)
Ga1	**O1**	**C1**	**C2**	-173.6(4)	**C28**	**C27**	**C26**	**C25**	-0.4(7)
Ga1	**N1**	**C6**	**C1**	-2.9(5)	**C28**	**C27**	**C26**	**C32**	179.7(4)
Ga1	**N1**	**C6**	**C5**	176.4(3)	**C28**	**C27**	**C31**	**C30**	-0.8(7)
Ga1	**N1**	**C7**	**C8**	-177.1(4)	**C6**	**N1**	**C7**	**C8**	0.4(7)
Ga1	**N3**	**C28**	**C23**	1.2(5)	**C6**	**C1**	**C2**	**C3**	0.0(7)
Ga1	**N3**	**C28**	**C27**	-179.5(3)	**C6**	**C1**	**C2**	**C11**	-176.6(5)
Ga1	**N3**	**C29**	**C30**	177.7(3)	**C1**	**C6**	**C5**	**C4**	0.8(7)
Ga1	**N2**	**C17**	**C12**	2.6(5)	**C1**	**C6**	**C5**	**C9**	-179.1(4)
Ga1	**N2**	**C17**	**C16**	-177.7(3)	**C25**	**C24**	**C23**	**O3**	-178.6(4)
Ga1	**N2**	**C18**	**C19**	177.8(4)	**C25**	**C24**	**C23**	**C28**	1.2(7)
O2	**C12**	**C17**	**N2**	-2.4(6)	**C5**	**C6**	**C1**	**O1**	177.8(4)
O2	**C12**	**C17**	**C16**	177.9(4)	**C5**	**C6**	**C1**	**C2**	-1.0(7)
O3	**C23**	**C28**	**N3**	-1.8(6)	**C31**	**C30**	**C29**	**N3**	2.7(8)
O3	**C23**	**C28**	**C27**	179.0(4)	**C31**	**C27**	**C26**	**C25**	179.9(5)
O1	**C1**	**C2**	**C3**	-178.7(5)	**C31**	**C27**	**C26**	**C32**	0.1(8)
O1	**C1**	**C2**	**C11**	4.6(8)	**C31**	**C27**	**C28**	**N3**	0.9(7)
N1	**C6**	**C1**	**O1**	-2.8(6)	**C31**	**C27**	**C28**	**C23**	-179.9(4)
N1	**C6**	**C1**	**C2**	178.3(4)	**C14**	**C15**	**C16**	**C20**	-178.5(5)

N1	**C6**	**C5**	**C4**	-178.5(4)	**C14**	**C15**	**C16**	**C17**	2.1(7)
N1	**C6**	**C5**	**C9**	1.6(7)	**C14**	**C13**	**C12**	**O2**	-176.5(4)
N2	**C17**	**C16**	**C15**	178.8(4)	**C14**	**C13**	**C12**	**C17**	2.2(7)
N2	**C17**	**C16**	**C20**	-0.6(7)	**C19**	**C20**	**C16**	**C15**	-179.3(5)
C3	**C4**	**C5**	**C9**	-179.6(5)	**C19**	**C20**	**C16**	**C17**	0.1(7)
C3	**C4**	**C5**	**C6**	0.4(7)	**C7**	**N1**	**C6**	**C1**	179.1(4)
C24	**C23**	**C28**	**N3**	178.4(4)	**C7**	**N1**	**C6**	**C5**	-1.6(7)
C24	**C23**	**C28**	**C27**	-0.8(7)	**C7**	**C8**	**C9**	**C5**	-0.6(8)
C4	**C3**	**C2**	**C11**	178.0(5)	**C21**	**C15**	**C14**	**C13**	178.9(5)
C4	**C3**	**C2**	**C1**	1.3(8)	**C21**	**C15**	**C16**	**C20**	1.8(8)
C8	**C9**	**C5**	**C4**	179.7(5)	**C21**	**C15**	**C16**	**C17**	-177.6(5)
C8	**C9**	**C5**	**C6**	-0.4(7)	**C32**	**C26**	**C25**	**C24**	-179.2(5)
C22	**C13**	**C12**	**O2**	2.9(7)	**C20**	**C19**	**C18**	**N2**	-0.7(8)
C22	**C13**	**C12**	**C17**	-178.5(4)	**C17**	**N2**	**C18**	**C19**	0.1(8)
C22	**C13**	**C14**	**C15**	179.2(5)	**C2**	**C3**	**C4**	**C10**	179.1(5)
C9	**C8**	**C7**	**N1**	0.7(8)	**C2**	**C3**	**C4**	**C5**	-1.5(8)
C33	**C24**	**C23**	**O3**	1.5(7)	**C29**	**N3**	**C28**	**C23**	-178.5(4)
C33	**C24**	**C23**	**C28**	-178.7(4)	**C29**	**N3**	**C28**	**C27**	0.8(7)
C33	**C24**	**C25**	**C26**	178.5(5)	**C29**	**C30**	**C31**	**C27**	-0.9(7)
C23	**C24**	**C25**	**C26**	-1.3(7)	**C16**	**C15**	**C14**	**C13**	-0.8(7)
C27	**C26**	**C25**	**C24**	0.9(7)	**C18**	**N2**	**C17**	**C12**	-179.3(4)
C13	**C12**	**C17**	**N2**	179.0(4)	**C18**	**N2**	**C17**	**C16**	0.5(7)
C13	**C12**	**C17**	**C16**	-0.8(7)	**C18**	**C19**	**C20**	**C16**	0.5(8)
C10	**C4**	**C5**	**C9**	-0.3(7)	**Cl2**	**C34**	**Cl1**	**Cl3**	102.5(10)
C10	**C4**	**C5**	**C6**	179.8(4)	**Cl2**	**C34**	**Cl3**	**Cl1**	-84.9(10)
C12	**C13**	**C14**	**C15**	-1.5(8)	**Cl4**	**C34**	**Cl1**	**Cl3**	93.6(11)
C12	**C17**	**C16**	**C15**	-1.4(7)	**Cl4**	**C34**	**Cl3**	**Cl1**	-90.9(10)

D. *mer*-[*tris*-(8-Hydroxyquinoline) indium (III)] ·2H_2O (4)

Table D.1: Fractional Atomic Coordinates (×10^4) and Equivalent Isotropic Displacement

Parameters ($Å^2×10^3$) for *mer*-[In(Ox_3)]·$2H_2O$ (4).

Atom	*x*	*y*	*z*	U(eq)
In1	9201.7(2)	4872.5(2)	2463.4(2)	22.27(10)
O2	7491(2)	5005.0(17)	2899.0(14)	24.3(5)
O3	11042(2)	5030.7(19)	2383.4(15)	30.2(6)
O1	9054(2)	3305.5(18)	2027.8(12)	26.1(5)
N2	9472(3)	4239(2)	3693.4(15)	25.3(6)
N1	8692(3)	5094(2)	1167.8(16)	24.0(6)
N3	9534(3)	6584(2)	2715.5(15)	25.3(6)
C13	8292(4)	5053(3)	-471(2)	36.3(10)
C12	8343(4)	5980(3)	-67(2)	39.3(10)
C36	13095(4)	7224(3)	2673(2)	36.7(10)
C17	8807(3)	2283(3)	851(2)	28.2(8)
C22	10488(4)	3467(4)	4828(2)	44.3(11)
C25	7313(4)	3785(3)	5184(2)	37.4(10)
C16	8576(3)	2231(3)	26(2)	32.3(8)
C19	8654(3)	4160(3)	774.8(18)	22.0(7)
C18	8853(3)	3227(3)	1242.3(18)	22.4(7)
C35	12371(4)	8028(3)	2839(2)	35.8(9)
C28	7407(3)	4598(3)	3616.1(19)	25.0(7)
C38	11475(3)	5958(3)	2531.4(17)	25.7(8)
C34	11144(4)	7845(3)	2869.7(19)	29.6(8)
C29	8441(3)	4204(3)	4054.9(18)	24.3(7)
C31	8784(3)	7324(3)	2912.1(19)	28.2(8)
C33	10320(4)	8599(3)	3077(2)	36.2(9)
C37	12665(3)	6200(3)	2527(2)	32.2(9)
C32	9155(4)	8342(3)	3104(2)	35.9(9)
C15	8403(3)	3109(3)	-427(2)	31.9(9)
C39	10711(3)	6816(3)	2699.6(17)	23.1(7)
C11	8531(3)	5971(3)	760(2)	31.9(9)
C23	9474(4)	3423(3)	5202(2)	38.7(10)
C26	6339(4)	4125(3)	4751(2)	38(1)
C21	10459(3)	3887(3)	4064(2)	34.3(9)
C27	6366(3)	4523(3)	3976(2)	31.2(8)
C24	8410(4)	3794(3)	4832.3(19)	31.4(9)
C14	8452(3)	4104(3)	-56.9(19)	27.2(8)
O4	5940(3)	6392(3)	2045.8(19)	81.5(14)
O5	4604(5)	5698(4)	692(3)	108(2)

Table D.2: Hydrogen Atom Coordinates (Å×104) and Isotropic Displacement Parameters (Å2×103) for *mer*-[In(Ox_3)]·$2H_2O$ (4).

Atom	*x*	*y*	*z*	U(eq)

H13	8152	5051	-1020	44
H12	8252	6611	-339	47
H36	13896	7352	2655	44
H17	8932	1667	1139	34
H22	11191	3222	5077	53
H25	7268	3550	5701	45
H16	8540	1579	-220	39
H35	12677	8695	2931	43
H31	7990	7158	2922	34
H33	10568	9278	3196	43
H37	13194	5671	2426	39
H32	8616	8840	3250	43
H15	8254	3054	-974	38
H11	8544	6605	1032	38
H23	9487	3143	5710	46
H26	5620	4095	4976	46
H21	11152	3919	3808	41
H27	5668	4738	3702	37
H4A	6093	5912	2386	122
H4B	5738	6945	2279	122
H5A	3992	5317	691	162
H5B	4746	5835	217	162

Table D.3: Anisotropic Displacement Parameters ($Å^2×10^3$) for *mer*-[In(Ox_3)]·$2H_2O$ (4).

Atom	U_{11}	U_{22}	U_{33}	U_{23}	U_{13}	U_{12}
In1	22.99(16)	22.79(15)	21.15(13)	-0.51(9)	2.42(10)	-1.46(10)
O2	17.6(13)	26.6(14)	29.0(12)	3.2(9)	3.6(10)	0(1)
O3	26.0(15)	30.4(15)	35.2(13)	-1.8(10)	7.8(11)	4.0(11)
O1	33.2(15)	22.1(13)	22.6(11)	-0.6(9)	0.3(10)	1.5(11)
N2	24.8(17)	28.4(17)	22.6(13)	-1.4(11)	2.5(12)	-0.1(13)
N1	28.4(17)	22.4(15)	21.4(13)	1.9(11)	1.8(12)	-0.6(12)
N3	28.0(17)	25.5(16)	22.2(13)	-0.5(11)	0.8(12)	0.1(13)
C13	46(3)	39(2)	23.7(17)	-0.3(15)	-2.2(17)	3.9(19)
C12	58(3)	29(2)	30.8(18)	10.6(16)	1.4(18)	4(2)
C36	26(2)	55(3)	29.0(18)	-2.3(17)	4.3(16)	-15.3(19)
C17	32(2)	20.5(18)	31.7(18)	-0.9(14)	1.7(16)	0.6(15)
C22	43(3)	57(3)	32.3(19)	7.2(18)	-5.1(19)	10(2)
C25	55(3)	29(2)	30.3(18)	-1.1(15)	16.5(18)	-2.8(19)
C16	36(2)	26(2)	34.4(19)	-8.1(15)	1.4(17)	2.7(17)
C19	19.8(19)	22.7(18)	23.4(15)	-0.7(13)	1.2(13)	0.1(14)
C18	21.1(19)	20.9(17)	25.3(15)	0.0(13)	1.6(14)	-0.3(14)
C35	41(3)	34(2)	32.4(19)	-4.5(16)	2.0(17)	-19.4(19)
C28	29(2)	17.4(17)	28.7(16)	-2.3(13)	5.8(15)	-3.7(15)

C38	26(2)	35(2)	16.2(14)	-1.1(13)	4.0(13)	-3.4(16)
C34	40(2)	25.4(19)	23.1(16)	-0.3(13)	0.6(15)	-13.2(17)
C29	32(2)	18.5(17)	22.4(15)	-3.2(12)	3.3(14)	-3.8(15)
C31	28(2)	28(2)	28.5(17)	0.8(14)	0.9(15)	3.8(16)
C33	52(3)	24(2)	32.8(19)	-0.3(15)	2.4(18)	-7.0(18)
C37	26(2)	43(2)	28.1(17)	-4.2(16)	4.9(15)	-1.5(17)
C32	41(3)	27(2)	39(2)	-1.8(16)	-0.5(18)	5.8(18)
C15	37(2)	35(2)	23.2(16)	-7.2(15)	0.3(16)	0.3(17)
C39	25(2)	25.1(18)	18.7(14)	0.9(12)	-1.4(14)	-5.0(15)
C11	41(2)	26(2)	28.3(17)	-0.1(14)	2.1(16)	0.8(17)
C23	49(3)	42(2)	24.6(17)	6.1(16)	-2.7(18)	-1(2)
C26	43(3)	28(2)	47(2)	-2.0(17)	22(2)	-5.3(18)
C21	28(2)	43(2)	31.8(18)	2.5(16)	0.7(16)	5.1(18)
C27	26(2)	26.0(19)	43(2)	-1.3(16)	6.2(16)	-2.1(16)
C24	48(3)	22.0(18)	25.5(16)	-1.6(14)	8.1(16)	-3.6(17)
C14	28(2)	29(2)	24.5(16)	1.7(14)	1.0(15)	4.4(16)
O4	104(3)	69(2)	64(2)	-30.5(19)	-41(2)	53(2)
O5	124(6)	72(4)	118(5)	22(3)	-47(4)	-26(4)

Table D.4: Bond Lengths for *mer*-[In(Ox$_3$)]·2H$_2$O (4).

Atom	Atom	Length/Å	Atom	Atom	Length/Å
In1	**O2**	2.142(3)	**C17**	**C18**	1.374(5)
In1	**O3**	2.121(3)	**C22**	**C23**	1.360(6)
In1	**O1**	2.135(2)	**C22**	**C21**	1.397(5)
In1	**N2**	2.231(3)	**C25**	**C26**	1.353(6)
In1	**N1**	2.241(3)	**C25**	**C24**	1.424(5)
In1	**N3**	2.253(3)	**C16**	**C15**	1.363(5)
O2	**C28**	1.330(4)	**C19**	**C18**	1.438(4)
O3	**C38**	1.300(4)	**C19**	**C14**	1.409(4)
O1	**C18**	1.334(4)	**C35**	**C34**	1.422(5)
N2	**C29**	1.366(4)	**C28**	**C29**	1.433(5)
N2	**C21**	1.322(5)	**C28**	**C27**	1.378(5)
N1	**C19**	1.365(4)	**C38**	**C37**	1.391(5)
N1	**C11**	1.320(4)	**C38**	**C39**	1.441(5)
N3	**C31**	1.333(4)	**C34**	**C33**	1.408(5)
N3	**C39**	1.375(4)	**C34**	**C39**	1.426(5)
C13	**C12**	1.365(5)	**C29**	**C24**	1.418(4)
C13	**C14**	1.405(5)	**C31**	**C32**	1.397(5)
C12	**C11**	1.399(5)	**C33**	**C32**	1.371(6)

C36	**C35**	1.360(6)	**C15**	**C14**	1.416(5)
C36	**C37**	1.411(5)	**C23**	**C24**	1.403(6)
C17	**C16**	1.402(5)	**C26**	**C27**	1.408(5)

Table D.5: Bond Angles for *mer*-[In(Ox$_3$)]·2H$_2$O (4).

Atom	Atom	Atom	Angle/°	Atom	Atom	Atom	Angle/°
O2	**In1**	**N2**	76.83(10)	**C14**	**C19**	**C18**	120.9(3)
O2	**In1**	**N1**	98.73(10)	**O1**	**C18**	**C17**	122.8(3)
O2	**In1**	**N3**	90.14(10)	**O1**	**C18**	**C19**	119.5(3)
O3	**In1**	**O2**	160.78(10)	**C17**	**C18**	**C19**	117.6(3)
O3	**In1**	**O1**	96.86(9)	**C36**	**C35**	**C34**	119.8(4)
O3	**In1**	**N2**	91.60(10)	**O2**	**C28**	**C29**	119.7(3)
O3	**In1**	**N1**	96.24(11)	**O2**	**C28**	**C27**	123.7(3)
O3	**In1**	**N3**	76.53(10)	**C27**	**C28**	**C29**	116.6(3)
O1	**In1**	**O2**	98.22(9)	**O3**	**C38**	**C37**	123.8(3)
O1	**In1**	**N2**	89.03(9)	**O3**	**C38**	**C39**	120.3(3)
O1	**In1**	**N1**	76.91(9)	**C37**	**C38**	**C39**	115.9(3)
O1	**In1**	**N3**	169.19(9)	**C35**	**C34**	**C39**	118.1(4)
N2	**In1**	**N1**	164.60(10)	**C33**	**C34**	**C35**	125.0(3)
N2	**In1**	**N3**	99.58(10)	**C33**	**C34**	**C39**	116.9(3)
N1	**In1**	**N3**	95.13(10)	**N2**	**C29**	**C28**	117.2(3)
C28	**O2**	**In1**	114.4(2)	**N2**	**C29**	**C24**	120.7(3)
C38	**O3**	**In1**	115.9(2)	**C24**	**C29**	**C28**	122.1(3)
C18	**O1**	**In1**	114.6(2)	**N3**	**C31**	**C32**	122.0(4)
C29	**N2**	**In1**	111.5(2)	**C32**	**C33**	**C34**	120.7(4)
C21	**N2**	**In1**	128.0(2)	**C38**	**C37**	**C36**	122.0(4)
C21	**N2**	**C29**	120.4(3)	**C33**	**C32**	**C31**	119.4(4)
C19	**N1**	**In1**	111.2(2)	**C16**	**C15**	**C14**	119.4(3)
C11	**N1**	**In1**	129.2(2)	**N3**	**C39**	**C38**	116.4(3)
C11	**N1**	**C19**	119.3(3)	**N3**	**C39**	**C34**	121.2(3)
C31	**N3**	**In1**	129.3(3)	**C34**	**C39**	**C38**	122.4(3)
C31	**N3**	**C39**	119.8(3)	**N1**	**C11**	**C12**	122.2(3)
C39	**N3**	**In1**	110.8(2)	**C22**	**C23**	**C24**	121.0(4)
C12	**C13**	**C14**	120.0(3)	**C25**	**C26**	**C27**	122.9(4)
C13	**C12**	**C11**	119.4(3)	**N2**	**C21**	**C22**	121.8(4)
C35	**C36**	**C37**	121.9(4)	**C28**	**C27**	**C26**	121.2(4)
C18	**C17**	**C16**	121.2(3)	**C29**	**C24**	**C25**	118.4(4)
C23	**C22**	**C21**	119.0(4)	**C23**	**C24**	**C25**	124.6(3)

C26	**C25**	**C24**	118.8(3)	**C23**	**C24**	**C29**	117.1(4)
C15	**C16**	**C17**	121.9(3)	**C13**	**C14**	**C19**	117.3(3)
N1	**C19**	**C18**	117.3(3)	**C13**	**C14**	**C15**	123.7(3)
N1	**C19**	**C14**	121.8(3)	**C19**	**C14**	**C15**	118.9(3)

Table D.6: Torsion Angles for *mer*-[In(Ox$_3$)]·2H$_2$O (4).

A	B	C	D	Angle/°	A	B	C	D	Angle/°
In1	**O2**	**C28**	**C29**	5.4(4)	**C16**	**C15**	**C14**	**C13**	179.6(4)
In1	**O2**	**C28**	**C27**	-174.4(3)	**C16**	**C15**	**C14**	**C19**	-1.3(6)
In1	**O3**	**C38**	**C37**	178.3(2)	**C19**	**N1**	**C11**	**C12**	-1.1(6)
In1	**O3**	**C38**	**C39**	-2.8(4)	**C18**	**C17**	**C16**	**C15**	0.9(6)
In1	**O1**	**C18**	**C17**	175.7(3)	**C18**	**C19**	**C14**	**C13**	-178.5(3)
In1	**O1**	**C18**	**C19**	-5.4(4)	**C18**	**C19**	**C14**	**C15**	2.4(5)
In1	**N2**	**C29**	**C28**	-2.1(4)	**C35**	**C36**	**C37**	**C38**	1.1(5)
In1	**N2**	**C29**	**C24**	177.9(2)	**C35**	**C34**	**C33**	**C32**	-178.8(3)
In1	**N2**	**C21**	**C22**	-177.1(3)	**C35**	**C34**	**C39**	**N3**	-179.7(3)
In1	**N1**	**C19**	**C18**	4.2(4)	**C35**	**C34**	**C39**	**C38**	2.6(5)
In1	**N1**	**C19**	**C14**	-174.6(3)	**C28**	**C29**	**C24**	**C25**	-0.5(5)
In1	**N1**	**C11**	**C12**	172.6(3)	**C28**	**C29**	**C24**	**C23**	179.5(3)
In1	**N3**	**C31**	**C32**	175.4(2)	**C34**	**C33**	**C32**	**C31**	-1.0(5)
In1	**N3**	**C39**	**C38**	0.1(3)	**C29**	**N2**	**C21**	**C22**	0.2(6)
In1	**N3**	**C39**	**C34**	-177.8(2)	**C29**	**C28**	**C27**	**C26**	3.0(5)
O2	**C28**	**C29**	**N2**	-2.2(5)	**C31**	**N3**	**C39**	**C38**	176.2(3)
O2	**C28**	**C29**	**C24**	177.8(3)	**C31**	**N3**	**C39**	**C34**	-1.7(5)
O2	**C28**	**C27**	**C26**	-177.2(3)	**C33**	**C34**	**C39**	**N3**	1.9(5)
O3	**C38**	**C37**	**C36**	178.5(3)	**C33**	**C34**	**C39**	**C38**	-175.8(3)
O3	**C38**	**C39**	**N3**	1.8(4)	**C37**	**C36**	**C35**	**C34**	0.1(5)
O3	**C38**	**C39**	**C34**	179.6(3)	**C37**	**C38**	**C39**	**N3**	-179.2(3)
N2	**C29**	**C24**	**C25**	179.5(3)	**C37**	**C38**	**C39**	**C34**	-1.4(4)
N2	**C29**	**C24**	**C23**	-0.5(5)	**C39**	**N3**	**C31**	**C32**	0.1(5)
N1	**C19**	**C18**	**O1**	0.6(5)	**C39**	**C38**	**C37**	**C36**	-0.5(5)
N1	**C19**	**C18**	**C17**	179.5(3)	**C39**	**C34**	**C33**	**C32**	-0.5(5)
N1	**C19**	**C14**	**C13**	0.2(5)	**C11**	**N1**	**C19**	**C18**	179.0(3)
N1	**C19**	**C14**	**C15**	-178.9(3)	**C11**	**N1**	**C19**	**C14**	0.2(5)
N3	**C31**	**C32**	**C33**	1.3(5)	**C23**	**C22**	**C21**	**N2**	-0.2(6)
C13	**C12**	**C11**	**N1**	1.6(7)	**C26**	**C25**	**C24**	**C29**	2.8(5)
C12	**C13**	**C14**	**C19**	0.3(6)	**C26**	**C25**	**C24**	**C23**	-177.2(4)
C12	**C13**	**C14**	**C15**	179.4(4)	**C21**	**N2**	**C29**	**C28**	-179.8(3)
C36	**C35**	**C34**	**C33**	176.4(3)	**C21**	**N2**	**C29**	**C24**	0.2(5)
C36	**C35**	**C34**	**C39**	-1.9(5)	**C21**	**C22**	**C23**	**C24**	-0.2(6)
C17	**C16**	**C15**	**C14**	-0.3(6)	**C27**	**C28**	**C29**	**N2**	177.7(3)

C22	**C23**	**C24**	**C25**	-179.5(4)	**C27**	**C28**	**C29**	**C24**	-2.4(5)
C22	**C23**	**C24**	**C29**	0.6(6)	**C24**	**C25**	**C26**	**C27**	-2.2(6)
C25	**C26**	**C27**	**C28**	-0.8(6)	**C14**	**C13**	**C12**	**C11**	-1.2(7)
C16	**C17**	**C18**	**O1**	179.0(3)	**C14**	**C19**	**C18**	**O1**	179.3(3)
C16	**C17**	**C18**	**C19**	0.1(5)	**C14**	**C19**	**C18**	**C17**	-1.7(5)

E. [*tris*-(5,7-dichloro-8-hydroxyquinoline)·(diaqua)·europium(III)] water · ethanol solvate (5)

Table E.1: Fractional Atomic Coordinates (×10^4) and Equivalent Isotropic Displacement Parameters (Å^2×10^3) for [Eu(57dcOx)$_3$(H_2O)$_2$]·EtOH·H_2O (5).

Atom	***x***	***y***	***z***	**U(eq)**

C11A	6520(30)	3000(30)	8320(20)	45(7)
C11B	3690(30)	7100(30)	1630(20)	40(6)
C11I	6690(30)	6170(20)	7110(30)	41(7)
C12A	6970(30)	1990(30)	8950(20)	53(9)
C12B	3060(40)	7930(30)	970(30)	59(9)
C12I	7850(30)	6890(20)	6890(20)	33(6)
C13A	6770(30)	860(30)	9100(30)	47(8)
C13B	3320(40)	9130(30)	1000(30)	55(11)
C13I	8940(40)	7030(30)	6000(30)	52(9)
C14A	5990(30)	690(20)	8440(20)	32(6)
C14B	3950(40)	9260(30)	1550(30)	49(9)
C14I	8930(30)	6480(20)	5290(30)	37(7)
C15A	5810(30)	-350(30)	8410(20)	49(8)
C15B	4350(30)	10430(20)	1520(30)	48(9)
C15I	9970(30)	6580(20)	4390(30)	34(6)
C16A	5040(30)	-550(20)	7900(20)	42(8)
C16B	5060(40)	10410(30)	2180(30)	53(8)
C16I	9900(20)	6160(20)	3750(20)	40(8)
C17A	4520(30)	620(20)	7160(20)	38(7)
C17B	5470(30)	9590(20)	2710(20)	37(6)
C17I	8660(30)	5620(20)	3920(20)	36(6)
C18A	4850(30)	1663(19)	7170(20)	32(7)
C18B	5170(20)	8290(30)	2940(20)	34(7)
C18I	7490(20)	5520(20)	4730(20)	25(6)
C19A	5530(30)	1700(20)	7790(20)	33(6)
C19B	4430(30)	8190(20)	2247(19)	32(6)
C19I	7710(20)	6010(20)	5420(20)	29(6)
C21A	1630(40)	2100(30)	8360(30)	82(13)
C21B	8140(19)	7783(17)	1728(15)	22(4)
C21I	3270(30)	3790(30)	2970(20)	40(8)
C22A	600(30)	1690(30)	9080(30)	42(7)
C22B	9460(40)	8460(40)	750(30)	60(10)
C22I	2160(40)	3250(30)	3010(30)	54(9)
C23A	70(30)	2040(30)	9990(20)	43(7)
C23B	9760(40)	8100(30)	100(30)	62(10)
C23I	1020(30)	3030(20)	3930(20)	36(6)
C24A	900(30)	2830(30)	10040(20)	47(8)
C24B	9130(30)	7010(30)	90(20)	37(7)
C24I	1050(30)	3360(20)	4730(20)	30(5)
C25A	580(30)	3370(30)	10780(20)	56(10)
C25B	9480(30)	6540(30)	-690(30)	42(8)
C25I	-40(30)	3270(30)	5660(20)	37(7)
C26A	1240(30)	4330(30)	10660(20)	55(10)
C26B	8670(30)	5720(30)	-640(30)	47(9)

C26I	100(30)	3870(30)	6320(20)	52(9)
C27A	2520(30)	4810(30)	9780(20)	43(7)
C27B	7570(30)	5200(30)	240(30)	44(8)
C27I	1320(30)	4550(30)	6080(20)	31(6)
C28A	2920(30)	4420(20)	8922(16)	23(5)
C28B	7140(30)	5540(30)	990(20)	45(8)
C28I	2420(30)	4520(20)	5260(20)	33(6)
C29A	2110(30)	3500(20)	9052(19)	43(8)
C29B	7910(20)	6600(20)	920(20)	34(7)
C29I	2300(30)	4060(30)	4500(20)	33(7)
C30A	4200(40)	7700(30)	6050(30)	71(12)
C30B	5920(40)	2500(30)	3870(30)	65(11)
N1A	5740(20)	2897(18)	7766(14)	21(4)
N1B	4280(30)	7170(20)	2300(20)	44(6)
N1I	6600(20)	5770(20)	6405(19)	32(5)
N2A	2510(30)	3140(20)	8193(17)	37(6)
N2B	7470(20)	7000(20)	1719(18)	33(5)
N2I	3370(30)	4270(20)	3642(18)	33(6)
O1A	4470(20)	2740(17)	6443(13)	33(5)
O1B	5470(20)	7359(16)	3557(15)	34(5)
O1I	6407(19)	5071(17)	4891(14)	29(4)
O2A	3950(20)	4872(16)	8116(16)	32(4)
O2B	6060(20)	4987(19)	1962(15)	41(5)
O2I	3701(17)	4938(16)	5130(15)	26(4)
O3A	4380(20)	6695(18)	5730(13)	43(6)
O3B	5580(20)	3262(15)	4331(17)	45(6)
Cl1A	6314(12)	-1734(9)	9198(9)	68(3)
Cl1B	3665(13)	11662(9)	786(9)	79(4)
Cl1I	11546(8)	7367(9)	4108(8)	59(3)
Cl2A	3550(13)	394(9)	6495(10)	73(3)
Cl2B	6484(11)	9653(8)	3454(9)	64(3)
Cl2I	8614(9)	4772(8)	3153(7)	44.3(19)
Cl3A	-981(12)	2687(11)	11861(8)	90(4)
Cl3B	10912(11)	7143(10)	-1838(7)	67(2)
Cl3I	-1541(9)	2652(9)	5900(8)	61(3)
Cl4A	3445(12)	5995(9)	9687(7)	64(3)
Cl4B	6585(12)	4029(11)	316(8)	73(3)
Cl4I	1381(9)	5185(8)	6878(6)	45(2)
Eu1A	4551.5(5)	4536.0(4)	6582.6(4)	26.8(3)
Eu1B	5440.4(5)	5467.3(5)	3425.6(4)	27.1(3)

Table E.2: Hydrogen Atom Coordinates (Å×104) and Isotropic Displacement

Parameters (Å2×103) for [Eu(57dcOx)$_3$(H$_2$O)$_2$]·EtOH·H$_2$O (5).

Atom	*x*	*y*	*z*	U(eq)
H11A	6750	3754	8279	54
H11B	3690	6351	1608	48
H11I	5982	5975	7757	49
H12A	7488	2109	9315	64
H12B	2582	7789	584	71
H12I	7875	7252	7347	40
H13A	7071	219	9580	57
H13B	2985	9806	588	66
H13I	9711	7501	5856	62
H16A	4838	-1322	7972	51
H16B	5236	11145	2193	64
H16I	10647	6191	3182	48
H21A	1918	1756	7875	98
H21B	7863	7985	2317	27
H21I	4053	3839	2422	48
H22A	88	1108	9060	50
H22B	9952	9099	710	72
H22I	2156	3037	2457	65
H23A	-777	1736	10505	51
H23B	10503	8527	-504	75
H23I	233	2654	3990	43
H26A	897	4698	11132	65
H26B	8862	5491	-1208	56
H26I	-632	3807	6912	62
H30A	3735	7391	6825	106
H30B	3696	8265	5661	106
H30C	5051	8105	5876	106
H30D	5892	2866	3139	98
H30E	5313	1768	4295	98
H30F	6803	2303	3849	98

Table E.3: Anisotropic Displacement Parameters (Å^2×10^3) for [Eu(57dcOx)$_3$(H$_2$O)$_2$]·EtOH·H$_2$O (5).

Atom	U_{11}	U_{22}	U_{33}	U_{23}	U_{13}	U_{12}
C11A	56(16)	55(14)	27(11)	-18(10)	-15(10)	-9(11)
C11B	31(10)	52(14)	53(14)	-30(12)	-26(10)	22(10)
C11I	50(17)	21(10)	47(16)	-9(10)	-17(14)	4(10)
C12A	67(18)	90(20)	47(14)	-45(14)	-55(14)	45(15)
C12B	70(20)	49(15)	47(15)	-21(13)	-3(13)	-11(13)

C12I	51(17)	31(12)	29(11)	-15(9)	-23(11)	1(11)
C13A	47(16)	66(19)	48(17)	-33(15)	-30(14)	22(14)
C13B	80(20)	42(16)	34(14)	0(12)	-26(15)	23(16)
C13I	36(17)	50(17)	60(19)	-10(14)	-21(15)	-4(13)
C14A	40(15)	27(12)	20(10)	-5(9)	-6(10)	7(10)
C14B	48(19)	41(17)	56(19)	-18(15)	-19(16)	23(14)
C14I	40(14)	23(10)	46(14)	-4(9)	-26(12)	-4(8)
C15A	42(13)	57(16)	21(10)	6(10)	-6(9)	15(11)
C15B	50(15)	23(11)	57(17)	-17(11)	0(12)	6(9)
C15I	34(14)	22(9)	42(14)	-5(9)	-16(11)	-5(8)
C16A	65(18)	7(8)	28(11)	2(8)	3(11)	9(9)
C16B	45(14)	45(18)	71(19)	-23(15)	-23(14)	11(12)
C16I	15(10)	42(15)	34(14)	2(12)	2(10)	9(10)
C17A	63(16)	16(9)	32(10)	-4(8)	-22(11)	5(9)
C17B	55(15)	22(10)	40(13)	-13(9)	-25(12)	4(10)
C17I	59(17)	21(9)	23(11)	-6(8)	-13(11)	7(9)
C18A	52(16)	10(8)	21(10)	0(8)	-6(10)	3(9)
C18B	21(11)	65(18)	30(12)	-32(13)	-9(9)	2(10)
C18I	26(13)	34(12)	24(11)	-14(10)	-17(10)	19(10)
C19A	27(12)	33(11)	43(14)	-20(10)	-11(11)	4(9)
C19B	41(14)	29(11)	13(9)	-6(8)	1(9)	7(9)
C19I	22(11)	18(9)	29(11)	-2(8)	1(9)	8(8)
C21A	120(30)	54(19)	110(30)	-50(20)	-70(30)	6(19)
C21B	16(7)	20(8)	26(8)	-10(7)	-1(6)	-3(6)
C21I	35(16)	63(19)	28(12)	-29(13)	-3(11)	-6(14)
C22A	36(14)	32(12)	40(12)	-10(10)	6(10)	-23(11)
C22B	44(18)	60(20)	50(18)	-8(15)	-9(14)	-5(15)
C22I	60(20)	46(16)	59(18)	-26(14)	-18(16)	-4(14)
C23A	36(13)	49(15)	33(12)	-9(11)	-9(10)	-5(11)
C23B	51(16)	44(15)	61(19)	-7(13)	0(13)	0(12)
C23I	49(16)	30(11)	38(12)	-19(9)	-20(11)	0(10)
C24A	49(16)	33(12)	33(13)	1(10)	-1(11)	13(11)
C24B	32(12)	45(14)	20(10)	4(9)	-17(9)	3(10)
C24I	28(11)	28(10)	36(11)	-18(9)	-6(9)	6(8)
C25A	54(16)	60(17)	10(10)	10(11)	9(10)	19(14)
C25B	36(14)	50(17)	35(14)	-14(13)	-14(11)	13(12)
C25I	24(12)	41(13)	46(15)	-28(12)	1(11)	0(9)
C26A	60(20)	51(16)	15(11)	1(11)	9(12)	11(15)
C26B	46(19)	70(20)	46(18)	-39(17)	-20(15)	23(17)
C26I	60(20)	47(16)	37(15)	-26(13)	9(13)	-13(13)
C27A	47(14)	41(14)	31(13)	-21(12)	8(11)	-5(11)
C27B	50(15)	69(19)	35(15)	-31(14)	-32(13)	31(14)
C27I	22(11)	42(13)	34(13)	-22(11)	-9(10)	16(10)
C28A	35(12)	35(11)	6(7)	-14(7)	-9(7)	12(9)

C28B	29(12)	46(15)	53(16)	-25(13)	-1(11)	6(10)
C28I	24(13)	32(13)	42(15)	-17(12)	-8(12)	-9(10)
C29A	60(17)	44(13)	17(10)	-13(9)	-5(10)	32(12)
C29B	20(10)	43(13)	28(12)	1(10)	-13(9)	-15(9)
C29I	40(15)	50(15)	15(9)	-12(9)	-15(10)	-3(12)
C30A	130(30)	19(9)	49(15)	-20(9)	-12(17)	19(13)
C30B	64(19)	62(19)	70(20)	-42(16)	-2(15)	-11(15)
N1A	33(10)	22(9)	14(8)	-8(6)	-16(7)	-1(7)
N1B	28(11)	57(14)	54(15)	-34(12)	-8(11)	10(10)
N1I	26(11)	33(11)	33(12)	-16(10)	-2(10)	8(9)
N2A	53(14)	33(10)	25(9)	-20(8)	-1(9)	-8(9)
N2B	23(10)	30(10)	35(10)	-2(8)	-11(8)	9(8)
N2I	42(14)	39(12)	23(11)	-16(9)	-11(10)	-3(10)
O1A	49(12)	35(9)	22(8)	-18(7)	-13(8)	1(8)
O1B	44(11)	19(8)	42(10)	-8(7)	-23(9)	15(7)
O1I	30(9)	36(9)	18(8)	-10(7)	-8(6)	15(7)
O2A	40(10)	31(7)	30(8)	-18(6)	-12(8)	7(7)
O2B	43(11)	52(11)	26(9)	-23(8)	1(8)	-11(8)
O2I	16(7)	34(8)	34(9)	-22(7)	-6(6)	-5(6)
O3A	65(14)	49(12)	14(7)	-17(7)	-8(8)	22(10)
O3B	52(13)	22(8)	69(13)	-27(9)	-19(10)	7(8)
Cl1A	75(7)	44(5)	68(6)	-12(4)	-23(5)	24(4)
Cl1B	97(9)	48(5)	71(6)	-3(5)	-34(6)	31(5)
Cl1I	30(4)	64(6)	67(6)	-17(5)	-10(4)	-6(4)
Cl2A	105(9)	53(5)	81(7)	-35(5)	-49(6)	-4(5)
Cl2B	88(8)	42(4)	82(6)	-33(4)	-46(6)	4(4)
Cl2I	46(5)	55(5)	40(4)	-30(4)	-12(4)	13(4)
Cl3A	63(6)	92(7)	51(5)	-4(4)	24(4)	3(5)
Cl3B	60(5)	82(5)	42(4)	-28(4)	8(4)	3(4)
Cl3I	41(5)	65(6)	73(6)	-40(5)	4(4)	-18(4)
Cl4A	91(8)	60(5)	49(5)	-32(4)	-20(5)	-4(5)
Cl4B	82(8)	95(7)	60(6)	-64(6)	-6(5)	-3(6)
Cl4I	42(5)	65(5)	33(4)	-28(4)	-11(4)	17(4)
Eu1A	30.5(7)	29.5(6)	20.8(6)	-12.6(5)	-6.5(5)	2.9(5)
Eu1B	30.9(7)	29.3(6)	22.3(6)	-13.3(5)	-7.3(5)	2.8(5)

Table E.4: Bond Lengths for $[Eu(57dcOx)_3(H_2O)_2]\cdot EtOH\cdot H_2O$ (5).

Atom	Atom	Length/Å	Atom	Atom	Length/Å
C11A	**C12A**	1.37(4)	**C23I**	**C24I**	1.38(4)
C11A	**N1A**	1.37(4)	**C24A**	**C25A**	1.42(5)
C11B	**C12B**	1.39(5)	**C24A**	**C29A**	1.51(4)
C11B	**N1B**	1.33(4)	**C24B**	**C25B**	1.41(5)

C11I	**C12I**	1.43(4)	**C24B**	**C29B**	1.38(4)
C11I	**N1I**	1.31(4)	**C24I**	**C25I**	1.42(3)
C12A	**C13A**	1.31(5)	**C24I**	**C29I**	1.48(4)
C12B	**C13B**	1.52(5)	**C25A**	**C26A**	1.31(5)
C12I	**C13I**	1.38(4)	**C25A**	**Cl3A**	1.80(3)
C13A	**C14A**	1.51(4)	**C25B**	**C26B**	1.31(5)
C13B	**C14B**	1.24(5)	**C25B**	**Cl3B**	1.74(3)
C13I	**C14I**	1.44(5)	**C25I**	**C26I**	1.44(4)
C14A	**C15A**	1.32(4)	**C25I**	**Cl3I**	1.67(3)
C14A	**C19A**	1.39(4)	**C26A**	**C27A**	1.47(4)
C14B	**C15B**	1.49(5)	**C26B**	**C27B**	1.35(4)
C14B	**C19B**	1.47(4)	**C26I**	**C27I**	1.44(4)
C14I	**C15I**	1.37(4)	**C27A**	**C28A**	1.44(3)
C14I	**C19I**	1.38(4)	**C27A**	**Cl4A**	1.71(3)
C15A	**C16A**	1.35(5)	**C27B**	**C28B**	1.25(4)
C15A	**Cl1A**	1.78(3)	**C27B**	**Cl4B**	1.76(4)
C15B	**C16B**	1.38(5)	**C27I**	**C28I**	1.38(4)
C15B	**Cl1B**	1.73(3)	**C27I**	**Cl4I**	1.65(3)
C15I	**C16I**	1.24(4)	**C28A**	**C29A**	1.35(4)
C15I	**Cl1I**	1.82(3)	**C28A**	**O2A**	1.25(3)
C16A	**C17A**	1.59(4)	**C28A**	**Eu1A**	3.18(2)
C16B	**C17B**	1.15(4)	**C28B**	**C29B**	1.51(4)
C16I	**C17I**	1.41(4)	**C28B**	**O2B**	1.40(3)
C17A	**C18A**	1.35(4)	**C28I**	**C29I**	1.46(4)
C17A	**Cl2A**	1.70(3)	**C28I**	**O2I**	1.40(3)
C17B	**C18B**	1.50(4)	**C29A**	**N2A**	1.41(3)
C17B	**Cl2B**	1.77(3)	**C29B**	**N2B**	1.37(4)
C17I	**C18I**	1.37(4)	**C29I**	**N2I**	1.32(4)
C17I	**Cl2I**	1.81(3)	**C30A**	**O3A**	1.47(3)
C18A	**C19A**	1.33(4)	**C30B**	**O3B**	1.33(4)
C18A	**O1A**	1.44(3)	**N1A**	**Eu1A**	2.62(2)
C18B	**C19B**	1.48(4)	**N1B**	**Eu1B**	2.60(3)
C18B	**O1B**	1.23(3)	**N1I**	**Eu1A**	2.59(3)
C18B	**Eu1B**	3.25(3)	**N2A**	**Eu1A**	2.60(2)
C18I	**C19I**	1.42(4)	**N2B**	**Eu1B**	2.69(2)
C18I	**O1I**	1.22(3)	**N2I**	**Eu1B**	2.56(3)
C19A	**N1A**	1.47(3)	**O1A**	**Eu1A**	2.294(18)
C19B	**N1B**	1.23(4)	**O1B**	**Eu1B**	2.401(19)
C19I	**N1I**	1.44(3)	**O1I**	**Eu1A**	2.429(18)
C21A	**C22A**	1.18(5)	**O1I**	**Eu1B**	2.488(19)
C21A	**N2A**	1.49(4)	**O2A**	**Eu1A**	2.281(19)
C21B	**C22B**	1.57(4)	**O2B**	**Eu1B**	2.292(19)
C21B	**N2B**	1.23(3)	**O2I**	**Eu1A**	2.386(18)

C21I	**C22I**	1.36(5)	**O2I**	**Eu1B**	2.382(17)
C21I	**N2I**	1.34(4)	**O3A**	**Eu1A**	2.432(19)
C22A	**C23A**	1.47(4)	**O3B**	**Eu1B**	2.481(17)
C22B	**C23B**	1.14(5)	**Cl2I**	**Eu1B**	3.418(9)
C22I	**C23I**	1.41(4)	**Cl4I**	**Eu1A**	3.397(9)
C23A	**C24A**	1.38(5)	**Eu1A**	**Eu1B**	3.9405(16)
C23B	**C24B**	1.53(5)			

Table E.5: Bond Angles for $[Eu(57dcOx)_3(H_2O)_2]\cdot EtOH\cdot H_2O$ (5).

Atom	Atom	Atom	Angle/°	Atom	Atom	Atom	Angle/°
N1A	**C11A**	**C12A**	119(3)	**C29A**	**N2A**	**Eu1A**	111.7(17)
N1B	**C11B**	**C12B**	132(3)	**C21B**	**N2B**	**C29B**	121(2)
N1I	**C11I**	**C12I**	121(3)	**C21B**	**N2B**	**Eu1B**	125.8(17)
C13A	**C12A**	**C11A**	129(3)	**C29B**	**N2B**	**Eu1B**	111.3(17)
C11B	**C12B**	**C13B**	106(3)	**C21I**	**N2I**	**Eu1B**	126.0(19)
C13I	**C12I**	**C11I**	118(3)	**C29I**	**N2I**	**C21I**	115(3)
C12A	**C13A**	**C14A**	114(3)	**C29I**	**N2I**	**Eu1B**	118.5(19)
C14B	**C13B**	**C12B**	124(3)	**C18A**	**O1A**	**Eu1A**	121.5(15)
C12I	**C13I**	**C14I**	122(3)	**C18B**	**O1B**	**Eu1B**	123.8(18)
C15A	**C14A**	**C13A**	123(3)	**C18I**	**O1I**	**Eu1A**	123.3(17)
C15A	**C14A**	**C19A**	119(3)	**C18I**	**O1I**	**Eu1B**	124.2(16)
C19A	**C14A**	**C13A**	118(3)	**Eu1A**	**O1I**	**Eu1B**	106.5(7)
C13B	**C14B**	**C15B**	126(3)	**C28A**	**O2A**	**Eu1A**	126.1(18)
C13B	**C14B**	**C19B**	119(3)	**C28B**	**O2B**	**Eu1B**	127(2)
C19B	**C14B**	**C15B**	116(3)	**C28I**	**O2I**	**Eu1A**	125.2(16)
C15I	**C14I**	**C13I**	125(3)	**C28I**	**O2I**	**Eu1B**	119.7(16)
C15I	**C14I**	**C19I**	118(3)	**Eu1B**	**O2I**	**Eu1A**	111.5(7)
C19I	**C14I**	**C13I**	116(3)	**C30A**	**O3A**	**Eu1A**	137.4(17)
C14A	**C15A**	**C16A**	124(3)	**C30B**	**O3B**	**Eu1B**	128(2)
C14A	**C15A**	**Cl1A**	125(3)	**C17I**	**Cl2I**	**Eu1B**	86.2(11)
C16A	**C15A**	**Cl1A**	110(2)	**C27I**	**Cl4I**	**Eu1A**	89.4(9)
C14B	**C15B**	**Cl1B**	115(3)	**C28A**	**Eu1A**	**Cl4I**	65.7(5)
C16B	**C15B**	**C14B**	118(3)	**C28A**	**Eu1A**	**Eu1B**	157.0(4)
C16B	**C15B**	**Cl1B**	126(2)	**N1A**	**Eu1A**	**C28A**	80.9(6)
C14I	**C15I**	**Cl1I**	118(2)	**N1A**	**Eu1A**	**Cl4I**	136.0(5)
C16I	**C15I**	**C14I**	124(3)	**N1A**	**Eu1A**	**Eu1B**	121.7(4)
C16I	**C15I**	**Cl1I**	118(2)	**N1I**	**Eu1A**	**C28A**	92.8(7)
C15A	**C16A**	**C17A**	116(2)	**N1I**	**Eu1A**	**N1A**	76.2(7)
C17B	**C16B**	**C15B**	127(4)	**N1I**	**Eu1A**	**N2A**	135.4(7)
C15I	**C16I**	**C17I**	118(3)	**N1I**	**Eu1A**	**Cl4I**	130.6(5)
C16A	**C17A**	**Cl2A**	117(2)	**N1I**	**Eu1A**	**Eu1B**	96.3(5)

C18A	**C17A**	**C16A**	115(3)	**N2A**	**Eu1A**	**C28A**	46.2(7)
C18A	**C17A**	**Cl2A**	128(2)	**N2A**	**Eu1A**	**N1A**	79.8(7)
C16B	**C17B**	**C18B**	126(3)	**N2A**	**Eu1A**	**Cl4I**	56.5(6)
C16B	**C17B**	**Cl2B**	124(3)	**N2A**	**Eu1A**	**Eu1B**	128.3(5)
C18B	**C17B**	**Cl2B**	110(2)	**O1A**	**Eu1A**	**C28A**	115.2(6)
C16I	**C17I**	**Cl2I**	118(2)	**O1A**	**Eu1A**	**N1A**	66.9(7)
C18I	**C17I**	**C16I**	126(3)	**O1A**	**Eu1A**	**N1I**	127.9(7)
C18I	**C17I**	**Cl2I**	115(2)	**O1A**	**Eu1A**	**N2A**	72.8(6)
C17A	**C18A**	**O1A**	116(3)	**O1A**	**Eu1A**	**O1I**	81.5(7)
C19A	**C18A**	**C17A**	122(3)	**O1A**	**Eu1A**	**O2I**	74.6(6)
C19A	**C18A**	**O1A**	122(2)	**O1A**	**Eu1A**	**O3A**	145.4(6)
C17B	**C18B**	**Eu1B**	162(2)	**O1A**	**Eu1A**	**Cl4I**	101.3(5)
C19B	**C18B**	**C17B**	112(3)	**O1A**	**Eu1A**	**Eu1B**	75.0(4)
C19B	**C18B**	**Eu1B**	81.5(16)	**O1I**	**Eu1A**	**C28A**	157.7(7)
O1B	**C18B**	**C17B**	130(3)	**O1I**	**Eu1A**	**N1A**	93.4(6)
O1B	**C18B**	**C19B**	118(3)	**O1I**	**Eu1A**	**N1I**	64.9(7)
O1B	**C18B**	**Eu1B**	37.8(14)	**O1I**	**Eu1A**	**N2A**	154.1(6)
C17I	**C18I**	**C19I**	110(3)	**O1I**	**Eu1A**	**O3A**	81.9(6)
O1I	**C18I**	**C17I**	127(3)	**O1I**	**Eu1A**	**Cl4I**	127.9(4)
O1I	**C18I**	**C19I**	122(2)	**O1I**	**Eu1A**	**Eu1B**	37.2(5)
C14A	**C19A**	**N1A**	121(3)	**O2A**	**Eu1A**	**C28A**	18.4(7)
C18A	**C19A**	**C14A**	123(3)	**O2A**	**Eu1A**	**N1A**	79.3(6)
C18A	**C19A**	**N1A**	115(2)	**O2A**	**Eu1A**	**N1I**	74.5(7)
C14B	**C19B**	**C18B**	121(3)	**O2A**	**Eu1A**	**N2A**	64.4(7)
N1B	**C19B**	**C14B**	124(3)	**O2A**	**Eu1A**	**O1A**	129.1(6)
N1B	**C19B**	**C18B**	115(3)	**O2A**	**Eu1A**	**O1I**	139.3(7)
C14I	**C19I**	**C18I**	124(2)	**O2A**	**Eu1A**	**O2I**	135.6(7)
C14I	**C19I**	**N1I**	120(3)	**O2A**	**Eu1A**	**O3A**	81.6(6)
C18I	**C19I**	**N1I**	115(2)	**O2A**	**Eu1A**	**Cl4I**	77.3(5)
C22A	**C21A**	**N2A**	125(3)	**O2A**	**Eu1A**	**Eu1B**	155.0(5)
N2B	**C21B**	**C22B**	121(2)	**O2I**	**Eu1A**	**C28A**	125.6(6)
N2I	**C21I**	**C22I**	127(3)	**O2I**	**Eu1A**	**N1A**	140.4(6)
C21A	**C22A**	**C23A**	125(3)	**O2I**	**Eu1A**	**N1I**	124.4(7)
C23B	**C22B**	**C21B**	115(4)	**O2I**	**Eu1A**	**N2A**	97.9(7)
C21I	**C22I**	**C23I**	117(3)	**O2I**	**Eu1A**	**O1I**	71.5(5)
C24A	**C23A**	**C22A**	116(3)	**O2I**	**Eu1A**	**O3A**	71.4(6)
C22B	**C23B**	**C24B**	129(4)	**O2I**	**Eu1A**	**Cl4I**	59.9(4)
C24I	**C23I**	**C22I**	120(3)	**O2I**	**Eu1A**	**Eu1B**	34.2(4)
C23A	**C24A**	**C25A**	126(3)	**O3A**	**Eu1A**	**C28A**	90.2(6)
C23A	**C24A**	**C29A**	119(3)	**O3A**	**Eu1A**	**N1A**	144.3(7)
C25A	**C24A**	**C29A**	112(3)	**O3A**	**Eu1A**	**N1I**	69.8(7)
C25B	**C24B**	**C23B**	131(3)	**O3A**	**Eu1A**	**N2A**	117.9(7)
C29B	**C24B**	**C23B**	109(3)	**O3A**	**Eu1A**	**Cl4I**	66.7(6)
C29B	**C24B**	**C25B**	119(3)	**O3A**	**Eu1A**	**Eu1B**	73.4(4)

C23I	**C24I**	**C25I**	127(3)	**Cl4I**	**Eu1A**	**Eu1B**	92.58(13)
C23I	**C24I**	**C29I**	115(2)	**C18B**	**Eu1B**	**Cl2I**	112.8(5)
C25I	**C24I**	**C29I**	117(3)	**C18B**	**Eu1B**	**Eu1A**	91.2(5)
C24A	**C25A**	**Cl3A**	112(3)	**N1B**	**Eu1B**	**C18B**	44.6(8)
C26A	**C25A**	**C24A**	126(3)	**N1B**	**Eu1B**	**N2B**	76.3(7)
C26A	**C25A**	**Cl3A**	122(3)	**N1B**	**Eu1B**	**Cl2I**	136.5(6)
C24B	**C25B**	**Cl3B**	121(3)	**N1B**	**Eu1B**	**Eu1A**	119.6(5)
C26B	**C25B**	**C24B**	120(3)	**N2B**	**Eu1B**	**C18B**	66.9(6)
C26B	**C25B**	**Cl3B**	118(3)	**N2B**	**Eu1B**	**Cl2I**	60.3(4)
C24I	**C25I**	**C26I**	120(3)	**N2B**	**Eu1B**	**Eu1A**	129.5(5)
C24I	**C25I**	**Cl3I**	120(2)	**N2I**	**Eu1B**	**C18B**	115.2(7)
C26I	**C25I**	**Cl3I**	119(2)	**N2I**	**Eu1B**	**N1B**	78.1(8)
C25A	**C26A**	**C27A**	119(3)	**N2I**	**Eu1B**	**N2B**	135.2(7)
C25B	**C26B**	**C27B**	121(3)	**N2I**	**Eu1B**	**Cl2I**	131.2(6)
C27I	**C26I**	**C25I**	122(2)	**N2I**	**Eu1B**	**Eu1A**	95.1(5)
C26A	**C27A**	**Cl4A**	119(2)	**O1B**	**Eu1B**	**C18B**	18.3(6)
C28A	**C27A**	**C26A**	120(3)	**O1B**	**Eu1B**	**N1B**	62.3(7)
C28A	**C27A**	**Cl4A**	120(2)	**O1B**	**Eu1B**	**N2B**	71.9(7)
C26B	**C27B**	**Cl4B**	118(3)	**O1B**	**Eu1B**	**N2I**	125.1(7)
C28B	**C27B**	**C26B**	125(4)	**O1B**	**Eu1B**	**O1I**	75.9(6)
C28B	**C27B**	**Cl4B**	117(3)	**O1B**	**Eu1B**	**O3B**	145.8(7)
C26I	**C27I**	**Cl4I**	119(2)	**O1B**	**Eu1B**	**Cl2I**	103.4(5)
C28I	**C27I**	**C26I**	118(3)	**O1B**	**Eu1B**	**Eu1A**	75.5(4)
C28I	**C27I**	**Cl4I**	123(2)	**O1I**	**Eu1B**	**C18B**	94.2(7)
C27A	**C28A**	**Eu1A**	157(2)	**O1I**	**Eu1B**	**N1B**	137.7(7)
C29A	**C28A**	**C27A**	116(2)	**O1I**	**Eu1B**	**N2B**	98.0(7)
C29A	**C28A**	**Eu1A**	86.7(14)	**O1I**	**Eu1B**	**N2I**	125.3(7)
O2A	**C28A**	**C27A**	122(3)	**O1I**	**Eu1B**	**Cl2I**	57.9(4)
O2A	**C28A**	**C29A**	122(2)	**O1I**	**Eu1B**	**Eu1A**	36.2(4)
O2A	**C28A**	**Eu1A**	35.4(12)	**O2B**	**Eu1B**	**C18B**	117.8(7)
C27B	**C28B**	**C29B**	118(3)	**O2B**	**Eu1B**	**N1B**	85.7(8)
C27B	**C28B**	**O2B**	127(3)	**O2B**	**Eu1B**	**N2B**	66.9(8)
O2B	**C28B**	**C29B**	114(3)	**O2B**	**Eu1B**	**N2I**	75.1(7)
C27I	**C28I**	**C29I**	121(3)	**O2B**	**Eu1B**	**O1B**	132.6(7)
C27I	**C28I**	**O2I**	122(3)	**O2B**	**Eu1B**	**O1I**	131.3(7)
O2I	**C28I**	**C29I**	118(2)	**O2B**	**Eu1B**	**O2I**	140.0(6)
C28A	**C29A**	**C24A**	125(2)	**O2B**	**Eu1B**	**O3B**	78.5(7)
C28A	**C29A**	**N2A**	115(2)	**O2B**	**Eu1B**	**Cl2I**	75.5(6)
N2A	**C29A**	**C24A**	119(3)	**O2B**	**Eu1B**	**Eu1A**	150.9(5)
C24B	**C29B**	**C28B**	116(3)	**O2I**	**Eu1B**	**C18B**	87.8(6)
N2B	**C29B**	**C24B**	124(2)	**O2I**	**Eu1B**	**N1B**	94.7(7)
N2B	**C29B**	**C28B**	120(2)	**O2I**	**Eu1B**	**N2B**	151.8(6)
C28I	**C29I**	**C24I**	120(2)	**O2I**	**Eu1B**	**N2I**	65.9(6)
N2I	**C29I**	**C24I**	124(3)	**O2I**	**Eu1B**	**O1B**	80.3(6)

N2I	**C29I**	**C28I**	116(3)	**O2I**	**Eu1B**	**O1I**	70.5(5)
C11A	**N1A**	**C19A**	117(2)	**O2I**	**Eu1B**	**O3B**	80.0(6)
C11A	**N1A**	**Eu1A**	130.0(19)	**O2I**	**Eu1B**	**Cl2I**	124.7(5)
C19A	**N1A**	**Eu1A**	112.8(16)	**O2I**	**Eu1B**	**Eu1A**	34.3(4)
C11B	**N1B**	**Eu1B**	125.8(19)	**O3B**	**Eu1B**	**C18B**	163.4(7)
C19B	**N1B**	**C11B**	115(3)	**O3B**	**Eu1B**	**N1B**	147.1(8)
C19B	**N1B**	**Eu1B**	118(2)	**O3B**	**Eu1B**	**N2B**	121.7(7)
C11I	**N1I**	**C19I**	121(3)	**O3B**	**Eu1B**	**N2I**	70.0(8)
C11I	**N1I**	**Eu1A**	126.1(19)	**O3B**	**Eu1B**	**O1I**	71.2(7)
C19I	**N1I**	**Eu1A**	113.2(19)	**O3B**	**Eu1B**	**Cl2I**	66.6(5)
C21A	**N2A**	**Eu1A**	134(2)	**O3B**	**Eu1B**	**Eu1A**	72.4(5)
C29A	**N2A**	**C21A**	114(3)	**Cl2I**	**Eu1B**	**Eu1A**	92.21(14)

Table E.6: Torsion Angles for [Eu(57dcOx)$_3$(H$_2$O)$_2$]·EtOH·H$_2$O (5).

A	B	C	D	Angle/°	A	B	C	D	Angle/°
C11A	**C12A**	**C13A**	**C14A**	4(5)	**C23B**	**C24B**	**C29B**	**C28B**	179(3)
C11B	**C12B**	**C13B**	**C14B**	-1(5)	**C23B**	**C24B**	**C29B**	**N2B**	-9(4)
C11I	**C12I**	**C13I**	**C14I**	0(5)	**C23I**	**C24I**	**C25I**	**C26I**	-168(3)
C12A	**C11A**	**N1A**	**C19A**	-6(4)	**C23I**	**C24I**	**C25I**	**Cl3I**	3(4)
C12A	**C11A**	**N1A**	**Eu1A**	176(2)	**C23I**	**C24I**	**C29I**	**C28I**	177(3)
C12A	**C13A**	**C14A**	**C15A**	173(3)	**C23I**	**C24I**	**C29I**	**N2I**	-7(4)
C12A	**C13A**	**C14A**	**C19A**	-3(4)	**C24A**	**C25A**	**C26A**	**C27A**	-9(5)
C12B	**C11B**	**N1B**	**C19B**	-8(5)	**C24A**	**C29A**	**N2A**	**C21A**	0(4)
C12B	**C11B**	**N1B**	**Eu1B**	-178(3)	**C24A**	**C29A**	**N2A**	**Eu1A**	177.1(19)
C12B	**C13B**	**C14B**	**C15B**	173(3)	**C24B**	**C25B**	**C26B**	**C27B**	-8(5)
C12B	**C13B**	**C14B**	**C19B**	-3(5)	**C24B**	**C29B**	**N2B**	**C21B**	2(4)
C12I	**C11I**	**N1I**	**C19I**	3(4)	**C24B**	**C29B**	**N2B**	**Eu1B**	-163(2)
C12I	**C11I**	**N1I**	**Eu1A**	-177.0(19)	**C24I**	**C25I**	**C26I**	**C27I**	-1(5)
C12I	**C13I**	**C14I**	**C15I**	-180(3)	**C24I**	**C29I**	**N2I**	**C21I**	0(4)
C12I	**C13I**	**C14I**	**C19I**	12(5)	**C24I**	**C29I**	**N2I**	**Eu1B**	-179(2)
C13A	**C14A**	**C15A**	**C16A**	175(3)	**C25A**	**C24A**	**C29A**	**C28A**	7(4)
C13A	**C14A**	**C15A**	**Cl1A**	5(4)	**C25A**	**C24A**	**C29A**	**N2A**	-175(3)
C13A	**C14A**	**C19A**	**C18A**	179(3)	**C25A**	**C26A**	**C27A**	**C28A**	14(5)
C13A	**C14A**	**C19A**	**N1A**	-2(4)	**C25A**	**C26A**	**C27A**	**Cl4A**	-175(3)
C13B	**C14B**	**C15B**	**C16B**	-179(4)	**C25B**	**C24B**	**C29B**	**C28B**	8(4)
C13B	**C14B**	**C15B**	**Cl1B**	9(5)	**C25B**	**C24B**	**C29B**	**N2B**	-180(3)
C13B	**C14B**	**C19B**	**C18B**	-179(3)	**C25B**	**C26B**	**C27B**	**C28B**	9(5)
C13B	**C14B**	**C19B**	**N1B**	2(5)	**C25B**	**C26B**	**C27B**	**Cl4B**	-175(3)
C13I	**C14I**	**C15I**	**C16I**	-175(3)	**C25I**	**C24I**	**C29I**	**C28I**	6(4)
C13I	**C14I**	**C15I**	**Cl1I**	5(4)	**C25I**	**C24I**	**C29I**	**N2I**	-177(3)
C13I	**C14I**	**C19I**	**C18I**	175(3)	**C25I**	**C26I**	**C27I**	**C28I**	-7(5)
C13I	**C14I**	**C19I**	**N1I**	-17(4)	**C25I**	**C26I**	**C27I**	**Cl4I**	-179(2)

C14A	**C15A**	**C16A**	**C17A**	9(4)	**C26A**	**C27A**	**C28A**	**C29A**	-7(4)
C14A	**C19A**	**N1A**	**C11A**	6(4)	**C26A**	**C27A**	**C28A**	**O2A**	175(3)
C14A	**C19A**	**N1A**	**Eu1A**	-175(2)	**C26A**	**C27A**	**C28A**	**Eu1A**	161(3)
C14B	**C15B**	**C16B**	**C17B**	6(6)	**C26B**	**C27B**	**C28B**	**C29B**	0(5)
C14B	**C19B**	**N1B**	**C11B**	3(4)	**C26B**	**C27B**	**C28B**	**O2B**	-175(3)
C14B	**C19B**	**N1B**	**Eu1B**	174(2)	**C26I**	**C27I**	**C28I**	**C29I**	14(4)
C14I	**C15I**	**C16I**	**C17I**	5(4)	**C26I**	**C27I**	**C28I**	**O2I**	-166(3)
C14I	**C19I**	**N1I**	**C11I**	10(4)	**C26I**	**C27I**	**Cl4I**	**Eu1A**	143(2)
C14I	**C19I**	**N1I**	**Eu1A**	-169.9(18)	**C27A**	**C28A**	**C29A**	**C24A**	-3(4)
C15A	**C14A**	**C19A**	**C18A**	3(4)	**C27A**	**C28A**	**C29A**	**N2A**	179(2)
C15A	**C14A**	**C19A**	**N1A**	-178(3)	**C27A**	**C28A**	**O2A**	**Eu1A**	-171(2)
C15A	**C16A**	**C17A**	**C18A**	-3(4)	**C27B**	**C28B**	**C29B**	**C24B**	-8(4)
C15A	**C16A**	**C17A**	**Cl2A**	180(2)	**C27B**	**C28B**	**C29B**	**N2B**	179(3)
C15B	**C14B**	**C19B**	**C18B**	5(4)	**C27B**	**C28B**	**O2B**	**Eu1B**	172(3)
C15B	**C14B**	**C19B**	**N1B**	-174(3)	**C27I**	**C28I**	**C29I**	**C24I**	-14(4)
C15B	**C16B**	**C17B**	**C18B**	-9(6)	**C27I**	**C28I**	**C29I**	**N2I**	169(3)
C15B	**C16B**	**C17B**	**Cl2B**	175(3)	**C27I**	**C28I**	**O2I**	**Eu1A**	43(3)
C15I	**C14I**	**C19I**	**C18I**	5(4)	**C27I**	**C28I**	**O2I**	**Eu1B**	-160(2)
C15I	**C14I**	**C19I**	**N1I**	174(2)	**C28A**	**C29A**	**N2A**	**C21A**	178(3)
C15I	**C16I**	**C17I**	**C18I**	0(4)	**C28A**	**C29A**	**N2A**	**Eu1A**	-5(3)
C15I	**C16I**	**C17I**	**Cl2I**	-169(2)	**C28B**	**C29B**	**N2B**	**C21B**	173(2)
C16A	**C17A**	**C18A**	**C19A**	-3(4)	**C28B**	**C29B**	**N2B**	**Eu1B**	9(3)
C16A	**C17A**	**C18A**	**O1A**	175(2)	**C28I**	**C27I**	**Cl4I**	**Eu1A**	-29(3)
C16B	**C17B**	**C18B**	**C19B**	9(5)	**C28I**	**C29I**	**N2I**	**C21I**	177(3)
C16B	**C17B**	**C18B**	**O1B**	-174(3)	**C28I**	**C29I**	**N2I**	**Eu1B**	-2(3)
C16B	**C17B**	**C18B**	**Eu1B**	147(5)	**C29A**	**C24A**	**C25A**	**C26A**	-1(5)
C16I	**C17I**	**C18I**	**C19I**	-1(4)	**C29A**	**C24A**	**C25A**	**Cl3A**	173(2)
C16I	**C17I**	**C18I**	**O1I**	180(2)	**C29A**	**C28A**	**O2A**	**Eu1A**	11(4)
C16I	**C17I**	**Cl2I**	**Eu1B**	-154(2)	**C29B**	**C24B**	**C25B**	**C26B**	0(4)
C17A	**C18A**	**C19A**	**C14A**	3(5)	**C29B**	**C24B**	**C25B**	**Cl3B**	173(2)
C17A	**C18A**	**C19A**	**N1A**	-176(3)	**C29B**	**C28B**	**O2B**	**Eu1B**	-3(4)
C17A	**C18A**	**O1A**	**Eu1A**	167(2)	**C29I**	**C24I**	**C25I**	**C26I**	1(4)
C17B	**C18B**	**C19B**	**C14B**	-7(4)	**C29I**	**C24I**	**C25I**	**Cl3I**	172(2)
C17B	**C18B**	**C19B**	**N1B**	172(3)	**C29I**	**C28I**	**O2I**	**Eu1A**	-137(2)
C17B	**C18B**	**O1B**	**Eu1B**	-162(2)	**C29I**	**C28I**	**O2I**	**Eu1B**	19(3)
C17I	**C18I**	**C19I**	**C14I**	-2(3)	**N1A**	**C11A**	**C12A**	**C13A**	1(5)
C17I	**C18I**	**C19I**	**N1I**	-170(2)	**N1B**	**C11B**	**C12B**	**C13B**	7(5)
C17I	**C18I**	**O1I**	**Eu1A**	165.6(19)	**N1I**	**C11I**	**C12I**	**C13I**	-8(4)
C17I	**C18I**	**O1I**	**Eu1B**	-45(3)	**N2A**	**C21A**	**C22A**	**C23A**	-7(7)
C18A	**C19A**	**N1A**	**C11A**	-175(3)	**N2B**	**C21B**	**C22B**	**C23B**	-5(5)
C18A	**C19A**	**N1A**	**Eu1A**	4(3)	**N2I**	**C21I**	**C22I**	**C23I**	-8(5)
C18B	**C19B**	**N1B**	**C11B**	-177(2)	**O1A**	**C18A**	**C19A**	**C14A**	-175(2)
C18B	**C19B**	**N1B**	**Eu1B**	-6(3)	**O1A**	**C18A**	**C19A**	**N1A**	6(4)
C18I	**C17I**	**Cl2I**	**Eu1B**	36(2)	**O1B**	**C18B**	**C19B**	**C14B**	175(3)

C18I	**C19I**	**N1I**	**C11I**	179(2)	**O1B**	**C18B**	**C19B**	**N1B**	-6(4)
C18I	**C19I**	**N1I**	**Eu1A**	-1(3)	**O1I**	**C18I**	**C19I**	**C14I**	178(2)
C19A	**C14A**	**C15A**	**C16A**	-9(4)	**O1I**	**C18I**	**C19I**	**N1I**	9(3)
C19A	**C14A**	**C15A**	**Cl1A**	-179(2)	**O2A**	**C28A**	**C29A**	**C24A**	175(2)
C19A	**C18A**	**O1A**	**Eu1A**	-15(4)	**O2A**	**C28A**	**C29A**	**N2A**	-3(4)
C19B	**C14B**	**C15B**	**C16B**	-4(4)	**O2B**	**C28B**	**C29B**	**C24B**	168(2)
C19B	**C14B**	**C15B**	**Cl1B**	-175(2)	**O2B**	**C28B**	**C29B**	**N2B**	-5(4)
C19B	**C18B**	**O1B**	**Eu1B**	16(3)	**O2I**	**C28I**	**C29I**	**C24I**	166(2)
C19I	**C14I**	**C15I**	**C16I**	-7(4)	**O2I**	**C28I**	**C29I**	**N2I**	-11(4)
C19I	**C14I**	**C15I**	**Cl1I**	172.7(19)	**Cl1A**	**C15A**	**C16A**	**C17A**	-180(2)
C19I	**C18I**	**O1I**	**Eu1A**	-13(3)	**Cl1B**	**C15B**	**C16B**	**C17B**	176(3)
C19I	**C18I**	**O1I**	**Eu1B**	135.6(19)	**Cl1I**	**C15I**	**C16I**	**C17I**	-175.3(19)
C21A	**C22A**	**C23A**	**C24A**	-5(5)	**Cl2A**	**C17A**	**C18A**	**C19A**	174(3)
C21B	**C22B**	**C23B**	**C24B**	-5(6)	**Cl2A**	**C17A**	**C18A**	**O1A**	-8(4)
C21I	**C22I**	**C23I**	**C24I**	0(5)	**Cl2B**	**C17B**	**C18B**	**C19B**	-174.1(19)
C22A	**C21A**	**N2A**	**C29A**	9(5)	**Cl2B**	**C17B**	**C18B**	**O1B**	3(4)
C22A	**C21A**	**N2A**	**Eu1A**	-166(3)	**Cl2B**	**C17B**	**C18B**	**Eu1B**	-36(7)
C22A	**C23A**	**C24A**	**C25A**	175(3)	**Cl2I**	**C17I**	**C18I**	**C19I**	167.8(18)
C22A	**C23A**	**C24A**	**C29A**	14(4)	**Cl2I**	**C17I**	**C18I**	**O1I**	-11(4)
C22B	**C21B**	**N2B**	**C29B**	6(4)	**Cl3A**	**C25A**	**C26A**	**C27A**	178(2)
C22B	**C21B**	**N2B**	**Eu1B**	168.6(19)	**Cl3B**	**C25B**	**C26B**	**C27B**	178(3)
C22B	**C23B**	**C24B**	**C25B**	-180(4)	**Cl3I**	**C25I**	**C26I**	**C27I**	-172(2)
C22B	**C23B**	**C24B**	**C29B**	11(6)	**Cl4A**	**C27A**	**C28A**	**C29A**	-179(2)
C22I	**C21I**	**N2I**	**C29I**	8(5)	**Cl4A**	**C27A**	**C28A**	**O2A**	3(4)
C22I	**C21I**	**N2I**	**Eu1B**	-173(3)	**Cl4A**	**C27A**	**C28A**	**Eu1A**	-11(7)
C22I	**C23I**	**C24I**	**C25I**	175(3)	**Cl4B**	**C27B**	**C28B**	**C29B**	-176(2)
C22I	**C23I**	**C24I**	**C29I**	6(4)	**Cl4B**	**C27B**	**C28B**	**O2B**	9(5)
C23A	**C24A**	**C25A**	**C26A**	-162(3)	**Cl4I**	**C27I**	**C28I**	**C29I**	-173(2)
C23A	**C24A**	**C25A**	**Cl3A**	11(4)	**Cl4I**	**C27I**	**C28I**	**O2I**	6(4)
C23A	**C24A**	**C29A**	**C28A**	170(3)	**Eu1A**	**C28A**	**C29A**	**C24A**	-178(3)
C23A	**C24A**	**C29A**	**N2A**	-12(4)	**Eu1A**	**C28A**	**C29A**	**N2A**	4(2)
C23B	**C24B**	**C25B**	**C26B**	-168(3)	**Eu1B**	**C18B**	**C19B**	**C14B**	-175(2)
C23B	**C24B**	**C25B**	**Cl3B**	5(5)	**Eu1B**	**C18B**	**C19B**	**N1B**	4(2)

F. κ^2-O,O'-*tris*-[(5,7-dichloro-8-hydroxyquinoline)(Methanol)Europium(III)]

Table F.1: Fractional Atomic Coordinates (×10^4) and Equivalent Isotropic Displacement Parameters (Å^2×10^3) for κ^2-O,O'-[Eu(57dcOx)$_3$·EtOH] (5).

Atom	***x***	***y***	***z***	**U(eq)**

Eu1	5369.5(2)	5109.2(2)	5715.4(2)	27.46(6)
Cl2	4647.2(7)	2896.6(6)	4849.3(3)	48.6(3)
Cl1	3075.3(8)	1180.6(6)	5920.1(4)	67.8(4)
O1	4941.0(14)	4080.7(13)	5363.6(6)	34.0(6)
C8	4519(2)	3428.2(19)	5477.8(10)	32.1(7)
N1	4505.7(17)	3921.1(16)	6040.1(8)	33.0(6)
C4	3824(2)	2626(2)	5982.9(11)	36.4(8)
C9	4265.5(19)	3313.0(19)	5838.4(10)	31.1(7)
C6	3859(2)	2129(2)	5413.4(13)	42.3(9)
C2	3860(2)	3187(2)	6540.4(12)	45.1(10)
C7	4307(2)	2817(2)	5278.3(10)	36.4(8)
C1	4305(2)	3848(2)	6379.1(11)	41.6(9)
C3	3630(2)	2584(2)	6345.2(12)	42.8(9)
C5	3626(2)	2039.6(19)	5755.2(14)	42.6(10)
O3	5759.3(13)	5323.7(13)	6324.0(6)	29.6(5)
O2	6120.7(14)	5564.3(13)	5209.3(6)	31.6(5)
O4	4657.9(14)	5364.1(14)	5293.3(7)	35.4(6)
N3	6357.5(17)	4851.9(16)	5849.5(8)	31.5(6)
O5	4587.8(17)	5447.4(18)	6015.9(7)	43.9(7)
Cl4	6073.8(5)	5503.8(6)	7119.6(2)	40.8(2)
C18	6629.7(19)	6747.9(19)	5425.6(9)	30.5(7)
N2	6212.4(18)	6463.2(16)	5720.3(8)	33.5(7)
C27	6568.1(18)	4910.1(17)	6198.3(9)	28.6(7)
C25	6442.9(19)	5208.2(19)	6797.5(9)	31.9(7)
C26	6230.1(18)	5162.4(17)	6442.5(9)	27.6(7)
Cl6	6928.0(7)	5966.6(6)	4514.3(3)	51.3(3)
C16	6981(2)	6536(2)	4854.6(10)	35.0(8)
C17	6562.0(19)	6246.5(19)	5157.7(9)	29.7(7)
C23	7261(2)	4792(2)	6674.2(12)	39.0(9)
C22	7082(2)	4722.2(19)	6309.2(11)	34.7(8)
C13	7096(2)	7494(2)	5386.6(11)	38.1(8)
Cl3	7861.7(7)	4540.8(7)	6826.9(4)	57.8(3)
C20	7151(2)	4432(2)	5696.4(12)	41.4(9)
C10	6248(3)	6897(2)	5975.0(11)	45.2(10)
C24	6950(2)	5032(2)	6914.5(11)	37.9(8)
C21	7365(2)	4475(2)	6041.1(12)	41.5(9)
C15	7437(2)	7267(2)	4807.6(11)	41.7(9)
C19	6652(2)	4630(2)	5610.8(10)	36.9(8)
C12	7119(3)	7930(2)	5670.0(12)	51.0(11)
Cl5	8048.5(8)	8640.3(6)	4996.6(4)	68.8(4)
C14	7493(2)	7732(2)	5065.5(12)	42.9(9)
C11	6699(3)	7637(2)	5959.8(12)	54.2(12)
C51	4961(3)	6189(4)	6933.7(16)	73.5(17)
O6	6061(8)	3949(9)	4401(3)	86(4)

O7	4829.7(19)	5622.6(19)	6699.6(8)	52.9(8)
C1B	4273(5)	6097(5)	7061(3)	143(4)

Table F.2: Hydrogen Atom Coordinates (Å×10^4) and Isotropic Displacement Parameters (Å^2×10^3) for κ^2-O,O'-[Eu(57dcOx)$_3$·EtOH] (5).

Atom	*x*	*y*	*z*	U(eq)
H6	3719	1726	5264	51
H2	3722	3162	6784	54
H1	4471	4265	6521	50
H3	3337	2132	6453	51
H4A	4461	5599	5402	53
H4B	4931	5640	5110	53
H5A	4627	5872	5923	66
H5B	4097	5098	5997	66
H20	7342	4268	5515	50
H10	5953	6700	6180	54
H24	7079	5078	7160	45
H21	7706	4338	6102	50
H15	7710	7439	4594	50
H19	6515	4605	5367	44
H12	7429	8431	5658	61
H11	6710	7930	6152	65
H51A	5232	6650	6807	88
H51B	5248	6192	7140	88
H1AA	5754	3599	4533	128
H1AB	5836	4069	4248	128
H7	4712	5699	6497	79
H1BA	3979	6066	6855	214
H1BB	4360	6505	7210	214
H1BC	4024	5658	7202	214

Table F.3: Anisotropic Displacement Parameters (Å^2×10^3) for κ^2-O,O'-[Eu(57dcOx)$_3$·EtOH] (5).

Atom	U_{11}	U_{22}	U_{33}	U_{23}	U_{13}	U_{12}
Eu1	35.72(11)	28.18(10)	17.23(9)	-0.41(6)	0.45(6)	15.03(8)
Cl2	69.1(7)	47.2(6)	35.5(5)	-11.9(4)	-6.4(5)	33.6(5)
Cl1	71.9(8)	28.3(5)	89.5(10)	5.0(5)	16.7(7)	14.9(5)
O1	45.1(15)	30.6(13)	23.0(12)	-1.1(10)	-2.1(10)	16.6(12)
C8	35.6(18)	31.4(18)	31.5(18)	-2.3(14)	-8.5(14)	18.5(15)
N1	38.8(17)	30.5(15)	27.7(15)	1.9(12)	0.8(12)	15.8(13)
C4	34.7(19)	29.2(18)	46(2)	2.6(15)	0.0(16)	16.4(15)

C9	30.1(17)	29.6(17)	32.6(18)	1.3(14)	-2.2(14)	14.1(14)
C6	43(2)	29.8(19)	55(3)	-10.0(17)	-10.4(19)	18.9(17)
C2	48(2)	45(2)	37(2)	11.0(17)	9.4(18)	18.8(19)
C7	44(2)	36.7(19)	35(2)	-5.9(15)	-8.7(16)	25.6(17)
C1	49(2)	39(2)	28.7(19)	2.0(15)	6.9(16)	16.6(18)
C3	40(2)	36(2)	50(2)	10.7(18)	7.7(18)	17.3(18)
C5	38(2)	24.8(18)	61(3)	0.8(17)	-0.4(18)	12.3(16)
O3	36.0(13)	33.7(13)	21.3(11)	-1.3(9)	-1.1(9)	19.1(11)
O2	39.6(14)	30.6(12)	23.3(12)	-0.1(9)	2.3(10)	16.7(11)
O4	44.4(15)	44.4(15)	22.2(12)	-2.2(10)	0.8(10)	25.8(13)
N3	38.0(16)	32.8(15)	25.1(14)	1.2(12)	5.8(12)	18.7(13)
O5	53.1(17)	62.7(19)	27.3(14)	-2.3(13)	-0.2(12)	37.4(16)
Cl4	39.3(5)	57.0(6)	23.0(4)	-4.0(4)	0.0(3)	21.7(4)
C18	34.6(18)	30.9(17)	26.3(17)	1.2(13)	-2.0(14)	16.5(15)
N2	45.6(18)	33.2(16)	21.1(14)	-0.7(12)	1.2(12)	19.4(14)
C27	30.1(17)	24.1(16)	28.1(17)	3.0(13)	3.7(13)	11.0(13)
C25	31.5(18)	32.0(18)	26.9(17)	-0.6(14)	0.1(14)	11.9(15)
C26	29.5(16)	23.5(15)	25.8(16)	1.4(12)	1.8(13)	10.3(13)
Cl6	65.1(7)	56.0(6)	32.4(5)	1.1(4)	17.5(5)	30.1(6)
C16	37.2(19)	41(2)	29.1(18)	4.6(15)	4.1(15)	21.0(17)
C17	33.3(18)	34.2(18)	23.4(16)	3.9(13)	-0.6(13)	18.2(15)
C23	33.1(19)	34.5(19)	48(2)	4.5(17)	-7.7(16)	15.6(16)
C22	31.7(18)	28.3(17)	40(2)	4.8(15)	1.7(15)	12.3(15)
C13	40(2)	33.6(19)	37(2)	4.1(15)	1.0(16)	15.7(17)
Cl3	53.0(6)	65.2(7)	68.2(8)	6.1(6)	-11.1(6)	39.2(6)
C20	43(2)	38(2)	45(2)	2.2(17)	13.7(18)	21.9(18)
C10	66(3)	39(2)	26.7(19)	-5.1(16)	3.1(18)	24(2)
C24	36(2)	39(2)	32.2(19)	2.3(15)	-7.0(15)	14.5(17)
C21	38(2)	35(2)	54(3)	5.3(17)	7.2(18)	21.1(17)
C15	40(2)	46(2)	38(2)	12.2(17)	10.8(17)	20.7(18)
C19	45(2)	34.0(19)	31.8(19)	3.1(15)	10.4(16)	20.0(17)
C12	64(3)	32(2)	46(3)	-3.8(18)	-2(2)	16(2)
Cl5	66.7(8)	37.0(6)	84.9(10)	16.8(6)	24.2(7)	12.7(6)
C14	36(2)	33(2)	52(3)	10.9(17)	7.4(18)	11.6(17)
C11	82(3)	38(2)	37(2)	-7.5(18)	3(2)	25(2)
C51	89(4)	89(4)	61(3)	-31(3)	-19(3)	58(4)
O6	122(11)	140(13)	52(7)	38(7)	31(7)	108(11)
O7	66(2)	73(2)	29.6(15)	-11.5(14)	-8.3(14)	41.4(18)
C1B	126(7)	121(7)	181(10)	-64(7)	42(7)	61(6)

Table F.4: Bond Lengths for κ^2-O,O'-[Eu(57dcOx)$_3$·EtOH] (5).

Atom	Atom	Length/Å	Atom	Atom	Length/Å

Eu1	**O1**	2.343(2)	**Cl4**	**C25**	1.735(4)
Eu1	**N1**	2.606(3)	**C18**	**N2**	1.361(5)
Eu1	**O3**	2.389(2)	**C18**	**C17**	1.430(5)
Eu1	**O2**	2.365(2)	**C18**	**C13**	1.422(5)
Eu1	**O4**	2.454(3)	**N2**	**C10**	1.313(5)
Eu1	**N3**	2.519(3)	**C27**	**C26**	1.438(5)
Eu1	**O5**	2.431(3)	**C27**	**C22**	1.426(5)
Eu1	**N2**	2.567(3)	**C25**	**C26**	1.391(5)
Eu1	**C26**	3.265(3)	**C25**	**C24**	1.403(5)
Cl2	**C7**	1.737(4)	**Cl6**	**C16**	1.735(4)
Cl1	**C5**	1.746(4)	**C16**	**C17**	1.390(5)
O1	**C8**	1.314(4)	**C16**	**C15**	1.398(6)
C8	**C9**	1.429(5)	**C23**	**C22**	1.405(6)
C8	**C7**	1.384(5)	**C23**	**Cl3**	1.739(4)
N1	**C9**	1.375(5)	**C23**	**C24**	1.371(6)
N1	**C1**	1.323(5)	**C22**	**C21**	1.413(6)
C4	**C9**	1.414(5)	**C13**	**C12**	1.404(6)
C4	**C3**	1.407(6)	**C13**	**C14**	1.415(6)
C4	**C5**	1.407(6)	**C20**	**C21**	1.356(6)
C6	**C7**	1.404(6)	**C20**	**C19**	1.385(6)
C6	**C5**	1.350(7)	**C10**	**C11**	1.402(6)
C2	**C1**	1.401(6)	**C15**	**C14**	1.356(6)
C2	**C3**	1.355(6)	**C12**	**C11**	1.351(7)
O3	**C26**	1.310(4)	**Cl5**	**C14**	1.738(4)
O2	**C17**	1.313(4)	**C51**	**O7**	1.416(6)
N3	**C27**	1.365(5)	**C51**	**C1B**	1.480(10)
N3	**C19**	1.320(5)			

Table F.5: Bond Angles for κ^2-O,O'-[Eu(57dcOx)$_3$·EtOH] (5).

Atom	Atom	Atom	Angle/°	Atom	Atom	Atom	Angle/°
O1	**Eu1**	**N1**	64.76(9)	**C2**	**C3**	**C4**	120.1(4)
O1	**Eu1**	**O3**	130.73(8)	**C4**	**C5**	**Cl1**	119.1(4)
O1	**Eu1**	**O2**	79.12(9)	**C6**	**C5**	**Cl1**	119.6(3)
O1	**Eu1**	**O4**	81.90(9)	**C6**	**C5**	**C4**	121.2(4)
O1	**Eu1**	**N3**	82.96(9)	**C26**	**O3**	**Eu1**	121.1(2)
O1	**Eu1**	**O5**	122.78(10)	**C17**	**O2**	**Eu1**	123.3(2)
O1	**Eu1**	**N2**	143.98(9)	**C27**	**N3**	**Eu1**	116.8(2)
O1	**Eu1**	**C26**	116.62(9)	**C19**	**N3**	**Eu1**	124.5(3)
N1	**Eu1**	**C26**	76.29(9)	**C19**	**N3**	**C27**	118.6(3)
O3	**Eu1**	**N1**	76.03(9)	**N2**	**C18**	**C17**	115.4(3)

O3	**Eu1**	**O4**	140.22(8)	**N2**	**C18**	**C13**	122.1(3)
O3	**Eu1**	**N3**	66.21(9)	**C13**	**C18**	**C17**	122.4(3)
O3	**Eu1**	**O5**	74.56(9)	**C18**	**N2**	**Eu1**	116.4(2)
O3	**Eu1**	**N2**	77.90(9)	**C10**	**N2**	**Eu1**	125.3(3)
O3	**Eu1**	**C26**	20.10(8)	**C10**	**N2**	**C18**	118.3(3)
O2	**Eu1**	**N1**	142.12(9)	**N3**	**C27**	**C26**	115.5(3)
O2	**Eu1**	**O3**	125.24(9)	**N3**	**C27**	**C22**	121.6(3)
O2	**Eu1**	**O4**	76.80(9)	**C22**	**C27**	**C26**	122.9(3)
O2	**Eu1**	**N3**	76.54(9)	**C26**	**C25**	**Cl4**	119.3(3)
O2	**Eu1**	**O5**	132.97(9)	**C26**	**C25**	**C24**	123.7(3)
O2	**Eu1**	**N2**	65.21(9)	**C24**	**C25**	**Cl4**	117.0(3)
O2	**Eu1**	**C26**	112.86(9)	**O3**	**C26**	**Eu1**	38.80(15)
O4	**Eu1**	**N1**	107.44(10)	**O3**	**C26**	**C27**	120.0(3)
O4	**Eu1**	**N3**	151.34(9)	**O3**	**C26**	**C25**	125.3(3)
O4	**Eu1**	**N2**	85.14(10)	**C27**	**C26**	**Eu1**	81.3(2)
O4	**Eu1**	**C26**	159.89(8)	**C25**	**C26**	**Eu1**	163.5(3)
N3	**Eu1**	**N1**	87.64(10)	**C25**	**C26**	**C27**	114.7(3)
N3	**Eu1**	**N2**	93.09(10)	**C17**	**C16**	**Cl6**	118.7(3)
N3	**Eu1**	**C26**	46.22(9)	**C17**	**C16**	**C15**	123.1(4)
O5	**Eu1**	**N1**	79.53(11)	**C15**	**C16**	**Cl6**	118.2(3)
O5	**Eu1**	**O4**	67.51(9)	**O2**	**C17**	**C18**	119.5(3)
O5	**Eu1**	**N3**	140.61(9)	**O2**	**C17**	**C16**	124.8(3)
O5	**Eu1**	**N2**	81.77(11)	**C16**	**C17**	**C18**	115.6(3)
O5	**Eu1**	**C26**	94.43(9)	**C22**	**C23**	**Cl3**	119.6(3)
N2	**Eu1**	**N1**	151.13(9)	**C24**	**C23**	**C22**	121.0(4)
N2	**Eu1**	**C26**	83.47(9)	**C24**	**C23**	**Cl3**	119.4(3)
C8	**O1**	**Eu1**	125.0(2)	**C23**	**C22**	**C27**	117.7(3)
O1	**C8**	**C9**	119.6(3)	**C23**	**C22**	**C21**	125.4(4)
O1	**C8**	**C7**	125.1(4)	**C21**	**C22**	**C27**	116.9(4)
C7	**C8**	**C9**	115.2(3)	**C12**	**C13**	**C18**	117.0(4)
C9	**N1**	**Eu1**	115.7(2)	**C12**	**C13**	**C14**	125.7(4)
C1	**N1**	**Eu1**	126.5(3)	**C14**	**C13**	**C18**	117.4(4)
C1	**N1**	**C9**	117.7(3)	**C21**	**C20**	**C19**	119.4(4)
C3	**C4**	**C9**	117.3(4)	**N2**	**C10**	**C11**	123.2(4)
C5	**C4**	**C9**	117.4(4)	**C23**	**C24**	**C25**	120.0(4)
C5	**C4**	**C3**	125.3(4)	**C20**	**C21**	**C22**	120.0(4)
N1	**C9**	**C8**	114.9(3)	**C14**	**C15**	**C16**	120.2(4)
N1	**C9**	**C4**	122.2(3)	**N3**	**C19**	**C20**	123.5(4)
C4	**C9**	**C8**	122.9(3)	**C11**	**C12**	**C13**	120.0(4)
C5	**C6**	**C7**	120.2(4)	**C13**	**C14**	**Cl5**	119.4(3)
C3	**C2**	**C1**	119.2(4)	**C15**	**C14**	**C13**	121.2(4)
C8	**C7**	**Cl2**	118.7(3)	**C15**	**C14**	**Cl5**	119.4(3)
C8	**C7**	**C6**	123.0(4)	**C12**	**C11**	**C10**	119.4(4)
C6	**C7**	**Cl2**	118.1(3)	**O7**	**C51**	**C1B**	109.2(6)

N1	**C1**	**C2**	123.5(4)

Table F.6: Torsion Angles for κ^2-O,O'-[Eu(57dcOx)$_3$·EtOH] (5).

A	B	C	D	Angle/°	A	B	C	D	Angle/°
Eu1	**O1**	**C8**	**C9**	2.6(5)	**C18**	**C13**	**C12**	**C11**	-1.1(7)
Eu1	**O1**	**C8**	**C7**	-175.0(3)	**C18**	**C13**	**C14**	**C15**	-0.9(6)
Eu1	**N1**	**C9**	**C8**	-1.0(4)	**C18**	**C13**	**C14**	**Cl5**	177.8(3)
Eu1	**N1**	**C9**	**C4**	176.7(3)	**N2**	**C18**	**C17**	**O2**	-0.4(5)
Eu1	**N1**	**C1**	**C2**	-177.3(3)	**N2**	**C18**	**C17**	**C16**	179.3(3)
Eu1	**O3**	**C26**	**C27**	5.5(4)	**N2**	**C18**	**C13**	**C12**	1.0(6)
Eu1	**O3**	**C26**	**C25**	-174.0(3)	**N2**	**C18**	**C13**	**C14**	-178.5(4)
Eu1	**O2**	**C17**	**C18**	3.4(4)	**N2**	**C10**	**C11**	**C12**	0.5(8)
Eu1	**O2**	**C17**	**C16**	-176.2(3)	**C27**	**N3**	**C19**	**C20**	2.0(6)
Eu1	**N3**	**C27**	**C26**	-4.3(4)	**C27**	**C22**	**C21**	**C20**	0.7(6)
Eu1	**N3**	**C27**	**C22**	174.9(3)	**C26**	**C27**	**C22**	**C23**	-0.1(5)
Eu1	**N3**	**C19**	**C20**	-174.1(3)	**C26**	**C27**	**C22**	**C21**	179.3(3)
Eu1	**N2**	**C10**	**C11**	-177.6(4)	**C26**	**C25**	**C24**	**C23**	-0.7(6)
O1	**C8**	**C9**	**N1**	-0.8(5)	**Cl6**	**C16**	**C17**	**O2**	0.1(5)
O1	**C8**	**C9**	**C4**	-178.5(3)	**Cl6**	**C16**	**C17**	**C18**	-179.5(3)
O1	**C8**	**C7**	**Cl2**	3.1(5)	**Cl6**	**C16**	**C15**	**C14**	179.6(3)
O1	**C8**	**C7**	**C6**	179.4(4)	**C16**	**C15**	**C14**	**C13**	0.2(7)
C9	**C8**	**C7**	**Cl2**	-174.6(3)	**C16**	**C15**	**C14**	**Cl5**	-178.6(3)
C9	**C8**	**C7**	**C6**	1.7(5)	**C17**	**C18**	**N2**	**Eu1**	-2.4(4)
C9	**N1**	**C1**	**C2**	-0.4(6)	**C17**	**C18**	**N2**	**C10**	-179.6(4)
C9	**C4**	**C3**	**C2**	0.5(6)	**C17**	**C18**	**C13**	**C12**	-179.5(4)
C9	**C4**	**C5**	**Cl1**	-179.5(3)	**C17**	**C18**	**C13**	**C14**	0.9(6)
C9	**C4**	**C5**	**C6**	0.9(6)	**C17**	**C16**	**C15**	**C14**	0.6(6)
C7	**C8**	**C9**	**N1**	177.1(3)	**C23**	**C22**	**C21**	**C20**	-179.9(4)
C7	**C8**	**C9**	**C4**	-0.6(5)	**C22**	**C27**	**C26**	**Eu1**	-176.2(3)
C7	**C6**	**C5**	**Cl1**	-179.5(3)	**C22**	**C27**	**C26**	**O3**	-179.7(3)
C7	**C6**	**C5**	**C4**	0.1(6)	**C22**	**C27**	**C26**	**C25**	-0.1(5)
C1	**N1**	**C9**	**C8**	-178.2(3)	**C22**	**C23**	**C24**	**C25**	0.4(6)
C1	**N1**	**C9**	**C4**	-0.5(5)	**C13**	**C18**	**N2**	**Eu1**	177.1(3)
C1	**C2**	**C3**	**C4**	-1.4(7)	**C13**	**C18**	**N2**	**C10**	-0.1(6)
C3	**C4**	**C9**	**C8**	177.9(4)	**C13**	**C18**	**C17**	**O2**	-179.9(3)
C3	**C4**	**C9**	**N1**	0.5(5)	**C13**	**C18**	**C17**	**C16**	-0.2(5)
C3	**C4**	**C5**	**Cl1**	2.0(6)	**C13**	**C12**	**C11**	**C10**	0.4(8)
C3	**C4**	**C5**	**C6**	-177.6(4)	**Cl3**	**C23**	**C22**	**C27**	177.8(3)
C3	**C2**	**C1**	**N1**	1.4(7)	**Cl3**	**C23**	**C22**	**C21**	-1.6(6)
C5	**C4**	**C9**	**C8**	-0.7(6)	**Cl3**	**C23**	**C24**	**C25**	-177.4(3)
C5	**C4**	**C9**	**N1**	-178.1(3)	**C24**	**C25**	**C26**	**Eu1**	166.8(7)
C5	**C4**	**C3**	**C2**	179.0(4)	**C24**	**C25**	**C26**	**O3**	-179.9(3)

C5	**C6**	**C7**	**Cl2**	174.8(3)	**C24**	**C25**	**C26**	**C27**	0.5(5)
C5	**C6**	**C7**	**C8**	-1.5(6)	**C24**	**C23**	**C22**	**C27**	0.0(6)
N3	**C27**	**C26**	**Eu1**	3.0(3)	**C24**	**C23**	**C22**	**C21**	-179.4(4)
N3	**C27**	**C26**	**O3**	-0.5(5)	**C21**	**C20**	**C19**	**N3**	-1.1(6)
N3	**C27**	**C26**	**C25**	179.1(3)	**C15**	**C16**	**C17**	**O2**	179.1(4)
N3	**C27**	**C22**	**C23**	-179.3(3)	**C15**	**C16**	**C17**	**C18**	-0.6(5)
N3	**C27**	**C22**	**C21**	0.2(5)	**C19**	**N3**	**C27**	**C26**	179.3(3)
Cl4	**C25**	**C26**	**Eu1**	-13.6(10)	**C19**	**N3**	**C27**	**C22**	-1.5(5)
Cl4	**C25**	**C26**	**O3**	-0.3(5)	**C19**	**C20**	**C21**	**C22**	-0.3(6)
Cl4	**C25**	**C26**	**C27**	-179.9(3)	**C12**	**C13**	**C14**	**C15**	179.6(4)
Cl4	**C25**	**C24**	**C23**	179.7(3)	**C12**	**C13**	**C14**	**Cl5**	-1.7(6)
C18	**N2**	**C10**	**C11**	-0.7(7)	**C14**	**C13**	**C12**	**C11**	178.4(5)